

**ANALYSIS OF HEAT STRESS ON POLLEN DEVELOPMENT
IN *ARABIDOPSIS THALIANA***

Yang Song, BSc, MSc

Thesis submitted to the University of Nottingham
for the degree of Doctor of Philosophy

January 2017

ACKNOWLEDGEMENTS

I would like to express my sincere gratitude to my supervisor Prof. Zoe A. Wilson for giving me the opportunity to do a PhD in her group, for her patience, motivation, and immense knowledge. Her continually guidance, endless support and invaluable advice helped me in all the time of research and writing of this thesis. I could not have imagined having a better advisor and mentor for my PhD study.

I greatly acknowledge my colleague Dr. A. Ferguson for her unlimited support and advice. I wish to thank Dr. J. Fernandez and Dr. I. Ferjentsikova for sharing their knowledge and many interesting discussion. And also thank my previous colleague Dr. S. Pierce for his support of bioinformatics. I am grateful to all other members of Wilson's group to create a wonderful working environment, and every one of Plant and Crop Sciences Division for their various contributions towards this thesis.

I owe my deepest gratitude to my family, to my Mum and Dad for their encouragement, support, patience and love. Thank you for always trusting me unconditionally in my life. To my wife for supporting me during the years, it is great to have you! Finally, I would like to specially thank my daughters, thank you bring me countless joy.

ABSTRACT

High temperature can have a serious impact on plant development; rising temperatures and environmental fluctuations mean that this is becoming an increasing problem for sustainable agriculture. Many studies have indicated that pollen development is very susceptible to high temperature (HT) stress, particularly during early development, and that the anther tapetum cell layer is extremely vulnerable, resulting in reduced fertility or complete male sterility (MS).

In this project, *Arabidopsis* plants were stressed with 32°C HT during flowering and then assessed by microscopy for phenotypic changes to anther and pollen development, and subsequent reproductive development. The results indicate that the HT had a significant negative impact on plant reproduction, particularly during the stress treatment, with some recovery of fertility post HT.

Samples of plant buds were divided into different growth stages and collected for analysis of fertility and for gene expression analysis. Several genes, which appear from available microarray data to be associated with HT stress and are also specifically expressed during tapetum development, were chosen to test for expression changes associated with temperature stress, both during and after HT stress. Phenotype analysis of insertional knockout mutants of these genes, both with and without HT stress, was used to assess their potential impact on resilience to temperature stress. Transcriptomic analysis of whole genome was conducted by RNA-seq in young (prior to polarized

microspore stage) and old buds (from polarized microspore stage to pollen mitosis) isolated from HT-stressed and non-stressed *Arabidopsis* Ler plants. This has identified a set of HT specific genes that are differentially expressed in different HT period treated plants.

The anther tapetum serves to regulate pollen development and is critical in the production of the pollen wall. It goes through a defined process of programmed cell death (PCD) to facilitate transfer of pollen wall materials onto the developing pollen grains. Disturbance of the timing or progression of this PCD process, for example by heat stress frequently results in male sterility.

Four GFP reporter constructs that have been used as markers during ovule PCD analysis were tested for expression during pollen development and particularly focusing upon the stages of tapetal PCD. These reporter genes showed different stage specific expression during anther development. They have now been introgressed into a number of *Arabidopsis* male sterile mutants that show PCD-related defects, including *ms1*, *ams* and *myb26* male sterile mutants. The F1 generation of these showed similar GFP expression to the parent plants, however the homozygous male sterile F2 generation plants appeared to show different patterns of GFP expression. Two of them (*BFN1* and *CEP1*) are expressed in the anther tapetum during the stages of tapetum PCD. Expression analysis suggests that HT-stress affects the expression of *BFN1* and *CEP1*, which may be linked to abnormal degeneration of the tapetum under HT-stress.

ACKNOWLEDGEMENTS	i
ABSTRACT	ii
TABLE OF CONTENT	iv
LIST OF FIGURES AND TABLES	ix
ABBREVIATIONS	xvi
CHAPTER 1. INTRODUCTION	1
1.1 GLOBAL WARMING AND FOOD SECURITY	1
1.2 <i>ARABIDOPSIS THALIANA</i>	4
1.3 ANther AND POLLEN DEVELOPMENT	7
1.3.1 Anther development	7
1.3.2 Pollen development	13
1.3.3 Regulation of anther and pollen development	16
1.3.4 The tapetum	19
1.4 MALE STERILITY	21
1.5 PROGRAMMED CELL DEATH	23
1.5.1 Tapetum programmed cell death	26
1.6 AIMS AND OBJECTIVES OF THE PROJECT	28
CHAPTER 2. MATERIALS AND METHODS	29
2.1 PLANT MATERIALS AND GROWTH CONDITION	29
2.2 HIGH TEMPERATURE (HT) STRESS	29
2.3 DAPI (4', 6-DIAMIDINO-2-PHENYLINDOLE) STAINING	30
2.4 POLLEN VITALITY STAINING AND COUNTING	30
2.5 <i>IN VITRO</i> POLLEN GERMINATION	31
2.6 MORPHOLOGY ANALYSIS	31
2.7 SEED STERILISATION AND GERMINATION	32
2.8 RNA EXTRACTION	33

2.9 PRIMER DESIGN	33
2.10 PCR PROCEDURE	33
2.11 cDNA SYNTHESIS	34
2.12 ACTIN AMPLIFICATION AND NORMALIZATION	35
2.13 QUANTITATIVE PCR	35
2.14 MICROSCOPY	36
2.14.1 Confocal microscopy	36
2.14.2 Fluorescence Microscopy	36
CHAPTER 3. IMPACTS OF HIGH TEMPERATURE STRESS DURING POLLEN DEVELOPMENT	38
3.1 INTRODUCTION	38
3.1.1 High temperature injury in barley and rice plants organ formation 	40
3.1.2 High temperature effects on <i>Arabidopsis thaliana</i> and auxin recovery	42
3.2 MATERIALS AND METHODS	44
3.2.1 Plant growth and staging	44
3.2.2 High temperature stress	44
3.2.3 Bud positions in inflorescence and pollen developmental stages 	45
3.2.4 Pollen developmental alteration under HT-stress	45
3.2.5 Morphology analysis and seed viability	45
3.3 RESULTS AND DISCUSSION	46
3.3.1 Identification of pollen samples developmental stages	46
3.3.2 HT-stress effect on flower and pollen development	47
3.3.2.1 Flower structure after HT-stress	47
3.3.2.2 Pollen viability analysis	49
3.3.2.3 Plant developmental analysis	51
3.3.2.4 Seed germination	58
3.4 DISCUSSION	59

CHAPTER 4. HIGH TEMPERATURE STRESS RELATED CANDIDATE GENES ANALYSIS	64
4.1 INTRODUCTION	64
4.2 MATERIALS AND METHODS	70
4.2.1 Plant materials and growth condition	70
4.2.2 HT-stress and sample collection	71
4.2.3 Sucrose method for DNA extraction	72
4.2.4 Primer list	73
4.2.5 RNA extraction and cDNA synthesis	73
4.2.6 RT-PCR and Quantitative RT-PCR	73
4.3 RESULTS	74
4.3.1 Expression analysis of HT related candidate genes	74
4.3.2 Analysis of T-DNA insertion mutants.	82
4.3.2.1 Expression analysis	82
4.3.2.2 Morphological analysis of T-DNA insertion mutants with and without HT-stress	101
4.4 DISCUSSION	114
CHAPTER 5. ANALYSIS OF GENE EXPRESSION CHANGE DUE TO HIGH TEMPERATURE STRESS	123
5.1 INTRODUCTION	123
5.1.1 Transcriptome research	123
5.1.2 Limitation of hybridisation- based transcriptomic methods	123
5.1.3 RNA-seq technology – Benefits and Challenges	125
5.1.4 RNA-Seq experiments processes	129
5.1.5 Data analysis software	131
5.2 MATERIALS AND METHODS	134
5.2.1 Plant materials, HT-stress and collection modes	134
5.2.2 RNA sample preparation for RNA-seq	135
5.2.3 Preparation of labelled targets, sequencing experiment (WTCHG, Oxford)	135

5.2.4 RNA-seq data analysis (The Advanced Data Analysis Centre, University of Nottingham)	136
5.2.5 Gene ontology (GO) and annotation	137
5.2.6 Validation of RNA-seq data with quantitative RT-PCR	137
5.3 RESULTS	138
5.3.1 Experiment design.....	138
5.3.2 Transcriptome sequencing.....	138
5.3.3 Data quantity assessment and exploratory.....	140
5.3.4 Interpreting the differential expression analysis results	146
5.3.5 Gene ontology enrichment analysis and annotation of the significantly regulated genes	152
5.3.6 Expression validation by quantitative RT-PCR.....	170
5.4 DISCUSSION.....	173
5.4.1 Data quality assessment.....	173
5.4.2 Gene Ontology (GO) enrichment analysis.....	176
5.4.3 RNA-seq data validation	177
CHAPTER 6. PROGRAMMED CELL DEATH RELATED GENES EXPRESSION AND REGULATION	179
6.1 INTRODUCTION	179
6.2 MATERIALS AND METHODS	185
6.2.1 Plant materials and growth.....	185
6.2.2 Introgression of PCD genes into male sterile mutants	185
6.2.3 BASTA screening	186
6.2.4 Samples dissection and microscopy.....	186
6.2.5 Bud samples collection.....	187
6.2.6 RNA extraction and cDNA synthesis	187
6.2.7 Quantitative RT-PCR	187
6.3 RESULTS	188
6.3.1 PCD related genes expression analysis	188
6.3.1.1 <i>APR1</i> expression in WT and male sterile mutants	188

6.3.1.2 <i>BFN1</i> expression in WT and male sterile mutants	196
6.3.1.3 <i>CEP1</i> expression in WT and male sterile mutants	202
6.3.1.4 <i>SAG12</i> expression in WT and male sterile mutants	208
6.3.2 Quantitative RT-PCR analysis of PCD genes in WT plant.....	213
6.3.3 Quantitative RT-PCR analysis of PCD genes in male sterile mutants.....	215
6.3.4 HT-stress effected PCD genes expression during pollen development	219
6.3.5 RNA-seq results of <i>BFN1</i> and <i>CEP1</i>	229
6.4 DISCUSSION.....	231
6.4.1 PCD genes expression with tapetum PCD	231
6.4.2 PCD genes expression in the male sterile mutants.....	236
6.4.3 Impacts of HT-stress on <i>BFN1</i> and <i>CEP1</i> during pollen development	238
CHAPTER 7. GENERAL DISCUSSION.....	241
7.1 HIGH TEMPERATURE STRESS ON PLANT MORPHOLOGY DURING POLLEN DEVELOPMENT	242
7.2 MOLECULAR ASPECT AND GENE FUNCTION ANALYSIS ON HT-STRESS DURING POLLEN DEVELOPMENT	243
7.3 TRANSCRIPTOME ANALYSIS OF HT-STRESS DURING POLLEN DEVELOPMENT.....	248
7.4 PROGRAMMED CELL DEATH WITH HT-STRESS DURING POLLEN DEVELOPMENT.....	252
7.5 SUGGESTING RELATIONSHIP BETWEEN HT-STRESS AND POLLEN DEVELOPMENT.....	254
REFERENCES.....	257
APPENDICES	298

LIST OF FIGURES AND TABLES

FIGURES

CHAPTER 1

Figure 1.1 Comparison of observed and simulated climate change.	3
Figure 1.2 Scheme of a transverse section through an <i>Arabidopsis</i> floral bud showing the number, position, and orientation of the floral organs	5
Figure 1.3 <i>Arabidopsis</i> flower.	6
Figure 1.4 Model for the differentiation of the microsporangial cell layers in <i>Arabidopsis</i>	8
Figure 1.5 Anther cell differentiations.	12
Figure 1.6 Morphological stages of microsporogenesis and microgametogenesis.	14
Figure 1.7 Anther and pollen development pathway.	19
Figure 1.8 Pollen wall structure.	21
Figure 1.9 Overview of developmentally controlled cell death in plants.	25

CHAPTER 3

Figure 3.1 <i>Arabidopsis</i> inflorescence.	45
Figure 3.2 Pollen stage by DAPI staining.	47
Figure 3.3 <i>Arabidopsis</i> flower structure after HT-stress.	49
Figure 3.4 Filament length (stamen without anther) data of non-stressed and 2 days HT-stressed <i>Arabidopsis</i> plants.	49
Figure 3.5 Pollen viability rate by FDA staining.	50
Figure 3.6 <i>In vitro</i> pollen germination rates.	51

Figure 3.7 Average silique lengths of all samples.	52
Figure 3.8 Average seed number of all samples.	53
Figure 3.9 Average silique length of each position.	55
Figure 3.10 Average seed number of each position.	56
Figure 3.11 Average silique lengths at different pollen developmental stages.	57
Figure 3.12 Average seed number at different pollen developmental stages.	58
Figure 3.13 Seed germination frequency (%) harvested from non-stressed and HT-stressed <i>Arabidopsis</i> plants.	59

CHAPTER 4

Figure 4.1 Bud collection modes for expression analysis.	72
Figure 4.2 RT-PCR for cDNA quality inspection.	76
Figure 4.3 Quantitative RT-PCR of HT related candidate genes expression level with and without HT-stress in different pollen developmental stages.	78-80
Figure 4.4 T-DNA insertion mutant information and genotyping of the <i>CRT1b</i> (AT1G09210) gene.	85
Figure 4.5 T-DNA insertion mutant information and genotyping of the <i>UTR1</i> (AT2G02810) gene.	86
Figure 4.6 T-DNA insertion mutant information and genotyping of the <i>MBF1c</i> (AT3G24500) gene.	87
Figure 4.7 T-DNA insertion mutant information and genotyping of the <i>HOP3</i> (AT4G12400) gene.	88
Figure 4.8 T-DNA insertion mutant information and genotyping of the <i>ABI1</i> (AT4G26080) gene.	89
Figure 4.9 T-DNA insertion mutant information and genotyping of the <i>HS83</i>	90

(AT5G52640) gene.

Figure 4.10 Expression analysis of T-DNA insertion mutants on *CRT1b* (AT1G09210) gene. 94

Figure 4.11 Expression analysis of T-DNA insertion mutants on *UTR1* (AT2G02810) gene. 95

Figure 4.12 Expression analysis of T-DNA insertion mutants on *MBF1c* (AT3G24500) gene. 96

Figure 4.13 Expression analysis of T-DNA insertion mutants on *HOP3* (AT4G12400) gene. 97

Figure 4.14 Expression analysis of T-DNA insertion mutants on *ABI1* (AT4G26080) gene. 98

Figure 4.15 Expression analysis of T-DNA insertion mutants on *HS83* (AT5G52640) gene. 99

Figure 4.16 Morphological analysis of WT and T-DNA insertion mutants of *CRT1b* (AT1G09210) gene with and without HT-stress. 108

Figure 4.17 Morphological analysis of WT and T-DNA insertion mutants of *UTR1* (AT2G02810) gene with and without HT-stress. 109

Figure 4.18 Morphological analysis of WT and T-DNA insertion mutants of *MBF1c* (AT3G24500) gene with and without HT-stress. 110

Figure 4.19 Morphological analysis of WT and T-DNA insertion mutants of *HOP3* (AT4G12400) gene with and without HT-stress. 111

Figure 4.20 Morphological analysis of WT and T-DNA insertion mutants of *ABI1* (AT4G26080) gene with and without HT-stress. 112

Figure 4.21 Morphological analysis of WT and T-DNA insertion mutants of *HS83* (AT5G52640) gene with and without HT-stress. 113

CHAPTER 5

Figure 5.1 Multidimensional scaling (MDS) showing the relationship between replicates in two dimensions (Leading logFC dimension 1 and 2), 142

generated by edgeR.

Figure 5.2 Multidimensional scaling (MDS) showing the relationship between replicates in two dimensions (Leading logFC dimension 1 and 2), generated by edgeR. 143

Figure 5.3 Multidimensional scaling (MDS) showing the relationship between replicates in two dimensions (Leading logFC dimension 1 and 2), generated by edgeR. 144

Figure 5.4 MA-plot generated in edgeR for evaluating the efficiency of normalisation. 150

Figure 5.5 Volcano plot of gene expression and significance. 151

Figure 5.6 Gene Ontology (GO) enrichment analysis of up-regulated genes in “Old” sample with 6 hours HT-stress. 155

Figure 5.7 Gene Ontology (GO) enrichment analysis of down-regulated genes in “Old” sample with 6 hours HT-stress. 156

Figure 5.8 Gene Ontology (GO) enrichment analysis of up-regulated genes in “Young” sample with 6 hours HT-stress. 157

Figure 5.9 Gene Ontology (GO) enrichment analysis of down-regulated genes in “Young” sample with 6 hours HT-stress. 158

Figure 5.10 Gene Ontology (GO) enrichment analysis of up-regulated genes in “Old” sample with 24 hours HT-stress. 159

Figure 5.11 Gene Ontology (GO) enrichment analysis of down-regulated genes in “Old” sample with 24 hours HT-stress. 160

Figure 5.12 Gene Ontology (GO) enrichment analysis of up-regulated genes in “Young” sample with 24 hours HT-stress. 161

Figure 5.13 Gene Ontology (GO) enrichment analysis of down-regulated genes in “Young” sample with 24 hours HT-stress. 162

Figure 5.14 Venn diagram analysis of the significantly regulated genes at different stages with different HT-stress period. 168

Figure 5.15 Heatmap of differential expression between all pairwise 169

comparisons using ANOVA analysis.

Figure 5.16 Quantitative RT-PCR verification of the differentially down-regulated expressed genes. 171

Figure 5.17 Quantitative RT-PCR verification of the differentially up-regulated expressed genes. 172

CHAPTER 6

Figure 6.1 APR1:GFP expression in anther tissues in WT background 190-191

Figure 6.2 APR1:GFP expression in anther tissue in *ams* mutant. 193

Figure 6.3 APR1:GFP expression in anther tissue in *ms1* mutant. 194

Figure 6.4 APR1:GFP expression in anther tissue in *myb26* mutant. 195

Figure 6.5 BFN1:GFP expression in anther tissue in WT mutant. 197

Figure 6.6 BFN1:GFP expression in anther tissue in *ams* mutant. 199

Figure 6.7 BFN1:GFP expression in anther tissue in *ms1* mutant. 200

Figure 6.8 BFN1:GFP expression in anther tissue in *myb26* mutant. 201

Figure 6.9 CEP1:GFP expression in anther tissue in WT mutant. 204

Figure 6.10 CEP1:GFP expression in anther tissue in *ams* mutant. 205

Figure 6.11 CEP1:GFP expression in anther tissue in *ms1* mutant. 206

Figure 6.12 CEP1:GFP expression in anther tissue in *myb26* mutant. 207

Figure 6.13 SAG12:GFP expression in anther tissue in WT mutant. 209

Figure 6.14 SAG12:GFP expression in anther tissue in *ms1* mutant. 210

Figure 6.15 SAG12:GFP expression in anther tissue in *myb26* mutant. 211

Figure 6.16 Quantitative RT-PCR of *BFN1* and *CEP1* expression in staged buds samples. 214

Figure 6.17 Quantitative RT-PCR of <i>BFN1</i> expression in staged male sterile mutant buds samples.	217
Figure 6.18 Quantitative RT-PCR of <i>CEP1</i> expression in staged male sterile mutant buds samples.	218
Figure 6.19 <i>BFN1</i> :GFP expression in Arabidopsis anther without HT-stress and HT-stressed for 1 day and 2 days.	221-224
Figure 6.20 <i>CEP1</i> :GFP expression in Arabidopsis anther without HT-stress and HT-stressed for 1 day and 2 days.	225-229
Figure 6.21 Relative expression levels of <i>BFN1</i> and <i>CEP1</i> in different pollen developmental stage after HT-stress.	230
Figure 6.22 A model for <i>BFN1</i> and <i>CEP1</i> regulation during anther and pollen development.	240

TABLES

CHAPTER 1

Table 1.1 Major events during <i>Arabidopsis</i> anther development.	11
--	----

CHAPTER 2

Table 2.1 PCR programme	34
-------------------------	----

CHAPTER 3

Table 3.1 List of transgenic plants, heat stress linked transgenes and their responsible role for enhancing plants towards stress tolerance	39
Table 3.2 Pollen development in <i>Ler</i> flower buds.	48

CHAPTER 4

Table 4.1 HT and tapetum specific related genes	66
Table 4.2 T-DNA insertion mutants used in HT-stress experiments.	70
Table 4.3 Buds samples information of HT-stress experiments.	75
Table 4.4 T-DNA insertion mutants used in the HT-stress experiments, and primers list for identification and expression analysis.	84
Table 4.5 Summary of T-DNA insertion mutant expression analysis.	100

CHAPTER 5

Table 5.1 Sequencing yields and alignment overview.	139
Table 5.2 Number of genes that present significant difference on expression level with HT-stress.	149
Table 5.3 Summary of the top 10 down- and up- regulated genes in “Old” group samples with 6 hours HT-stress (P -value<0.05).	163
Table 5.4 Summary of the top 10 down- and up- regulated genes in “Young” group samples with 6 hours HT-stress (P -value<0.05).	164
Table 5.5 Summary of the top 10 down- and up- regulated genes in “Old” group samples with 24 hours HT-stress (P -value<0.05).	165
Table 5.6 Summary of the top 10 down- and up- regulated genes in “Young” group samples with 24 hours HT-stress (P -value<0.05).	166
Table 5.7 Comparison of gene expression fold change in RNA-seq and quantitative RT-PCR.	170

CHAPTER 6

Table 6.1 Expression pattern of PCD genes in <i>Arabidopsis</i> anther.	213
Table 6.2 Detailed relative expression level of <i>BFN1</i> and <i>CEP1</i> in different staged buds.	219

ABBREVIATIONS

ANOVA	analysis of variance
bp	base pair
Col-0	Columbia-0
CPM	counts per million
DAPI	4',6-diamidino-2-phenylindole
ddH ₂ O	double distilled water
DE	differential expression
FC	Fold change
FDA	Fluorescein Diacetate
GFP	green fluorescent protein
GO	Gene Ontology
HT	high temperature
kb	kilo base pair
<i>Ler</i>	Landsberg <i>erecta</i>
MDS	Multidimensional Scaling
MS medium	Murashige and Skoog medium
PCD	programmed cell death
WT	wild type

CHAPTER 1

INTRODUCTION

CHAPTER 1. INTRODUCTION

1.1 GLOBAL WARMING AND FOOD SECURITY

Our world is suffering serious climate changes; in the twentieth century, global average temperature increased between 0.6°C and 0.9°C (Riebeek, 2010). There have also been more natural and artificial influences on the world climate change in the recent five to six decades, such as the increasing volcanic activities between 1960 and 1991 which induced a net negative natural radiative forcing in the last two decades of twentieth century; and a slight overall increase in solar activity from 1900 to 1950 which may have accounted for about one of six of that century's observed temperature increase. These also include more greenhouse gas (GHG) emission associated with population increase, and industry and city development (Stocker et al., 2013). Data from the Intergovernmental Panel on Climate Change (IPCC)(Stocker et al., 2013) showed that the global average temperature has risen 0.13°C every decade since 1950, and a faster pace of 0.2°C temperature ascent every decade is expected over the next two to three decades, with substantially larger trend likely for cultivated land areas (Fig. 1.1). By 2100, the world average temperature even is expected to increase within the range 2.6-4.8°C (Stocker et al., 2013). However, Battisti and Naylor (2009) suggest that the temperature in some areas such as Sahara would increase by about 10°C according to their model.

Food security was defined by the Food and Agriculture Organization of the United Nations (FAO) as “situation that exists when all people, at all times, have physical, social, and economic access to sufficient, safe, and nutritious

food that meets their dietary needs and food preferences for an active and healthy life” (Dept, 2002), which separated the food supplies into four dimensions: availability, stability, access and utilization. These four dimensions relate to 1) food production, supplement, and farmers performance in response to markets in the entire global range; 2) the individuals who lose their access to achieve adequate food temporarily or permanently; 3) the entitlement of individuals for a nutrition diet; and 4) safe and healthy utilization of food (Schmidhuber & Tubiello, 2007). In all these aspects, food supplement plays a basic but important role for food security, while other considerations are built on the basis of sufficient food supplement. Lobell et al. (2011) indicate that more food production is demanded with the increasing population and economics, however, global climate change is leading toward severe risks to food production, which will result in serious impacts, including significant impacts on plant growth and development, and crop yields. It has been predicted that the average summer temperature will exceed the hottest on record throughout the tropics and subtropics, which will lead to potentially serious consequences for food production and is likely to affect 50% of people who live in these areas (Battisti & Naylor, 2009).

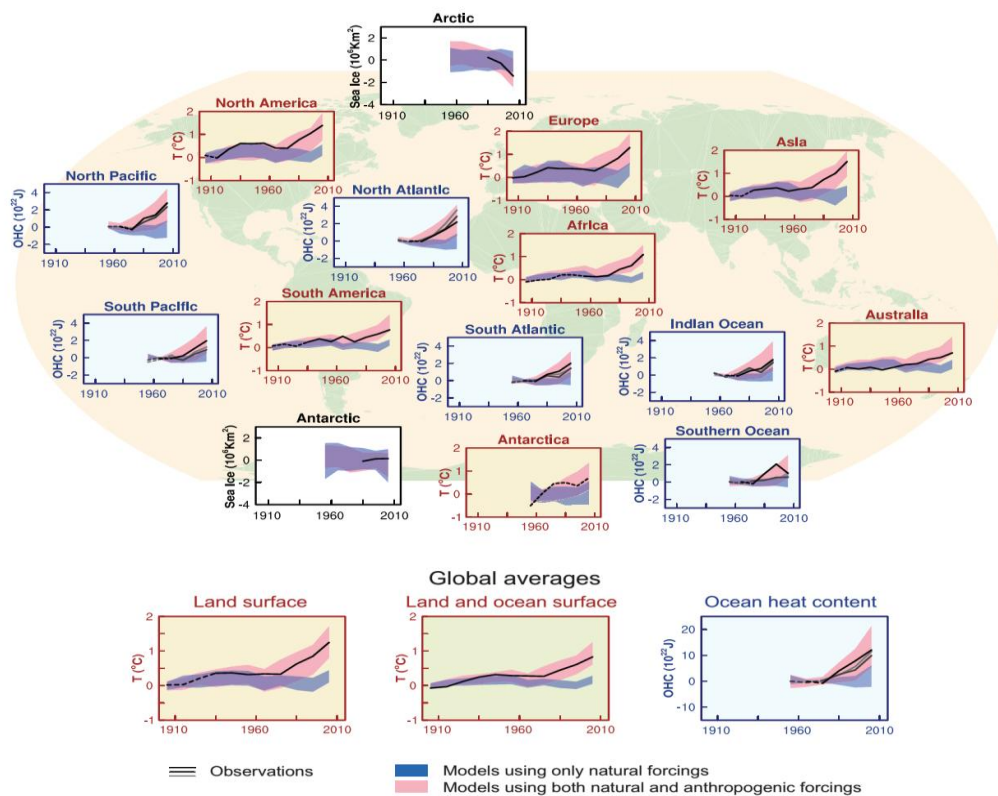


Figure 1.1 Comparison of observed and simulated climate change (Stocker et al., 2013). The climate change is based on three large-scale indicators in the atmosphere, the cryosphere and the ocean: change in continental land surface air temperatures (yellow panels), Arctic and Antarctic September sea ice extent (white panels), and upper ocean heat content in the major ocean basins (blue panels). Global average changes are also given. Anomalies are given relative to 1880–1919 for surface temperatures, 1960–1980 for ocean heat content and 1979–1999 for sea ice. All time-series are decadal averages, plotted at the centre of the decade. For temperature panels, observations are dashed lines if the spatial coverage of areas being examined is below 50%. For ocean heat content and sea ice panels the solid line is where the coverage of data is good and higher in quality, and the dashed line is where the data coverage is only adequate, and thus, uncertainty is larger. Model results shown are Coupled Model Intercomparison Project Phase 5 (CMIP5) multi-model ensemble ranges, with shaded bands indicating the 5 to 95% confidence intervals (Stocker et al., 2013).

High temperature affects crop yields in the following pathways, firstly high temperature causes faster crop development as well as shorter crop duration, which in most cases is associated with lower yields (Hatfield & Prueger, 2015). Second, temperature impacts the rates of photosynthesis, respiration, and grain filling, such as high temperature at night that raises respiration costs without any potential benefit for photosynthesis (Yano et al., 2007). Third, high temperature, which leads to an increase in the saturation vapour pressure of air, will cause reduced water-use efficiency in plants (Bita & Gerats, 2013). Fourth, high temperature can damage plant cells directly, and then affect plant development (Oshino et al., 2007). Fifth, high temperature may increase the growth and survival of many pests and diseases specific to agricultural crops (Schmidhuber & Tubiello, 2007). Finally, high temperature may increase evapotranspiration and lower soil moisture levels, which will cause a much drier environment with damage to the plants (Schmidhuber & Tubiello, 2007, Lobell & Gourджи, 2012). Therefore, the potential decrease of crop yields caused by high temperature has become a serious problem in this century.

1.2 ARABIDOPSIS THALIANA

The genus *Arabidopsis* belongs to a member of the Brassicaceae family (mustard or crucifer). There are several species in the *Arabidopsis* genus, while the most well known and most extensively used one is *Arabidopsis thaliana*. *Arabidopsis* is a small flowering plant native to Europe, Asia, and north-western Africa and has been widely introduced to North America, Australia and some other areas (Wilson et al., 1991).

Arabidopsis grows a rosette from 2-10 cm in diameter, depending on different growth conditions and genotype. A mature *Arabidopsis* plant consists of a rosette of 2-30 leaves, from which a flowering stem can extend to a height of 20-70 cm. The *Arabidopsis* flowers are approximately 3 mm long and 1 mm wide; the flowers typically produce four whorls of floral organs, which contain four sepals, four petals, six stamens (four long and two short), and a gynoecium consisting of two fused carpels, from whorl 1 to whorl 4 (Scott et al., 2004)(Fig. 1.2). After fertilization, the ovary develops into a silique which contains about 50 seeds and this shatters on ripening to allow the distribution of seed. Mature seeds are less than 1mm in length. The entire life cycle of *Arabidopsis* plants is completed in 6 weeks, from seed germination, formation of of rosette, main stem elongation, flowering and maturation of first seeds. (TAIR: www.arabidopsis.org)

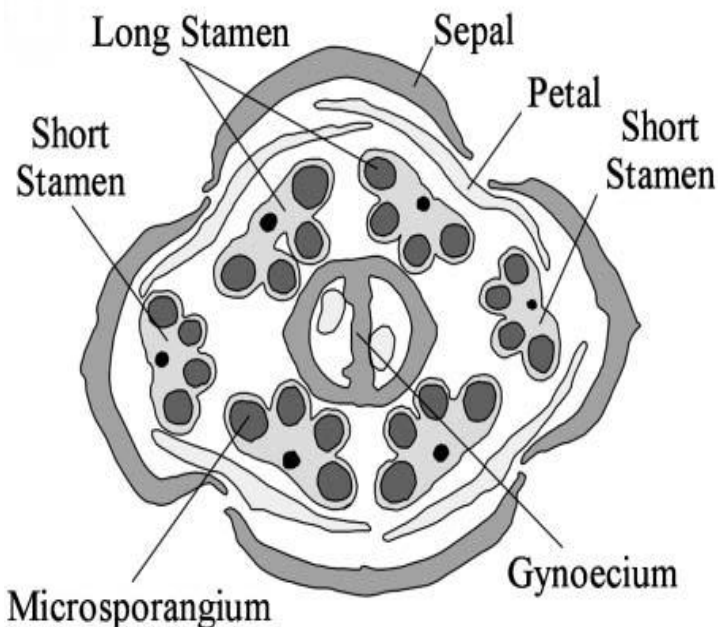


Figure1.2 Scheme of a transverse section through an *Arabidopsis* floral bud showing the number, position, and orientation of the floral organs (Scott et al., 2004).

Whorl 1: Sepals

Whorl 2: Petals

Whorl 3: Stamens

Whorl 4: Carpels (Gynoecium)

Arabidopsis attracts researchers as a model plant in development and genetics because of its many advantages, which include a rapid life cycle, small plant size, abundant seed production, a relatively small genome, and associated genetic resources. Furthermore, the *Arabidopsis* genome sequencing had been completed in 2000 (*Arabidopsis* Genome Initiative, 2000), which provide more information for gene mapping and function of analysis.

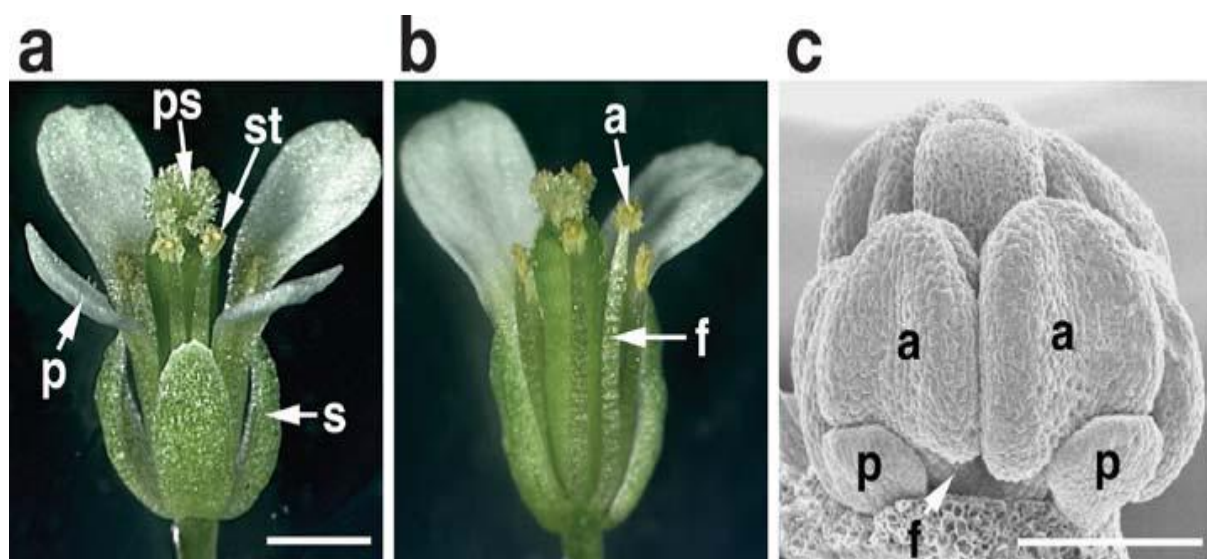


Figure 1.3 *Arabidopsis* flower (Ma, 2005). (A) An intact mature (stage 13) *Arabidopsis* flower with four types of organs, sepals (s), petals (p), stamens (st), and the pistil (ps). (B) A mature flower with one sepal and two petals removed to reveal some of the stamens, which have an anther (a) and a filament (f). A and B are of the same magnification; bar = 1.0 mm. (C) A scanning electron micrograph of a stage 9 flower, with its sepals removed to show the inner organs; two petal primordia (p) are round and small; two of the four long stamens can be easily seen with their anthers (a) having attained the characteristic lobed shape and the filaments (f) still very short. Bar= 100 μ m.(Ma, 2005)

1.3 ANTHOR AND POLLEN DEVELOPMENT

In flowering plants, male reproductive processes take place in the stamen. There are six stamens in *Arabidopsis*, each containing a filament and an anther (Ma, 2005) (Fig.1.3). The filament is a vascular tube of tissue that links the stamen to the flower and supplies water and nutrients, and also attaches to the anther by connective tissues. The anther contains the reproductive and non-reproductive tissues that are responsible for producing and releasing pollen grains so that pollination and fertilization processes can occur within the flower (Goldberg et al., 1993).

1.3.1 Anther development

The *Arabidopsis* anther development initiates from a single archesporial cell with the formation of stamen primordia in whorl 3 of the floral meristem. A model of this differentiation in microsporangial cell layers in *Arabidopsis* is shown by Scott et al. (2004)(Fig 1.4). During the early developmental stages, cell and tissue differentiation occur in the anthers, and microspore mother cells undergo meiosis, until the specialized anther cells and tissues are produced, and the pollen sacs contain the tetrads of microspores. The next process is that as pollen grains differentiate, and the anther enlarges and grows upward in the flower by filament extension, then tissue degeneration, dehiscence, and the process concludes with the release of the pollen grains (Goldberg et al., 1993). Major events in *Arabidopsis* anther development have been described in Table 1.1 (Sanders et al., 1999).

These developmental stages are recognized by morphological and cellular features from light microscopy, and are divided into two main phases. Phase

1 consists of stages 1-8, whilst stages 9-14 make up phase 2 (Fig. 1.5)(Ma, 2005). During phase 1, the anther tissues are forming via cell division and differentiation. There are four lobes in the anther, several sporophytic (somatic) tissues surround the microspore mother cells (MMCs), also called pollen mother cell (PMCs), or male sporocytes in every lobe. The anther lobes develop and attach to a vascular bundle, which is continuous with the vasculature of the filament, by a contiguous connective tissue. The circular cell cluster and stomium are two additional non-reproductive anther tissues, which are important for pollen release. During phase 2, the filament elongates greatly; meanwhile, the anther further enlarges and the microspores develop into pollen grains, followed by the degeneration of anther tissues, anther dehiscence, and pollen release (Ma, 2005).

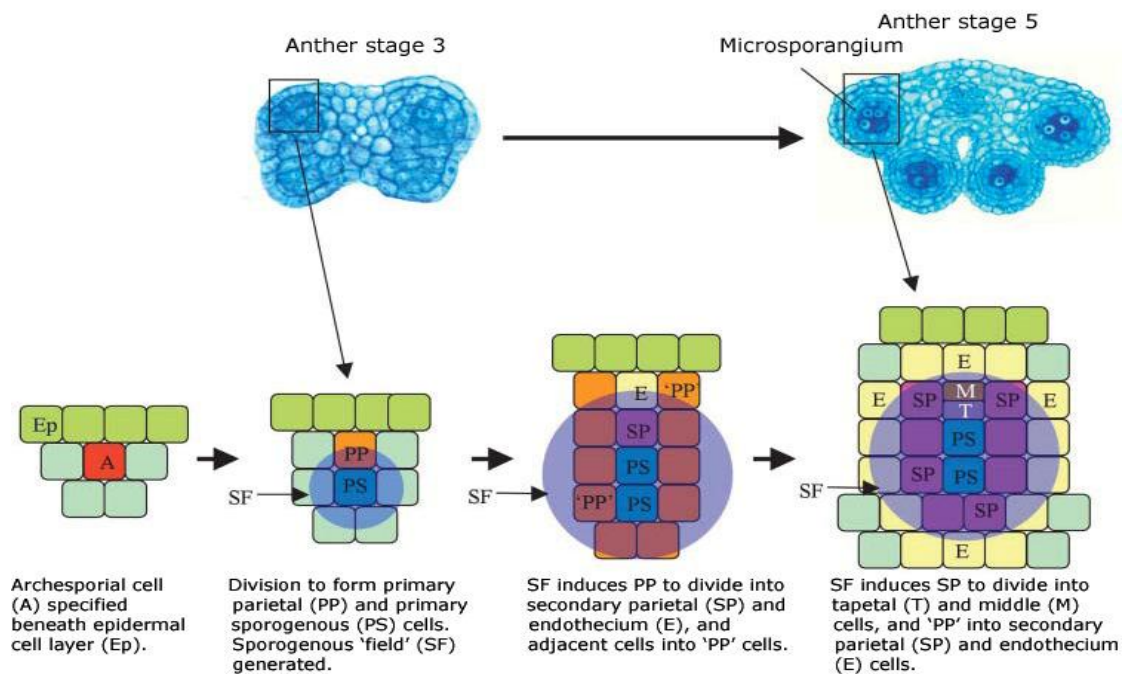


Figure 1.4 Model for the differentiation of the microsporangial cell layers in *Arabidopsis* (Scott et al., 2004).

During stage 1, L1, L2, and L3 layers of the floral meristem divide to form the stamen (anther) primordium. In stages 2 to 5, anticlinal cell division in L1 then expands the surface area of the anther and results in the formation of the epidermis. Meanwhile, cell divisions and differentiation occurs in the L3 layer and then form the connective and vascular tissues. Periclinal and anticlinal cell also divisions to form the internal cell layers in the four anther lobes. At stage 2, there are four clusters of archesporial cells form from the periclinal division of L2 cells. At stage 3, division of the archesporial cells initiates and then to form the primary parietal layer and the sporogenous cells. The primary parietal layer is beneath the epidermal layer and surrounds the sporogenous cells. The primary parietal layer then divides to form two secondary parietal layers. The inner secondary parietal layer divides and develops into the tapetum layer, and the outer secondary parietal layer divides and differentiates to an endothecium layer and a middle layer at stage 4 (Sanders et al., 1999; Smyth et al., 1990).

At stage 5, involves completion of the four lobes characteristic morphology and anther morphogenesis, four non-reproductive layers form from the surface to the interior in each lobe: the epidermis, the endothecium, the middle layer, and the tapetum. The reproductive MMCs are surrounded by these somatic layers. At stage 6, the MMCs undergo meiosis, and the callose is deposited on the wall of the meiotic cells. Subsequently, the meiotic cells dissociate from each other and also the tapetum, leading to a space called the locule, which is inside the tapetum. The meiosis completes at stage 7 and a tetrad of four haploid microspores form. At stage 8, the callose wall degrades and the microspores are released from the tetrad. During stages 9–12, the

microspores develop into pollen grains, and the tapetum degenerates at stages 10 and 11. During stage 12, pollen mitosis occurs to produce the tricellular haploid pollen grains. The anther dehiscent to release the pollen grains at stage 13. At stage 14, anther cells shrink (Sanders et al., 1999; Smyth et al., 1990).

Table 1.1 Major events during *Arabidopsis* anther development.

(Sanders et al., 1999)

Anther stage	Major events and morphological markers	Flower stage ^a	Pollen stage ^b
1	Rounded stamen primordia emerge	5	
2	Archesporial cells arise in four corners of the anther primordia. Primordia oval shaped.		
3	1° parietal and sporogenous layers generated by mitotic activity. They generate the 2° parietal layers and sporogenous cells, respectively.		
4	Four-lobed anther pattern with two developing stomium regions. Vascular region initiated.		
5	Four defined locules established. All anther cell types present. Pollen mother cells appear.	9	3
6	Pollen mother cells enter meiosis. Middle layer is crushed and degenerates. Tapetum becomes vacuolated and the anther undergoes a general increase in size.		
7	Meiosis completed. Tetrads of microspores free within each locule. Remnants of middle layer present.		
8	Callose wall surrounding tetrads degenerates and individual microspores released.	10	4
9	Growth and expansion of anther continues. Microspores generate an exine wall and become vacuolated.		5
10	Tapetum degeneration initiated.		6-7
11	Pollen mitotic divisions occur. Tapetum degenerates. Expansion of endothelial layer. Secondary thickenings appear in endothecium and connective cells. Septum cell degeneration initiated. Stomium differentiation begins.	11-12	8-9
12	Anther contains tricellular pollen grains. Anther becomes bilocular after degeneration and breakage of septum below stomium. Stomium differentiates.		10
13	Dehiscence. Breakage along stomium and pollen release.	13-14	
14	Senescence of stamen. Shrinkage of cells and anther structure.	15-16	
15	Stamen falls off senescing flower	17	

a. Flower development stages taken from Smyth et al. (1990) and Bowman et al.(1991). b. Pollen development stages taken from Regan and Moffatt (1990).

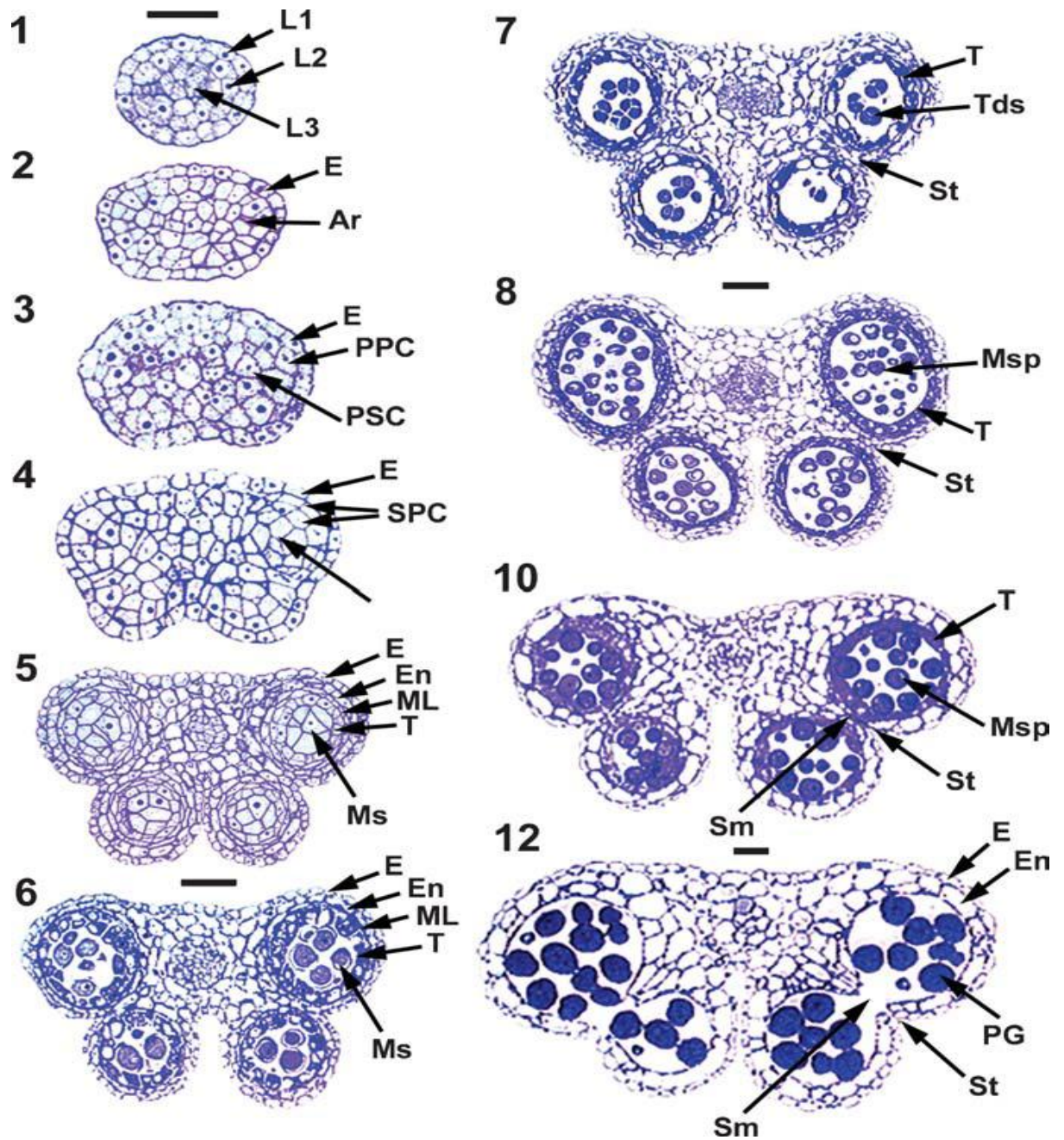


Figure 1.5 Anther cell differentiations. Stages are shown of wild-type *Arabidopsis thaliana* anther development. The numbers indicate stages. Bar = 25 μ m and stages 1 to 5, 6 and 7, 8 and 10, and 12 alone have same-sized bars. Ar, archesporial; E, epidermis; En, endothecium; L1, L2, L3, Layer 1, 2, 3; ML, middle layer; Ms, microsporocytes; Msp, microspore; PG, pollen grain; PPC, primary parietal cell; PSC, primary sporogenous cell; Sm, septum; SPC, secondary parietal cell; St, stomium; T, tapetum; Tds, tetrads. (Ma, 2005)

1.3.2 Pollen development

Pollen development is a series of intricate and tightly controlled set of structural and molecular changes, which begin with meiosis and culminate in the formation and release of the pollen grain from the plant (McCormick, 1993). The pollen grains develop from microspores to form a vegetative cell and two sperm cells undergoing cell divisions and cell differentiation after meiosis (Li & Ma, 2002, McCormick, 1993, Tanaka, 1997). There are three major developmental stages include in pollen development, microsporogenesis (differentiation of the sporogeneous cells and meiosis), postmeiosis development of microspores, and microspore mitosis (microgametogenesis) (Chaudhury, 1993). The primary sporogenous layer develops to the microsporocytes or meiocytes. The diploid microsporocytes undergo meiosis and produce the tetrads of four haploid microspores enclosed by the callosic walls. These haploid microspores are then separated into individual microspores and released from the tetrad by an enzyme complex (callase) secreted by the tapetum (Fig. 1.7) (Owen & Makaroff, 1995, Yamamoto et al., 2003). An eccentric microspore nucleus appears against the microspore was to form the polarised microspore with vacuole morphogenesis and microspore expansion. The polarised microspores then divide asymmetrically at pollen mitosis I (PMI) to produce bicellular pollen grains.

Then the pollen mitosis I occurs and produces a large vegetative cell and a small generative cell asymmetrically. During pollen mitosis I, there are two daughter cells, which are completely different in structures and cell fates, are generated through an asymmetric division (Twell & Howden, 1998). The

dispersed nuclear chromatin and constitutes the bulk of the pollen cytoplasm exist in the large vegetative cell, and the condensed nuclear chromatin and relatively few organelles and stored metabolites are contained in the smaller generative cell. The vegetative cell only exits the cell cycle at G1 phase, but the generative cell remains division until form the two sperm cells through pollen mitosis II (PMII).

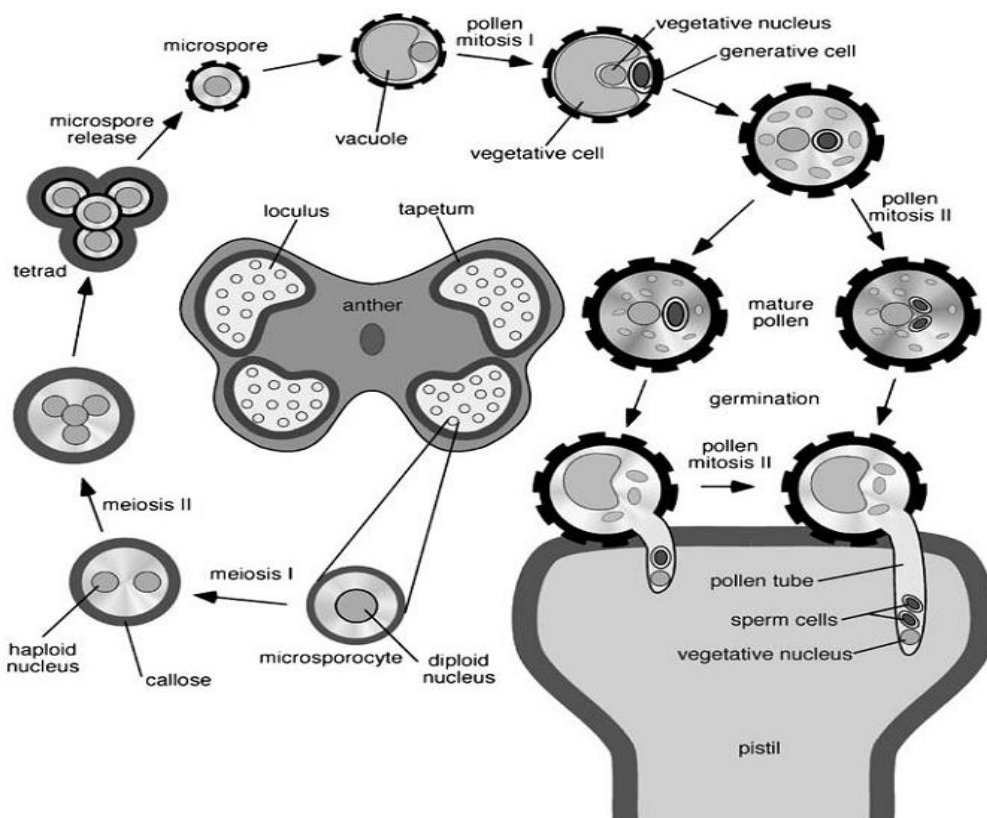


Figure 1.6 Morphological stages of microsporogenesis and microgametogenesis. During microsporogenesis, microsporocytes undergo two nuclear divisions at meiosis followed by cytokinesis to produce a tetrad of four haploid microspores. During microgametogenesis, microspores undergo two stereotypical mitotic divisions, pollen mitosis I and pollen mitosis II to produce bicellular (70% of species) or tricellular pollen grains (e.g., *Arabidopsis*). In species with bicellular pollen grains, pollen mitosis II occurs in the growing pollen tube within the pistil (Twell et al., 2006).

After pollen mitosis I, the generative cell migrates inward and is completely engulfed by the cytoplasm of the vegetative cell to form a “cell within a cell” structure, which enables gamete transport within the pollen tube. Generative cell migration follows with the degradation of the hemispherical callose wall which functions to separate the vegetative and generative cells. Subsequently, the generative cell elongates to a spindle-like shape, and is maintained by a cortical cage of bundled microtubules. In *Arabidopsis*, and other plants with tri-nucleate pollen, the pollen mitosis II, which produces two sperm cells from the generative cell, occurs before pollen maturation (Ma, 2005). Pollen mitosis II takes place within a membrane bound compartment of the vegetative cell cytoplasm, while a physical association is established between the gametic cells and the vegetative nucleus, which is known as the male germ unit (MGU). The MGU exists in both bicellular and tricellular pollen, and it is thought to be important for the coordinated delivery in the gametes and sperm cell fusion events (Dumas et al., 1998). The MGU is first assembled in tricellular pollen in *Arabidopsis* plant (Lalanne & Twell, 2002). Lately in the pollen maturation process, the vegetative cell accumulates carbohydrate and/or lipid reserves required for the demands of plasma membrane and pollen tube wall synthesis (Pacini, 1996). Pollen grains are usually suffered strong dehydration when they are released from the anthers. The accumulation of sugars and amino acids as osmoprotectants, including disaccharides and glycine-betaine or proline, is thought to protect the vitality of membranes and proteins from damage in dehydration (Schwacke et al., 1999).

The generative cell is completely engulfed by the cytoplasm of the vegetative cell.

1.3.3 Regulation of anther and pollen development

To investigate the developmental pathway, the ABCDE model has been established by Robles and Pelaz (2004). The key genes that regulate the development of different cell layers in anther and pollen formation have been identified (Fig. 1.8) (Wilson et al., 2011, Gómez et al., 2015).

At the beginning of anther and pollen development, *WUSCHEL (WUS)* activates the expression of *AGAMOUS (AG)* at the centre of the floral apex and then to increase the number of pluripotent cells, lately *WUS* was repressed by *AG* and cell differentiation was promoted. *APETALA3 (AP3)*, *PISTILLATA (PI)*, and *AG* are three homeotic genes to control stamen initiation, which belongs with the primordia forming as a tetrad of archesporial cells. *AG* also induces microsporogenesis through activating *NOZZLE/SPOROCTELESS (NZZ/SPL)* (Ito et al., 2004). *JAGGED (JAG)* and *NUBBIN (NAB)* are two transcription factors that involve in stamen formation (Dinneny et al., 2006). The expression of *AG* is prolonged, which regulates stamen and carpel specification as the early roles in floral initiation (Ito et al., 2004) and induces the *DEFECTIVE IN ANOTHER DEHISCENCE1 (DAD1)* (Ito et al., 2007), which catalyses jasmonic acid (JA) biosynthesis and results in stamen filament extension and flower opening, during later development. *BARELY ANY MERISTEM1 (BAM1)* and *BAM2* are two CLAVATA 1-related leucine-rich repeat receptor-like protein kinases, which regulate *NLZ/SPL* to promote somatic cell types and to restrict *NZL/SPL*

expression to the inner region of the locule (Hord et al., 2006, Feng & Dickinson, 2010). *EXTRA SPOROGENOUS CELLS/EXCESS MICROSPOROCTES1 (EXS/EMS1)* is a leucine-rich repeat receptor kinase and controls the archesporial cell number and tapetal cell fate (Canales et al., 2002, Zhao et al., 2002), and its ligand *TAPETAL DETERMINANT1 (TPD1)* (Jia et al., 2008) act to establish tapetal cell initiation and microsporocyte identity. The SERK1 and SERK2 complex, which acts downstream of *NZZ/SPL*, is thought to form a receptor complex with EMS1 in the tapetal plasma membrane (Albrecht et al., 2005, Colcombet et al., 2005), and then binds to TPD1 (Yang et al., 2003, Shu-Lan et al., 2005). *DYSFUNCTIONAL TAPETUM1 (DYT1)* (Zhang et al., 2006) and *DEFECTIVE IN TAPETAL DEVELOPMENT AND FUNCTION1 (TDF1)* (Zhu et al., 2008) initiate tapetal development, and several other genes, such as *ABORTED MICROSPORES (AMS)*, *MALE STERILITY1 (MS1)* (Wilson et al., 2001), *ABCWBC27* (Sorensen et al., 2003, Yang et al., 2007, Xu et al., 2010), *MALE STERILITY2 (MS2)*, and *LEUCINE AMINOPEPTIDASE (LAP3)*, involve with the following tapetal maturation, pollen wall formation, and tapetal programmed cell death (PCD). The *MALE GAMETOGENESIS IMPAIRED ANTHEAS (MIA)* gene, which encodes a type V P-type ATPase, also involves in these processes. *DYT1* functions in meiotic progression and regulates many tapetal genes (Feng et al., 2012). The downstream of *DYT1* is *TDF1/MYB35*, which is upstream of *AMS* (Zhu et al., 2008, Zhu et al., 2011). Recent research indicates that *DYT1* directly regulates *TDF1* in the tapetum. The expression of *TDF1* in the *dyt1* mutant can recover the expression of several downstream genes, such as *AMS*, *MS188*, *TEK* and other sporopollenin genes (Gu et al.,

2014). The *AMS* gene encodes a putative bHLH-type transcription factor, which expresses in anther at a low level before meiosis and then increases after meiosis (Sorensen et al., 2003). *AMS* is a master regulator gene in tapetum, which associate with tapetum function and biosynthesis, such as the synthesis of lipidic and phenolic components which are essential for pollen wall patterning, and flavonoids (Xu et al., 2010, Xu et al., 2014a). There are premature microspore degeneration presenting in *ams* mutant due to the reduced callose wall and the absence of sporopollenin secretion (Xu et al., 2014a), the tapetum also becomes abnormally enlarged and vacuolated in this mutant (Sorensen et al., 2003). *ASHR3*, *Arabidopsis* SET-domain protein, shows interact with *AMS*, which indicates that *ASHR3* may regulate stamen development through targeting *AMS* to chromatin (Thorstensen et al., 2008). During in the final stage of dehiscence, there are several jasmonic acid (JA)-induced genes involve, such as *MYB26* (Steiner-Lange & Unte, 2003, Yang et al., 2007) and the *NAC SECONDARY WALL THICKENING PROMOTING FACTOR1 (NST1)* and *NST2* (Mitsuda et al., 2007), which are also the transcription factors associated with endothecium secondary thickening.

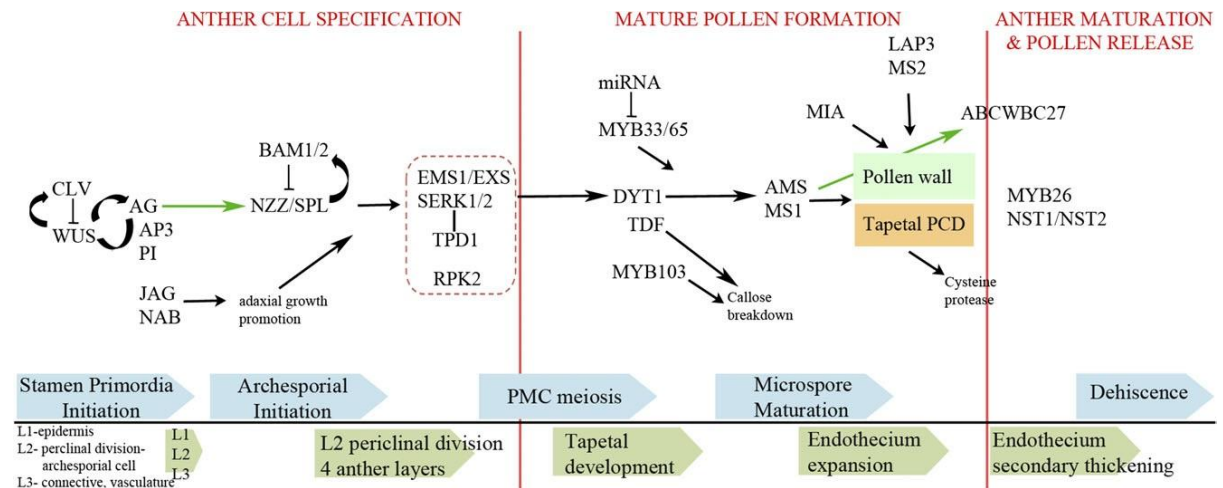


Figure 1.7 Anther and pollen development pathway. Regulation is indicated by arrows; green arrows indicate proven direct regulation; inhibition is shown by a T-bar (Wilson et al., 2011).

1.3.4 The tapetum

The anther consists of four cell layers that surround the microspores: the epidermis, endothecium, middle layer, and tapetum. The tapetum is a layer of nutritive cells which is closest to the sporogenous tissue in developing anthers, and helps form the pollen wall (Polowick & Sawhney, 1993). The tapetum is also known to act as a supplier of metabolites, and sporopollenin precursors (Piffanelli et al., 1998, Scott et al., 2004). In higher plants, the tapetum is highly active with multiple nuclei and large numbers of plastids, mitochondria, Golgi bodies, both rough and smooth ER, some vacuoles, and lipid bodies (Ariizumi & Toriyama, 2011).

In *Arabidopsis* and other many insect-pollinated (entomophilous) plants, the tapetum provides material for the exine and also the tryphine (the pollen coat), which are deposited on the to the outer exine surface (Fig 1.9) (Ariizumi & Toriyama, 2011). In *Arabidopsis*, there are several kinds of short- and long-

chain fatty acids, and proteins, such as glycine-rich oleosin and calcium-binding protein, in the tapetum degenerative debris. These types of sticky lipids are crucial in the signalling pathway that switches on pollen hydration upon contact with the stigmatic surface (Edlund et al., 2004). The flavonoids and a mixture of carotenoids exist in the tryphine which functioned in pollen pigmentation and served as protectors from pathogen attacks, photo-oxidative damage, and UV radiation damage (Hernández-Pinzón et al., 1999, Piffanelli et al., 1998). These also attract animal vectors for pollination.

The tapetum is involved in the synthesizing and secretion of hydrolytic enzymes which are involved in tapetum cell wall breakdown (Mepham & Lane, 1969). Another function of the tapetum is to produce the β -1, 3-glucanase (callase) into the locule to degrade the special callose wall, which lies beneath the cellulose wall of the microsporocytes (pollen mother cells), and then to ensure the free microspores are released into the locule (Ariizumi & Toriyama, 2011).

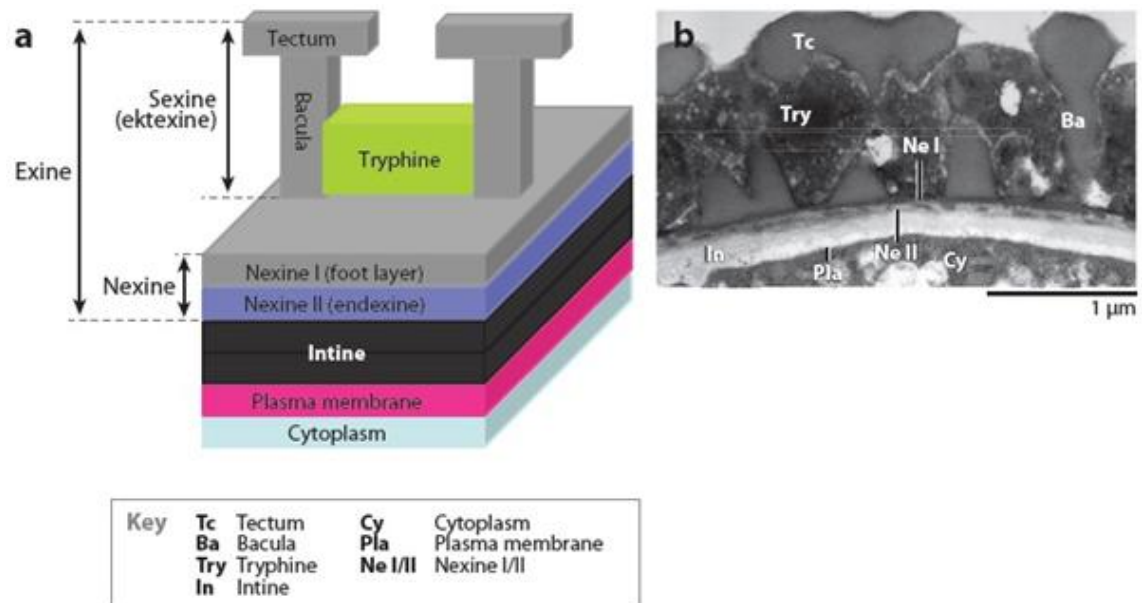


Figure 1.8 Pollen wall structure. (a) A typical angiosperm pollen grain. (b) Transmission electron micrographs of a cross-section of exine architecture in *Arabidopsis*. This diagram represents a cross-section from a nonaperture area of pollen grains (Ariizumi & Toriyama, 2011).

1.4 MALE STERILITY

Male sterility is defined as the failure of plants to produce functional anthers, pollen, male gametes, or to release pollen. Generally, there are several types of male sterility, such as absence or malformation of male organs (stamens) in bisexual plants or no male flowers in dioecious plants, failure to develop normal microsporogenous tissues in the anther, abnormal microsporogenesis in deformed or inviable pollen, abnormal pollen maturation, viable pollen but non-dehiscent anthers, also the barriers which prevent pollen reaching the ovule can lead to male sterility (Kaul, 1988).

Male sterility is classified into three types according to phenotype. 1) Structural male sterility, when the plants produce anomalies in male sex

organs. 2) Sporogenous male sterility, where stamens form successfully but rare pollen presents or even no pollen is produced due to the abortion of microsporogenous cell before, during, or after meiosis. 3) Functional male sterility, where viable pollen form but there is barriers that prevent fertilization such as anther indehiscence, inability of pollen to migrate to stigma, or pollen cannot be released. Also there are three groups classified on the basis of genotype. 1) Genic male sterility (GMS), which is caused by nuclear genes. This type of male sterility shows Mendelian inheritance. It is usually governed by a single recessive gene, but also a dominant gene can govern male sterility. 2) Cytoplasmic male sterility (CMS) is controlled by cytoplasmic genes, with mutations in the mitochondrial genome. Usually the cytoplasm of the zygote comes primarily from the egg cell and due to this progeny of such male sterile plants would always be male sterile. This type of male sterility does not show Mendelian inheritance and sterility is inherited maternally. 3) Gene-cytoplasmic Male Sterility (GCMS), when both nuclear and cytoplasmic genes are involved (Frankel, 1973, Friedlander et al., 1977, Kaul, 1988).

Male sterility is important in flowering plants for the molecular and developmental studies of stamen and evolutionary studies on the origin of dioecy, and also in its commercial application for hybrid breeding. Male sterility in crop plants is of agronomic importance because of its potential value in breeding and hybrid seed programs. Male sterile (ms) systems are also powerful tools to investigate the fundamental mechanisms involved in the development of stamens and the male gametophyte (Sawhney & Shukla, 1994).

1.5 PROGRAMMED CELL DEATH

Most cells in multicellular organisms possess an intrinsic program for cell suicide. This programme instructs the cell to eliminate itself for the overall survival of the organism (Kimchi, 2007). Over evolutionary time, the cell suicide programme is exploited for associating with the development of reproductive organisms. Many of these developmental cell deaths are genetically “programmed cell death” (PCD), often requiring the induction of specific genes to activate the cell death machinery (Williams & Dickman, 2008). PCD genetically regulated cellular suicide that is executed by the intrinsic cellular machinery, has been described in all multicellular organisms.

PCD can be part of a developmental programme (dPCD) or be triggered by environmental conditions (ePCD) (Van Durme & Nowack, 2016). In plants, dPCD is an integral part of development, and ePCD is a reaction to abiotic and biotic environmental confrontations (Lam, 2004). There are two kinds of distinct dPCD: (i) differentiation-induced PCD as the ultimate differentiation step in specific cell types, for example, in the anther tapetum layer or the root cap (Olvera-Carrillo et al., 2015) and (ii) age-induced PCD that occurs in all tissues of an organ or even the entire plant at the end of its life cycle as the last step of organ senescence (Thomas, 2013, Avila-Ospina et al., 2014). For ePCD, one of the most studied processes is the hypersensitive response (HR), which is a localized cell death that is induced by pathogen recognition (Wu et al., 2014). Another well-studied process is the formation of aerenchyma which facilitates gas diffusion within roots in waterlogged soil and the aerial environment. Several investigations, notably in maize roots, have shown that

aerenchyma formation is initiated by hypoxia and triggered by the accumulation of ethylene (Voesenek & Bailey - Serres, 2015). Other abiotic stresses such as heat, salt and oxidative stress, and UV radiation can also lead to cell death that displays as certain marks of PCD (Nawkar et al., 2013, Petrov et al., 2015).

The plant life cycle alternates between the haploid gametophytes and the diploid sporophyte (Fig. 1.10) (Van Hautegeem et al., 2015). During gametophyte development, fertilisation, and the following seed development, developmentally regulated PCD (dPCD) is crucial to determine the success of reproductive of a plant.

Van Durme and Nowack (2016) propose the following three-phase chronological progression of the molecular mechanisms involved in the control of dPCD processes in plant cells: (i) modifications of the cell fate and differentiation programme in response to an internal and/or external signal; (ii) an intracellular signal triggering PCD initiation and execution in specific cells; (iii) the breakdown of cellular compartmentalization and cell clearance processes.

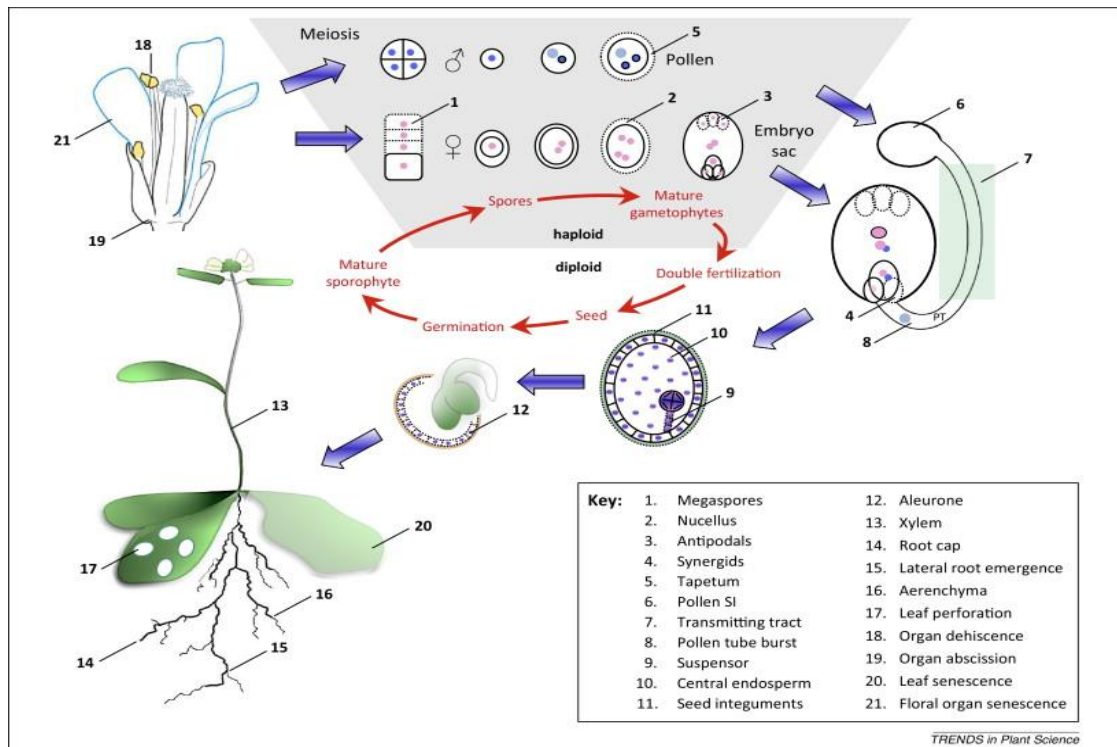


Figure 1.9 Overview of developmentally controlled cell death in plants (Van Hautegeem et al., 2015). During development of the male and female gametophytes, both gametophytic cells (e.g., synergid) and supporting sporophytic tissues (e.g., tapetum) need to undergo cell death for fertilization. After fertilization, cell death occurs in most seed tissues in the course of seed development, only the embryo proper will survive germination to form the next sporophytic generation. During vegetative development, developmentally controlled cell death occurs in the xylem of stems, leaves, and roots, in the root cap of some species, during aerenchyma formation, and as part of organ senescence. Dehiscence and abscission processes might also involve cell death events. PT, Pollen tube (Van Hautegeem et al., 2015).

During Phase (i), the PCD module of the differentiation programme is activated by several different TFs, and then the differentiated cell initiates for cell death through accumulating lytic enzymes in different specialised

compartments. In Phase (ii), signal transduction by second messengers, such as Ca^{2+} and ROS, and other unknown signalling cascades results in the initiation of cell death execution. Furthermore, the vital components of the dying cells are degraded through autophagy and the lytic enzymes that are released from various stores. In Phase (iii) tonoplast rupture and plasma membrane permeabilisation indicate cell death. In addition, the lytic processes that is initiated in Phase (ii) is completed to release enzymes to degrade the cell corpse (Van Durme & Nowack, 2016).

1.5.1 Tapetum programmed cell death

Solís et al. (2014) named and identified three main tapetum developmental stages related to tapetum PCD: “active tapetum”, “tapetum at PCD” and “tapetum at late PCD”. The “active tapetum stage” corresponded to a long stage starting with the microsporocyte at the meiotic prophase stage and finishing with the initiation of tapetum PCD. At this stage, tapetum cells were large with a rectangular shape and large rounded nuclei, with a chromatin pattern in a network of threads of different sizes; they showed a dense cytoplasm with abundant ribosomes, a feature indicative of very active cells, to accomplish both nutritive and secretory functions. Later in development, at the early vacuolated microspore stage, tapetum cells showed initial features of PCD: they lost their geometrical shape and presented elongated nuclei and fragmented nucleoli. This stage was named “tapetum at PCD”. The chromatin appeared more condensed, forming irregular and large chromatin masses, the nucleus became compacted and lobulated and the nucleolus fragmented. In this stage, the high vacuolation and the very thin layer of cytoplasm present in

anther cell layers which behind the tapetum. As development progressed, at the early pollen stage, tapetum cells became degraded and began to disappear, and the nuclear remnants displayed much smaller size and a lobular or elongated shape with highly condensed chromatin. This stage was selected and named “tapetum at late PCD”. The shapes and organization of tapetal cells was irregular, while massive ribosome and transcript degradation occurred at this stage. Anther cell layers behind the tapetum were highly vacuolated at this stage. (Solís et al., 2014)

Precise timing of tapetum degeneration is crucial for pollen maturation (Gomez et al., 2015), GA-regulated myeloblastosis (GAMYB) are TFs in rice and *Arabidopsis thaliana* that regulate tapetum differentiation and dPCD with Gibberellic acid (GA) (Plackett et al., 2011). The microRNA *mirR159*, which is GA regulated in *Arabidopsis thaliana* but GA independent in rice, represses the GAMYBs post-transcriptionally (Tsuji et al., 2006, Alonso-Peral et al., 2010, He et al., 2015). There are several TFs that control tapetum differentiation and PCD in *Arabidopsis thaliana*, including *aborted microspores (ams)* (Sorensen et al., 2003), *dysfunctional tapetum 1 (dvt1)* (Feng et al., 2012), *defective in tapetal development and function 1 (tdf1)* (Zhu et al., 2008), and *male sterility 1 (ms1)* (Vizcay-Barrena & Wilson, 2006), display delayed tapetum PCD and pollen abortion. Conversely, mutation of *MYB80* leads to precocious tapetum degeneration in *Arabidopsis thaliana* and other species (Phan et al., 2012, Xu et al., 2014b). Few downstream TF targets that control PCD initiation and execution are known. The PCD-inhibiting aspartic protease UNDEAD is activated by *MYB80* in *Arabidopsis thaliana* (Phan et al., 2011). On the contrary, *CYSTEINE ENDOPEPTIDASE 1 (CEP1)* is indirectly

repressed by *MYB80* and promotes tapetal PCD (Zhang et al., 2014). Tapetal TFs also regulate the *ROS-producing enzyme RESPIRATORY BURST OXIDASE HOMOLOG E (RBOHE)*, which is antagonistically regulated by *AMS* and *MYB80*. Loss of function of *RBOHE* results in delayed tapetal PCD but gain of function of *RBOHE* leads to tapetal PCD occur precociously (Xie et al., 2014).

1.6 AIMS AND OBJECTIVES OF THE PROJECT

The main aim of this project is to analyse the impact of high temperature on pollen development and analyse male sterile mutant gene role during tapetum PCD, and then to establish a bioinformatics database for transcriptomic analysis.

1. Phenotype analysis of Arabidopsis pollen and reproductive development with and without HT-stress. (Chapter 3)
2. Expression and function analysis of high temperature inducible genes during pollen development under HT-stress condition. (Chapter 4)
3. Transcriptomic analysis of HT inducible genes by RNA-seq. (Chapter 5)
4. Regulation and relationship between male sterile genes and PCD genes, and HT-stress influence on PCD related genes during pollen development. (Chapter 6)

CHAPTER 2

MATERIALS AND METHODS

CHAPTER 2. MATERIALS AND METHODS

2.1 PLANT MATERIALS AND GROWTH CONDITION

Arabidopsis thaliana wild type genotype Col and Ler, and mutants *ms1*, *ams*, *myb26*, *dyt1* and *tdf1*, and all T-DNA insertion mutants (See Table 4.1 for detailed list) were obtained from Nottingham Arabidopsis Stock Centre (NASC). Four PCD-GFP transcriptional fusion lines [*APR1* (At4G04610), *BFN1* (At1G11190), *CEP1* (At5G50260), and *SAG12* (At5G45890)] were obtained from Nowack's lab. All seeds mentioned above were sown on Levington M3 and placed in the growth room. The plants were grown under the following conditions: 16h of light ($180\pm 20\mu\text{mol}\cdot\text{m}^{-2}\cdot\text{sec}^{-1}$) at $20\pm 2^\circ\text{C}$ and 8hr dark at 18°C .

2.2 HIGH TEMPERATURE (HT) STRESS

To identify the HT-stress effect on pollen development and plant morphological change, the *Arabidopsis* plants, including wild-type (WT) (Col and Ler ecotypes), T-DNA insertion mutants, and PCD-GFP lines were stressed with high temperature at 30-day-old stage, which was at the point where they had established flowering and produced 3 siliques. All of the opened and semi-opened flowers on the main shoot were removed prior to HT stress, as well as the siliques on the main shoot. The humidity in the incubator was kept between 60%-70%. The plants were treated at 32°C for 2 days with continuous light. The control plants were moved to another growth chamber which had same condition as the HT treated samples but with a temperature of 22°C . Both of the HT-stressed group and non-stressed group

plants were moved back to glasshouse after the 2 days treatment for recovery. Buds were dissected and separated in different groups according to their relative position within the inflorescence. During the HT stress period, samples were collected at four different time points, D1 (1 day in treated in HT), D2 (2 days treated in HT), R1 (1 day recovery after HT), and R2 (2 days recovery after HT).

2.3 DAPI (4', 6-DIAMIDINO-2-PHENYLINDOLE) STAINING

To stage pollen development, anthers were dissected from a series of flower buds onto separate microscope slides and covered with a cover slip. Then anthers were infiltrated with 1 µg/ml DAPI solution (dH₂O solvent) and 30% (v/v) glycerol, and visualized using fluorescence microscopy under ultraviolet illumination from a 100W mercury lamp.

2.4 POLLEN VITALITY STAINING AND COUNTING

Arabidopsis pollen was collected from 20 anthesis stage flowers at D1, D2, R1 and R2 time points during the HT stressing period, then stained with 2 µg/ml FDA (fluorescein diacetate) solution (BK buffer S15 MOPS solvent, Appendix I). The pollen with FDA-buffer suspension solution was mixed gently and then dropped on a slide and covered with a cover slip for observation by Leica fluorescence microscope in blue light (wavelength=495 nm). For each time point, 10 slides were observed in both HT-treated group and non-treated group, respectively. Numbers of viable and non-viable pollen were recorded.

2.5 IN VITRO POLLEN GERMINATION

Newly opened flowers were used for *in vitro* pollen germination experiments. For each experiment, 20 flowers were randomly collected from HT-stressed plants and non-stressed plants, respectively. The dehisced anthers from two randomly picked flowers were carefully dipped into the growth medium in a 3.5 cm diameter Petri Dish. The growth medium for *in vitro* pollen germination contained 5 mM MES (pH 5.8 adjusted with TRIS), 1 mM KCl, 10 mM CaCl₂, 0.8 mM MgSO₄, 1.5 mM boric acid, 1% (w/v) sucrose, 3.65% (w/v) sorbitol, and 10µg/ml myo-inositol. The medium was prepared with double-distilled water, and each plate contained 500 µl liquid growth medium. Following pollen application, the dishes were immediately transferred to a growth chamber at 25°C with 100% relative humidity (controlled with a humidifier) without light for 5 hours. The total and germinated pollen grains were counted under a light microscope. All experiments were repeated three times and six medium plates were included in each treatment for both HT-stressed and non-stressed groups. For each plate, about 500 pollen grains were counted for calculation of germination percentage (Fan et al., 2001).

2.6 MORPHOLOGY ANALYSIS

After HT-stress the *Arabidopsis* plants were recovered in a growth room (22° C, 16h light) for two weeks, and then the siliques on the main shoot were measured from bottom to top in growth succession. Simultaneously, the seed number in the siliques was counted. Six plants in both HT-stressed and non-stressed groups were selected randomly.

To evaluate the HT-stress effect on plant development, ANOVA and *t*-test statistical analysis was applied to different factors. Average silique length and seed number of all samples indicated the overall change with and without HT-stress, and average silique length and seed number of each position reflected the trend of intensity of HT-stress on different pollen developmental stages.

2.7 SEED STERILISATION AND GERMINATION

The siliques on the main shoot were harvested once they had turned completely brown from HT-stressed and non-stressed group plants. Seeds were allowed to dry in paper seed bags for at least three days and were surface sterilized with ethanol before sowing. The seeds were placed in a 1.5 ml microfuge tube and 1 ml 70% (v/v) ethanol added, they were vortexed thoroughly for a few seconds, and ethanol removed. Another 1 ml of 70% (v/v) ethanol was added and left for 10 minutes, shaking the tube occasionally to ensure all seeds and all parts of the tube came into contact with the ethanol. Tubes were then centrifuged to pellet the seeds at 3000 RPM. Ethanol supernatant was removed in a sterile laminar flow cabinet. 0.5 ml absolute ethanol was added to the tube, the seeds were mixed for no more than a few seconds and then tipped onto a sterile piece of filter paper to allow the ethanol to evaporate entirely. When dried, seeds were sown on half-strength MS media (Appendix I) in Petri dishes (9 cm diameter). Seeds sown on plates were treated in dark room at 4°C for 24h. After the treatments, seeds were immediately placed in growth room at 22°C with 24h light. Germination frequencies were measured 7d after growing in growth room. 50 seeds were sown on each plate with enough space between them, and ten plates were

included in each experiment. The experiments were repeated three times. Numbers of germinated and non-germinated seeds was recorded.

2.8 RNA EXTRACTION

Total RNA was extracted using the RNeasy Plant Mini Kit (Qiagen, UK) following the manufacturer's protocol. DNase treatment was carried out to eliminate DNA contamination. RNA (60 µl) samples were eluted from the RNeasy column and were mixed with 1 µl RNase inhibitor (40 u/µl, Promega, USA), 5 µl RQ1 (RNA-Qualified) RNase-free DNase (1 u/µl, Promega, USA), RQ1 10 X reaction buffer (Promega, USA), and 24 µl distilled water, and then incubated at 37°C for 45 min. RNA was subsequently purified using the RNeasy Plant Mini Kit. RNA quality and quantity were tested on a NanoDrop fluorospectrometer. RNA samples were stored at -80°C.

2.9 PRIMER DESIGN

Primers were designed using Primer5 software (www.PrimerBiosoft.com, Version 5.0). Conditions were specific for individual products. Each pair of primers was tested using SnapGene[®] Viewer (www.snapgene.com, version 2.3.5) and primer BLAST analysis to confirm their specificity.

2.10 PCR PROCEDURE

PCR reactions were performed in 10 µl and comprised the following reagents: 4.5 µl 2xRed Taq[®] Ready Mix[®] (VWR[®], USA), 0.25 µl of each primer (10 µM), 0.5 µl DNA/cDNA template and molecular grade distilled water to make up to

10 μ l. The annealing temperature depended on the primer set and ranged from 55°C to 60°C. The PCR reaction programme is shown in Table 2.1.

Table 2.1 PCR programme

Cycles	Duration of cycle	Temperature
1	3 min	94°C
25-35	30 sec	94 °C
	30 sec	Tm ^a
	30 sec – 1 min ^b	72 °C
1	10 min	72 °C

^a An appropriate annealing temperature was chosen depending on the primers used. ^b An appropriate duration for extension was chosen for the target size amplified: 1 min for less than 2kb, 30 sec for less than 500bp.

Electrophoresis was carried out after PCR to check the size and/or amount of the products. PCR products were run in agarose gels (Sigma, USA, ranging from 1%-2% [w/v] depending on DNA size) at 100 V in 0.5X TBE (Appendix I) and visualised by ethidium bromide staining. Size of the PCR products was determined using a HyperLadder I (Bioline, USA) marker (unless otherwise stated).

2.11 cDNA SYNTHESIS

cDNA was synthesized from total RNA with following components in nuclease free microcentrifuge tubes: 2 μ g RNA depending on the extracted RNA concentration to uniform all of the experiments, 1 μ l of Oligodt (0.5 μ g/ μ l, Invitrogen, USA), 1 μ l of dNTP (10 mM, Bioline, USA), and ddH₂O to a total volume of 13 μ l. This mixture was incubated at 65°C for 5 mins then quickly moved onto ice to stop the reaction. Then 1 μ l of dTT (0.1 M), 1 μ l of RNAaseOUT recombinant RNase inhibitor, 1 μ l of Superscript III (2200 u/ μ l,

Invitrogen, USA) and 4 µl of 5× First-Strand buffer were added and incubated at 50°C for 1 hour, and subsequently to inactivate the reaction by heating at 70°C for 15 mins. The cDNA was used as a template for PCR or quantitative RT-PCR (qRT-PCR) analysis. cDNA samples were stored at -20°C.

2.12 ACTIN AMPLIFICATION AND NORMALIZATION

The house-keeping ACTIN transcripts were amplified from cDNA templates (primers ACTIN7F and ACTIN7R, primer sequences in Appendix II) to determine the initial quantity of the cDNA templates. Comparisons between extent of amplification and band intensity were used to confirm that initial template levels were equivalent between samples and that cDNA synthesis had been successful.

2.13 QUANTITATIVE PCR

Quantitative gene expression analysis was performed using the fluorescent dye SYBR[®] Green I (provided in the Maxima[®] SYBR[®] Green/ROX qPCR Master Kit, Fermentas). The dye exhibits minimal fluorescence in the unbound state; the fluorescence is detectable when bound non-specifically to double-stranded DNA. As PCR products accumulate during amplification, the fluorescence from SYBR[®] Green increases, making it possible for the detection of product accumulation in real-time.

QPCR was performed using the LightCycler[®] 480 Real-Time PCR system (Roche Applied Science). LightCycler[®] 480 was used to operate the machine and analyse the data. All reagents were provided in a Maxima[®] SYBR[®] Green/ROX qPCR Master Kit (Fermentas, USA), except primers and

templates. The experimental reaction comprised 4.5 µl 2x master mix (provided in the kit), 0.1 µl of each primer (10 µM), 0.2 µl cDNA template and nuclease-free water to adjust the final volume to 10 µl. All samples were run at least in three replicates.

The standard program for running the plate on the LightCycler was: 95°C 10 min; 45x (95°C 30 sec, T_m, 30 sec, 72°C for 1 min); 72°C 6 min. Annealing temperature (T_m) was chosen for each primer separately.

2.14 MICROSCOPY

2.14.1 Confocal microscopy

Confocal microscopy was used to screen the GFP fluorescence in whole anthers. Experimental samples were imaged on a Leica SP2 confocal laser scanning microscope (Leica Microsystems). The microscope is equipped with the Leica confocal software (Leica Confocal Software V2.61 Build 1537); the Argon Laser was used at 488 nM and 514 nM to view fluorescence of GFP and YFP, respectively. Images were processed using the Leica SP2 Image Analysis software. During experiments, two channels for GFP fluorescence and background were set to 400, and gain value was 4.00.

2.14.2 Fluorescence Microscopy

Fluorescence microscopy was used in this project to stage pollen development by staining pollen nuclei with 4',6-diamidino-2-phenylindole (DAPI). Fluorescence was visualised using fluorescence microscopy under ultraviolet illumination from a 100W mercury lamp. Anthers were visualised on

a Leica DM5000B microscope, using ultraviolet illumination. A Leica camera Df320 was used to capture images and processed using the software of Leica Application Suite V3.3.0.

CHAPTER 3

IMPACTS OF HIGH TEMPERATURE STRESS DURING POLLEN DEVELOPMENT

CHAPTER 3. IMPACTS OF HIGH TEMPERATURE STRESS DURING POLLEN DEVELOPMENT

3.1 INTRODUCTION

There are several impacts of high temperature on plant growth which have been referred to in section 1.1. The reduction of fertility caused by high temperature is an important and serious impact causing decreases in crop yields. Plants are highly sensitive to high temperature during reproductive development (Endo et al., 2009, Oshino et al., 2011). Hasanuzzaman et al. (2013) summarised some commonly used transgenes and their functions for making heat stress tolerant transgenic plants (Table 3.1).

High temperature environment may lead to various physiological injuries in plant growth, such as scorching of stems and leaves, leaf senescence and abscission, root and shoot growth inhibition, and fruit damage that leads to a decreasing of plant productivity (Vollenweider & Gunthardt-Goerg, 2006). Plants exposed to high temperature conditions also present a set of cellular and metabolic characteristic responses, which include the variations of the organization of cellular structures and the functions of membrane (Weis & Berry, 1988), and decreasing in the synthesis of normal proteins and the accelerating of transcription and translation of heat shock proteins (HSPs) (Bray EA, 2000), as well as the production of phytohormones such as abscisic acid (ABA) and antioxidants and other protective molecules (Maestri et al., 2002).

Table 3.1 List of transgenic plants, heat stress linked transgenes and their role in enhancing plants towards stress tolerance (Hasanuzzaman et al., 2013).

Transgenic plants	Transgenes	Function of transgenes	Reference
<i>A. thaliana</i>	<i>Hsp70</i>	HSP synthesis for thermotolerance	(Montero-Barrientos et al., 2010)
<i>A. thaliana</i>	<i>AtHSF1</i>	Heat shock transcription factor HSF1::GUS (β -glucuronidase) fusion and such modification will increase HSP production in large scale with small investment of HSFs	(Lee et al., 1995)
<i>A. thaliana</i>	<i>gusA</i>	β -glucuronidase synthesis and bind with HSFs to form active trimer	(Lee et al., 1995)
<i>A. thaliana</i>	<i>CodA</i> (choline oxidase A) from <i>A. globiformis</i>	Glycine betaine synthesis for tolerance to HT during imbibition and seedling germination	(Alia et al., 1998)
<i>A. thaliana</i>	Ascorbate peroxidase (<i>APX1</i> from <i>P. sativum</i> and <i>HvAPX1</i> from <i>H. vulgare</i>)	H ₂ O ₂ detoxification and conferred heat tolerance	(Shi et al., 2001)
<i>Daucus carota</i>	<i>Hsp17.7</i> from <i>D. carota</i>	Synthesis of sHsp	(Murakami et al., 2004)
<i>N. tabacum</i>	<i>Fad7</i> from <i>N. tabacum</i> and <i>O. sativa</i>	Desaturation of fatty acids (trienoic fatty acids and hexa-decatrienoic acid) that increased the level of unsaturated fatty acids and provide HT tolerance	(Sohn & Back, 2007)
<i>N. tabacum</i>	<i>TLHS1</i>	Synthesis of sHSP (Class I)	(Park & Hong, 2002)
<i>N. tabacum</i>	<i>MT-sHSP</i> from <i>L. esculentum</i>	Molecular chaperone function <i>in vitro</i>	(Sanmiya et al., 2004)
<i>N. tabacum</i>	<i>Dnak1</i> from <i>Aphanotheca halophytica</i>	High temperature tolerance	(Ono et al., 2001)
<i>N. tabacum</i>	<i>BADH</i> (betain aldehyde dehydrogenase) from <i>Spinacia oleracea</i>	Over production of GB osmolyte that will enhance the heat tolerance	(Yang et al., 2005)
<i>N. tabacum</i>	<i>ANP1/NPK1</i>	H ₂ O ₂ responsive MAPK kinase (MAPKKK) production to protect against the lethality in HT	(Kovtun et al., 2000)
<i>Z. mays</i> and <i>O. sativa</i>	<i>Hsp100, Hsp101</i> from <i>A. thaliana</i>	HSP synthesis for HT tolerance	(Queitsch et al., 2000, Katiyar-Agarwal et al., 2003)

A complicated set of sensors, which locate in various cellular compartments, is used to sense the variations of environment temperature by plants, for example, the increased fluidity of the membrane leads to a activation of lipid-based signalling cascades and an increasing Ca^{2+} influx and cytoskeletal reorganization (Saidi et al., 2009). Recent reports also indicate that the differences in the tissue-specific activation of various signalling pathways may occur between vegetative and reproductive tissues (Mittler et al., 2011).

High temperature induces several variations in respiration and photosynthesis and may also results in a shortened life cycle and damage of plant productivity (Barnabas et al., 2008). Plant biosynthesis and compartmentalization of metabolites, is also disturbed in these HT-stressed plant tissues (Maestri et al., 2002), such as the sucrose synthesis, , starch accumulation, and activities of carbon metabolism enzymes (Ruan et al., 2010).

The level of several key phytohormones increase under HT stress, such as salicylic acid (SA), ethylene (ET), and ABA , while others such as auxin (AUX), gibberellic acids (GAs), and cytokinin (CK), decrease. These fluctuations ultimately cause plant premature senescence (Talanova et al., 2003, Larkindale & Huang, 2004, Larkindale et al., 2005). HT stress also results in the denaturation of existing proteins and the mis-folding of newly synthesized proteins (Nover et al., 2001).

3.1.1 High temperature injury in barley and rice plants organ formation

High temperature influences plant development and cellular morphology. According to Sakata and Higashitani (2008), exposure of barley plants to high temperatures (30°C day/25°C night) for 5 days at the 4-leaf stage resulted in

an observation of typical damage being lack of cytoplasm during pollen grain development. Another type of damage occurs 5 days after HT-stress that between the early stages of panicle differentiation and PMC meiosis (the 5-leaf stage), which then results in the completely lack pollen grains in the anthers at the heading stage. The last type of damage caused by HT-stress leads to the formation of abnormal and immature microspores that do not accumulate starch in the meiotic stage of PMCs (the 6- to 7-leaf stage).

High temperature also causes cytological injury in barley plant. Barley that exposed in high temperatures at the 5-leaf stage (2–3 mm panicles) results in the complete abortion of organ development, and also the differentiation of PMCs and tapetum cells (Sakata et al., 2000, Abiko et al., 2005). HT-stress at the 4-leaf stage and the following meiotic stage of PMCs (the six- to seven-leaf stages) leads to the anther wall cells exhibit increased vacuolization and over-development of chloroplasts (Sakata & Higashitani, 2008). In PMCs, meiotic prophase chromosomes show premature synapses and nuclear membranes are partially disrupted. There are irregular rough endoplasmic reticulum (RER), abnormal swelling of mitochondria and premature degradation of tapetum cells exist in the anther wall cells of 15 mm size panicles (Sakata & Higashitani, 2008). In addition, nuclear density of microsporocytes significantly reduced in the 15–20 mm size panicles under HT-stress (Sakata & Higashitani, 2008). These results indicate clearly that HT-stress causes male tissue-specific arrest of cell proliferation at either the 4- or 5-leaf stage.

In non-stressed conditions, the mitotic index of anther wall cells reduces

gradually in 5, 10 and 15 mm size panicles. Division of sporogenous cells occurs frequently in 5 and 10 mm size panicles, but division significantly decreases in 15 mm size panicles, as the cells proceed into meiotic prophase (Oshino et al., 2007). On the contrary, HT-stress results in a serious reduction in the mitotic index of anther wall cells and primary sporogenous cells (Sakata & Higashitani, 2008). Few premature PMCs are found to be dividing in 10 mm panicles, as well as anther wall cells in 15 mm size panicles (Sakata & Higashitani, 2008). In contrast, ovule cell division is observed in both of HT-stressed and non-stressed samples (Oshino et al., 2007).

Similar injuries have also been revealed in rice plants. Early research indicates HT induces sterility during rice flower development. Endo et al. (2009) reported that the spikelet fertility was completely lost at microspore stage when the rice plants were exposed to temperatures of 39°C in the daytime and 30°C at night for 7d. Further results revealed that the pollen viability of each spikelet was decreased and also the pollen germination on the stigma. To investigate the effects of HT stress on the pistil, the pollen from non-HT treated plants was introgressed into HT-treated plants as female parents. The results showed the pollen from untreated plants could germinate on the HT treated pistil, which suggested that high temperatures at the microspore stage did not damage the ability of the pistil to receive pollen by the stigma, but impaired the ability of pollen to attach and/or germinated on the stigma (Endo et al., 2009).

3.1.2 High temperature effects on *Arabidopsis thaliana* and auxin recovery

High temperature also leads to male sterility in *Arabidopsis*. Sakata et al. (2010)

reported that cell-proliferation is arrested, vacuoles are distended, chloroplast development is altered, and mitochondrial abnormalities occur in *Arabidopsis* anthers developing under high temperature.

Previous research on *Arabidopsis thaliana* injury by high temperature stress was shown a reduction of silique length and seed number (Suzuki et al., 2013). However, a deficiency in the *ascorbate peroxidase 2 (APX2)* gene leads to a more high temperature sensitive seedling stage of plants, but more high temperature tolerance at the reproductive stage. In their experiment, *apx2 Arabidopsis* plants showed longer siliques and a higher number of seeds per silique compared to the other lines in response to the 42°C treatment, but presented a significantly smaller plant diameter compared to wild type samples with this kind of HT-stress (Suzuki et al., 2013).

Alternatively, Sakata et al. (2010) have reported sterility caused by high temperature stress which was displayed as repressed pollen maturation and filament elongation. *Arabidopsis* plants formed short stamens and rarely produced any pollen under high temperature, and then produced sterile plants (Sakata et al., 2010). This sterility could be recovered partly by applying exogenous auxin such as IAA/NAA when plants were treated in the high temperature environment. Different types and concentration of auxin were used on *Arabidopsis* and also barley plants. As a result, the filament elongation in *Arabidopsis* plants was rescued after the auxin IAA/NAA treatment, and the auxin restored stamen length of mature flowers in a dose-dependent manner. In their experiment, auxin recovery appeared in barley plants as well. With auxin application during HT stressing period, anther length and pollen viability

in barley plants exhibited obviously recovery. As with the auxin effect in *Arabidopsis*, all auxin application in barley also restored anther length in a dose-dependent manner at the heading stage (Sakata et al., 2010).

In summary, high temperatures negatively affect various biological processes, such as tapetum degeneration and pollination, which then results in defect of plant growth and development. Pollen developmental stages are sensitive to high temperature stress, which would lead to male sterility during pollen development. In this chapter, the establishment of an efficient HT-stress system for affecting pollen development is described as well as experiment to find out the HT sensitive stages during pollen development, and then to verify the morphological changes during pollen development under HT-stress.

3.2 MATERIALS AND METHODS

3.2.1 Plant growth and staging

Seeds of *Arabidopsis thaliana* genotype Ler were obtained from Nottingham *Arabidopsis* Stock Centre (NASC). The seeds were sown on Levington M3 in 9 cm pots and insured 4 plants grow in each pot. For growth conditions see section 2.1.

3.2.2 High temperature stress

The 30-day-old *Arabidopsis* plants (Ler) seedlings were stressed with high temperature (see Section 2.2). All of the opened and semi-opened flowers on the main shoot were removed prior to HT stress, as well as the siliques on the main shoot. HT-stress treatment and bud samples were collected as mentioned in section 2.2. Samples were frozen in liquid nitrogen and stored at

-80° C.

3.2.3 Bud positions in inflorescence and pollen developmental stages

DAPI staining was applied to identify the stages of pollen development with the position of each bud in the inflorescence. DAPI staining protocol was described in section 2.3. The bud was labelled as “1” for the oldest one in the inflorescence, and then counted to the younger ones in numerical order (Fig. 3.1).

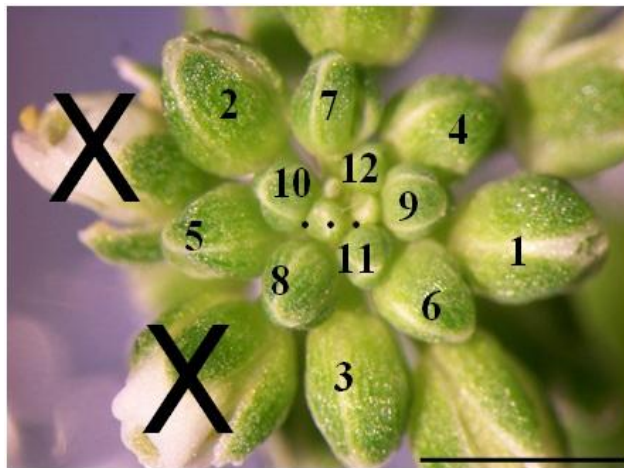


Figure 3.1 *Arabidopsis* inflorescence.

Helical arrangement of buds, each bud has been numbered according to its position within the inflorescence. Bar: 2.5mm. (PhD thesis of Dr. GemaVizcay-Barrena)

3.2.4 Pollen developmental alteration under HT-stress

To find out the impacts of HT-stress on pollen development, pollen viability and *in vitro* pollen germination, analyses were applied according to section 2.4 and 2.5, respectively.

3.2.5 Morphological analysis and seed viability

The *Arabidopsis* plants were recovered in a growth room for two weeks, and then 30 siliques on the main shoot were measured from bottom to top in growth succession. Simultaneously, the seed number in the siliques was

counted for the same sequence. Six plants in both HT-stressed and non-stressed groups were selected randomly.

Seed germination tests were also carried out as section 2.7. Data were analysed and statistical analyses were performed using GraphPad Prism 6.

3.3 RESULTS AND DISCUSSION

3.3.1 Identification of pollen samples developmental stages

To determine the developmental stage, bud samples on the main shoot of *Arabidopsis* Ler plants were infiltrated using DAPI solution before HT-stress. The bud samples were labelled from the oldest to youngest in numerical order, and the numerical label of bud position in each inflorescence is shown in Fig 3.1. In the experiment, 20 buds from each inflorescence were observed, and six inflorescences on the main shoot were selected randomly from *Arabidopsis* Ler plants. Briefly the relationship between bud position in each inflorescence and the developmental stage was: 1-2, mature pollen stage; 3-4, tricellular stage; 5-6, bicellular stage; 7-8, polarized microspore stage; 9-12, free microspore stage; 13-14, tetrad stage; 15-20, PMCs (Fig 3.2). The position of each bud was also linked with flower, anther and pollen developmental stages in Table 3.2 according to previous results (Regan & Moffatt, 1990, Sanders et al., 1999, Smyth et al., 1990)

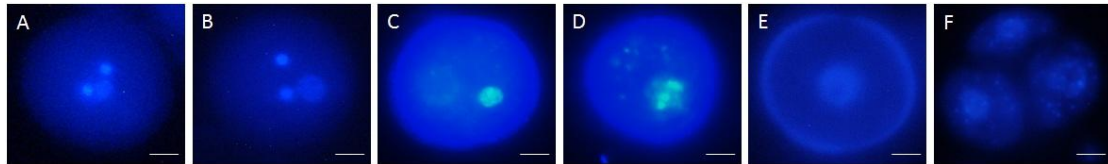


Figure 3.2 Pollen stage by DAPI staining. A, mature pollen stage; B, tricellular stage; C, bicellular stage; D, polarized microspore stage; E, free microspore stage; F, tetrad stage. Bar: 10 μ m.

3.3.2 HT-stress effect on flower and pollen development

3.3.2.1 Flower structure after HT-stress

Previous research by Sakata et al. (2010) had indicated the filament length of *Arabidopsis* plant flower was suppressed with 7d HT treatment at 32°C with 16h light period. However, the results here showed that 2d HT-stress at 32°C with 24h light period caused significant flower defects. The filament in a fully opened flower at anthesis after 2d HT-stress was shorter compared with the non-stressed anthers (Fig. 3.3). Twenty filaments from ten randomly selected flowers were measured from both non-stressed and HT-stressed plants, and the average filament length of HT-stressed plants was significantly shorter than that of non-stressed plants. (Fig. 3.4)

Table 3.2 Pollen development in *Ler* flower buds. (a) Flower developmental stages taken from Smyth et al. (1990). (b) Anther developmental stages taken from Sanders et al. (1999). (c) Pollen developmental stages taken from Regan and Moffatt (1990).

Bud position	Pollen development stage	Flower stage (a)	Anther stage (b)	Pollen Stage (c)
1	Bilocular anther containing tricellular	13	13	10
2				
3				
4				
5	Pollen mitosis I&II. Tapetum has degenerated. Septum cell degeneration initiated. Stomium differentiation begins. Septum breakage.	11-12	12	8-9
6			11	
7	Tapetum degeneration. Late ring stage.	10	10	6-7
8				
9	Ring stage. Exine wall formation.	10	9	5
10				
11				
12				
12	Microspores free with the locule.	10	8	5
13	Tetrads of microspores free within anther locule.		7	4
14	PMC meiosis.		6	
15	PMC appear.		9	5
16				



Figure 3.3 *Arabidopsis* flower structure after HT-stress. A. Flower from non-stressed plant; B. Flower from 2 days HT-stressed plant. Bar: 200 μ m.

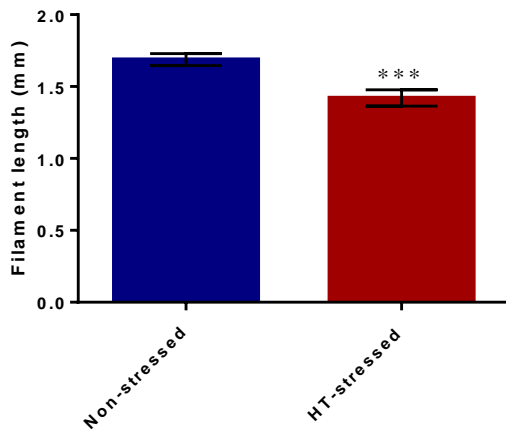


Figure 3.4 Filament length (stamen without anther) data of non-stressed and 2 days HT-stressed *Arabidopsis* plants. Error bars: standard error. n=20. *** Significant different from Non-stressed by *t*-test. *p* value < 0.001.

3.3.2.2 Pollen viability analysis

FDA staining results revealed that the pollen viability decreased most significantly after 1 day HT stress, and the decreased viability showed

recovery as time went on. Moreover, the plants produced 3-4 flowers every day, which meant that the pollen which was collected at D1 time point had mostly come from mature pollen stage and tricellular stage, D2 was collected from bicellular and polarized microspore stages, R1 was from free micospore and tetrad stages, and R2 was from PMCs and younger. According to these results, it could make a hypothesis that the pollen would be affected at late stages (mature pollen stage and tricellular stage), but seems be protected at the earlier stages. (Fig. 3.5)

Meanwhile, pollen which was collected during the HT-stress was cultured *in vitro* to test the percentage germination (Fig. 3.6). The result showed a similar change as seen for pollen viability, which also indicated the defect of pollen at late stages.

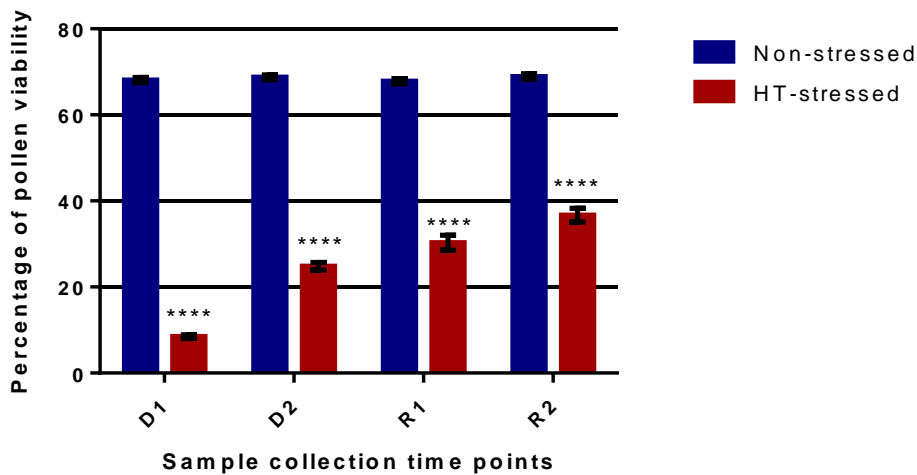


Figure 3.5 Pollen viability rate by FDA staining. Pollen which was collected at D1 was the oldest in the inflorescence before HT-stress, and D2, R1, R2 were younger successively. Error bar: standard error. **** Significant different from Non-stressed by ANOVA. *p* value < 0.0001.

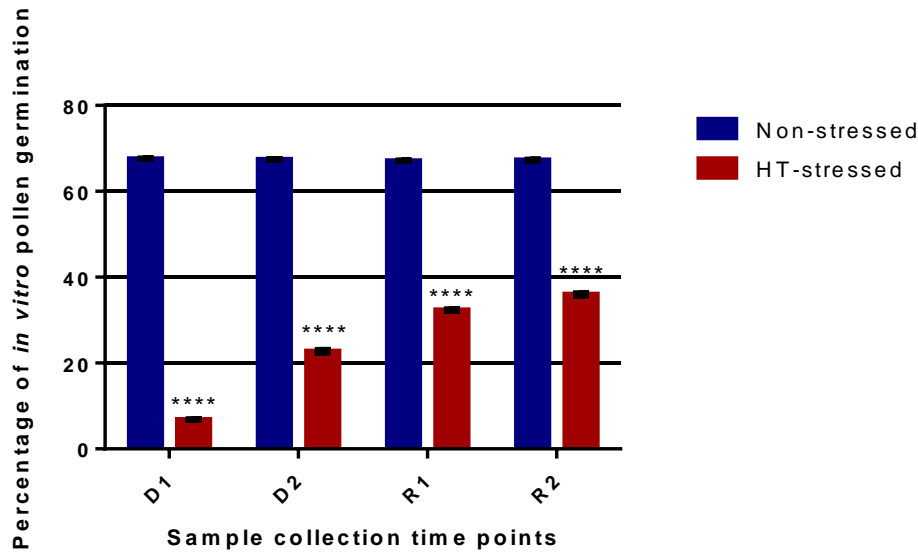


Figure 3.6 *In vitro* pollen germination rates. Pollen which was collected at D1 was the oldest in the inflorescence before HT-stress, and D2, R1, R2 were younger successively. Error bar: standard error. **** Significant different from Non-stressed by ANOVA. p value < 0.0001.

3.3.2.3 Plant developmental analysis

Previous studies suggested that the HT-stressed pistil could still receive pollen but the stigma and the pollination process would not be impacted if the pollen was viable (Sakata & Higashitani, 2008). Therefore, the reproductive developmental status of silique length and seed number could indicate the impacts of HT-stress on pollen development. To investigate the HT-stress effect on pollen development after pollination, the HT-stressed and non-stressed plants were used to analyse the silique growth status and seed production in the seed pot.

As mentioned previously, all of the siliques, open and about to open flowers on the main shoot were discarded before the start of the HT-stress experiment.

This ensured that all the siliques were produced during and after HT-stress. Furthermore, according to the DAPI staining results the oldest bud in the inflorescence was at the mature pollen stage when the HT-stress began. After two weeks recovery in the glasshouse, silique length on the main shoot was measured and the seed number in the silique counted. For this experiment, 30 siliques on the main shoot were used from each *Arabidopsis* plant, and six plants were selected randomly for each replicate. The results are shown in Fig. 3.7 and 3.8. These revealed that the average silique length of all HT-stressed samples was significantly shorter than the non-stressed ones, and also the seed number in corresponding siliques was significantly reduced between the non-stressed samples and HT-stressed samples. These results indicate that silique development is significantly repressed after HT-stress, as well as seed production.

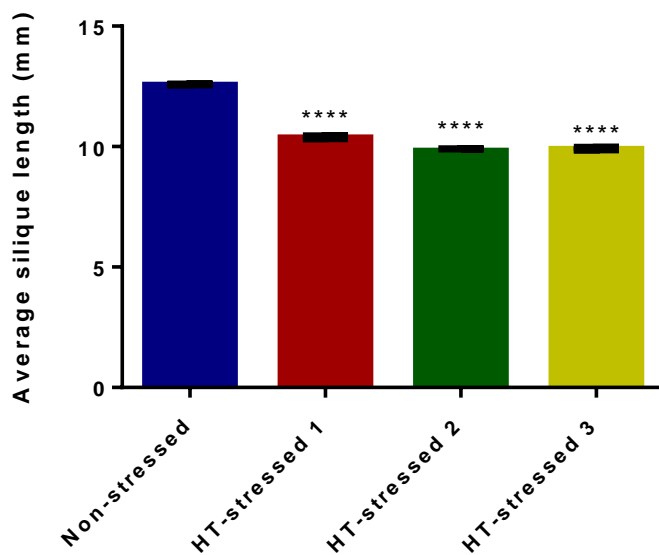


Figure 3.7 Average silique lengths of all samples. HT-stressed 1, 2, and 3 indicate three replicates of HT-stress experiments. Bars mean the average of silique length of all measured samples. Error bar: standard error. **** Significant different from Non-stressed by ANOVA. p value < 0.0001 .

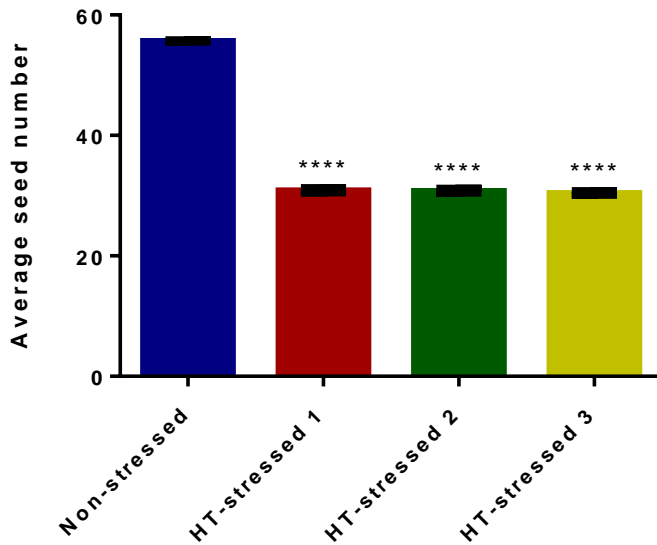


Figure 3.8 Average seed number of all samples. HT-stressed 1, 2, and 3 indicate three replicates of HT-stress experiments. Bars mean the average of seed number of all measured samples. Error bar: standard error. ****Significant different from Non-stressed by ANOVA. p value < 0.0001.

Detailed analysis was performed to compare the variation of each silique on different plant. For each HT-stress experiment, siliques, which were labelled as same numerical order, were measured the length as well as the seed numbers in the siliques. These results are shown in Fig 3.9 and 3.10. The trend lines of three replicates were very similar and display a recovery from the oldest to the youngest. In Fig. 3.9 and 3.10, the oldest siliques were the shortest ones in all of the samples measured, and had the lowest seed numbers. According to previous results of the relationship between bud positions and pollen developmental stages the trend lines here revealed that impact of HT-stress was most significant on the pollen in the late developmental stages. However, this impact was decreased in earlier pollen developmental stages which were displayed by the recovery of silique length and seed number. Furthermore,

there was no significant variation in plant height, it might indicate that the HT-stress would not effect on shoot growth or that this 2D HT-stress period was not long enough to affect it.

Detailed analysis was carried of the data between non-stressed samples and HT-stressed samples depending on pollen developmental stages. Based on my previous DAPI staining results of pollen developmental stages, the silique samples for silique length and seed number measurement were divided into four groups according to their pollen developmental stages when HT-stress experiments started: 1) "Old group" containing siliques No. 1-4, which were produced from the buds contained mature and tricellular staged pollen before HT-stress; 2) "Young group" contained siliques No. 5-8, which were produced from the buds of bicellular stage and polarized microspore stage before HT-stress; 3) "Immature group" contained siliques No. 9-14, from buds of free microspore and tetrad stages; and 4) "PMCs" included siliques No. 15-30, from all of the buds younger than tetrad stage. To evaluate the data, ANOVA was performed between the pair of non-stressed samples and each replicate of HT-stressed sample at the same stage. Silique length and seed number decreased significantly at each stage compared with the non-stressed samples at the same stages (p value < 0.0001) (Fig. 3.11 & 3.12). Further analysis was carried out to compare the difference between the pairs of each stage period in each individual HT-stress replicate. The ANOVA results also indicated the samples in different stages in each individual replicate showed a significantly increasing recovery trend, but the variation of the samples in same stages among different replicates was not significant.

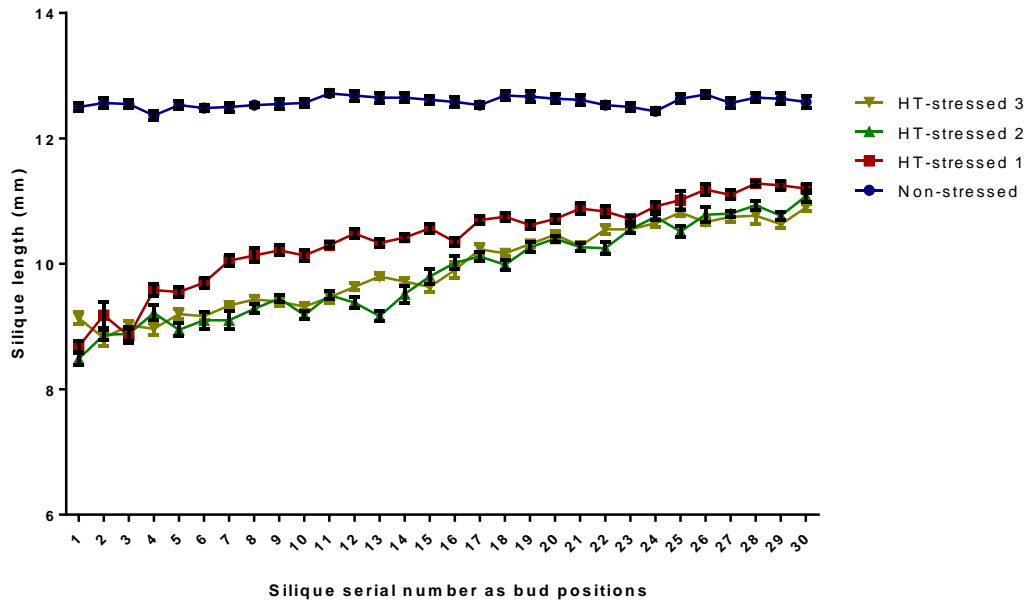


Figure 3.9 Average silique length of each position. HT-stressed 1, 2, and 3 indicate three replicates of HT-stress experiments. X axis indicates the measured siliques produced on main shoot 2 weeks after HT-stress from oldest which was labelled as “1” and the youngest which was labelled as “30”. Siliques from six plants of each replicate were measured to achieve the average length data. Error bar: standard error.

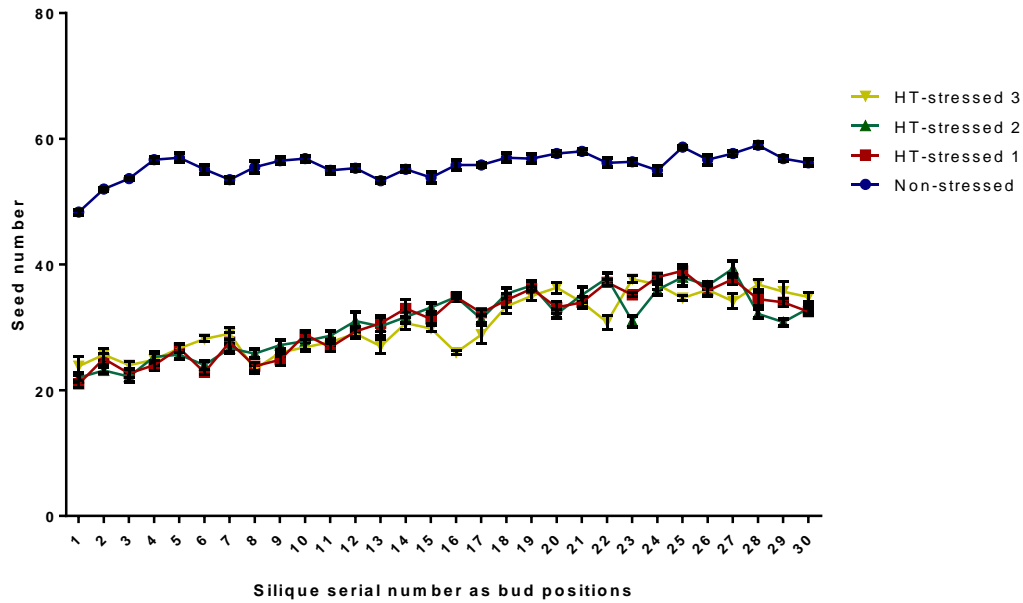


Figure 3.10 Average seed number of each position. HT-stressed 1, 2, and 3 indicate three replicates of HT-stress experiments. X axis indicates the counted seeds in the siliques that produced on main shoot 2 weeks after HT-stress from oldest which was labelled as “1” and the youngest which was labelled as “30”. Seed numbers from six plants of each replicate were counted to achieve the average data. Error bar: standard error.

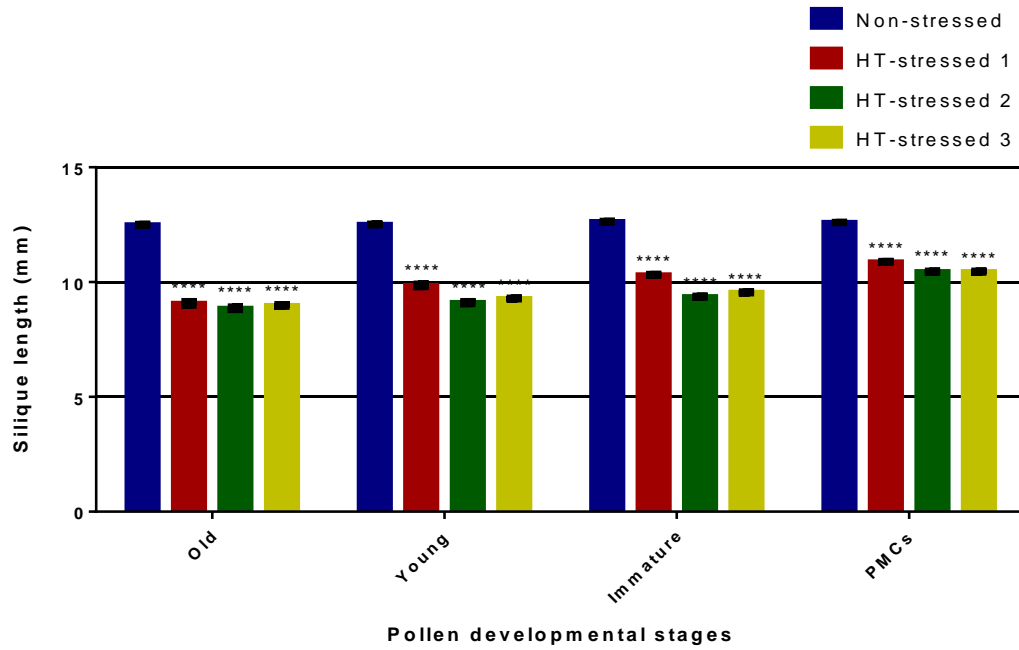


Figure 3.11 Average silique lengths at different pollen developmental stages. Pollen developmental stages (x axis) were identified according to DAPI staining results. **** Each different stage group of HT-stressed samples was significantly different from the corresponding non-stressed group by ANOVA. Error bar: standard error. p value < 0.0001.

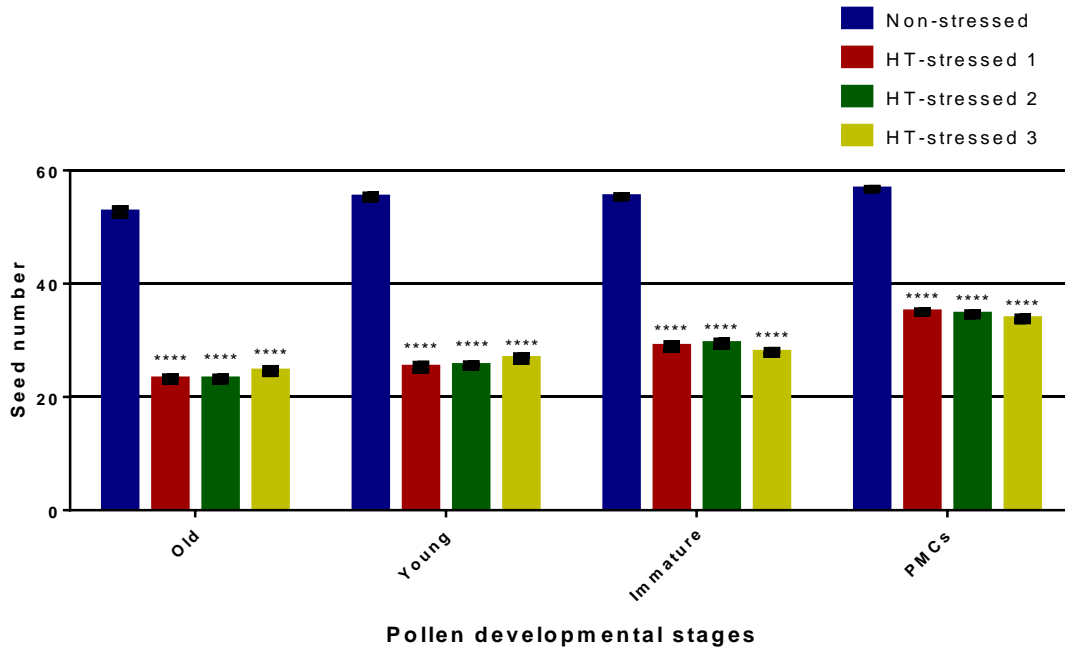


Figure 3.12 Average seed number at different pollen developmental stages. Pollen developmental stages (x axis) were identified according to DAPI staining results. **** Each different stage group of HT-stressed samples was significantly different from the corresponding non-stressed group by ANOVA. Error bar: standard error. p value < 0.0001.

3.3.2.4 Seed germination

The seeds which were harvested from both HT-stressed and non-stressed *Arabidopsis* plants were surface sterilized by the ethanol method (see section 2.7), and then they were plated on Petri dishes with half MS-agar medium (Appendix I) in a growth room for 7d. However, there was not any significant difference in germination frequency between non-stressed seeds and HT-stressed seeds. Statistical analysis by t -test between HT-stressed and non-stressed samples of each replicate revealed there was no significant difference between the two groups (p value > 0.05) (Fig. 3.13), which indicated

that HT-stress did not influence the seed production process although the pollen viability was significantly depressed.

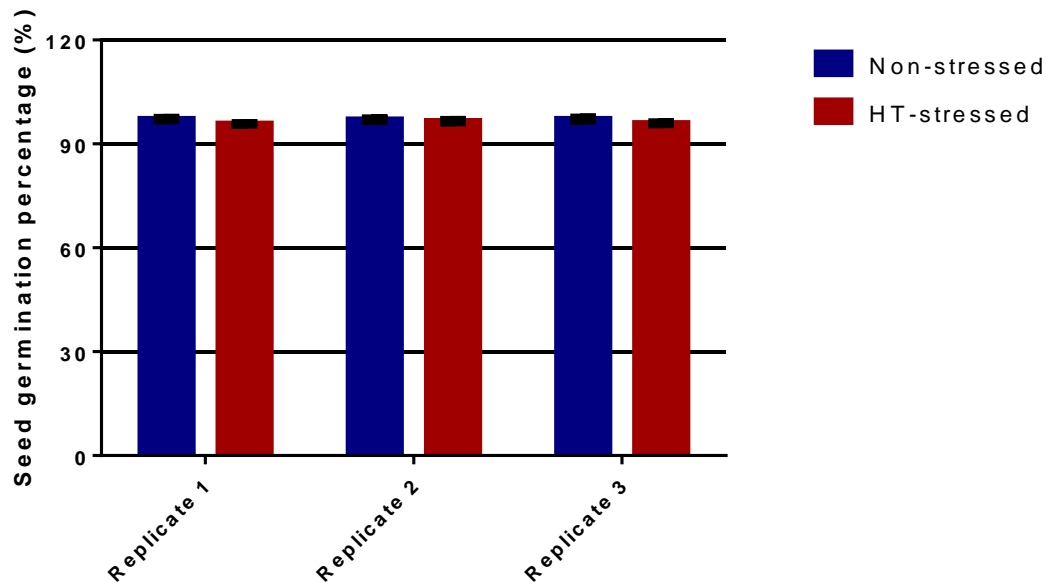


Figure 3.13 Seed germination frequency (%) harvested from non-stressed and HT-stressed *Arabidopsis* plants. Replicate 1, 2, and 3 indicate three replicates of seed germination experiment. Bars indicate average of seed germination percentages on each Petri dish. Error bar: standard error.

3.4 DISCUSSION

Previous research has indicated that the *Arabidopsis* plants would produce sterile and/or defective phenotype in HT environment (Endo et al., 2009, Oshino et al., 2011), and also revealed the HT-stress resulted in serious defects in pollen development. In this experiment, 32°C for 2 days treatment was efficient at influencing the development of 30-day old *Arabidopsis* plants, which would lead to many morphological changes in the reproductive organs. It was obvious that the filament length, silique length and seed number

decreased in HT-stressed plants. Furthermore, pollen viability and germination rates were found to reduce in the HT-stressed samples although the reduction showed a recovery trend as the HT-stress in progress. However, these results confirmed that 2 days HT-stress at 32° C could significantly repress pollen development and the following reproductive growth.

HT-stress leads to a set of negative affection on plant developmental and physiological processes. For example, sexual reproduction and flowering processes in crop plants show high sensitivity to HT-stress, which often leads to a reduction yield (Hedhly et al., 2009). However, there is no clear evidence to be able to identify HT-stress affection with different pollen developmental stages. In this experiment, detailed data such as silique length and seed number were utilised. In the HT-stressed plants, the most serious change happened in the later pollen developmental stages which reflected the lowest percentage of pollen viability and germination, and shortest silique production. The results in section 3.3 reveal that the average pollen viability and pollen germination decreased most significantly after one day HT-stress (Fig. 3.5, 3.6). According to DAPI staining results, these samples include the stages of mature pollen and tricellular stages which could be identified by the flowers' maturation number every sample collection point, for about 3-4 flowers opened every day during the whole HT-stress experiment. Also in the data of silique length and seed number, the mature and tricellular stages were much more defective than other stages (Fig. 3.11, 3.12). This decrease was recovered in the samples collected at later time points. The data in Fig. 3.9 and 3.10 present the recovery of silique length and seed numbers on the 2-day HT-stressed plants by comparing the data for siliques and seeds produced at each point. In

Fig. 3.11 and 3.12 show the change of silique length and seed number in different stages, that the silique length and seed numbers were significantly decreased in HT-stressed samples than those of non-stressed. Alternatively, variation was also significant among the samples in different pollen developmental stages in the same replicate but was not significant in the samples of the same stages among different replicates through ANOVA analysis. Compared with female gametophyte which are more tolerant on high temperature environment, the male gametophyte show more sensitivity to high temperatures at all stages of development (Endo et al., 2009, Hedhly, 2011). Male sterility can be widely observed in many sensitive crop plants as a consequence of HT-stress, and the impairment of pollen development also involves in yield reduction as the main factor under heat stress (Sakata & Higashitani, 2008, Wassmann et al., 2009). Furthermore, previous research has certified that there was little effect on female organ development, such as HT-stressed pistil was not affected on pollination but HT-stressed mature pollen almost totally lost viability (Endo et al., 2009), the defects of silique and seed development were mainly caused by male reproductive organ. Seed germination result also did not show significant variation between HT-stressed and non-stressed samples. This experiment performed the final percentage of germination when seeds were sown on Petri dishes for seven days rather than the rate every day. Furthermore, seeds are also needed to be separated into different groups as the pollen developmental stages when HT-stress began to be sure the effect of high temperature on matured seeds. However, the germination rate of HT-stressed seeds did not present significant difference with non-stressed ones indicates that high temperature might not leads to

serious defection on successfully matured seeds, while also confirm that HT-stress injuries mainly happen in male gametophyte and male organ development rather than female ones.

Except shorter filament on HT-stress plants that leads to less pollen reach pistil and pollination, another aspect which results in defection of silique and seed development is damage during pollen development. The results here indicate that protection of anther wall might be crucial for pollen development because pollen viability decreased most significantly at late pollen developmental stages when HT-stressed began. Moreover, the results of silique length and seed number (Fig. 3.9, 3.10) present the level of anther wall protection was proportional to tapetum degeneration.

Tapetum development and degeneration is essential for male fertility as well as pollen development, for numerous studies on male sterile mutants have been reported (Prasad et al., 2003, Young et al., 2004, Christensen & Christensen, 2007, Tauber et al., 2007, Ainsworth et al., 2008, Jaggard et al., 2010, Zinn et al., 2010). HT-stress leads to an early abortion of tapetal cells, which then causes the pollen mother cells progress toward meiotic prophase rapidly and undergoes PCD, thus leading to a pollen sterility (Oshino et al., 2007, Sakata & Higashitani, 2008, Parish et al., 2012). Therefore, abnormal tapetum PCD results in reduction of pollen viability and seed production. Major variations in gene expression under HT-stress are possibly related with tapetum degeneration and pollen sterility in kinds of plant species (Oshino et al., 2007, Endo et al., 2009). Existence of the tapetum could protect pollen and pollen development, but defects of pollen development occur in the anthers that

pre-degenerated tapetum under HT-stress. Fig. 3.9 and 3.10 show that the most seriously injured pollen developmental stages were more in which the tapetum had degenerated, while this reduction displayed recovery in parallel with the tapetum degeneration process. Therefore, tapetum development and degeneration is key point for HT tolerance of *Arabidopsis* plant. As a nutrition layer in anther wall, tapetum provides not only physical protection on pollen, but also supply some molecular to ensure pollen development. For example, starch and sugars show fewer amounts in maturing pollen grains with HT-stress, this kind of defects may be the result of decreased hexose supply by the tapetum (Müller & Rieu, 2016). Some tapetum specific and gibberellin acid signalling related genes in rice were also down-regulated with HT-stress (Endo et al., 2009), while a higher GA content results in a higher pollen viability under HT-stress in rice (Tang et al., 2008).

HT stress has a negative effect on pollen development and on various aspects of this process including molecular, cellular, and physiological defects. Pollen development is sensitive to HT-stress as well as reproductive growth, which results in a reduction of seed production. The tapetum is crucial for HT tolerance during pollen development, HT induced tapetum pre-maturation and early degeneration lead to male sterility.

For future, detailed microscopic structure of different staged anther under HT-stress may be necessary to analyse the morphological change of tapetum. Further challenges lies in understanding high temperature caused variation metabolite and secretions from tapetum such as proteins and hormones.

CHAPTER 4

HIGH TEMPERATURE STRESS RELATED CANDIDATE GENES ANALYSIS

CHAPTER 4. HIGH TEMPERATURE STRESS RELATED CANDIDATE GENES ANALYSIS

4.1 INTRODUCTION

Many abiotic stresses, such as water, temperature, light and nutrients, affect plant development directly and seriously. related to (Rodziewicz et al., 2014).

As plants cannot move autonomously, their ability to adapt to environmental change may be better than that of animals. Nevertheless, plant reproductive development is more sensitive to abiotic stresses than vegetative growth, and these sensitivities are often reflected in reduced fertility of plants (Bita & Gerats, 2013). Global environmental changes caused by human activities and global activities could have serious impacts since high temperature (HT) may result in reduced food production (Pachauri et al., 2014). The results in Chapter 3 have indicated that HT-stress can lead to a reduction of pollen viability, which results in a decrease of plant reproductive efficiency. These results also indicate that the most sensitive stages to HT-stress during pollen development were the late stages including the mature pollen stage and tricellular stage when the tapetum is degrading and the pollen wall is forming. The tapetum is a layer of nutritive cells found within the sporangium of the anther in flowering plants (Ariizumi & Toriyama, 2007). It is important for the development of pollen grains, as it helps in pollen wall formation, transportation of nutrients to developing pollen and synthesis of callase for the breakdown of callase and

the separation of microspore tetrads (Liu & Fan, 2013). Previous research has indicated that the tapetum undergoes an incorrect early degradation in a HT environment, which would be disadvantageous for pollen development (Sakata & Higashitani, 2008). Discovery of high temperature sensitive and/or resistant genes expressed specifically in the tapetum could help to understand the regulation of tapetum development in a HT environment. Manipulation of these genes could then positively influence pollen development and plant growth under high temperature stress (Endo et al., 2009).

To investigate the molecular regulation during pollen development under HT stress, a bioinformatics approach was applied to select the candidate genes which were differentially expressed during heat stress. The first category was "Heat", which implied that the candidate gene expression would result in a change in state or activity as a result of a temperature stimulus above the optimal temperature for plant growth. About 200 genes were characterised by the heat definition by Gene Ontology (GO) analysis, these were then further characterised to focus on those expressed specifically within the tapetum. To focus on those genes involved in flower development and in particular the tapetum, further categories were selected for in this dataset (Pearce et al., 2015), such as 10-fold higher expression level in the stamen than flower samples; on the stamen specific expression list; 2-fold higher in the tapetum than the other 3 samples (endothecium, vascular, connective, anther); 2-fold higher in the tetrads tapetum than at least 2 of the other tetrads samples;

expression level over 10 in one of the tapetum samples (Appendix III). Based on these conditions, 6 candidate genes were selected for analysis (Table 4.1)

Table 4.1 HT and tapetum specific related genes.

Gene name	AGI codes	Annotation	References
<i>CRT1b</i>	AT1G09210	Encodes one of three Arabidopsis calreticulins.	(Kim et al., 2013)
<i>UTR1</i>	AT2G02810	Functions as transporter of UDP-galactose and UDP-glucose into the Golgi	(Reyes et al., 2006)
<i>MBF1c</i>	AT3G24500	Highly conserved transcriptional coactivator	(Suzuki et al., 2011)
<i>HOP3</i>	AT4G12400	Potential to interact with Hsp90/Hsp70 as co-chaperones	(Chang et al., 2007)
<i>ABI1</i>	AT4G26080	Involved in abscisic acid (ABA) signal transduction.	(Lu et al., 2015a)
<i>HS83</i>	AT5G52640	Encodes a cytosolic heat shock protein AtHSP90.1 and interacts with disease resistance signaling components	(Wang et al., 2016)

CALRETICULIN 1B (CRT1b, AT1G09210) is an isoform belong to the CRT family, an Endoplasmic Reticulum (ER)-localized Ca²⁺-binding protein, which is highly conserved in all multi-cellular eukaryotes including humans, nematodes, fruit flies and plants (Kim et al., 2013). In *Arabidopsis*, CRT1b locates in the apoplast, chloroplast, endoplasmic reticulum (ER), mitochondria, and vacuole (Ge et al., 2011, Nikolovski et al., 2012, Sweetlove et al., 2002, Carter et al., 2004). It is involved in many abiotic responses, such as elevated temperature, high light, hydrogen peroxide, oxidative, salt and water stress (Heyndrickx & Vandepoele, 2012, Sweetlove et al., 2002, Jiang et al., 2007, Kim et al., 2013). Christensen et al. (2010) demonstrated that loss of *AtCRT1b*

results in altered tunicamycin responsiveness, and in retarded seedling growth. In *Petunia*, *PhCRT* gene expression is also indicated to be up-regulated during secretory activity of pistil transmitting tract cells, pollen germination and outgrowth of the tubes, and then during gamete fusion and early embryogenesis (Lenartowski et al., 2014).

UDP-GALACTOSE TRANSPORTER 1 (UTR1, AT2G02810) is characterized as a nucleotide sugar transporter in *Arabidopsis thaliana* (Norambuena et al., 2002), which encodes a multi-transmembrane hydrophobic protein that functions as a transporter of UDP-galactose and UDP-glucose into the Golgi. UTR1 localised in the ER, and is involved in the unfolded protein response, which is a mechanism that controls proper protein folding in the ER, and also responds to heat and light stress (Heyndrickx & Vandepoele, 2012, Reyes et al., 2010).

MULTIPROTEIN BRIDGING FACTOR 1C (MBF1C, AT3G24500) is a transcriptional co-activator that mediates transcriptional activation by bridging between an activator and a TATA-box binding protein (TBP) (Tsuda & Yamazaki, 2004), and possibly functioned as a DNA-binding transcriptional regulator and also a putative transcription factor (Suzuki et al., 2011). *MBF1c* protein accumulates rapidly and is localized to nuclei during heat stress (Suzuki et al., 2008), it was reported as a key regulator of thermo tolerance in *Arabidopsis thaliana*. It had been reported that plants overexpressing *MBF1c*

showed enhanced basal resistance to drought and infection (Bechtold et al., 2013). Furthermore, the homologous gene in wheat (*TaMBF1c*) was reported to be induced by HT-stress and also other abiotic stresses, and overexpression of *TaMBF1c* increased tolerance of yeast and rice under high temperature stress. (Qin et al., 2015).

HSP70-HSP90 ORGANIZING PROTEIN 3 (HOP3, AT4G12400) is a carboxylate clamp-tetratricopeptide repeat protein which mediates the association of the molecular chaperones HSP70 and HSP90 and nuclear encoded chloroplast preproteins binding to HSP90 prior to chloroplastic sorting (Charng et al., 2007). *AtHOP3* is a member of the HOP family that functions as partner components in the HSP90 cycle, which are present in the pre-protein containing high-molecular-weight complexes (Fellerer et al., 2011).

ABA INSENSITIVE 1 (ABI1, AT4G26080) is a protein phosphatase, it is key component and repressor of the abscisic acid (ABA) signalling pathway that regulates numerous ABA responses, such as osmotic water permeability in the plasma membrane and stomata closure, (Leung et al., 1994). *ABI1* functions in drought resistance, responds to high strength of light stress, seed germination and inhibition of vegetative growth, and is involved in acquired thermo-tolerance of root growth and seedling survival (Chak et al., 2000, Fryer et al., 2003, Larkindale et al., 2005, Parcy & Giraudat, 1997). Moreover, *ABI1* acts to inhibit MAPKKK18 kinase activity, but also affects MAPKKK18 protein

turnover via the ubiquitin-proteasome pathway (Tajdel et al., 2016). It is also reported that *ABI1* directly regulates cross-talk between the carbon/nitrogen and non-canonical ABA signalling pathways (Lu et al., 2015a).

HEAT SHOCK PROTEIN 83 (HS83, AT5G52640), which is also known as HSP90.1 encodes a heat shock protein (HSP) belonging to the 83 to 90 kilodalton HSP family of *Arabidopsis thaliana* (HSP90) (Conner et al., 1990). Previous research confirmed that *HS83* exists in monomeric, dimeric and higher oligomeric states and was stress-inducible; its activity was enhanced in oligomeric stages (Cha et al., 2013). HSP90 prevents the denaturation of substrate proteins with foldase chaperone function, and promotes the refolding of heat-denatured proteins in the foldase chaperone function under HT stress conditions (Cha et al., 2013). HSP90 interacts with *TRANSPORT INHIBITOR RESPONSE1 (TIR1)* by forming HSP90-TIR1 dimer, integrating environmental temperature and auxin signalling to regulate plant development. This reveals a link between the molecular networks regulating plant growth response to ambient temperature module and the HSPs-HSFs module that plays a central role in heating sensing and signalling (Wang et al., 2016). HS83 is a cytosolic HSP90 which localises to the cytosol, and it has been reported that cytosolic HSP90 negatively regulates heat-inducible genes by actively suppressing HSF function in the absence of heat shock (Yamada et al., 2007).

In this chapter, the expression analysis of these 6 candidate genes in different

staged buds samples with and without HT-stress was analysed. Furthermore, T-DNA insertion mutants of these genes were also utilised to investigate the function of these genes during pollen development in response to HT-stress treatment compared to WT.

4.2 MATERIALS AND METHODS

4.2.1 Plant materials and growth condition

Seeds of *Arabidopsis thaliana* genotype Ler and seeds of T-DNA insertion mutants were obtained from Nottingham Arabidopsis Stock Centre (NASC). A detailed list of T-DNA insertion mutants are shown in Table 4.2. The seeds were sown on Levington M3 in 9 cm pots and allowed there were 4 plants grow in each pot. For growth conditions see section 2.1.

Table 4.2 T-DNA insertion mutants used in HT-stress experiments. T-DNA insertion positions of these mutants are shown in Fig. 4.4-4.9.

Gene	AGI code	T-DNA insertion mutant code
CRT1b	AT1G09210	SALK_062083
CRT1b	AT1G09210	SALK_099778
UTR1	AT2G02810	SALK_123541
UTR1	AT2G02810	GABI_493A10
MBF1c	AT3G24500	SALK_083813
MBF1c	AT3G24500	GABI_434G08
ABI1	AT4G26080	SALK_072009
ABI1	AT4G26080	GABI_334A12
HOP3	AT4G12400	SALK_000794
HOP3	AT4G12400	SALK_023494
HS83	AT5G52640	SALK_004008
HS83	AT5G52640	SALK_075596

4.2.2 HT-stress and sample collection

The *Arabidopsis* plants (Ler) and all of the T-DNA insertion mutants were stressed with high temperature at the 30-day-old stage, which was at the point when they had produced 3 siliques. All of the opened and semi-opened flowers on the main shoot were removed prior to HT stress, as well as the siliques on the main shoot. The humidity in the incubator was kept between 60%-70%. The plants were treated at 32°C for 2 days with continuous light. The control plants were moved to another growth chamber which had same conditions as the HT treated samples but with a temperature of 22°C. Both of the HT-stressed group and non-stressed group plants were moved back to the glasshouse after the 2 days treatment for recovery. All opened flowers and buds that were about to open were discarded and buds were grouped and collected into three groups named “Mature”, “Old” and “Young” (Fig. 4.1) according to previous DAPI staining (see section 3.3.1). Buds 1, 2, 3 and 4 constituted the “Mature group”; buds 5, 6, 7 and 8 formed the “Old group”; and buds 9 and all of the younger ones belonged to the “Young group”. Only the inflorescences on the main shoots were collected. The plant materials were collected and frozen immediately in liquid nitrogen and stored at -80°C for subsequent RNA extraction. During the HT stress period, samples were collected at four different time points, D1 (1 day HT treated), D2 (2 days HT treated), R1 (1 day recovery after HT), and R2 (2 days recovery after HT). Morphological analysis was performed to characterise the difference between

HT-stressed and non-stressed samples in the T-DNA insertion mutants and wild type plants. Pollen viability (see section 2.4), germination (see section 2.5), silique length and seed number (see section 2.6) data were recorded.

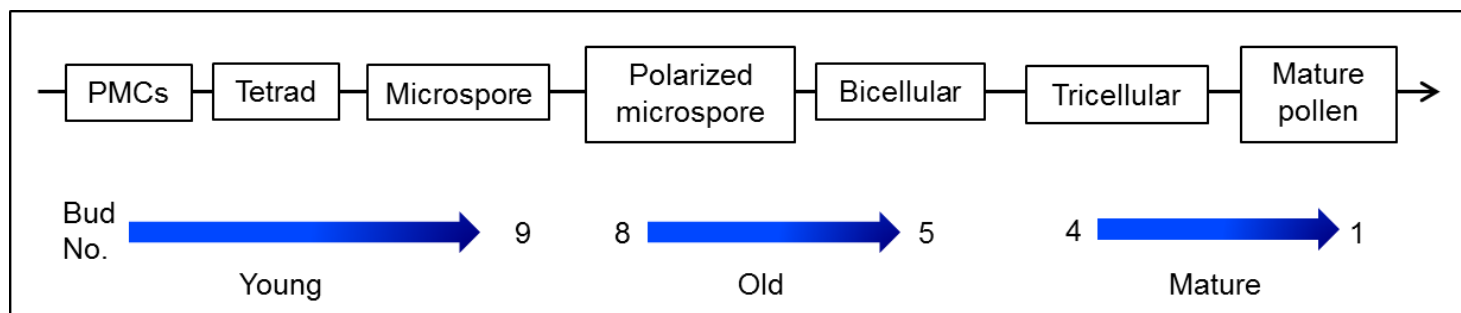


Figure 4.1 Bud collection modes for expression analysis. Bud groups were constructed for different tapetum developmental processes. Tapetum was formed in the “Young group” buds, and initiated PCD in “Old group” bud, while it degenerated in “Mature group” buds. No. 1 indicates the oldest bud at mature pollen stage in inflorescence, and No. 9 indicates very small young bud at microspore stage.

4.2.3 Sucrose method for DNA extraction

The sucrose DNA extraction method was used on leaf tissues of *Arabidopsis thaliana* to characterise the segregating T-DNA insertion lines (Berendzen et al., 2005). Young leaf tissues were collected from *Arabidopsis* seedlings, and then were placed directly into 100 µl of Sucrose Buffer (Appendix I) on ice in 96-well PCR-plates. The tissues were crushed with a yellow pipette tip, which was then used to mark the sampled plant. The samples were then heated to 99-100°C for 10 min using a PCR machine and briefly spun at 3000 rpm for 5

min. Then the samples were stored at -20°C until needed.

4.2.4 Primer list

Primers were designed using Primer5 software (www.PrimerBiosoft.com, Version 5.0). Conditions were specific for individual products. Each pair of primers was tested using SnapGene[®] Viewer (www.snapgene.com, version 2.3.5) and BLAST analysis to confirm their specificity. Primers for RT-PCR and quantitative RT-PCR, and genotyping are listed in Appendix II.

4.2.5 RNA extraction and cDNA synthesis

Total RNA from the whole inflorescence (or particular bud stage) was extracted using a QIAGEN RNA extraction kit following the manufacturer's protocol, and the quality of RNA samples was tested by Nanodrop. cDNA was synthesised from the RNA template using SuperscriptIII[®], and the quality was then checked by RT-PCR using a housekeeping gene (*ACTIN7*), as previously mentioned in section 2.3 and 2.6.1. The amount of RNA for cDNA synthesis was adjusted to 2 µg for all of the experiments.

4.2.6 RT-PCR and Quantitative RT-PCR

RT-PCR was used to verify the cDNA products from RNA samples before quantitative RT-PCR with primers of HT related genes were tested on WT cDNA. Components of the quantitative RT-PCR were as mentioned previously

(see section 2.12). Primers for HT genes are as listed in Appendix II. The standard program for running the plate on the LightCycler was: 95°C 10 min; 45x (95°C 30 sec, T_m, 30 sec, 72°C for 1 min); 72°C 6 min. Cp values were calculated by the LightCycler[®] 480 software. Expression level was analysed and performed using MicroSoft Excel. Annealing temperature (T_m) was chosen by each primer separately.

4.3 RESULTS

4.3.1 Expression analysis of HT related candidate genes

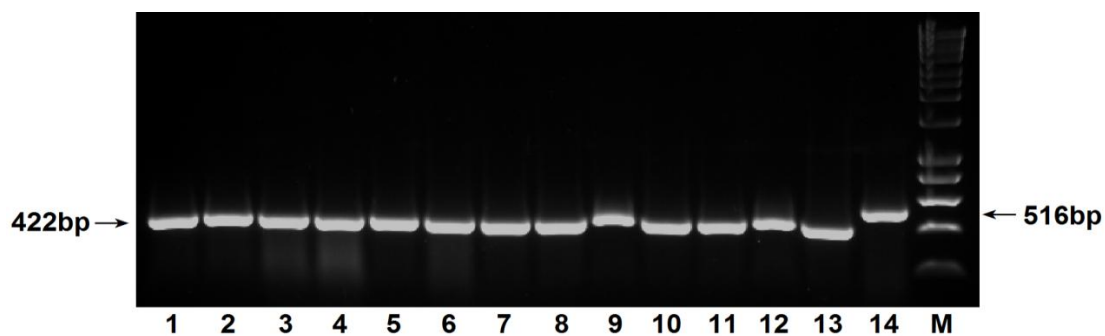
To explore the relationship between tapetum and HT-stress, six HT related and tapetum expressed genes were chosen (Table 4.1). 30-day-old *Arabidopsis* Ler ecotype plants were treated with and without HT for 2 days in two separate growth chambers at the same time. Total RNA of buds separated into three groups according to growth stage (mature (B1), old (B2) and young (B3)) was extracted for expression analysis. Four time points were collected, after 1 day HT- stress (D1), 2 days HT- stress (D2), 1 day after recovery (R1) and 2 days after recovery (R2) with and without HT-stress (see section 4.2.2), and were labelled according to Table 4.3. The quality of the cDNA and a comparison between samples was assessed by RT-PCR using the housekeeping gene *ACTIN7* (Fig 4.2).

Table 4.3 Buds samples information of HT-stress experiments. “Mature”, “Old” and “Young” groups’ details see section 4.2.2. D1, D2, R1 and R2 details see section 4.2.2.

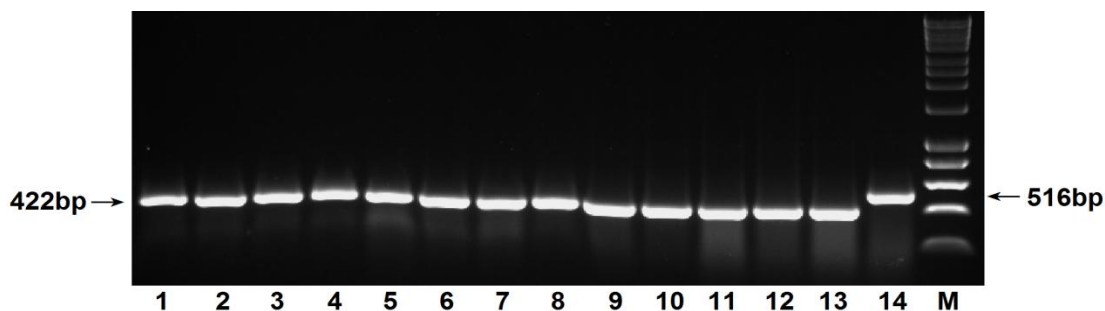
Sample name	Description
D1-C-B1	Non-stressed “Mature” buds collected at D1
D1-C-B2	Non-stressed “Old” buds collected at D1
D1-C-B3	Non-stressed “Young” buds collected at D1
D2-C-B1	Non-stressed “Mature” buds collected at D2
D2-C-B2	Non-stressed “Old” buds collected at D2
D2-C-B3	Non-stressed “Young” buds collected at D2
R1-C-B1	Non-stressed “Mature” buds collected at R1
R1-C-B2	Non-stressed “Old” buds collected at R1
R1-C-B3	Non-stressed “Young” buds collected at R1
R2-C-B1	Non-stressed “Mature” buds collected at R2
R2-C-B2	Non-stressed “Old” buds collected at R2
R2-C-B3	Non-stressed “Young” buds collected at R2
D1-HS-B1	HT-stressed “Mature” buds collected at D1
D1-HS-B2	HT-stressed “Old” buds collected at D1
D1-HS-B3	HT-stressed “Young” buds collected at D1
D2-HS-B1	HT-stressed “Mature” buds collected at D2
D2-HS-B2	HT-stressed “Old” buds collected at D2
D2-HS-B3	HT-stressed “Young” buds collected at D2
R1-HS-B1	HT-stressed “Mature” buds collected at R1
R1-HS-B2	HT-stressed “Old” buds collected at R1
R1-HS-B3	HT-stressed “Young” buds collected at R1
R2-HS-B1	HT-stressed “Mature” buds collected at R2
R2-HS-B2	HT-stressed “Old” buds collected at R2
R2-HS-B3	HT-stressed “Young” buds collected at R2

Figure 4.2 RT-PCR for cDNA quality inspection.

A). cDNA samples from non-stressed buds materials. Lanes 1-13, cDNA as templates; lane 14, genomic DNA as template. 1, D1-C-B1; 2, D1-C-B2; 3, D1-C-B3; 4, D2-C-B1; 5, D2-C-B2; 6, D2-C-B3; 7, R1-C-B1; 8, R1-C-B2; 9, R1-C-B3; 10, R2-C-B1; 11, R2-C-B2; 12, R2-C-B3; 13, WT cDNA synthesized from RNA of whole inflorescence; 14, WT genomic DNA of whole inflorescence. Primers used: *ACTIN7* (Act7_2F and Act7_443R) (30 cycles), primer sequences see Appendix II. cDNA bands size: 422bp; genomic DNA band size: 516bp. M, marker: HyperLadder I. For sample stage information, see Table 4.3.



B). cDNA samples from HT-stressed buds samples. Lanes 1-13, cDNA as template; lane 14, genomic DNA as template. 1, D1-HS-B1; 2, D2-HS-B2; 3, D1-HS-B3; 4, D2-HS-B1; 5, D2-HS-B2; 6, D2-HS-B3; 7, R1-HS-B1; 8, R1-HS-B2; 9, R1-HS-B3; 10, R2-HS-B1; 11, R2-HS-B2; 12, R2-HS-B3; 13, WT cDNA synthesized from RNA of whole inflorescence; 14, WT genomic DNA of whole inflorescence. Primers used: *ACTIN7* (Act7_2F and Act7_443R) (30 cycles), primer sequences see Appendix II. cDNA bands size: 422bp; genomic DNA band size: 516bp. M, marker: HyperLadder I. For sample stage information, see Table 4.3.



Expression of the six HT related genes was analysed in these bud samples. In wild type under non-stressed conditions, all of these six HT related genes showed different expression level in the three different stages buds groups, “Mature”, “Old” and “Young”. However, these non-stressed materials also exhibited some variation at different time points which might be caused by variation between sample stage and time of collection.

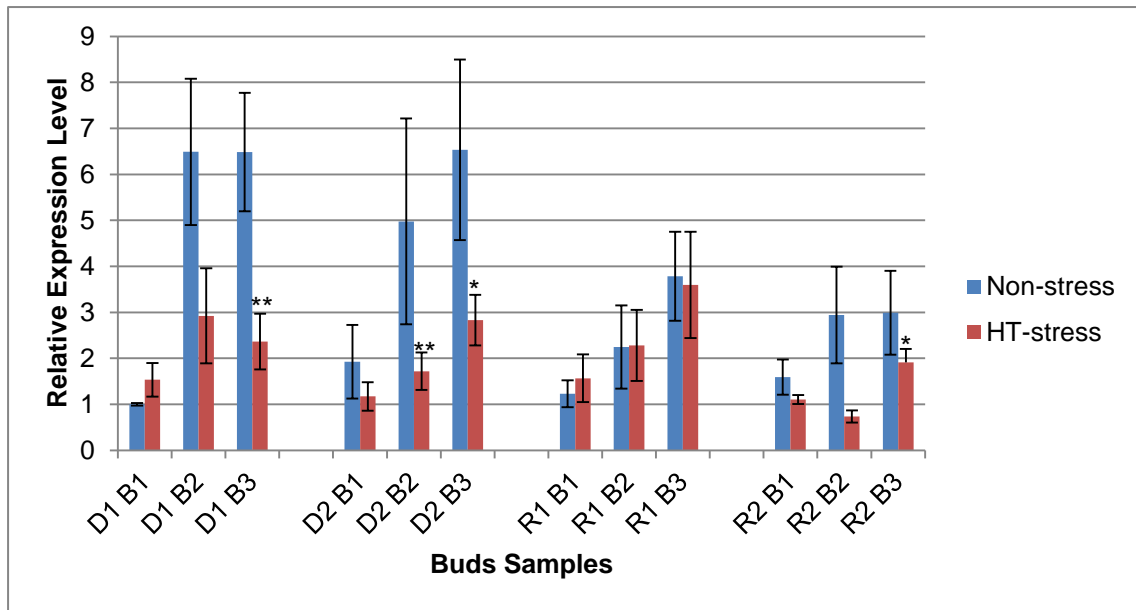
Figure 4.3 Quantitative RT-PCR of HT related candidate genes expression level with and without HT-stress in different pollen developmental stages.

Bud samples were collected after 1 day (D1), 2 days (D2), and 1 day recovery (R1), 2 days recovery (R2) with and without HT stress. B1, B2, and B3 indicates three bud stages, “mature” (B1), “old” (B2) and “young” (B3) respectively. For collection time point details see section 4.2.2, for bud stage group details see Table 4.2. Column bars are means of three biological replicate, error bars represent standard error. Each biological replicates represents RNA pooled from six plants. For each gene relative expression level, the non-stressed “Old” buds sample which were collected at D1 time point was defined as “1”, and all of other values were compared with it. Primers used: CRT1b (CRT1bF-qPCR and CRT1bR-qPCR), UTR1 (UTR1F-qPCR and UTR1R-qPCR), MBF1c (MBF1cF-qPCR and MBF1cR-qPCR), HOP3 (HOP3F-qPCR and HOP3R-qPCR), ABI1 (ABI1F-qPCR and ABI1R-qPCR), HS83 (HS83F-qPCR and HS83R-qPCR), and ACTIN7 as reference gene (ACT7_2F and ACT7_443R) (primer sequences see section Appendix II). *, **, *

, * Relatively expression level under HT-stress was significantly different from Non-stressed by *t*-test. *p* value < 0.1, 0.01, 0.001, 0.0001, respectively.

Figure 4.3 Quantitative RT-PCR of HT related candidate genes expression level with and without HT-stress in different pollen developmental stages.

A). Expression level of *CRT1b* (At1G09210).



B). Expression level of *UTR1* (At2G02810).

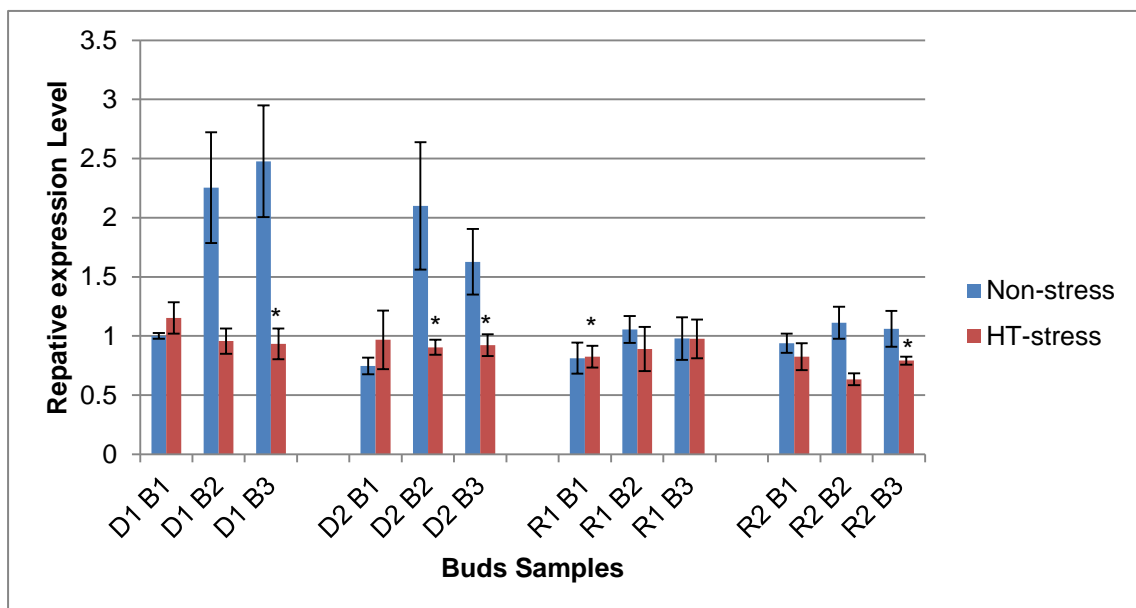
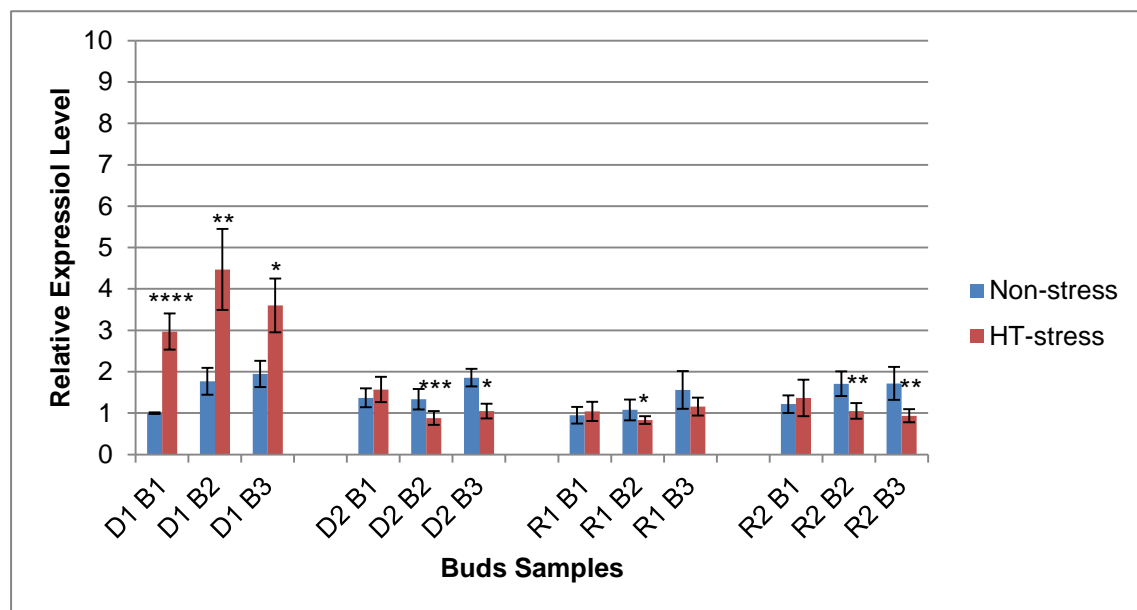


Figure 4.3 Quantitative RT-PCR of HT related candidate genes expression level with and without HT-stress in different pollen developmental stages (continued).

C). Expression level of *MBF1c* (At3G24500).



D). Expression level of *HOP3* (At4G12400).

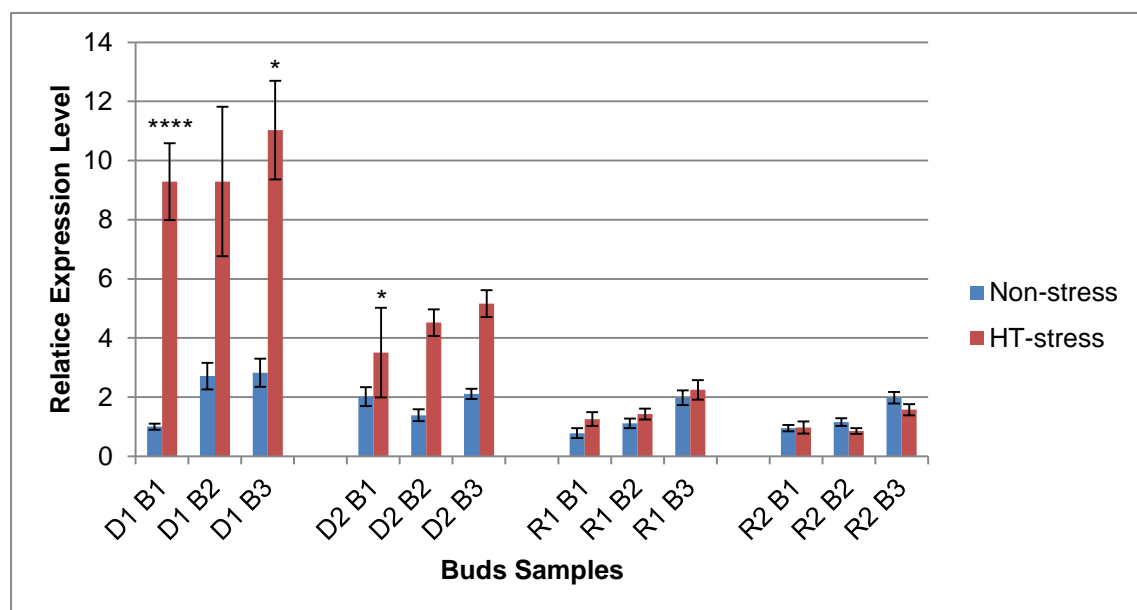
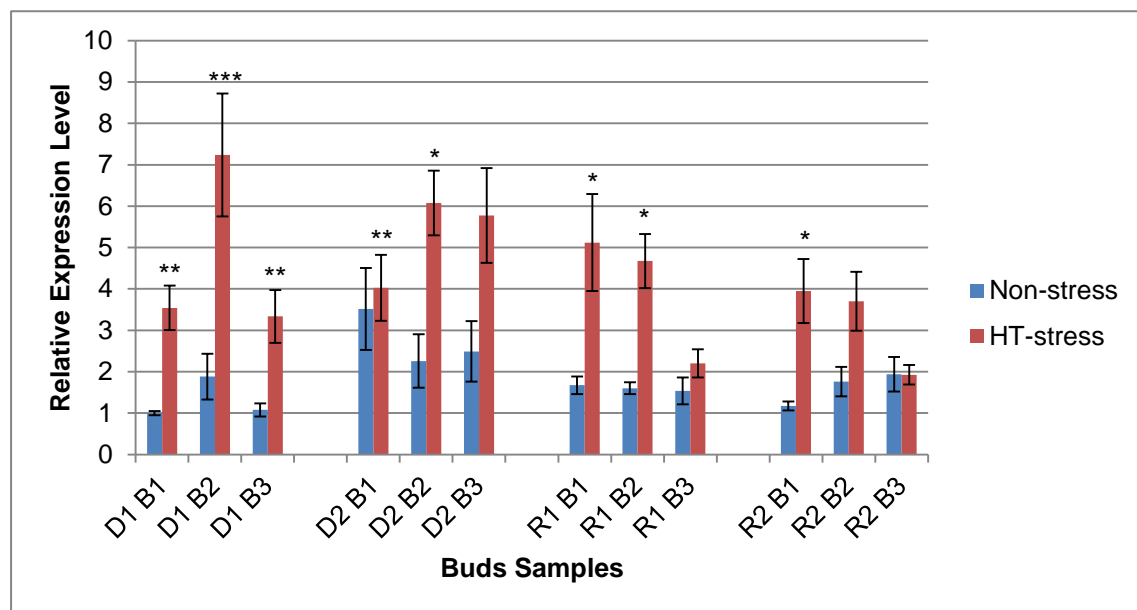
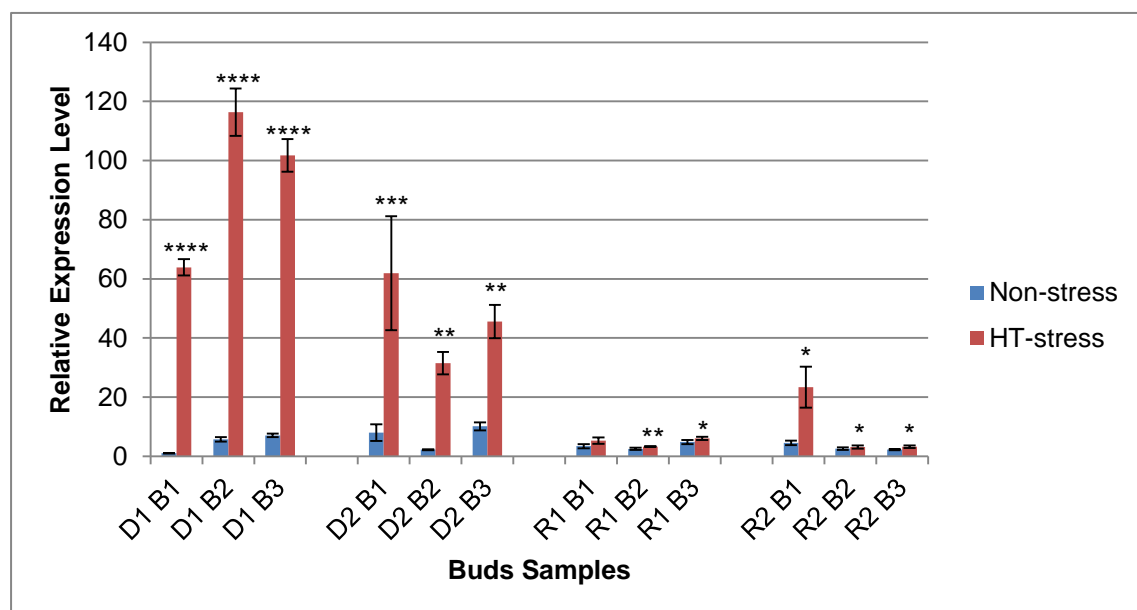


Figure 4.3 Quantitative RT-PCR of HT related candidate genes expression level with and without HT-stress in different pollen developmental stages (continued).

E). Expression level of *ABI1* (At4G26080).



F). Expression level of *HS83* (At5G52640).



The *AtCRT1b* gene was clearly reduced in “Old” (B2) and “Young” (B3) buds (stage details see section 4.2.2) during the HT-stress experiment compared to the non-stressed control and also down-regulated during recovery in the non-stressed environment. In “Mature” (B1) group buds this gene was up-regulated at D1 and down-regulated at D2 and then up-regulated at R1 and down-regulated at R2 in HT treated compared to untreated control. However, this relative expression level change in “Mature” group materials was not significant to compare the values between HT-stressed and non-stressed samples by *t*-test at each collection time point, while the “Young” group materials showed significant difference in HT-stressed samples with non-stressed ones at all of time points (Fig. 4.3a).

The variation of expression level of *AtUTR1* showed a similar trend as *AtCRT1b*. *AtUTR1* expression reduced was also in groups “Old” and “Young” during HT-stress but the expression level changed to the similar level when the plants were back to non-stressed condition. However, *AtUTR1* expression level in “Mature” group buds materials also did not change significantly in the HT-stress environment compared to that in the non-stressed treatment (Fig. 4.3b).

AtMBF1c was up-regulated in the all three bud sample groups after 1 day HT-stress and its expression decreased to a similar level as the in non-stressed samples after 2 days HT-stress, and also did not show significant

variation during the 2 days recovery period (Fig. 4.3c).

AtHOP3 and *AtHS83* genes showed up-regulated expression in all of the samples during the whole HT-stress period but this up-regulation reduced to non-stressed level after recovery. Furthermore, the values indicate that the genes' expression level increased more level after 1 day HT-stress than that after 2 days HT-stress in the "Old" and "Young" groups (Fig. 4.3d, Fig. 4.3f).

AtABI1 gene was also up-regulated in the whole inflorescence during the HT-stress experiment, but it did not return to untreated level when the HT-stress finished in "Mature" and "Old" groups samples although the expression level in "Young" group reduced to non-stressed level (Fig. 4.3e).

To conclude, the expression level of most genes in the recovery period did not represent a significant difference between HT-stressed and non-stressed samples as that seen in HT-stress active phase. This suggests the temperature effect on these genes is not maintained when the HT-stress finishes.

4.3.2 Analysis of T-DNA insertion mutants.

4.3.2.1 Expression analysis

T-DNA insertion mutants of these genes were used to investigate the function of HT related genes during pollen development. SALK lines and GABI-KAT

lines seeds were obtained from Nottingham *Arabidopsis* Stock Centre and genotyped to confirm the T-DNA insertion. Detailed information of T-DNA insertion mutants are listed in Table 4.4. For each gene, the T-DNA insertion position and genotyping were showed separately in Fig. 4.4-4.9.

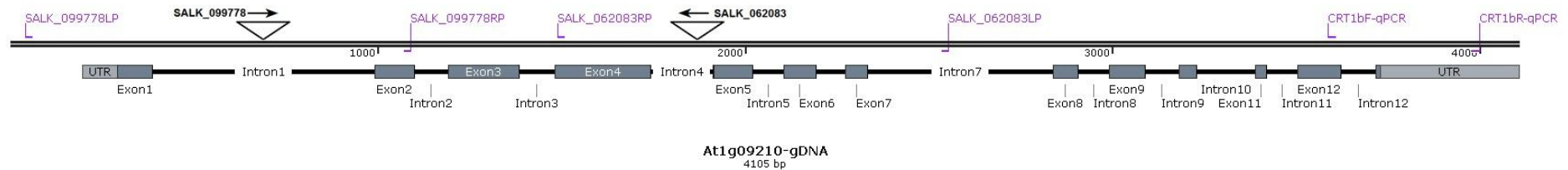
For each insertion line, DNA from the T-DNA insertion mutant was amplified with three primers, in combination LBb1.3 (for SALK lines)/o8409 (for GABI lines) and the respective gene-specific primers (LP and RP); wild type materials were amplified only with gene specific primers without LBb1.3 and 08409. Primer sequences are listed in Appendix II.

Table 4.4 T-DNA insertion mutants used in the HT-stress experiments, and primers list for identification and expression analysis.

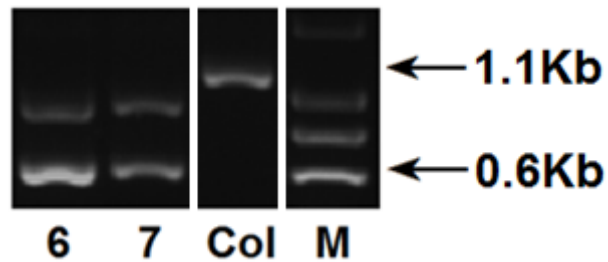
Gene	T-DNA insertion mutant ID	Primers	
		Genotyping	RT-PCR
<i>AT1G09210</i> <i>CRT1b</i>	SALK_062083	SALK_062083LP, SALK_062083RP, LBb1.3	CRT1bF-qPCR CRT1bR-qPCR
	SALK_099778	SALK_099778LP, SALK_099778RP, LBb1.3	
<i>AT2G02810</i> <i>UTR1</i>	SALK_123541	SALK_123541LP, SALK_123541RP, LBb1.3	UTR1F-qPCR UTR1R-qPCR
	GABI_493A10	GABI_493A10LP, GABI_493A10RP, o8409	
<i>AT3G24500</i> <i>MBF1c</i>	SALK_083813	SALK_083813LP, SALK_083813RP, LBb1.3	MBF1cF-qPCR MBF1cR-qPCR
	GABI_434G08	GABI_434G08LP, GABI_434G08RP, o8409	
<i>AT4G26080</i> <i>ABI1</i>	SALK_072009	SALK_072009LP, SALK_072009RP, LBb1.3	HOP3F-qPCR HOP3R-qPCR
	GABI_334A12	GABI_334A12LP, GABI_334A12RP, o8409	
<i>AT4G12400</i> <i>HOP3</i>	SALK_000794	SALK_000794LP, SALK_000794RP, LBb1.3	ABI1F-qPCR ABI1R-qPCR
	SALK_023494	SALK_023494LP, SALK_023494RP, LBb1.3	
<i>AT5G52640</i> <i>HS83</i>	SALK_004008	SALK_004008LP SALK_004008RP, LBb1.3	HS83F-qPCR HS83R-qPCR
	SALK_075596	SALK_075596LP SALK_075596RP, LBb1.3	

Figure 4.4 T-DNA insertion mutant information and genotyping of the *CRT1b* (AT1G09210) gene.

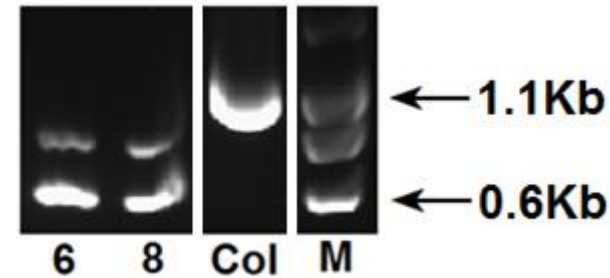
A)



B)



C)



A). T-DNA insertion positions on *CRT1b* genomic DNA. Triangles indicate the positions of the T-DNA inserts, arrows represent the direction of the T-DNA insertion.

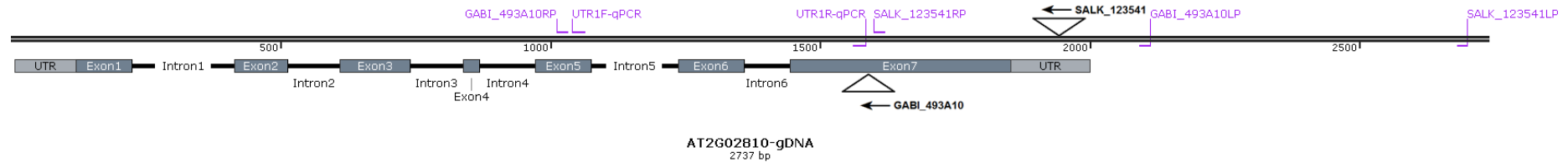
B). Genotyping for SALK_062083. 6 and 7 are two homozygous plants that were identified; Col: *Arabidopsis* Col-0 as WT; M: HyperLadder I as marker. Arrow indicates WT band (1.1Kb) and homozygous insertion line (0.6Kb). Primers used: LP, SALK_062083LP; RP, SALK_062083RP; LB, LBb1.3.

C). Genotyping for SALK_099778. 6 and 8 are two homozygous plants that were identified; Col: *Arabidopsis* Col-0 as WT; M: HyperLadder I as marker. Arrow indicates WT band (1.1Kb) and homozygous insertion line (0.6Kb). Primers used: LP, SALK_099778LP; RP, SALK_099778RP; LB, LBb1.3.

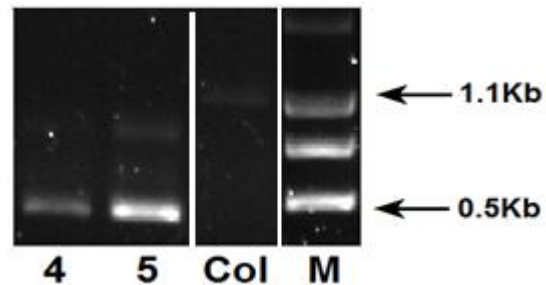
Sequences of primer for genotyping are listed in Appendix II.

Figure 4.5 T-DNA insertion mutant information and genotyping of the *UTR1* (AT2G02810) gene.

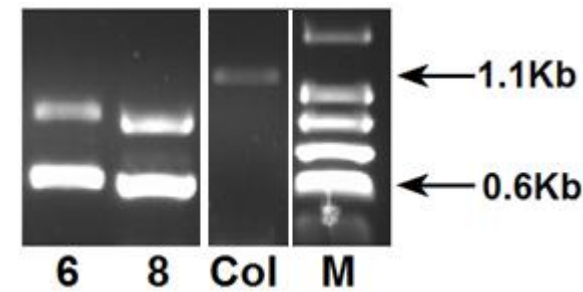
A)



B)



C)



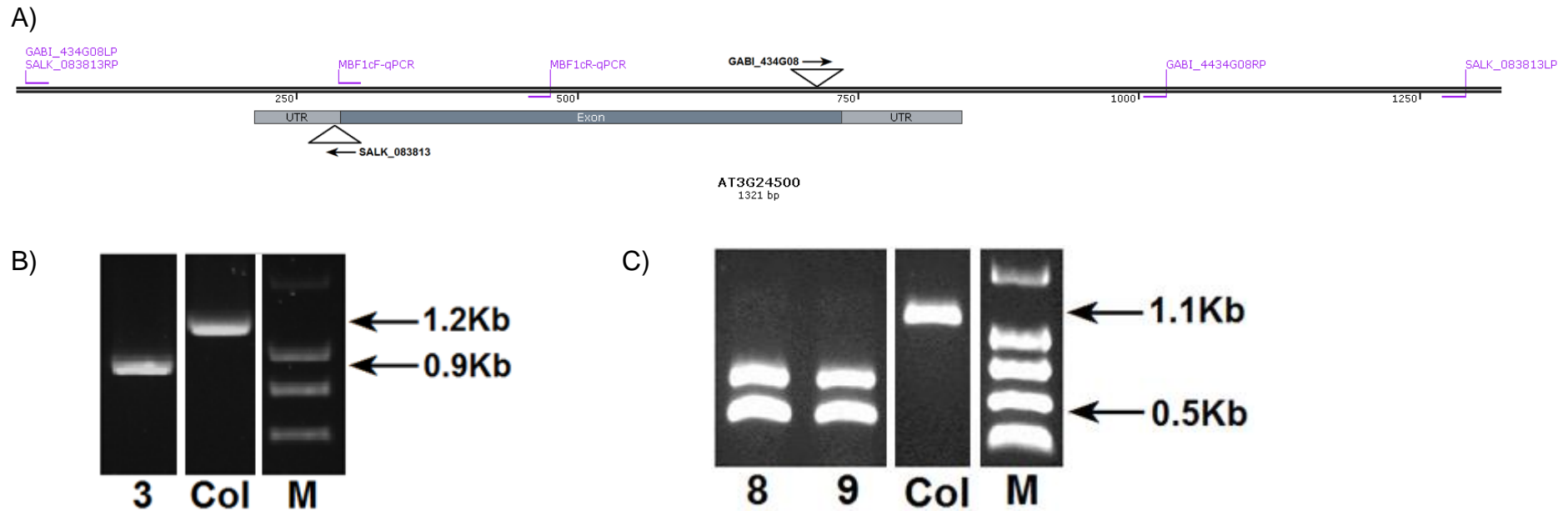
A). T-DNA insertion positions on *UTR1* genomic DNA. Triangles indicate the positions of the T-DNA inserts, arrows represent the direction of the T-DNA.

B). Genotyping for SALK_123541. 4 and 5 are two homozygous plants that were identified; Col: *Arabidopsis* Col-0 as WT; M: HyperLadder I as marker. Arrow indicates WT band (1.1Kb) and homozygous insertion line (0.5Kb). Primers used: LP, SALK_123541LP; RP, SALK_123541RP; LB, LBb1.3.

C). Genotyping for GABI_493A10. 6 and 8 are two homozygous plants that were identified; Col: *Arabidopsis* Col-0 as WT; M: HyperLadder I as marker. Arrow indicates WT band (1.1Kb) and homozygous insertion line (0.6Kb). Primers used: LP, GABI_493A10LP; RP, GABI_493A10RP; LB, LBb1.3.

Sequences of primer for genotyping are listed in Appendix II.

Figure 4.6 T-DNA insertion mutant information and genotyping of the *MBF1c* (AT3G24500) gene.



A). T-DNA insertion positions on *MBF1c* genomic DNA. Triangles indicate the positions of the T-DNA inserts, arrows represent the direction of the T-DNA.

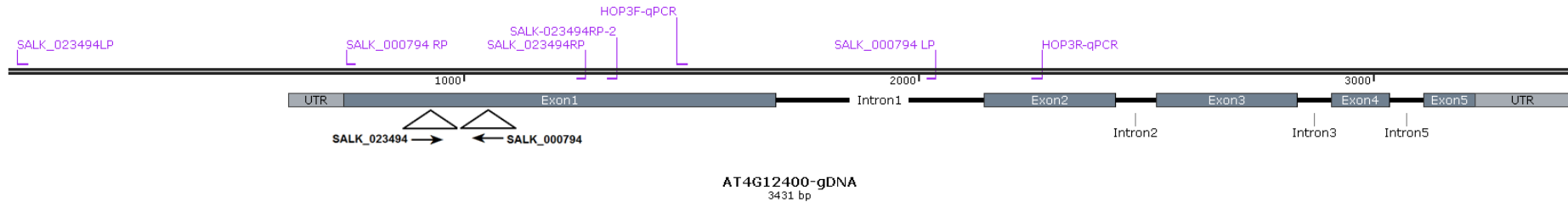
B). Genotyping for SALK_083813. 4 is the homozygous plant that was identified; Col: *Arabidopsis* Col-0 as WT; M: HyperLadder I as marker. Arrow indicates WT band (1.2Kb) and homozygous insertion line (0.9Kb). Primers used: LP, SALK_083813LP, SALK_083813RP; RP; LB, LBb1.3.

C). Genotyping for GABI_434G08. 8 and 9 are two homozygous plants that were identified; Col: *Arabidopsis* Col-0 as WT; M: HyperLadder I as marker. Arrow indicates WT band (1.1Kb) and homozygous insertion line (0.5Kb). Primers used: LP, GABI_434G08LP, GABI_434G08RP; RP; LB, LBb1.3.

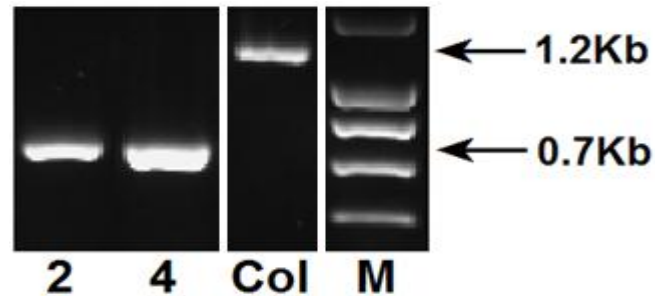
Sequences of primer for genotyping are listed in Appendix II.

Figure 4.7 T-DNA insertion mutant information and genotyping of the *HOP3* (AT4G12400) gene.

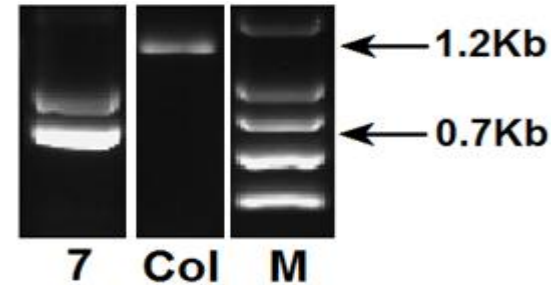
A)



B)



C)



A). T-DNA insertion positions on *HOP3* genomic DNA. Triangles indicate the positions of the T-DNA inserts, arrows represent the direction of the T-DNA.

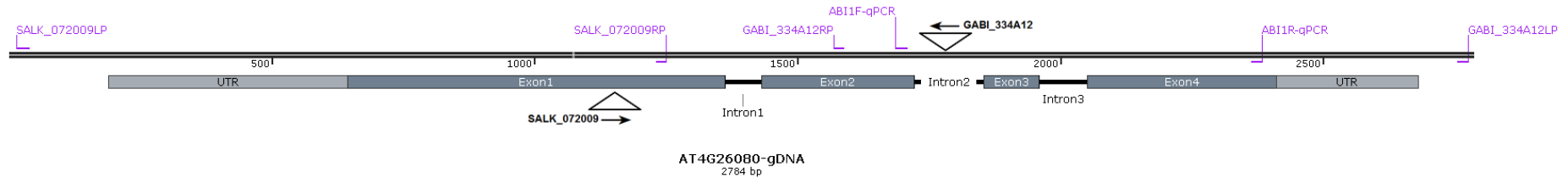
B). Genotyping for SALK_000794. 2 and 4 are two homozygous plants that were identified; Col: *Arabidopsis* Col-0 as WT; M: HyperLadder I as marker. Arrow indicates WT band (1.2Kb) and homozygous insertion line (0.7Kb). Primers used: LP, SALK_000794LP, SALK_000794RP; RP; LB, LBb1.3.

C). Genotyping for SALK_023494. 7 is the homozygous plant that was identified; Col: *Arabidopsis* Col-0 as WT; M: HyperLadder I as marker. Arrow indicates WT band (1.2Kb) and homozygous insertion line (0.7Kb). Primers used: LP, SALK_023494LP, SALK_023494RP; RP; LB, LBb1.3.

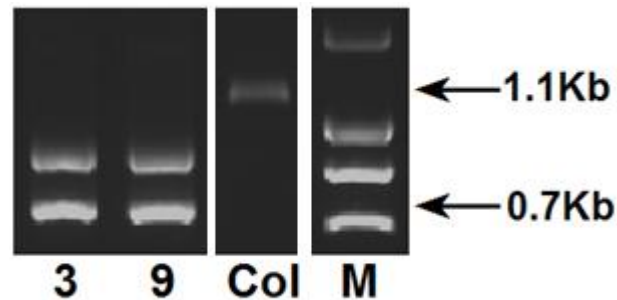
Sequences of primer for genotyping are listed in Appendix II.

Figure 4.8 T-DNA insertion mutant information and genotyping of the *ABI1* (AT4G26080) gene.

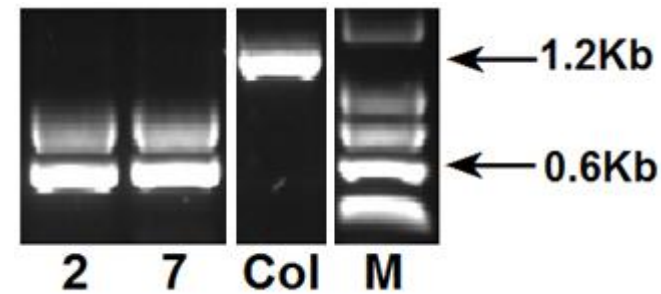
A)



B)



C)



A). T-DNA insertion positions on *ABI1* genomic DNA. Triangles indicate the positions of the T-DNA inserts, arrows represent the direction of the T-DNA.

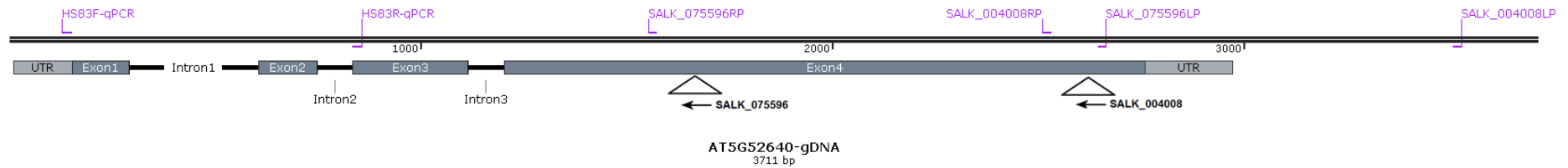
B). Genotyping for SALK_072009. 3 and 9 are two homozygous plants that were identified; Col: *Arabidopsis* Col-0 as WT; M: HyperLadder I as marker. Arrow indicates WT band (1.1Kb) and homozygous insertion line (0.7Kb). Primers used: LP, SALK_072009LP, SALK_072009RP; RP; LB, LBb1.3.

C). Genotyping for GABI_334A12. 2 and 7 are two homozygous plants that were identified; Col: *Arabidopsis* Col-0 as WT; M: HyperLadder I as marker. Arrow indicates WT band (1.2Kb) and homozygous insertion line (0.6Kb). Primers used: LP, GABI_334A12LP, GABI_334A12RP; RP; LB, LBb1.3.

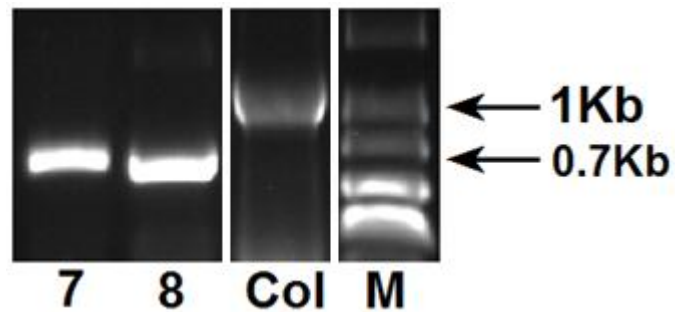
Sequences of primer for genotyping are listed in Appendix II.

Figure 4.9 T-DNA insertion mutant information and genotyping of the *HS83* (AT5G52640) gene.

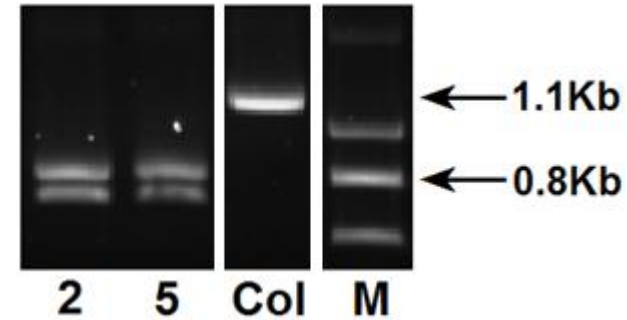
A)



B)



C)



A). T-DNA insertion positions on *HS83* genomic DNA. Triangles indicate the positions of the T-DNA inserts, arrows represent the direction of the T-DNA.

B). Genotyping for SALK_004008. 7 and 8 are two homozygous plants that were identified; Col: *Arabidopsis* Col-0 as WT; M: HyperLadder I as marker. Arrow indicates WT band (1Kb) and homozygous insertion line (0.7Kb). Primers used: LP, SALK_004008LP, SALK_004008RP; RP; LB, LBb1.3.

C). Genotyping for SALK_075596. 2 and 5 are two homozygous plants that were identified; Col: *Arabidopsis* Col-0 as WT; M: HyperLadder I as marker. Arrow indicates WT band (1.1Kb) and homozygous insertion line (0.8Kb). Primers used: LP, SALK_075596LP, SALK_075596RP; RP; LB, LBb1.3.

Sequences of primer for genotyping are listed in Appendix II.

Homozygous lines were identified as a lack of WT gene amplification and amplification of T-DNA insert did not have this kind of WT DNA. WT control plants showed amplification of the target genes of the expected size, however, no equivalent amplification was seen in the homozygous insertion mutants. Therefore, the genotyping of mutants could be confirmed to be homozygous T-DNA insertion mutants.

The seeds of the homozygous mutants were harvested from individual plants and then were sown in soil according to the conditions mentioned before (see section 2.1). These 30-day old plants were treated with HT-stress at 32° C for 2 days. *Arabidopsis* Col-0 was used as control. The non-stressed samples were kept in the growth room. All of the growth conditions were kept the same as the previous HT-stress environment. Whole inflorescences on the main shoots were collected from 30-day old plants. Total RNA was extracted and cDNA synthesised. Expression analysis was performed using these cDNA as template for RT-PCR and quantitative RT-PCR for each T-DNA insertion mutant (Fig. 4.10, Fig. 4.11, Fig. 4.12, Fig. 4.13, Fig. 4.14, Fig. 4.15). The wild type *Arabidopsis* Col-0 was also analysed as control.

AtCRT1b was expressed in inflorescence in wild type Col, and no expression was seen in the SALK line 099778 in both RT-PCR and quantitative RT-PCR results (Fig. 4.10c, Fig. 4.10d, Fig. 4.10e). However, the RT-PCR results showed that there was expression in homozygous SALK line 062082, and

quantitative RT-PCR indicated the significantly down-regulated expression level in SALK_062082 than that in WT materials. The SALK_062083 and SALK_099778 insertions are present in the intron (Fig. 4.4a).

AtUTR1 was expressed but was down-regulated in the inflorescence in both of the homozygous T-DNA insertion mutant lines SALK_123541 and GABI_493A10 compared to wild type Col according to RT-PCR and quantitative RT-PCR results (Fig. 4.11b, Fig. 4.11c, Fig. 4.11d). These two mutants have the T-DNA insertion in the last two exons of the *AtUTR1* gene (Fig. 4.5a).

AtMBF1c showed a significantly repressed expression level in SALK_083813 and GABI_434G08 homozygous mutants compared with wild type Col according to RT-PCR and quantitative RT-PCR results (Fig. 4.12b, Fig. 4.12c, Fig. 4.12d). The sequence information indicates that the T-DNA insertion is present in the 5'-UTR in SALK_083813 and C-terminal end of the exon of GABI_434G08 (Fig. 4.6a). There is no intron in *AtMBF1c*.

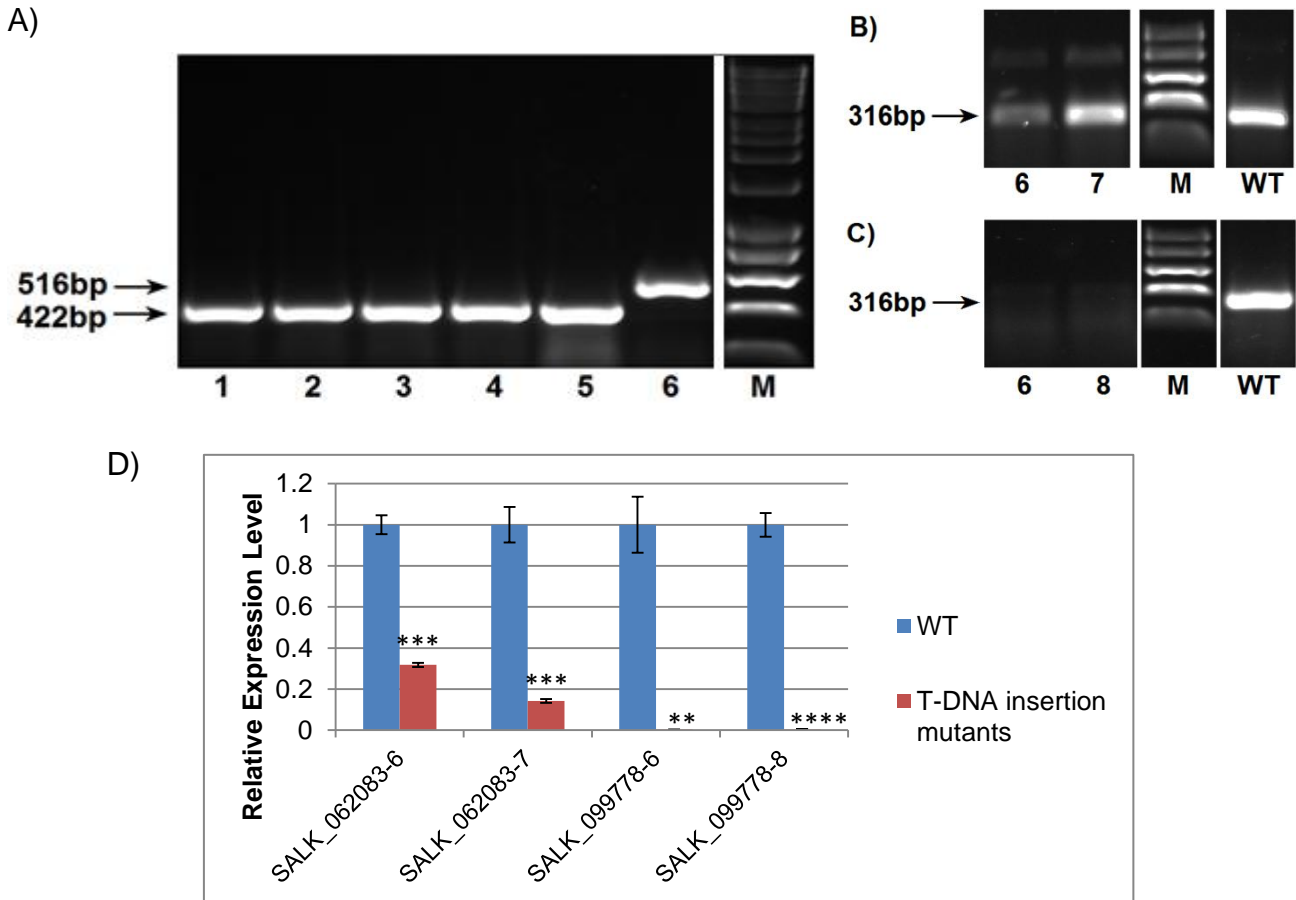
Two SALK lines T-DNA insertion homozygous mutants were identified, SALK_000794 and SALK_023494 for the *AtHOP3* gene. There was no expression of *HOP3* in SALK_000794 (Fig. 4.13b, Fig. 4.13d) but *AtHOP3* was extremely up-regulated in SALK_023494 compared to wild type Col (Fig. 4.13c, Fig. 4.13d). The T-DNA insertions of these two mutants are present in the same exon (first exon of the gene) but in reverse directions (Fig. 4.7a).

AtABI1 showed a greatly reduced expression level in the homozygous SALK_072009 mutant and a reduced expression in GABI_334A12 mutant (Fig. 4.14e) by quantitative RT-PCR, although hardly any difference could be observed from the RT-PCR results (Fig. 4.14b, Fig. 4.14c). The SALK_072009 insertion is present in the first exon from 5'-UTR and GABI_334A12 insertion is in the intron (Fig. 4.8a).

AtHS83 was significantly repressed in homozygous SALK lines 004008 and 075596 in bud tissue (Fig. 4.15b, Fig. 4.15c, Fig. 4.15d). The T-DNA was inserted on the same exon (Exon4) of *HS83* gene for both of these two mutant lines (Fig. 4.9a).

In summary, all of the HT related genes showed reduced expression or were totally silenced in their corresponding homozygous T-DNA insertion mutants. However, there no phenotype difference was observed in these mutants under normal growth conditions. The summary of expression analysis for T-DNA insertion mutants is listed in Table 4.5.

Figure 4.10 Expression analysis of T-DNA insertion mutants for *CRT1b* (AT1G09210) gene.



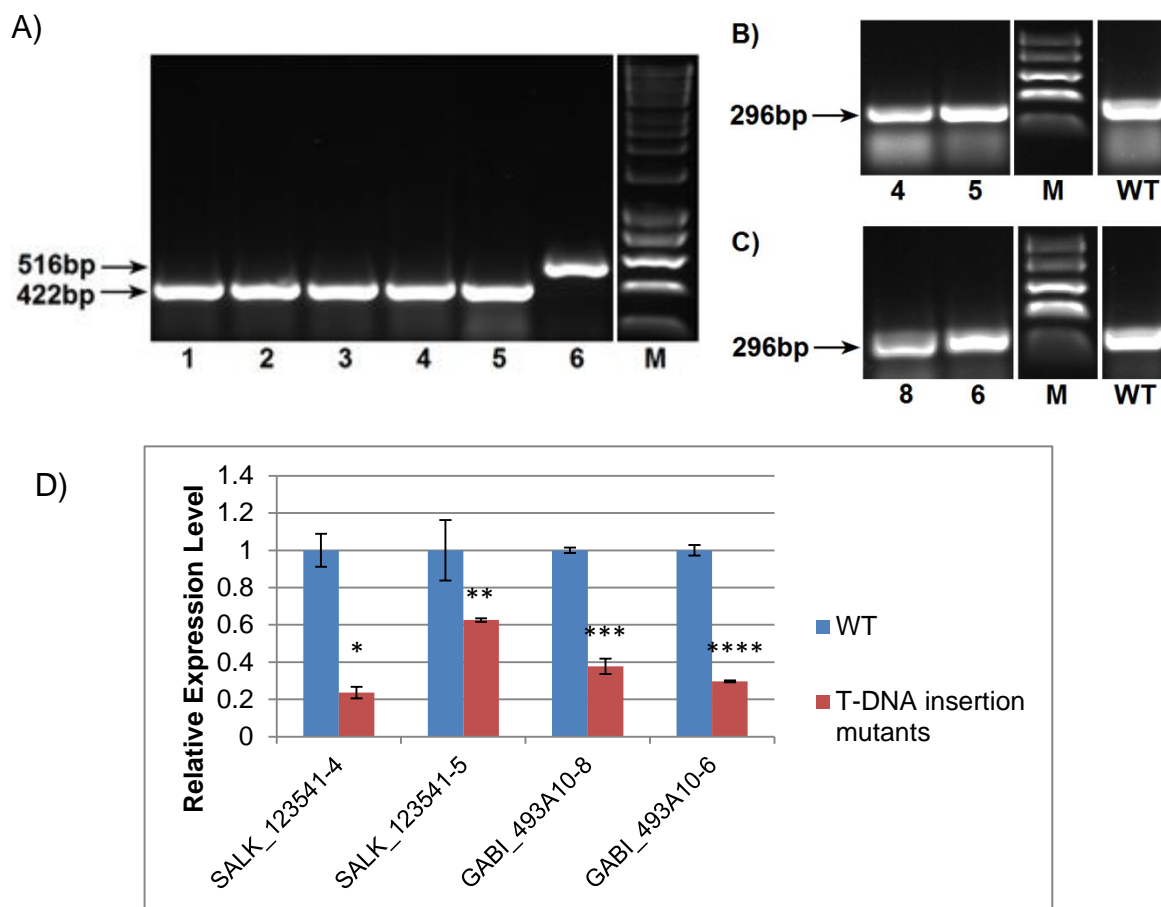
A). RT-PCR to check cDNA quality with *ACTIN7* gene. Lanes 1-5, cDNA as template; 1, SALK_062083-6; 2, SALK_062083-7; 3, SALK_099778-8; 4, SALK_099778-8; 5, *Arabidopsis* Col-0 as WT; 7, *Arabidopsis* Col-0 genomic DNA as template. Primers used: *ACTIN7* (Act7_2F and Act7_443R) (30 cycles), primer sequences see section 4.X). cDNA bands size: 422bp; genomic DNA band size: 516bp. M, HyperLadder I.

B). RT-PCR for SALK_062083 expression analysis. 6, SALK_062083-6; 7, SALK_062083-7; WT, Col-0.

C). RT-PCR for SALK_099778 expression analysis. 6, SALK_099778-6; 8, SALK_099778-8; WT, Col-0.

D). Quantitative RT-PCR for *CRT1b* expression in T-DNA insertion mutants and WT. Primers for target gene: CRT1bF-qPCR and CRT1bR-qPCR; target gene was normalised against internal control *ACTIN7* (primers used: ACT7_2F and ACT7_443R). For each T-DNA insertion line, the expression level was compared with that in WT background (the expression level was defined as 1). Error bars represent standard error. *, **, ***, **** Relatively expression level under HT-stress was significantly different from Non-stressed by *t*-test. *p* value < 0.1, 0.01, 0.001, 0.0001, respectively.

Figure 4.11 Expression analysis of T-DNA insertion mutants for *UTR1* (AT2G02810) gene.



A). RT-PCR to check cDNA quality with *ACTIN7* gene. Lanes 1-5, cDNA as template; 1, SALK_123541-4; 2, SALK_123541-5; 3, GABI_493A10-8; 4, GABI_493A10-6; 5, *Arabidopsis* Col-0 as WT; 6, *Arabidopsis* Col genomic DNA as template. Primers used: *ACTIN7* (Act7_2F and Act7_443R) (30 cycles), primer sequences see section 4.X). cDNA bands size: 422bp; genomic DNA band size: 516bp. M, HyperLadder I.

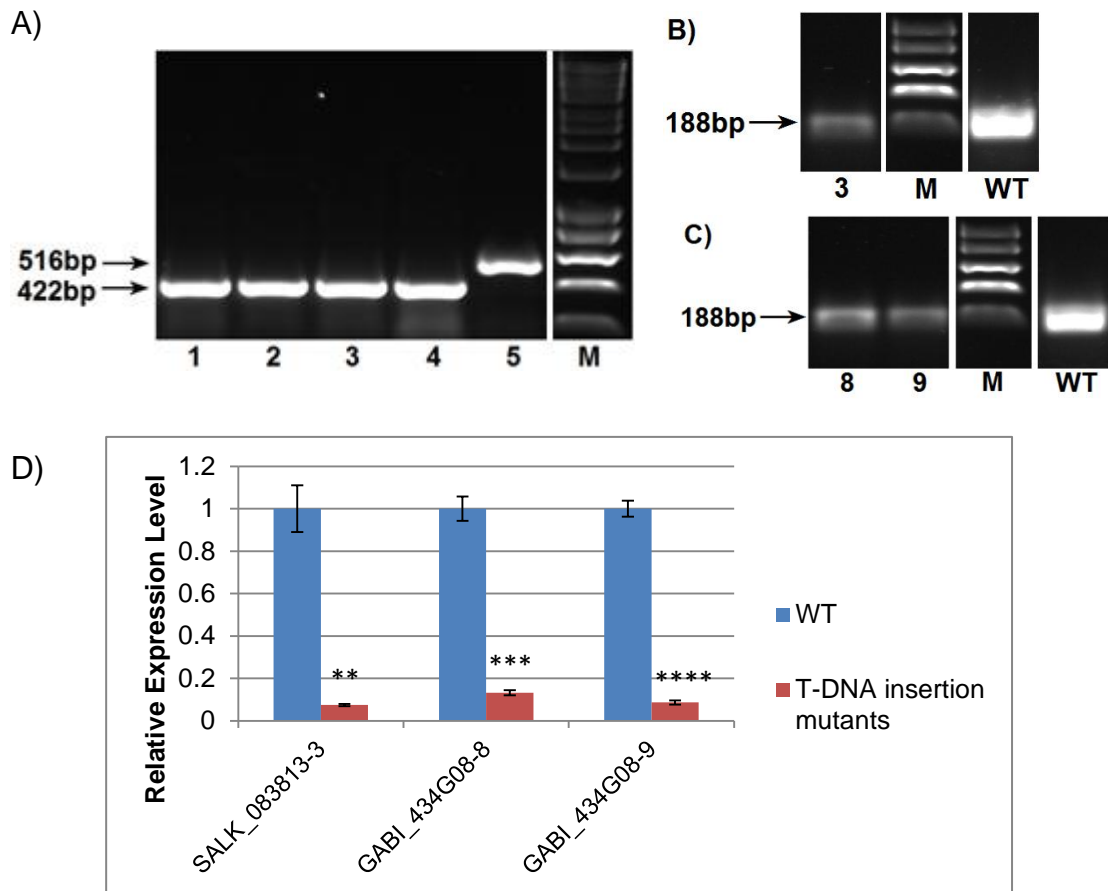
B). RT-PCR for *SALK_062083* expression analysis. 4, SALK_123541-4; 5, SALK_123541-5; WT, Col-0.

C). RT-PCR for *GABI_493A10* expression analysis. 8, GABI_493A10-8; 6, GABI_493A10-6; WT, Col-0.

For RT-PCR, primers used: *UTR1F*-qPCR and *UTR1R*-qPCR.

D). Quantitative RT-PCR for T-DNA insertion mutants expression analysis. Primers for target gene: *UTR1F*-qPCR and *UTR1R*-qPCR; target gene was normalised against internal control *ACTIN7* (primers used: ACT7_2F and ACT7_443R). For each T-DNA insertion line, the expression level was compared with that in WT background (the expression level was defined as 1). Error bars represent standard error. *, **, ***, **** Relatively expression level under HT-stress was significantly different from Non-stressed by *t*-test. *p* value < 0.1, 0.01, 0.001, 0.0001, respectively.

Figure 4.12 Expression analysis of T-DNA insertion mutants for *MBF1c* (AT3G24500) gene.



A). RT-PCR to check cDNA quality with *ACTIN7* gene. Lanes 1-4, cDNA as template; 1, SALK_083813-3; 2, GABI_434G08-8; 3, GABI_434G08-; 4, *Arabidopsis* Col-0 as WT; 5, *Arabidopsis* Col genomic DNA as template. Primers used: *ACTIN7* (Act7_2F and Act7_443R) (30 cycles), primer sequences see section 4.X). cDNA bands size: 422bp; genomic DNA band size: 516bp. M, HyperLadder I.

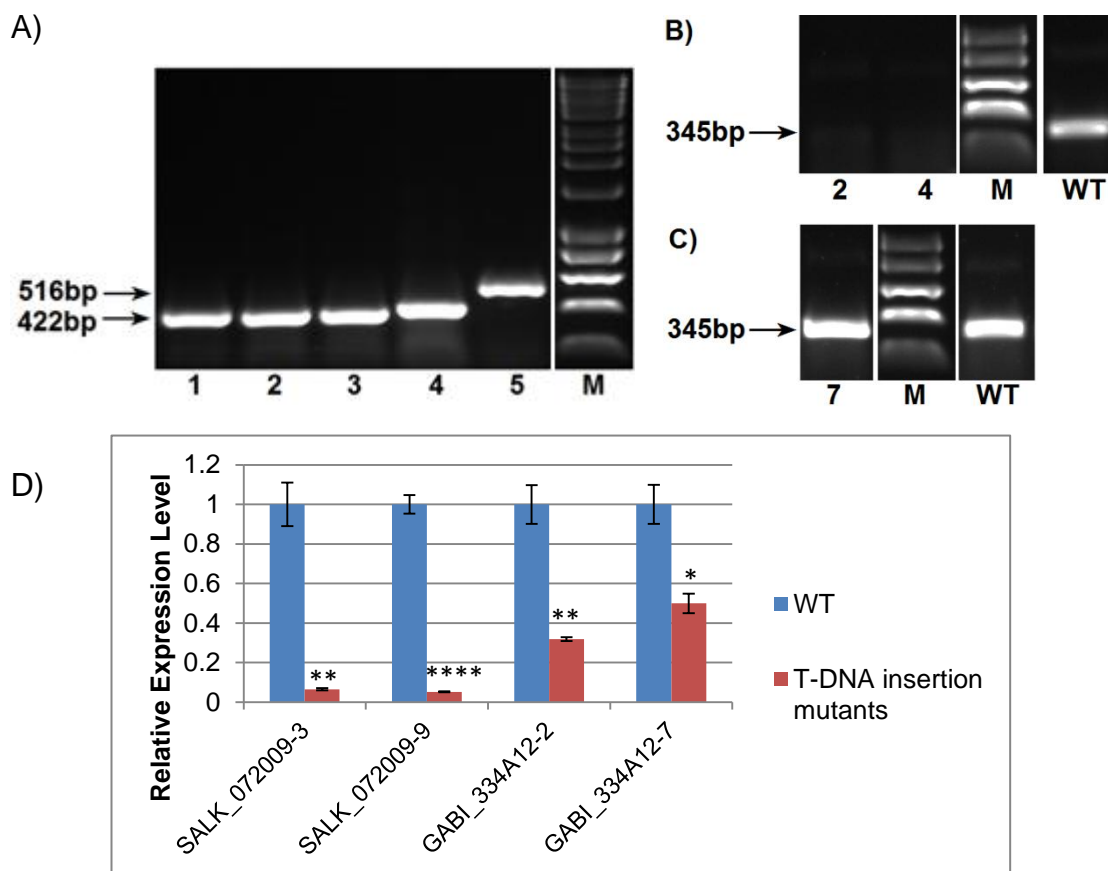
B). RT-PCR for SALK_083813 expression analysis. 3, SALK_083813 WT, Col-0.

C). RT-PCR for GABI_434G08 expression analysis. 8, GABI_434G08-8; 9, GABI_434G08-9; WT, Col-0.

For RT-PCR, primers used: *MBF1cF*-qPCR and *MBF1cR*-qPCR.

D). Quantitative RT-PCR for T-DNA insertion mutants expression analysis. Primers for target gene: *MBF1cF*-qPCR and *MBF1cR*-qPCR; target gene was normalised against internal control *ACTIN7* (primers used: ACT7_2F and ACT7_443R). For each T-DNA insertion line, the expression level was compared with that in WT background (the expression level was defined as 1). Error bars represent standard error. *, **, ***, **** Relatively expression level under HT-stress was significantly different from Non-stressed by *t*-test. *p* value < 0.1, 0.01, 0.001, 0.0001, respectively.

Figure 4.13 Expression analysis of T-DNA insertion mutants for *HOP3* (AT4G12400) gene.



A). RT-PCR to check cDNA quality with *ACTIN7* gene. Lanes 1-5, cDNA as template; 1, SALK_000794-2; 2, SALK_000794-4; 3, SALK_023494-7; 4, *Arabidopsis* Col-0 as WT; 5, *Arabidopsis* Col genomic DNA as template. Primers used: *ACTIN7* (Act7_2F and Act7_443R) (30 cycles), primer sequences see section 4.X). cDNA bands size: 422bp; genomic DNA band size: 516bp. M, HyperLadder I.

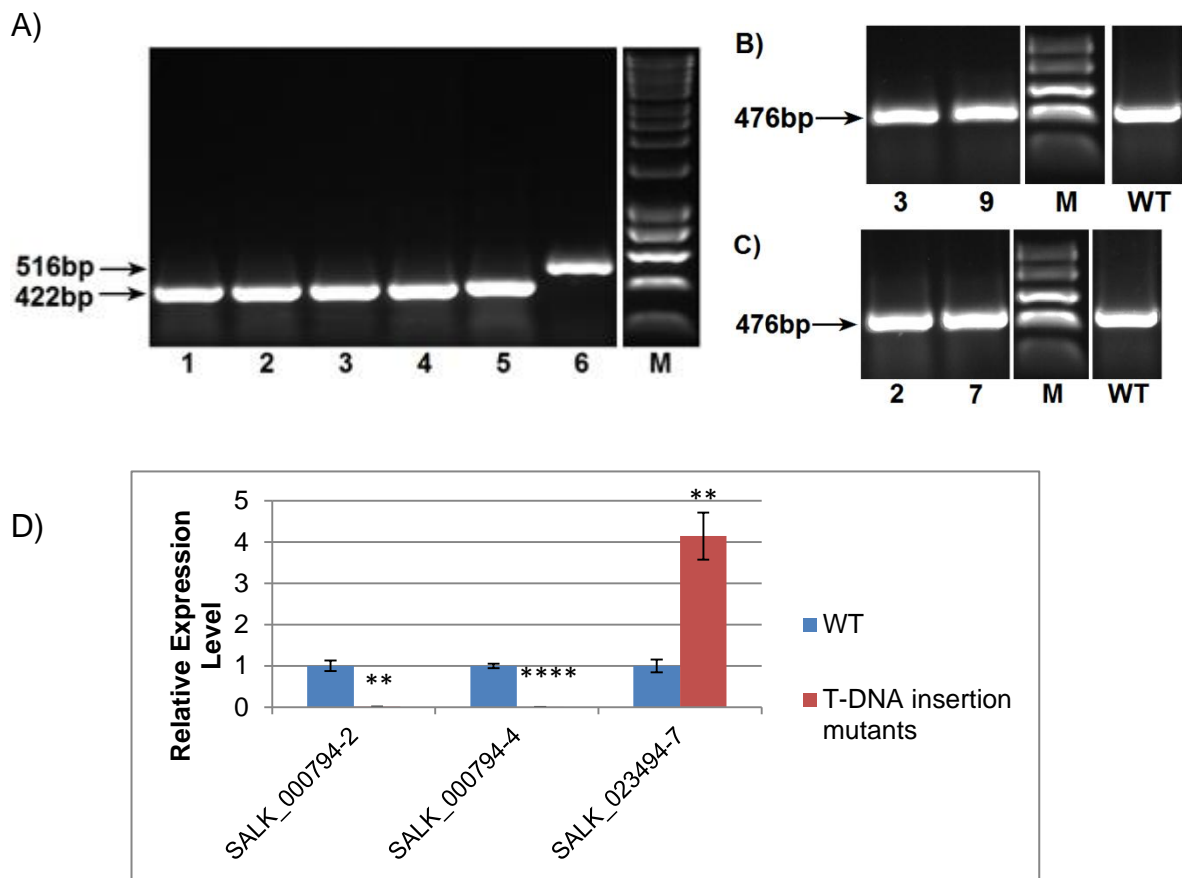
B). RT-PCR for SALK_000794 expression analysis. 2, SALK_000794-2; 4, SALK_000794-4; WT, Col-0.

C). RT-PCR for SALK_023494 expression analysis. 7, SALK_023494-7; WT, Col-0.

For RT-PCR, primers used: *MBF1cF*-qPCR and *MBF1cR*-qPCR.

D). Quantitative RT-PCR for T-DNA insertion mutants expression analysis. Primers for target gene: *HOP3F*-qPCR and *HOP3R*-qPCR; target gene was normalised against internal control *ACTIN7* (primers used: ACT7_2F and ACT7_443R). For each T-DNA insertion line, the expression level was compared with that in WT background (the expression level was defined as 1). Error bars represent standard error. *, **, ***, **** Relatively expression level under HT-stress was significantly different from Non-stressed by *t*-test. *p* value < 0.1, 0.01, 0.001, 0.0001, respectively.

Figure 4.14 Expression analysis of T-DNA insertion mutants for *ABI1* (AT4G26080) gene.



A).

RT-PCR to check cDNA quality with *ACTIN7* gene. Lanes 1-5, cDNA as template; 1, SALK_072009-3; 2, SALK_072009-9; 3, GABI_334A12-2; 4, GABI_334A12-7; 5, *Arabidopsis* Col-0 as WT; 6, *Arabidopsis* Col genomic DNA as template. Primers used: *ACTIN7* (Act7_2F and Act7_443R) (30 cycles), primer sequences see section 4.X). cDNA bands size: 422bp; genomic DNA band size: 516bp. M, HyperLadder I.

B). RT-PCR for *SALK_062083* expression analysis. 3, SALK_072009-3; 9, SALK_072009-9; WT, Col-0.

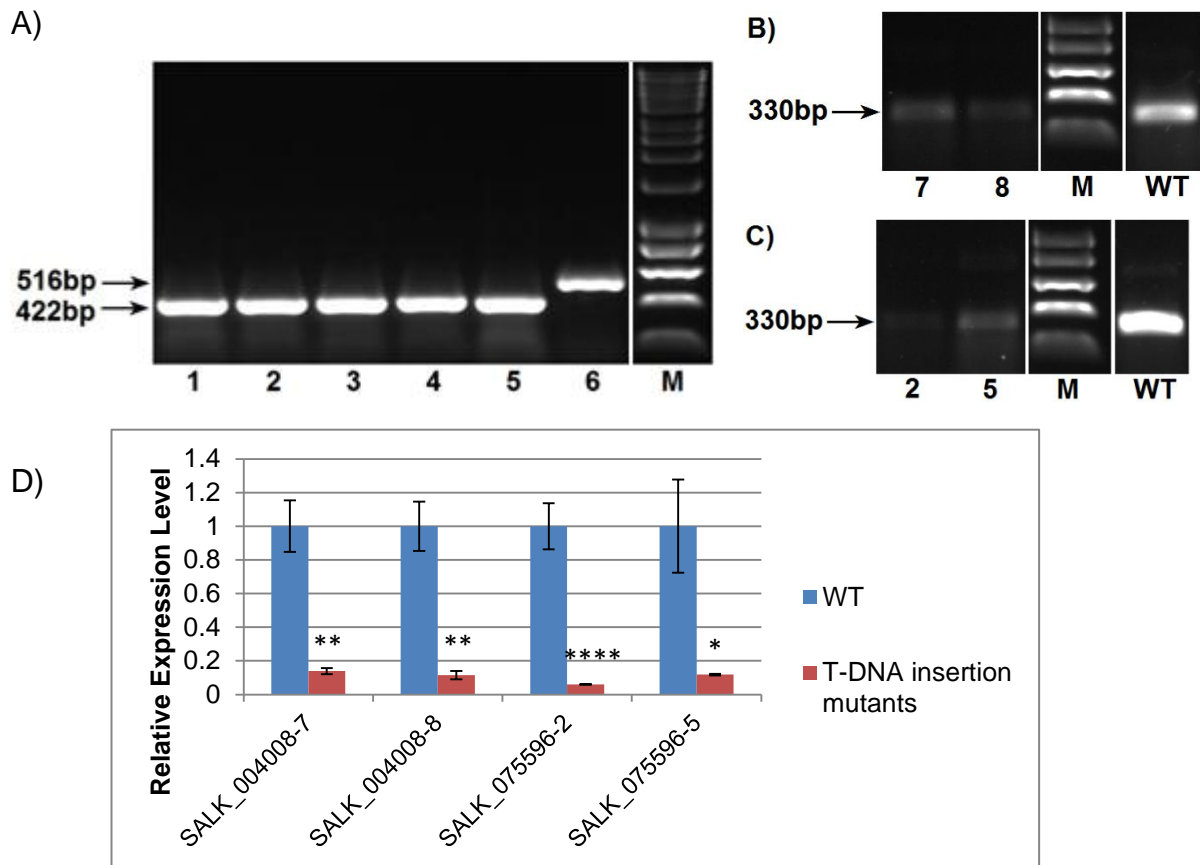
C). RT-PCR for *GABI_334A12* expression analysis. 2, GABI_334A12-2; 7, GABI_334A12-7; WT, Col-0.

For RT-PCR, primers used: *ABI1F*-qPCR and *ABI1R*-qPCR.

D). Quantitative RT-PCR for T-DNA insertion mutants expression analysis.

Primers for target gene: *ABI1F*-qPCR and *ABI1R*-qPCR; target gene was normalised against internal control *ACTIN7* (primers used: ACT7_2F and ACT7_443R). For each T-DNA insertion line, the expression level was compared with that in WT background (the expression level was defined as 1). Error bars represent standard error. *, **, ***, **** Relatively expression level under HT-stress was significantly different from Non-stressed by *t*-test. *p* value < 0.1, 0.01, 0.001, 0.0001, respectively.

Figure 4.15 Expression analysis of T-DNA insertion mutants for *HS83* (*AT5G52640*) gene.



A). RT-PCR to check cDNA quality with *ACTIN7* gene. Lanes 1-5, cDNA as template; 1, SALK_004008-7; 2, SALK_004008-8; 3, SALK_075596-2; 4, SALK_075596-5; 5, *Arabidopsis* Col-0 as WT; 6, *Arabidopsis* Col genomic DNA as template. Primers used: *ACTIN7* (Act7_2F and Act7_443R) (30 cycles), primer sequences see section 4.X). cDNA bands size: 422bp; genomic DNA band size: 516bp. M, HyperLadder I.

B). RT-PCR for **SALK_004008** expression analysis. 7, SALK_004008-7; 8, SALK_004008-8; WT, Col-0.

C). RT-PCR for **SALK_075596** expression analysis. 2, SALK_075596-2; 4, SALK_075596-5; WT, Col-0.

For RT-PCR, primers used: *HS83F*-qPCR and *HS83R*-qPCR.

D). Quantitative RT-PCR for T-DNA insertion mutants expression analysis. Primers for target gene: *HS83F*-qPCR and *HS83R*-qPCR; target gene was normalised against internal control *ACTIN7* (primers used: ACT7_2F and ACT7_443R). For each T-DNA insertion line, the expression level was compared with that in WT background (the expression level was defined as 1). Error bars represent standard error. *, **, ***, **** Relatively expression level under HT-stress was significantly different from Non-stressed by *t*-test. *p* value < 0.1, 0.01, 0.001, 0.0001, respectively.

Table 4.5 Summary of T-DNA insertion mutant expression analysis. “↑” and “↓” indicate up- and down- regulated in RT-PCR results, respectively. “-” indicates no band seen and “=” indicates similar expression in RT-PCR results. Values of quantitative RT-PCR show the relative expression level compare to WT.

Gene	T-DNA insertion lines	Homozygous plant No.	Expression in RT-PCR	Expression in quantitative RT-PCR
<i>CRT1b</i>	SALK_062083	6	↓	0.32
		7	↓	0.14
	SALK_099778	6	-	0
		8	/	0
<i>UTR1</i>	SALK_123541	4	=	0.24
		5	=	0.63
	GABI_493A10	8	↓	0.38
		6	=	0.3
<i>MBF1c</i>	SALK_083813	3	↓	0.07
	GABI_434G08	8	↓	0.13
		9	↓	0.09
<i>HOP3</i>	SALK_072009	2	-	0.01
		4	-	0
	GABI_334A12	7	↑	4.14
<i>ABI1</i>	SALK_000794	3	=	0.07
		9	=	0.05
	SALK_023494	2	=	0.32
		7	=	0.5
<i>HS83</i>	SALK_004008	7	-	0.14
		8	-	0.12
	SALK_075596	2	-	0.06
		5	-	0.12

4.3.2.2 Morphological analysis of T-DNA insertion mutants with and without HT-stress

The homozygous T-DNA insertion mutants and wild type Col plants were grown under normal conditions (as mentioned in section 2.1) until 30-day stage and were then treated with HT-stress at 32° C for 2 days. Control samples of these mutants and wild type were maintained in the normal environment according to the method mentioned in section 2.2. Pollen viability (see section 2.4) and *in vitro* pollen germination (see section 2.5) were performed at D1 and D2 time points. Silique length and seed number measurements (see section 2.6) were carried out 15 days after completion of HT-stress. According to the previous data of DAPI staining for pollen development stages, the pollen samples which were collected at D1 time point were in the mature pollen and tricellular pollen at the start of HT-stress, and the buds which would produce to the siliques No. 1-3 were also in the mature pollen and tricellular pollen when HT-stress began. Those that were collected at D2 time point included silique No. 4-6 which were at pollen mitosis stages at the start of HT-stress.

AtCRT1b is repressed in homozygous SALK_062083 and is knocked out in the homozygous SALK_099778 mutant. The average pollen viability and *in vitro* pollen germination rate were higher than that in wild type Col materials after 1 day HT-stress, which showed almost same level with non-stressed sample.

But these rates reduced after 2 day HT-stress (Fig. 4.16a, Fig. 4.16b). The results were similar with the data of silique length and seed number. The oldest siliques produced were longer with more seeds than those in wild type samples (Fig. 4.16c No.1-3 silique, Fig. 4.16d No.1-3 silique). However, the siliques that were produced after these were more stressed than wild type (Fig. 4.16c No.4-20 silique, Fig. 4.16d No.4-20 silique), which HT-stressed samples presented a shorted length than non-stressed control ones. Moreover, previous expression analysis of *AtCRT1b* in wild type indicates it expresses higher in the stages before PMII than that after tricellular stages according to quantitative RT-PCR (Fig. 4.3a) and the bioinformatics GO analysis (Appendix III), indicates expression of *AtCRT1b* is specific during tapetum PCD. These results indicate the loss of function of *AtCRT1b* may delay HT response in late pollen developmental stages but strongly depresses the HT tolerance in all of the younger stages.

Both of two homozygous T-DNA insertion mutants SALK_123541 and GABI_493A10 showed reduced *AtUTR1* expression rather than no expression. T-DNA insertions are present in exons in both of the two mutant lines but in different exon of the gene sequence (Fig. 4.5a) and the expression in the inflorescence was repressed to similar level (Fig. 4.11d) according to quantitative RT-PCR. However, the morphological alteration was not similar in these two mutants. Average pollen viability and *in vitro* pollen germination was reduced more in wild type and SALK_123541 than those not HT-stressed, but

almost no variation was seen in GABI_493A10 between HT-stressed samples and non-stressed after 1 day HT-stress (Fig. 4.11a, Fig. 4.11b). The percentage of pollen viability and *in vitro* pollen germination was decreased to an approximately similar level in both of these T-DNA insertion mutants and wild type after 2 days HT-stress (Fig. 4.11a, Fig. 4.11b). Silique length and seed number were not reduced in the oldest siliques in homozygous GABI_493A10 mutant, but decreased soon after. Nevertheless, the silique length in homozygous SALK_123541 was relatively longer, and the seed number was always less than that in wild type after 2 days HT-stress. However, all of these morphological variations in SALK_123541 after HT-stress were similar to those in WT, which indicates that exon No.6 (Fig. 4.5) possible has more important role than exon No.7 in *AtUTR1* gene, and T-DNA inserts in exon No.6 may lead to more obvious alteration on pollen development and reproductive growth. The expression analysis showed that *AtUTR1* also expresses higher in the stages before PMII than that after tricellular according to quantitative RT-PCR (Fig. 4.3b) and GO (Appendix III), which indicates *AtUTR1* is induced during tapetum development. Comparing the silique length and seed number in SALK_123541, GABI_493A10 showed a very rapid recovery, while there was no difference of the silique length and seed number in the youngest samples compared with wild type after HT-stress. Therefore, the result suggests reduced expression of *AtUTR1* would not lead to a clear alteration of HT resistance during pollen development.

RT-PCR and quantitative RT-PCR results indicated the *AtMBF1c* gene was not knocked out but significantly repressed in homozygous SALK_083813 and GABI_434G08 mutants (Fig. 4.12b, Fig. 4.12c, Fig. 4.12d). Quantitative RT-PCR analysis showed *MBF1c* was up-regulated in all three staged group samples but was then repressed after 2 days HT-stress as well as during recovery (Fig. 4.3c), which indicates *AtMBF1c* is sensitive to HT-stress but this altered expression level recovered. In the knock down mutants of *AtMBF1c*, average pollen viability and *in vitro* germination was not seriously affected in SALK_083813 but showed a difference in the GABI_434G08. Pollen viability and *in vitro* germination was increased after 1 day HT-stress and then decreased to a very low level after 2 days HT-stress in the GABI_434G08 mutant (Fig. 4.18a, Fig. 4.18b). Previous results indicate these pollen materials were collected from mature pollen and *AtMBF1c* expression level was more repressed at D2 in the “Mature” group than that at D1 according to previous quantitative RT-PCR results (Fig. 4.3c), and loss of function of *AtMBF1c* in these staged samples lead to higher pollen viability. Furthermore, the bud samples after 2 days HT-stress produced longer siliques and more seeds in the oldest siliques on the main shoot, but the development was repressed in the following younger ones to result in shorter siliques and less seeds (Fig. 4.18c, Fig. 4.18d). These results indicate loss of function of *AtMBF1c* may increase HT resistance in the late pollen developmental stages but decrease the HT tolerance in the other stages during pollen development.

T-DNA insertions were present at almost the same position on *AtHOP3* gene sequence in SALK_000794 and SALK_023494 (Fig. 4.7a). Interestingly, *AtHOP3* was completely knocked out in homozygous SALK_000794 mutants but showed an up-regulated expression level in homozygous SALK_023494 (Fig. 4.13b, Fig. 4.13c, Fig. 4.13d). Average pollen viability and the *in vitro* germination rate was high in the homozygous SALK_000794 mutant compared to wild type after both of 1 day and 2 days HT-stress, but average viability and germination rate was higher only after 1 day HT-stress in SALK_023494 and decreased to a similar percentage as wild type. Therefore, both the loss of function and up-regulation of *AtHOP3* may decrease HT sensitivity but the loss of function mutant displayed longer sensitive period than that of the up-regulated mutant. After 2 days HT-stress, the siliques produced much longer in the several oldest ones and there were also more seeds in these siliques although the following younger ones those were produced later were shorter than wild type and had less seeds, which also support the putative function of *AtHOP3*.

AtABI1 expression was almost completely silenced in homozygous SALK_072009 but just down-regulated in homozygous GABI_334A12 according to expression analysis results (Fig. 4.14d). For the following morphological analysis, the GABI_334A12-2 which showed lower *AtABI1* expression level was used rather than GABI_334A12-7. Average pollen viability and *in vitro* germination represented higher percentage in both of

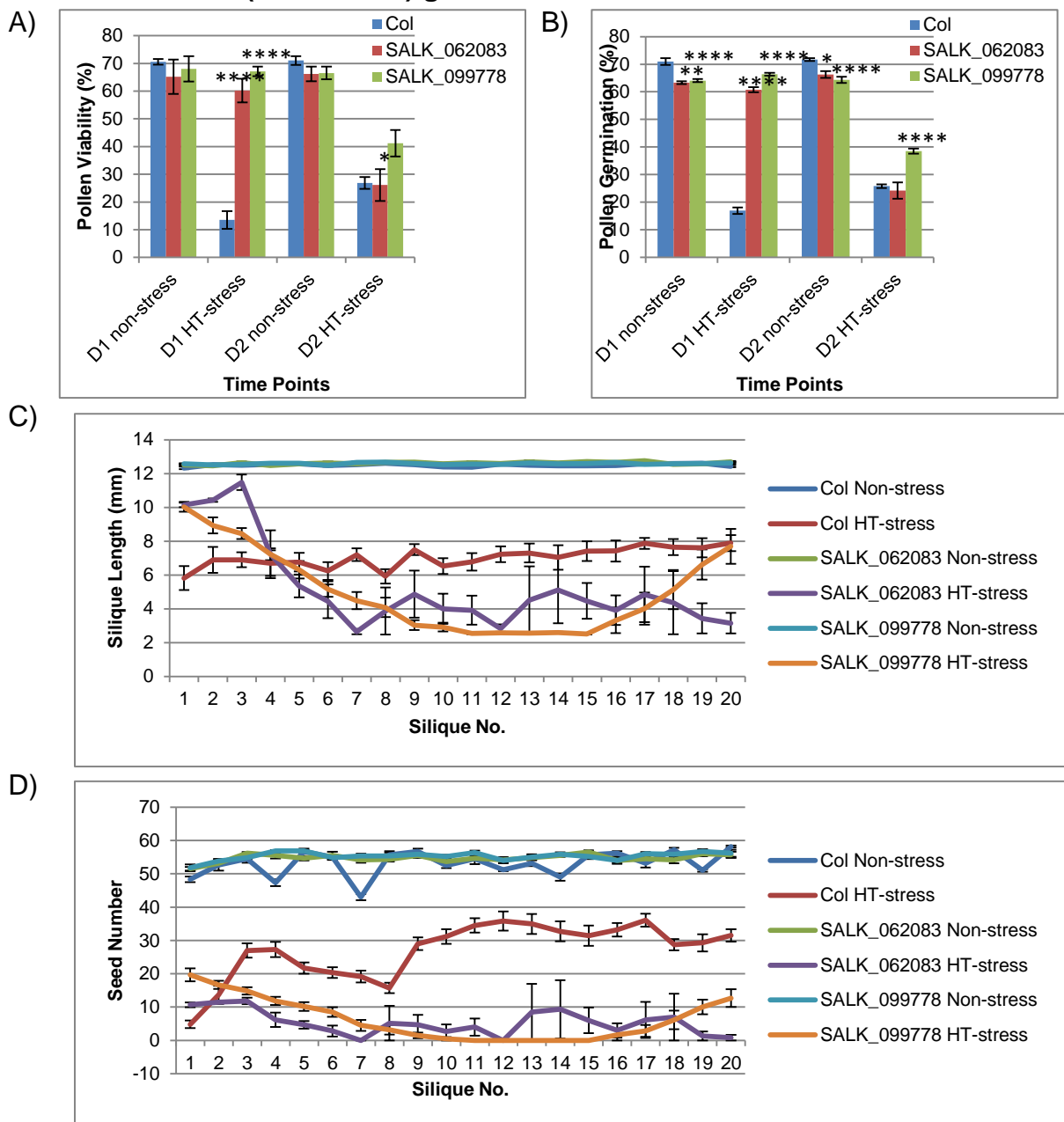
these two mutants after 1 day HT-stress, while these rates were higher in GABI_334A12 than those in SALK_072009 (Fig. 4.20a, Fig. 4.20b). However, pollen viability and *in vitro* germination rate reduced rapidly in SALK_072009 after 2 days HT-stress, and were much less than that in wild type. These were also decreased in GABI_334A12 but still showed a higher level than wild type (Fig. 4.20a, Fig. 4.20b). Siliques were longer with more seeds than WT in GABI_334A12 mutant in the oldest siliques, but were always shorter with less seeds in SALK_072009 (Fig. 4.20c, Fig. 4.20d). The results indicate loss of function of *AtABI1* may reduce HT resistance quickly during pollen development.

AtHS83 expression was significantly repressed in the homozygous SALK line mutants 004008 and 075596 to a similar level (Fig. 4.15c, Fig. 4.15c, Fig. 4.15d), although the T-DNA insertions were present in different positions on the gene sequence (Fig. 4.9a). The average pollen viability and *in vitro* germination rate was higher in SALK_004008 than that in wild type samples after 1 day HT-stress although this increase was not significant, but decreased to a significantly lower level than wild type after 2 days HT-stress (Fig. 4.21a, Fig. 4.21b). The silique length and seed number data of SALK_004008 after 2 days HT-stress showed longer silique size and a greater seed number in the oldest siliques than those in wild type, and then seriously decreased in the following siliques produced which resulted in smaller size of siliques and lower seed number than wild type (Fig. 4.21c, Fig. 4.21d). These data in

SALK_075596 were not same in SALK_004008. Pollen viability and *in vitro* germination rate were maintained at a higher level than that in wild type after both of 1 day and 2 days HT-stress, and then produced siliques that were longer with more seeds than wild type after 2 days HT-stress (Fig. 4.21). This difference may be due to the function domain on *AtHS83* gene. Nevertheless, loss of function of *AtHS83* lead to defects on seeds produced under HT-stress (Fig. 4.21d).

To summarise these HT related and tapetum specific genes, loss of function of these genes lead to a delayed HT response in pollen viability and seed production than in WT under HT-stress, but the ultimate impact by losing function of these genes is reduced seed production after HT-stress.

Figure 4.16 Morphological analysis of WT and T-DNA insertion mutants of *CRT1b* (AT1G09210) gene with and without HT-stress.

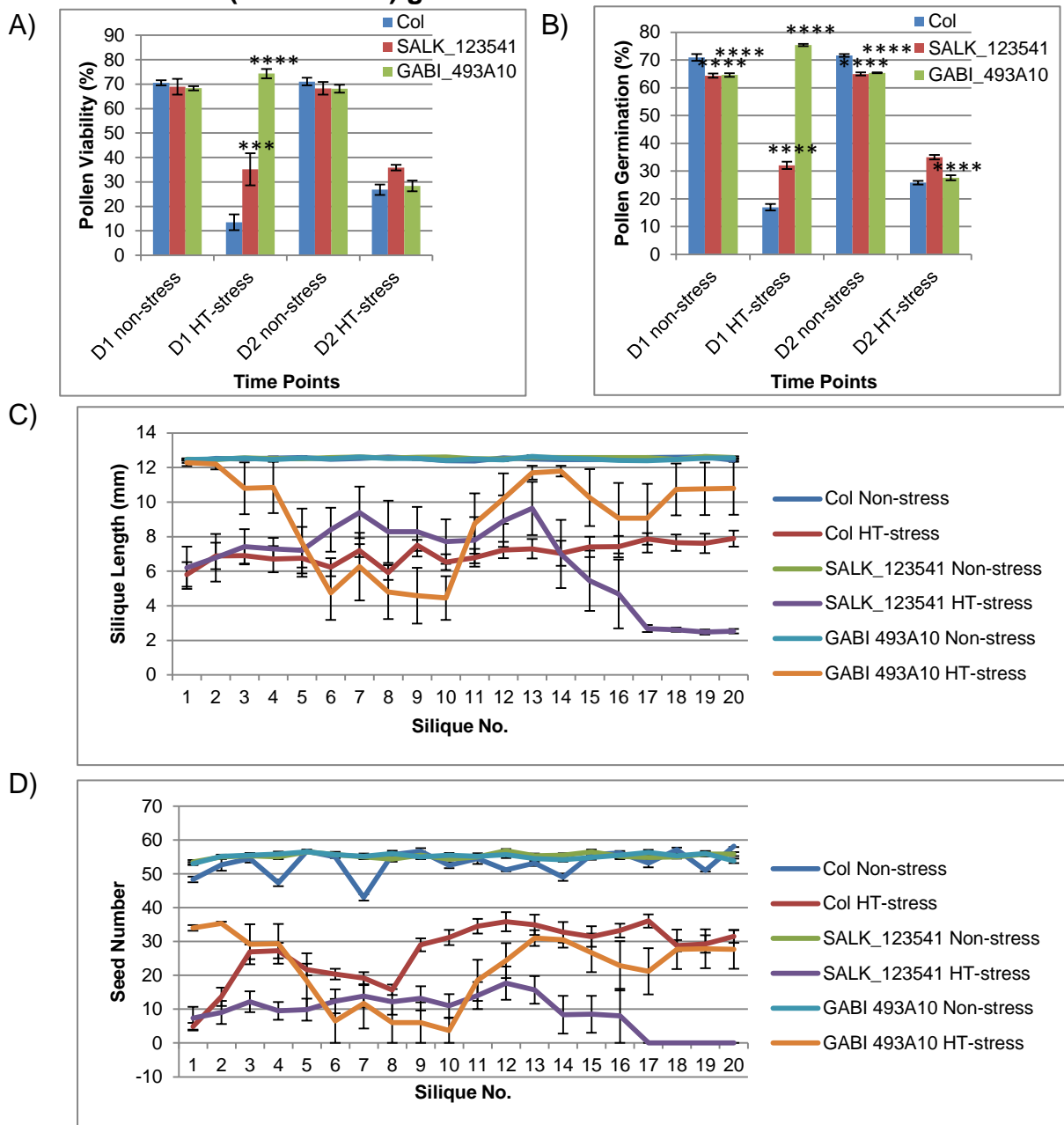


A) Pollen viability by FDA staining and B) *In vitro* pollen germination percentage. Pollen was collected from fully opened flowers after 1 day (D1) and 2 days (D2) HT-stress and at corresponding non-stressed points. Error bars represent the standard error. *, **, **** Relatively expression level under HT-stress was significantly different from Non-stressed by ANOVA. p value < 0.1, 0.01, 0.0001, respectively.

C) Silique length measurement and D) seed number per silique. Samples were measured 15-days after HT-stress experiment. The first produced silique after HT-stress was labelled as 1 and then to 20 according to the growth sequence. Only the siliques on the main shoot were used.

CRT1b is down-regulated in SALK_062038 and knock out in SALK_099778.

Figure 4.17 Morphological analysis of WT and T-DNA insertion mutants of *UTR1* (AT2G02810) gene with and without HT-stress.

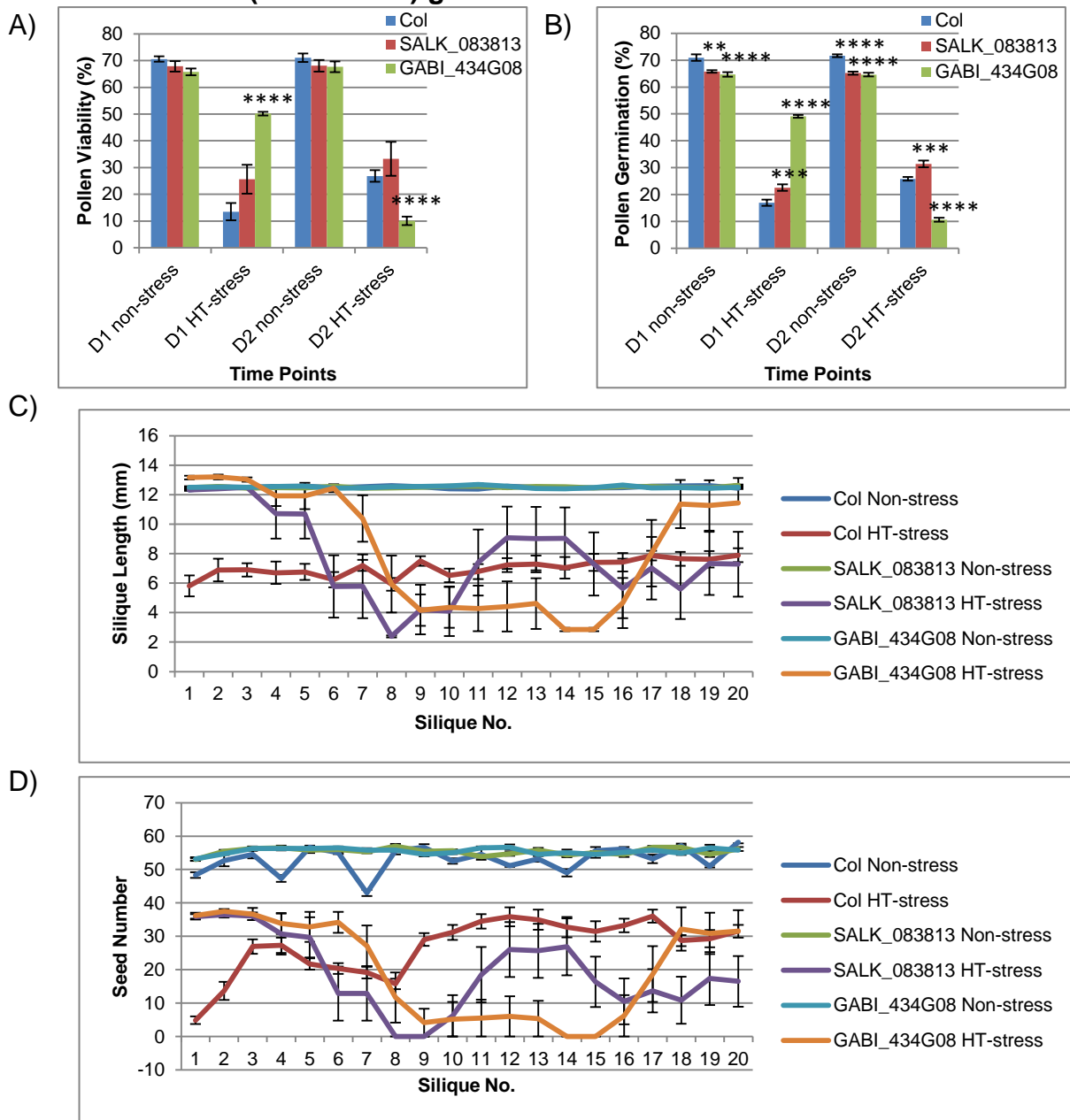


A) Pollen viability by FDA staining and B) *In vitro* pollen germination percentage. Pollen was collected from fully opened flowers after 1 day (D1) and 2 days (D2) HT-stress and at corresponding non-stressed points. Error bars represent the standard error. ***, **** Relatively expression level under HT-stress was significantly different from Non-stressed by ANOVA. p value < 0.001, 0.0001, respectively.

C) Silique length measurement and D) seed number per silique. Samples were measured 15-days after HT-stress experiment. The first produced silique after HT-stress was labelled as 1 and then to 20 according to the growth sequence. Only the siliques on the main shoot were used.

UTR1 is down-regulated in both SALK_123541 and GABI_493A10.

Figure 4.18 Morphological analysis of WT and T-DNA insertion mutants of *MBF1c* (AT3G24500) gene with and without HT-stress.

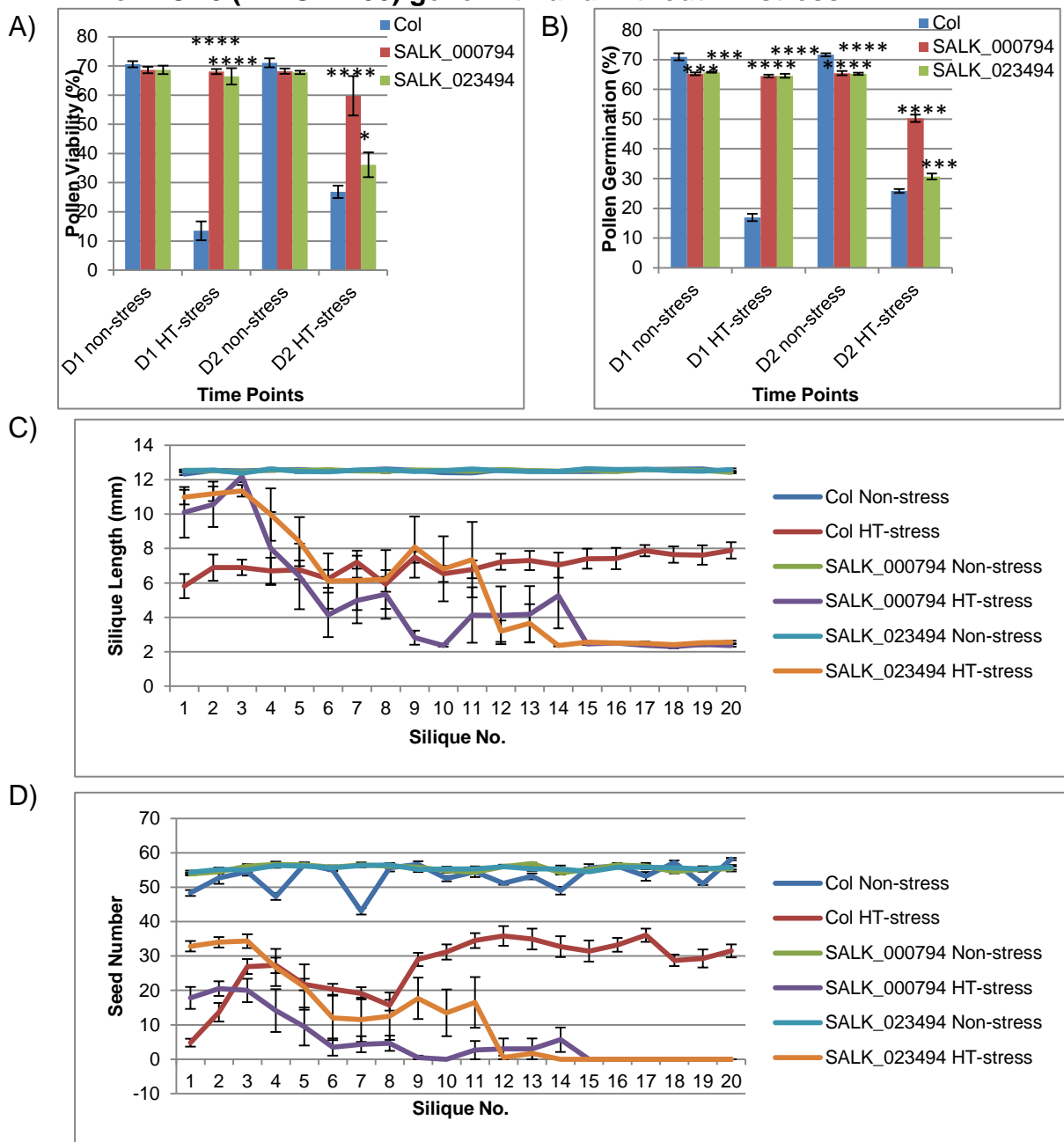


A) Pollen viability by FDA staining and B) *In vitro* pollen germination percentage. Pollen was collected from fully opened flowers after 1 day (D1) and 2 days (D2) HT-stress and at corresponding non-stressed points. Error bars represent the standard error. **, ***, **** Relatively expression level under HT-stress was significantly different from Non-stressed by ANOVA. p value < 00.1, 0.001, 0.0001, respectively.

C) Silique length measurement and D) seed number per silique. Samples were measured 15-days after HT-stress experiment. The first produced silique after HT-stress was labelled as 1 and then to 20 according to the growth sequence. Only the siliques on the main shoot were used.

MBF1c is down-regulated in both SALK_083813 and GABI_434G08.

Figure 4.19 Morphological analysis of WT and T-DNA insertion mutants of *HOP3* (AT4G12400) gene with and without HT-stress.

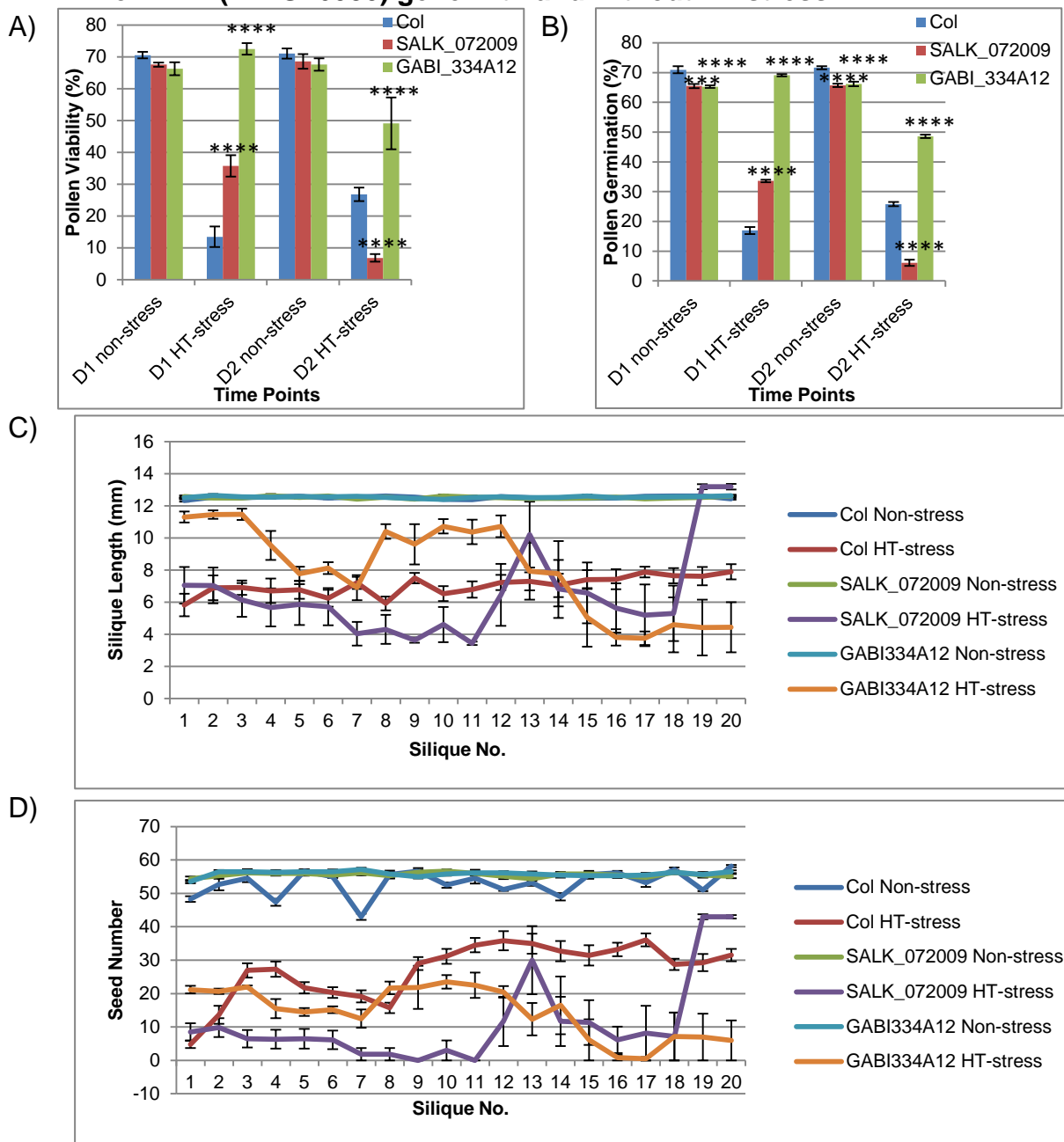


A) Pollen viability by FDA staining and B) *In vitro* pollen germination percentage. Pollen was collected from fully opened flowers after 1 day (D1) and 2 days (D2) HT-stress and at corresponding non-stressed points. Error bars represent the standard error. *, ***, **** Relatively expression level under HT-stress was significantly different from Non-stressed by ANOVA. p value < 0.1, 0.001, 0.0001, respectively.

C) Silique length measurement and D) seed number per silique. Samples were measured 15-days after HT-stress experiment. The first produced silique after HT-stress was labelled as 1 and then to 20 according to the growth sequence. Only the siliques on the main shoot were used.

HOP3 is knock out in SALK_000794 and up-regulated in SALK_023494.

Figure 4.20 Morphological analysis of WT and T-DNA insertion mutants of *ABI1* (AT4G26080) gene with and without HT-stress.

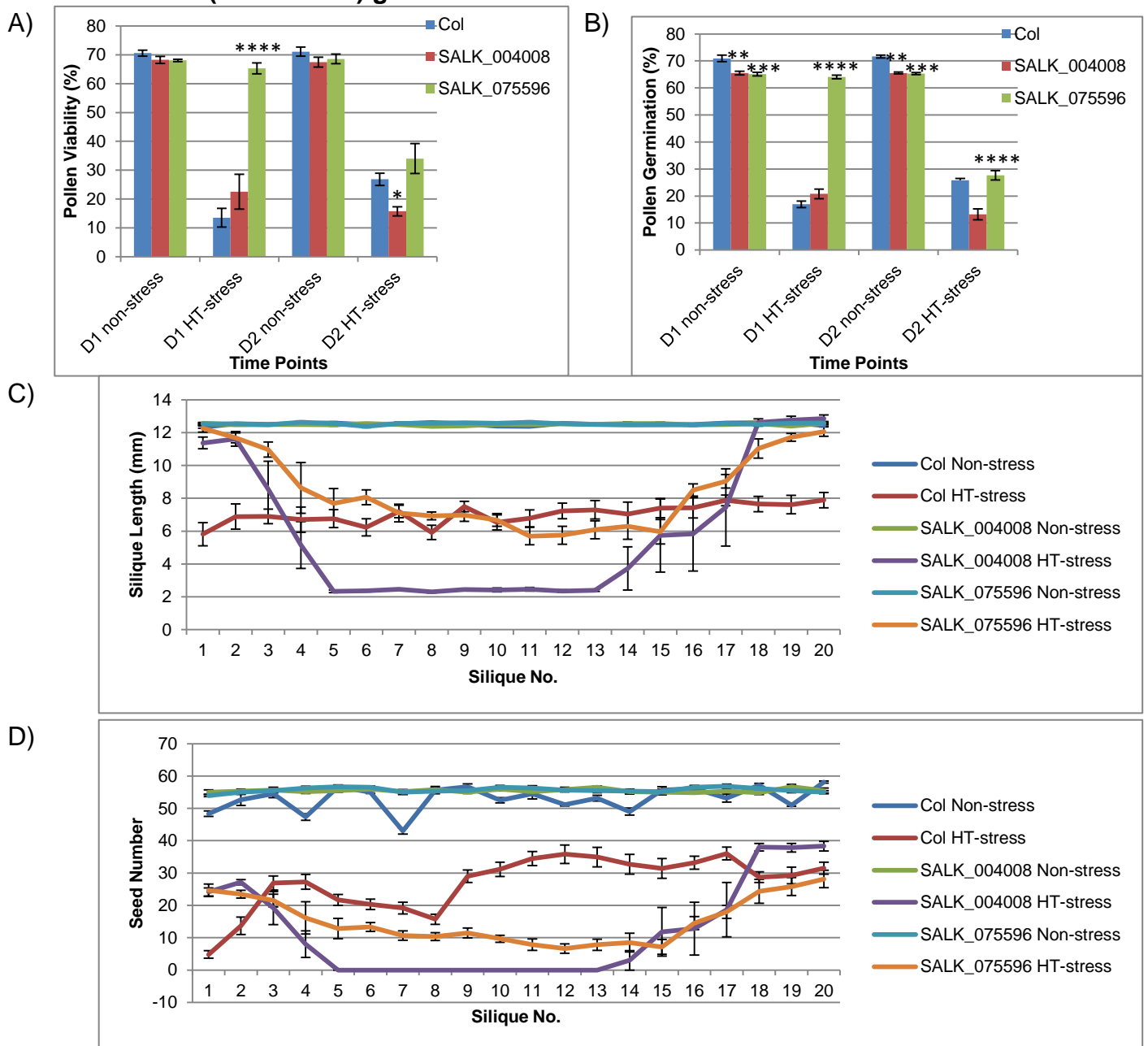


A) Pollen viability by FDA staining and B) *In vitro* pollen germination percentage. Pollen was collected from fully opened flowers after 1 day (D1) and 2 days (D2) HT-stress and at corresponding non-stressed points. Error bars represent the standard error. ***, **** Relatively expression level under HT-stress was significantly different from Non-stressed by ANOVA. p value < 0.001, 0.0001, respectively.

C) Silique length measurement and D) seed number per silique. Samples were measured 15-days after HT-stress experiment. The first produced silique after HT-stress was labelled as 1 and then to 20 according to the growth sequence. Only the siliques on the main shoot were used.

ABI1 is down-regulated in both SALK_072009 and GABI_334A12.

Figure 4.21 Morphological analysis of WT and T-DNA insertion mutants of *HS83* (AT5G52640) gene with and without HT-stress.



A) Pollen viability by FDA staining and B) *In vitro* pollen germination percentage. Pollen was collected from fully opened flowers after 1 day (D1) and 2 days (D2) HT-stress and at corresponding non-stressed points. Error bars represent the standard error. *, **, ***, **** Relatively expression level under HT-stress was significantly different from Non-stressed by ANOVA. *p* value < 0.1, 0.01, 0.001, 0.0001, respectively.

C) Silique length measurement and D) seed number per silique. Samples were measured 15-days after HT-stress experiment. The first produced silique after HT-stress was labelled as 1 and then to 20 according to the growth sequence. Only the siliques on the main shoot were used.

HS83 is down-regulated in both SALK_004008 and SALK_075596.

4.4 DISCUSSION

AtCRT1b is expressed at a higher level before pollen mitosis compared to tricellular and mature pollen stages in wild type without HT-stress (Fig. 4.3a). The expression level in tricellular and mature pollen stages showed little difference throughout HT-stress and the following recovery period, but samples before tricellular stage displayed significantly repressed expression level under HT-stress (Fig. 4.3a). However, the quantitative RT-PCR results of WT buds indicated the expression of *AtCRT1b* was reduced in the entire pollen developmental stages during both the HT-stress and recovery phases compared to non-stressed WT ones. Morphological analysis of T-DNA insertion mutants, which are silenced in *AtCRT1b* expression, with HT-stress showed enhanced HT sensitivity during pollen development as the HT-stressed plants produced shorter siliques and less seeds compared to HT-stressed WT control samples (Fig. 4.16). Previous research has revealed *AtCRT1b* was down-regulated in mature pollen by cold-stress and involved with signal transduction (Changsong & Diqiu, 2010), and loss of function of *AtCRT1b* and two other calreticulins, *AtCRT1a* and *AtCRT3*, increased sensitivity to drought, indicating a possible role of calreticulins in the *Arabidopsis* response to drought stress (Kim et al., 2013). It has been also speculated that *AtCRT1b* is co-expressed with *CRT1a* as part of a larger network of Endoplasmic Reticulum (ER) chaperones, which provides a basal folding apparatus for the newly synthesized proteins in the ER (Christensen et

al., 2010). The ER is an organelle found in the cells of eukaryotic organisms and functions as a manufacturing and packaging system (Kato et al., 2011). In animal cells, CRT is an important component for protein folding and Ca^{2+} homeostasis in the ER (Michalak et al., 1999) and the over-expressed maize *CRT Arabidopsis* plants showed reduction of leaf chlorosis when grown on Ca^{2+} -depleted media compared to wild-type control plants (Wyatt et al., 2002). Christensen et al. (2010) reported that there was strong activation of the *AtCRT1a* and *AtCRT1b* promoters in response to tunicamycin which is indicative of an association to tunicamycin-induced ER stress, or the unfolded protein response (UPR), with loss of *AtCRT1b* constitutively triggering a stress similar to UPR in the seedlings. There are two very prominent components of the tapetum: the plastids and lipid bodies (Quilichini et al., 2014). The lipid bodies first form as simple lipid droplets in association with the ER, and as the tapetal cells mature, the developing and new lipid bodies are intimately associated with the rough ER (Platt et al., 1998). The components of the lipidic pollen coat are produced and stored in the tapetum and deposited onto pollen upon tapetum programmed cell death, and the pollen coat components are liberated upon the breakdown of two specialized organelles in the tapetum, elaioplasts and tapetosomes, which are unique, densely packed organelles that are intimately associated with the ER (Quilichini et al., 2014). It is possible that loss of function of *AtCRT1b* would lead to a defect of UPR in the ER and then affect the structure of the tapetum and its PCD, which might release

defective tapetosomes that could not form an efficient pollen coat. This would cause insufficient protection of pollen in the T-DNA insertion mutants compared with that of the wild type, which would result in reduced HT resistance and less seeds produced.

Similarity with *AtCRT1b*, the expression of *AtUTR1* is higher in the buds before tricellular stage, and is also significantly depressed by HT-stress (Fig. 4.3b). Reyes et al. (2010) have reported there are no developmental abnormalities in the *AtUTR1* mutant compared to wild type but pollen grains in the *atutr1* and *atutr3* double mutant have an abnormal development, and loss of function of *AtUTR1* could be recovered by *AtUTR3*. However, *AtUTR1* is reported partially penetrant for the female gametophyte and important for embryo sac development (Reyes et al., 2010). *AtUTR1*, which works together with *AtUTR3*, is exclusively located in the ER and involved in the transport of UDP-glucose and UDP-galactose, and is co-expressed with ER chaperones and genes related to UPR (Reyes & Orellana, 2008). Therefore, *AtUTR1* is considered as part of a common transcriptional network integrated of genes that code for proteins involved in the protein folding machinery (Reyes et al., 2010). *AtUTR1* is up-regulated under conditions that induce UPR, which would trigger the accumulation of misfolded proteins (Reyes et al., 2006). Although the lack of *AtUTR1* seems to result in the constitutive activation of the UPR, suggesting that these plants are continuously under stress (Reyes et al., 2006), there is no significant variation of phenotype after HT-stress in the loss of function of the

AtUTR1 mutant. This would also suggest that function of *AtUTR1* is acting redundantly with another gene, possibly *AtUTR3*. Therefore, although *AtUTR1* expression is repressed by HT-stress this down-regulation would not reflect on the phenotype.

AtMBF1c expression level is up-regulated in inflorescence tissue after 1 day of HT-stress but is depressed rapidly to a lower level equivalent to wild type level in the tricellular and mature pollen developmental stages, and maintained in the following recovery period once HT-stress is finished (Fig. 4.3c), which indicated *AtCRT1b* was sensitive to temperature change at late pollen developmental stages when the tapetum was degenerating. The T-DNA insertion mutant SALK_083813 that was identified for *AtMBF1c* showed reduced pollen viability and germination rate decreased more slowly than that of the wild type but reached a similar even lower level later (Fig. 4.18a, Fig. 4.18b), while another mutant GABI_434G08 showed less affection after 1 day HT-stress but lower percentage of pollen viability and germination after 2 days HT-stress. These results indicate that the function region maybe in the front part of the *MBF1c* gene sequence. The trend for silique length and seed number data of the two T-DNA insertion mutants with 2 days HT-stress indicate that these data continue to reduce although the oldest several siliques were longer and produced more seeds than wild type (Fig. 4.18c, Fig. 4.18d). There are three subtypes of the *Arabidopsis MBF1* gene, *MBF1a* and *MBF1b* show similar amino acid sequences and tissue-specific expression patterns but are

quite different from *MBF1c* (Tsuda & Yamazaki, 2004). It has been reported that *AtMBF1c* is a key regulator of HT tolerance in *Arabidopsis* and other abiotic stress (Suzuki et al., 2005). Loss of function of *AtMBF1c* leads to reduced survival of seedlings with HT-stress but overexpression of *AtMBF1c* increased the survival percentage (Suzuki et al., 2008). *MBF1c* is required for HT tolerance and functions upstream to trehalose, ethylene, SA, and pathogenesis-related protein 1 during HT stress (Suzuki et al., 2008). Ectopic expression of *MBF1c* in *Arabidopsis* and soybean can improve the growth and yield under normal growth conditions (Suzuki et al., 2011). In *Arabidopsis* pollen development, *MBF1c* is sensitive to HT after 1 day HT-stress and loss of function of *AtMBF1c* leads to a slow HT response on pollen viability and reproductive development, but results in reduced HT resistance of plants. However, there is no clear evidence how *AtMBF1c* affect pollen development, future microscopy work may be needed to identify the function of this gene.

AtHOP3 shows strong up-regulation in all stages of buds tested in wild type after 1 day HT-stress and was up-regulated after 2 days HT-stress but at a lower level than that of 1 day; expression level decreased to similar level as non-stressed samples when moved to recovery conditions (Fig. 4.3d). This result suggests *HOP3* is a heat inducible gene but expression is not maintained once HT is over. There is no *AtHOP3* expression seen in homozygous T-DNA insertion mutant SALK_000794, interestingly, *AtHOP3* was highly up-regulated in the homozygous SALK_023494 (Fig. 4.13b, Fig.

4.13c, Fig. 4.13d). The phenotype of homozygous SALK_000794 when *AtHOP3* is totally silenced, presents a slower reduction of pollen viability and *in vitro* germination, but the reproductive development data of silique length and seed number reveals loss of function of *AtHOP3* appears to increase HT sensitivity of plants during pollen development (Fig. 4.19). However, increased expression level of *AtHOP3* in homozygous SALK_023494 also lead to increased percentage of pollen viability and germination after 1 day HT-stress in the oldest buds in the inflorescence, and the later produced siliques and seeds showed a less reduction than that in SALK_000794 (Fig. 4.19). Previous research has reported *AtHOP3* is a potential interactor and co-chaperone of HSP70/HSP90 (Prasad et al., 2010, Zhang et al., 2003), and is a heat-inducible transactivator a key regulator in the induction of the defence system for several kinds of environmental stress including HT stress and loss of function of HsfA2 leads to less survival of *Arabidopsis* seedlings with HT-stress (Nishizawa et al., 2006, Charng et al., 2007). These results suggest *AtHOP3* is sensitive to HT-stress and loss of function would reduce HT resistance during pollen development.

AtABI1 shows a continued enhanced expression in whole *Arabidopsis* inflorescences after HT-stress, not only during the HT-stress treatment but during the recovery period (Fig. 4.3e), which suggests *AtABI1* is highly sensitive to HT and heat is inducible. *AtABI1* is not expressed in homozygous SALK_072009 but depressed in homozygous GABI_334A12 according to

quantitative RT-PCR (Fig. 4.14d). Loss of function of *AtABI1* results in a reduction of pollen viability and germination with 1 day HT-stress but this reduction was less serious than the WT. However, pollen viability and germination quickly decreased after 2 days HT-stress to a much lower level compared to WT (Fig. 4.20a, Fig. 4.20b). The morphology of reproductive growth in SALK_072009 after 2 days HT-stress showed a significant reduction in silique length and seed number (Fig. 4.20c, Fig. 4.20d). Down-regulation of *AtABI1* expression in homozygous GABI334A12 presents a different status compared to SALK_072009 in that the pollen viability and germination rate are not decreased immediately with HT-stress but were still maintained to a high level (Fig. 4.20). *ABI1* is a type 2C phosphatase that negatively regulates abscisic acid (ABA) signalling (Moes et al., 2008). It globally represses ABA responses and has emerged as a focal point in the network of ABA signal transduction (Raghavendra et al., 2010). *ABI1* regulates or is regulated by several other genes in the ABA regulation network (Chen et al., 2016, Kong et al., 2015, Krzywinska et al., 2016). Mutant of *ABI1* change ABA insensitivity resulting in morphological alterations in different species (Arend et al., 2009, Kong et al., 2015, Li et al., 2015, Lu et al., 2015b). Although previous research has indicated that ABA synthesis would be repressed with HT (Toh et al., 2008), the *ABI1* mutations might confer a partial or tissue-specific ABA insensitivity, resulting in sufficient residual ABA signalling in cells (Mang et al., 2012), which would lead to a suppression of pollen development.

AtHS83 is expressed at an extremely high level in the entire *Arabidopsis* inflorescence tissue during the HT-stress treatment but expression is reduced immediately when returned to normal conditions (Fig. 4.3f), which suggests *AtHS83* is very sensitive to HT and also to temperature variation. In homozygous T-DNA insertion mutant SALK_004008 with loss of function of *AtHS83*, the average percentage of pollen viability and germination is higher than wild type after 1 day HT-stress but lower after 2 days stress (Fig. 4.21a, Fig. 4.21b). The variation of silique length and seed number is similar as pollen viability and germination, which produced longer silique and more seeds in the oldest siliques but decrease in the younger siliques which developed from bicellular and other younger stage buds when HT-stress began (Fig. 4.21c, Fig. 4.21d). These results suggest that loss of function of *AtHS83* leads to a reduction of HT resistance for pollen development. However, another T-DNA insertion mutant SALK_075596 does not show such decreases, which implies that the sequence near the 5' of the gene contributes more to gene function of *AtHS83* (Fig. 4.9a). As a member of Heat Shock Protein (HSP), transcripts for *AtHS83* could be detected only in roots of control *Arabidopsis thaliana* plants but were abundant in all organs after heat shock (Krishna & Gloor, 2001, Samakovli et al., 2014). There would be no *AtHS83* protein accumulated in a loss of function *AtHS83* mutant and this would result in a reduction of HT resistance. Moreover, it has been reported *AtHS83* interacts with several other genes that could modulate HT tolerance (Kim et al., 2014, Meiri & Breiman,

2009), which suggests that *AtHS83* is part of a complex regulating network and is a key interactor for plant HT resistance.

Therefore, all these six genes are HT inducible during HT-stress but not in recovery, except *ABI1*. Loss of function of these genes leads to delayed HT response but a decreased HT tolerance in seed production and silique development. To investigate more detailed function of these genes, further ultrastructure analysis of the anther during pollen development is needed to compare the difference between T-DNA insertion mutants with and without HT-stress. Proteomics for regulation analysis may also be needed to find more HT inducible that functioned during pollen development.

CHAPTER 5

ANALYSIS OF GENE EXPRESSION CHANGE DUE TO HIGH TEMPERATURE STRESS

CHAPTER 5. ANALYSIS OF GENE EXPRESSION CHANGE DUE TO HIGH TEMPERATURE STRESS

5.1 INTRODUCTION

5.1.1 Transcriptome research

The transcriptome is the complete set of transcripts in a cell, and is specific for a developmental stage or physiological condition (Hoeijmakers et al., 2013).

The central theme of transcriptome analysis is to understand the functional elements of the genome and evince the molecular components of species, and thus to interpret development processes and resolve diseases. There are several main purposes of transcriptomics analysis, which include (1) cataloguing transcript in all species, such as small RNAs, mRNAs, and non-coding RNAs; (2) interrogating the transcriptional structure of genes, include the start sites, 5' and 3' ends, splicing patterns and other post-transcriptional modifications; and (3) evaluating the variations of expression levels of each transcript that occurs during development and/or in different conditions (Wang et al., 2009).

5.1.2 Limitation of hybridisation- based transcriptomic methods

There are various technologies that have been developed to deduce and quantify the transcriptome, initial transcriptomics studies largely relied on hybridisation- based microarray technologies, which is a kind of commercial

high-density oligo or custom-made microarrays to incubate fluorescently labelled cDNA (Faghihi & Wahlestedt, 2009). Microarrays are well-known technology to understand large-scale of gene expression level, which have been used to identify more than thousands of transcripts simultaneously. This has led to many core progresses in extensive biological problems, including to identify the variations of gene expression in different tissues and organs, novel and precise understanding of the responses to biotic and abiotic stress, developmental processes, and the pathways of gene regulation (Marioni et al., 2008). Moreover, specialised microarrays have also been designed for detecting and quantifying distinct spliced isoforms through arrays with probes spanning exon junctions (Wang et al., 2009).

Nonetheless, there are several limitations of these hybridisation-based microarray technologies in their applicability. Firstly, the dynamic range for the detection of transcript levels in microarrays is limited due to saturation, background, and spot quality and density, and reliance upon existing knowledge about genome sequence (Bloom et al., 2009). The second limitation of microarrays is that the sequences of different samples are needed, due to hybridisation efficiency is significantly affected by mismatches and applying of the oligonucleotide probes designed for a single sample may lead to a high background as cross- or nonspecific- hybridisation. Furthermore, it is a challenge that complex normalisation methods are normally required to analyse the transcription levels between experiments (Hinton et al., 2004).

Finally, only the relative level of RNA could be measured through microarrays, but differences between modified transcripts and *de novo* synthesized transcripts cannot be identified, and the accuracy of promoter that is used in *de novo* transcription also cannot be determined.

5.1.3 RNA-seq technology – Benefits and Challenges

Compared to microarray methods, sequence-based approaches are high throughput and directly determine the cDNA sequence, therefore they can provide precise and real-time gene expression analysis. However, there are also some disadvantages of these kinds of methods, such as non-unique mapping to the reference gene of the short tags, only part of the transcripts can be analysed, and isoforms are frequently indistinguishable from each other. RNA-sequencing (RNA-seq), a sequence-based high-throughput method, provides a useful option for transcriptomics research. This method has been applied to several species for transcriptomics research such as *Saccharomyces cerevisiae*, *Schizosaccharomyces pombe*, *Arabidopsis thaliana*, mouse and human cells (Cloonan et al., 2008, Lister et al., 2008, Marioni et al., 2008, Morin et al., 2008, Mortazavi et al., 2008, Nagalakshmi et al., 2008, Wilhelm et al., 2008).

Many different platforms have been applied for RNA-Seq deep-sequencing technology. Initially, total or fractionated long RNA are converted to a cDNA fragments library through either DNA fragmentation or RNA fragmentation with

adaptors that are attached to one or both ends. Every molecule, no matter amplified or not, is then sequenced using high throughput manner for obtaining short sequences, which are the reads, from one end (single-end sequencing) or both ends (pair-end sequencing). Different DNA sequencing technologies could result in different size of reads from 30 to 400 bp. Generally, all of the high-throughput platforms of sequencing technology can be used for RNA-Seq, however several systems, such as the Applied Biosystems SOLiD, Roche 454 Life Science and Illumina IG are usually used in RNA-seq experiments. After sequencing, the resulting reads are aligned to a reference transcripts or reference genome, or assembled *de novo* without the genomic sequence to generate a genome-scale transcription map that includes the transcriptional structure and/or expression level of each gene (Wang et al., 2009).

Compared to other current technologies, the RNA-seq method provides several core advantages. First of all, there is no limitation of RNA-Seq to detect transcripts that corresponded to the existing genomic sequences compared to the hybridization-based approaches, which means RNA-Seq could be applied for non-model organisms that the genomic sequences are not determined (Vera et al., 2008).. RNA-Seq can identify the exact location of transcription boundaries even to the resolution of single base pair. Moreover, the short reads from RNA-Seq, such as 30-bp, can provide details about connection between two exons, whereas the multiple exons connection could be revealed

by longer reads or pair-end short reads. All of these advantages make RNA-Seq efficient to understand complex transcriptomes. Furthermore, RNA-Seq can also reveal sequence variations in the transcribed regions (Cloonan et al., 2008, Morin et al., 2008).

Another advantage of RNA-Seq is the very low background signal of RNA-seq results because DNA sequences can be mapped to unique regions of the genome precisely. There is no upper limit of RNA-seq for quantification, this is correlated with the number of sequences obtained. Therefore, RNA-seq has a large dynamic range of expression levels and to detect the transcripts accurately. In contrast, DNA microarrays have a much smaller dynamic range due to the insensitivity to the very high or low level gene expression. RNA-Seq also presents highly accurate to quantify expression levels. The results of RNA-Seq can also show high levels of reproducibility, for both of biological and technical replicates (Cloonan et al., 2008, Mortazavi et al., 2008, Nagalakshmi et al., 2008). Finally, RNA-Seq requires lower amount of RNA due to the cloning step is not needed and also no amplification step with the Helicos technology.

Taking all of these together, RNA-Seq was the first sequence-based method that to survey the entire transcriptome in a very quantitative and high-throughput approach. This method offered both single-base resolution, which is used to reveal gene expression levels at the genome scale and

annotate their functions, or large-scale Sanger EST sequencing (Wang et al., 2009).

However, there are still some challenges that cannot be ignored. First challenge is to construct the cDNA library. The demand of highly efficient method for transcriptomics is to identify and quantify all RNAs directly. Compared to the few steps in RNA-Seq, several manipulation stages to produce of cDNA libraries could complicate the using in profiling all kinds of transcript.

The second challenge relates to bioinformatics analysis. Similar to other high-throughput sequencing technologies, RNA-Seq has to overcome some other challenges of information, such as the large amounts of data need to be stores, retrieved and processed by more efficient methods.

Another challenge is sequence coverage which has implications for the cost. Considerable sequencing depth is required for better and larger sequences coverage, and to detect an uncommon transcript. Therefore, adequate coverage usually requires more sequencing depth for the large genome and the complex transcriptome. Meanwhile, previous studies have suggested it is effective to increase power and accuracy in large-scale differential expression RNA-seq studies with less sequencing read and more biological replicates (Liu et al., 2014).

5.1.4 RNA-Seq experiments processes

To optimise RNA-seq experimental designs, it is necessary to evaluate the biological and technical replication, and sequencing depth, since inefficient designs of RNA-seq studies would lead to suboptimal power and waste of resources, especially in large-scale treatment-control studies (Auer & Doerge, 2010).

Sequencing depth is usually defined as the expected mean coverage at all loci over the target sequences, of assumes all transcripts are assumed to have similar levels of expression in RNA-seq experiments (Soneson & Delorenzi, 2013). In most cases, it is difficult to estimate the optimal sequencing depth to detect differential expression (DE) of the interesting transcriptome adequately before data generation. Differential expression (DE) is referenced to be that a gene is declared differentially expressed whether an observed difference or change in read counts between two experimental conditions is statistically significant or not (Soneson & Delorenzi, 2013). RNA-seq sequencing depth is usually chosen according to the estimation of total transcriptome length and the expected dynamic range of transcript abundances.. Previous research has indicated that transcripts with low to moderate expression levels were still difficult to quantify with good precision even at higher read depths over existing RNA-Seq protocols (Fang & Cui, 2011). Therefore, it is crucial to understand the increased sequencing depth provide whether raised or reduced return with

regard to transcript detection and DE testing prior to design an efficient experimental.

Replication is also a key point to be considered for statistical analysis of DE. In RNA-seq, multiple technical replicates are used depending upon several factors, such as the sequence data generation, library preparation or RNA extraction technical processes, to verify the materials are replicated to the same biological sample, while the main source of technical change is library preparation (Roberts et al., 2011). Biological replication is used to measure the variation of the target population and counteract random technical variation as part of independent sample preparation simultaneously (Fang & Cui, 2011). However, more utility and availability of multiplex experimental are designed recent, which lead the strategy of efficient increased biological replicates with decreased sequencing depth to be becoming attractive and cost-effective.

Liu *et al.* (2014) has shown that increasing the number of biological replicates consistently increased the power significantly, regardless of sequencing depth. Additionally, estimation accuracy for logFC and absolute expression levels greatly improved across the board when more biological replicates were added, whereas sequencing depth improved the accuracy of these estimations only in some situations. Therefore, they suggested that, when possible, more biological replication with lower sequencing depth should be used rather than sequencing few samples in great depth, and that this would result in a more

efficient strategy for RNA-seq DE studies.

5.1.5 Data analysis software

Following sequencing, millions of short reads are taken from one end of the cDNA fragments, the data that consist list of short sequences with quality scores. A typical RNA-seq pipeline for DE analysis includes the following aspects. First, the reads are mapped to the reference genome or transcriptome. Second, mapped reads of each sample are assembled into expression summaries on transcript-level, exon-level, or gene-level , depending on the purposes of the experiment. Next, the summarised data are normalized together with the statistical tested DE, and then generate a ranking list of genes with associated fold changes and *P*-values. Finally, further analysis such as gene function prediction and target gene investigation can be preceded.

Hierarchical Indexing for Spliced Alignment of Transcripts (HISAT) is highly efficient to align reads from RNA sequencing experiments (Kim et al., 2015). An indexing scheme, which is based on the Ferragina-manzini (FM) index and Burrows-Wheeler transform, is applied by HISAT, and then two kinds of indexes for alignment are generate, including numerous local FM indexes for very rapid extensions of these alignments and a whole-genome FM index to anchor each alignment . HISAT is currently thought to be the fastest analysis system with better accuracy than any other method through comparing the real

and simulated data sets. Due to the large number of indexes, HISAT requires very limited storage space and also supports genomes of any size, even those larger than 4 billion bases.

The Sequence Alignment/Map (SAM) is used to produce a type of generic alignment data format to store read alignments against reference sequences, which supports both short and long reads produced from kinds of sequencing platforms (Li et al., 2009). There are several advantages of SAM format, including the efficiency of random access, compacted in size, flexibility of style. SAM tools have been applied on various utilities for post-processing alignments, such as data indexing, variant caller and alignment viewer, and even universal tools for processing read alignments (Li et al., 2009).

StringTie is a computational method that used to assemble the complex *de novo* data sets into transcripts (Pertea et al., 2015). Compared to other transcript assembly methods, StringTie can produce much more accurate and integral reconstructions of genes, and then evaluate better of expression levels for analysing real or simulated data sets. . StringTie also produce the data sets much faster compared to other assembly software (Pertea et al., 2015).

HTSeq is a Python library provided to process data from high-throughput sequencing assays (Anders et al., 2014). HTSeq includes parsers, which is used to input all types of data of common file formats, and is suitable for different range of tasks as a general platform. Container class is the core

element of HTSeq, which functions to reduce the workload of data associated with genomic coordinates, such as read coverage and genomic features. Two unique applications of HTSeq are distributed with the software package, which are “htseq-qa” for quality assessment of read and “htseq-count” for pre-processing RNA-Seq alignments for differential expression calling (Anders et al., 2014).

EdgeR is a set of Bioconductor software package for inspecting differential expression of different replicated count data (Robinson et al., 2010). The edgeR software contains many features and options, and opens up flexible possibilities for RNA-seq data analysis (McCarthy et al., 2012). Alongside edgeR, there several additional function and attachments are developed, such as the over-dispersed Poisson model which is used to calculate the variability on biological and technical aspects, and Empirical Bayes methods that are used to adjust the over-dispersion of transcripts and then to improve the reliability of hypothesis. This type of method can be applied even with the smallest numbers of replication. Beyond sequencing data, EdgeR also has some other functions such as proteome peptide count data (Robinson et al., 2010, McCarthy et al., 2012).

Genesis is a tool to analyse the entire set of gene expression experiments and generate the visible results simultaneously (Sturn et al., 2002). This software generates several graphical representations that show a matrix of genes and

experiments, which is easily to compare the multiple genes and experiments.

5.2 MATERIALS AND METHODS

5.2.1 Plant materials, HT-stress and collection modes

Plant material *Arabidopsis thaliana* genotype Ler seeds were sown as in Section 2.1 but grown in controlled environment chambers to keep the growth conditions as constant as possible. The latter were fixed to: 16h of daylight ($180\pm 20\mu\text{mol}\cdot\text{m}^{-2}\cdot\text{sec}^{-1}$) and 8h of night, the temperature was kept at 22°C. Moreover, daylight started at 6am in the morning and ended at 10pm in night. High temperature stress commenced as soon as the plants showed 3 fertile or sterile siliques (28-30 days old approx.). Plant material was treated with HT at 32°C for 1 day, during a time series of buds samples were collected, these were dissected and separated into different groups according to their relative position within the inflorescence (see section 3.2.3). All opened flowers and buds that were about to open were discarded and buds were grouped and collected into three groups named “Mature”, “Old” and “Young” (Fig. 4.1) as mentioned in section 4.2. The plant materials were collected and frozen immediately in liquid nitrogen and stored at -80°C for subsequent RNA extraction. However, because the focus was on the genes which specifically functioned during tapetum development, bud samples in the “Old group” and “Young group” were used for the RNA-seq experiment.

HT-stress treatment for *Arabidopsis thaliana* (Ler genotype) initiated at 8am in the morning, the bud samples were collected and labelled as T0-control at this time point prior to HT-stress. Both of HT-stressed and non-stressed samples were collected after six hours at 2pm in the afternoon as T6-HS and T6-control, and then T24-HS and T24-control samples were collected from the HT-stressed and non-stressed plants at 8am on the second day.

5.2.2 RNA sample preparation for RNA-seq

Three biological replicates were used in the RNA-seq experiment. For each replicate, total RNA was extracted from about 30mg of tissue from HT-stressed and non-stressed bud samples using a commercially available total RNA isolation kit (RNeasy Plant Kit, Qiagen). RNA samples were DNase treated for 20 min at 28°C and then purified using RNeasy spin columns (Qiagen). RNA concentrations were estimated spectrophotometrically with the NanoDrop ND-1000 (Thermo), and also were tested for RNA integrity using the Agilent 2100 Bioanalyzer. RNA stocks were stored at -80°C until ready for submission to RNA-seq.

5.2.3 Preparation of labelled targets, sequencing experiment (WTCHG, Oxford)

Approximate 3µg RNA samples were submitted for RNA-seq analysis. Wellcome Trust Centre for Human Genetics (WTCHG) concluded the following

analysis. The mRNA fraction was selected from the total RNA provided before conversion to cDNA. Second strand cDNA synthesis incorporated dUTP. The cDNA was then end-repaired, A-tailed and adapter-ligated. Prior to amplification, samples underwent uridine digestion. The prepared libraries were size selected, multiplexed and QC'ed before paired end sequencing over one lane of a flow cell. Data were aligned to the reference and quality checked. Standard data files, fastq and bam, were delivered via an ftp link.

5.2.4 RNA-seq data analysis (The Advanced Data Analysis Centre, University of Nottingham)

The WTCHG returned the data obtained from the RNA-seq experiments as base-pairs reads. The following analysis pipeline was performed by The Advanced Data Analysis Centre (ADAC) on the data. The pipeline aligns reads to a genome sequence using HISAT2. Technical replicates from different lanes were merged using Samtools and then assembled to identify transcript level expression using StringTie. Gene level counts were generated using HTseq. Differentially expressed (DE) genes were identified using the R package "DESeq" (Anders & Huber, 2010). *P*-value of 0.05 and fold change of 2.0 genes was chosen as the threshold for significant differential expression. Final pre-normalised data for expression level of transcripts and genes were obtained as Microsoft Excel and Adobe PDF files.

5.2.5 Gene ontology (GO) and annotation

Statistically significantly down-regulated and up-regulated genes were analysed for GO and other annotations enrichment using TAIR GO tools [<http://www.Arabidopsis.org>], with an *P*-value of 0.05 and a fold change of category representation of 2.0 as the threshold of significance. The GO term enrichment analysis was performed by PANTHER to compare classifications of multiple clusters of genes to a reference list to statistically determine over- or under- representation of GO ontology classification categories (Mi et al., 2016).

5.2.6 Validation of RNA-seq data with quantitative RT-PCR

To validate the RNA-seq data, 10 genes which were differentially expressed by HT and specifically in the tapetum were chosen according to the data from Pearce *et al.* (2015). Six of these genes were used in Chapter 4 and four others were newly selected. Total RNA was extracted from bud samples, which were treated with 1 day HT-stress and separated into the same groups as mentioned previously, and then cDNA was synthesised by reverse transcription with 2 µg of RNA, uniform all of the experiment. For RNA extraction and cDNA synthesis see sections 2.8 and 2.11.1, respectively. Quantitative RT-PCR was described in section 2.12, and primers are listed in Appendix II. The standard program for running the plate on the LightCycler was: 95°C 10 min; 45x (95°C 30 sec, T_m, 30 sec, 72°C for 1 min); 72°C 6 min.

Cp values were calculated by the LightCycler[®] 480 software. The expression level was analysed using MicroSoft Excel. Annealing temperature (T_m) was chosen for each primer separately.

5.3 RESULTS

5.3.1 Design of experiment

Three biological replicates were used in the RNA-seq experiment. Samples were collected at the T0 time point (prior to HT-stress) from non-stressed plants, and then were collected at T6 (6 hours after the start of HT-stress began) and T24 (24 hours of HT-stress) from HT-stressed and non-stressed plants. RNA was extracted from young and old buds from HT-stressed and non-stressed plants and then submitted to WTCHG. For each sample, X0-Control-Old, X0-Control-Young, X6-Control-Old, X6-Control-Young, X6-Treatment-Old, X6-Treatment-Young, X24-Control-Old, X24-Control-Young, X24-Treatment-Old, and X24-Treatment-Young samples three sets of data were generated (one for each replicate).

5.3.2 Transcriptome sequencing

To generate RNA-seq data sets, cDNA libraries for different staged bud samples different treatments were prepared and then sequenced to generate several libraries within between 33 and 50 million 75-bp-paired reads. The reads were aligned onto the reference *Arabidopsis* genome assembly (TAIR10)

to obtain the reads, in which the designated single-mapping reads mapped exactly onto the genome. Table 5.1 shows the yields and alignment percentages for each library in each replicate sample.

Table 5.1 Sequencing yields and alignment overview. Each library was sequenced in two lanes. X0: samples were collected before HT- stress treatment, X6: samples were collected 6 hours after HT-stress treatment, X24: samples were collected 24 hours after HT-stress treatment. Control: samples were not treated with HT-stress, Treatment: samples were treated with HT-stress. Old: bud samples in polarized microspore and pollen mitosis I and II, Young: bud samples in microspore and all younger stages. R1, R2 and R3: replicates 1, 2 and 3.

Library name	Reads (million)	Aligned (%)
X0.Control.Old.R1	41.18	89.19
X0.Control.Old.R2	40.87	89.53
X0.Control.Old.R3	47.42	89.62
X0.Control.Young.R1	43.15	89.56
X0.Control.Young.R2	45.00	89.96
X0.Control.Young.R3	41.20	89.83
X6.Control.Old.R1	43.20	89.53
X6.Control.Old.R2	46.57	89.29
X6.Control.Old.R3	35.51	89.64
X6.Control.Young.R1	34.93	89.80
X6.Control.Young.R2	35.53	89.99
X6.Control.Young.R3	41.88	89.47
X6.Treatment.Old.R1	34.46	89.23
X6.Treatment.Old.R2	29.46	84.58
X6.Treatment.Old.R3	39.20	89.20
X6.Treatment.Young.R1	41.46	89.22
X6.Treatment.Young.R2	43.08	89.78
X6.Treatment.Young.R3	44.07	89.83
X24.Control.Old.R1	44.63	89.97
X24.Control.Old.R2	43.85	89.64
X24.Control.Old.R3	40.42	89.45
X24.Control.Young.R1	37.55	89.77
X24.Control.Young.R2	37.70	89.80
X24.Control.Young.R3	42.81	89.77
X24.Treatment.Old.R1	42.04	89.70
X24.Treatment.Old.R2	42.12	89.56
X24.Treatment.Old.R3	41.48	89.86
X24.Treatment.Young.R1	39.87	89.28
X24.Treatment.Young.R2	43.12	89.52
X24.Treatment.Young.R3	46.11	88.71

5.3.3 Data quantity assessment and exploratory

Multidimensional Scaling (MDS) plots (Fig. 5.1) are used to provide a visual representation of the pattern of proximities (i.e., similarities or distances) among a set of objects. MDS takes a set of similarities and returns a set of points such that the distances between the points are approximately equal to the similarities. Distances on the plot can be interpreted as leading log₂-fold-change, meaning the typical (root-mean-square) log₂-fold-change between the samples for the genes that distinguish those samples. The three replicates of X24-Treatment-young are close to each other but distant compared to the other clusters. Moreover, both of X24-Treatment-old and X24-Treatment-young samples show greater distance to the other samples which were collected at different time points and X24 non-stressed ones, but those samples which were collected at X24 time point show a closer distance in the individual clusters (Fig. 5.1). This means that after 24 hours HT-stress treatment, the gene expression level is changed much more in those samples that were treated with HT for less than 24 hours. However, it was not easy to recognise the distance of other replicates in Fig. 5.1, so detailed MDS plots of HT-stressed and non-stressed samples were generated according to sample collection time points (Fig 5.2). The expression of non-stressed “Old” samples show obvious difference according to the time points by dimension 2, while the gene expression level of non-stressed “Young” samples are more closely related in dimension 1 at different time point (Fig. 5.2a, Fig. 5.2b). The samples

that were treated for different periods with HT are close to their replicates but distant from those collected at other time points and non-stressed samples, regardless the “Old” groups or “Young” groups (Fig. 5.2c, Fig. 5.2d). The “Control” group replicates are less well distinguished (Fig. 5.2a, Fig. 5.2b) than that between “Control” and “Treatment” groups (Fig. 5.2c, Fig. 5.2d), which indicates that the gene expression levels were affected more by HT-stress than different time period in one day cycle. To determine the difference between HT-stressed sample replicates and non-stressed ones, MDS plot maps for HT-stressed replicates versus non-stressed replicates at different collection time points were generated (Fig. 5.3). All of the samples show clear differentiation on corresponding to the different treatments (HT-stressed or non-stressed) in plot dimension 1. The “Old” samples that were treated with HT show closer distance compared to those that were not stressed at the same stages (Fig. 5.3a, Fig. 5.3b), but the HT-stressed “Young” samples (Fig. 5.3c, Fig. 5.3d) are closer in dimension 1 than dimension 2. This indicates that the gene expression level in “Old” samples is more sensitive to HT-stress than that in “Young” samples, it means HT-stress possibly affects gene expression alteration during tapetum degeneration more seriously than before that period.

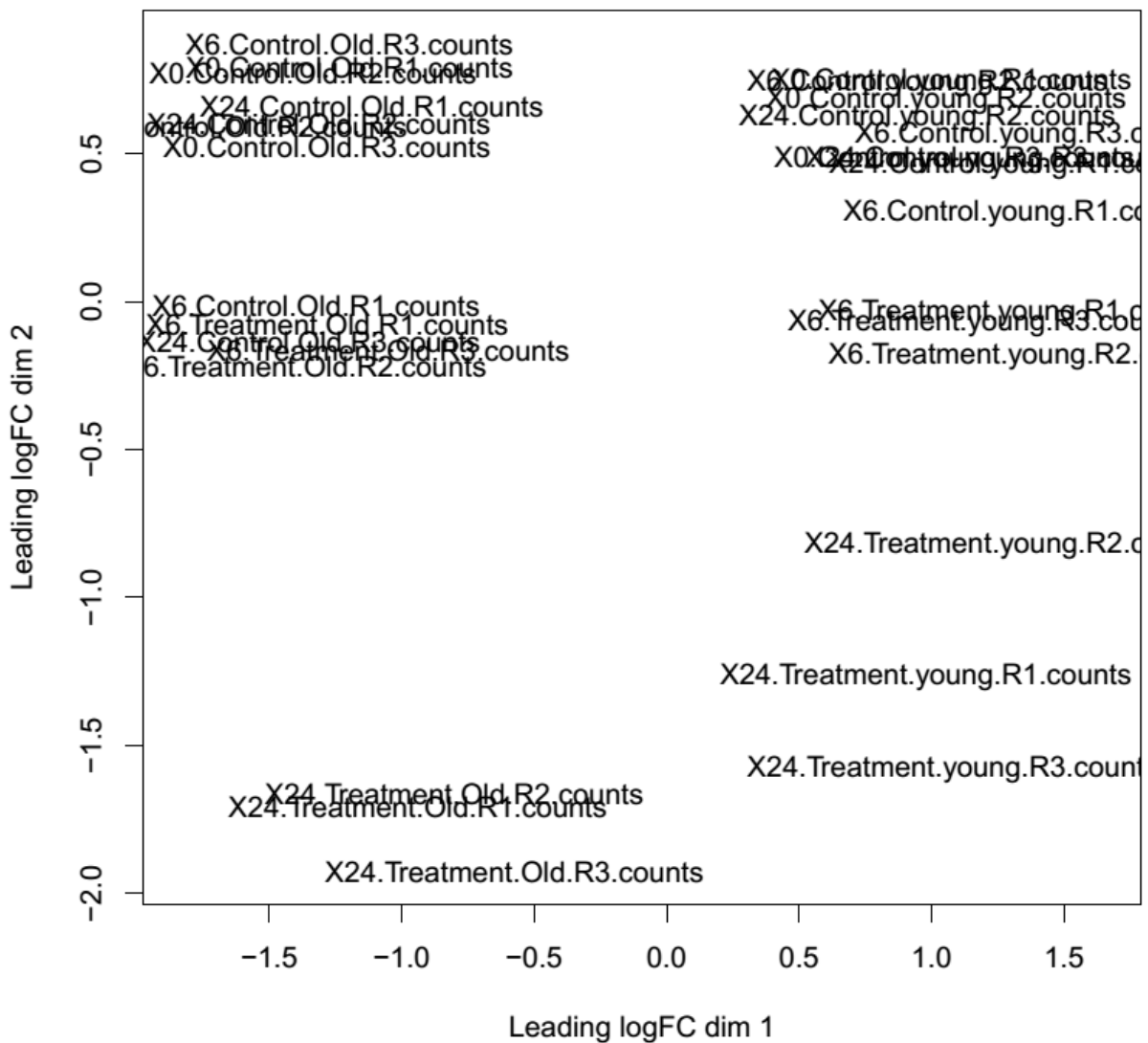
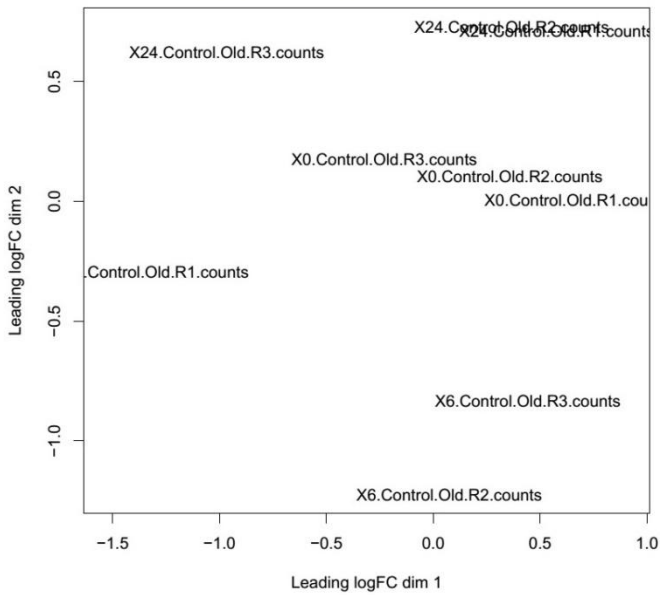
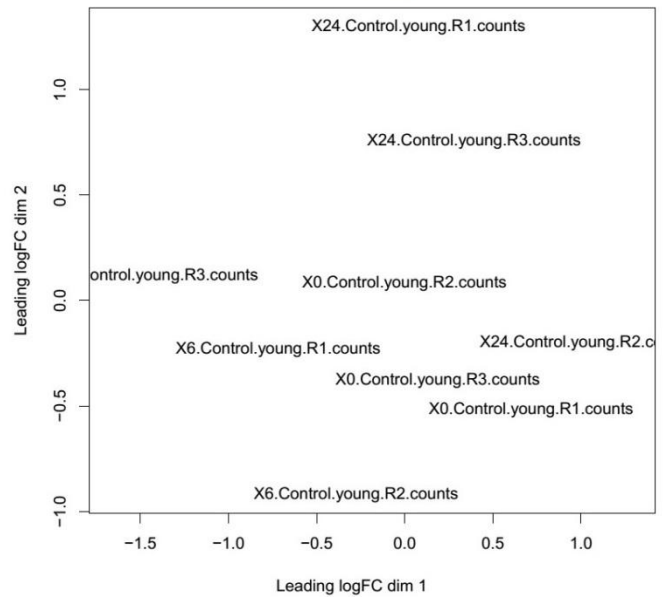


Figure 5.1 Multidimensional scaling (MDS) showing the relationship between replicates in two dimensions (Leading logFC dimension 1 and 2), generated by edgeR. Three replicates (R1, R1 and R3) for the samples X24.Treatment.Old and X24.Treatment.Young are closely related in both dimensions, respectively, whereas other sample replicates were so closely related that it was difficult to recognise the detailed distance. Axes x and y are representations of all the gene expression levels between groups based on bud stages and replicates.

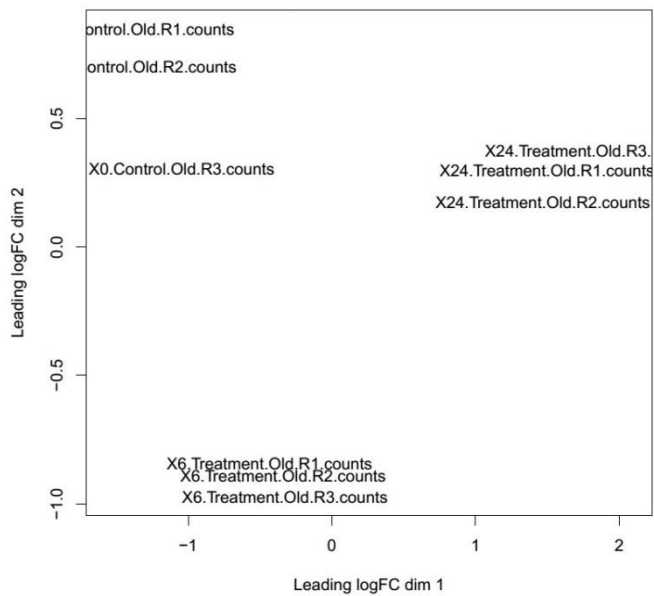
A. MDS Plot for all "Old" Control replicates of X0, X6 and X24 time points



B. MDS Plot for all "Young" Control replicates of X0, X6 and X24 time points



C. MDS Plot for "Old"X6 and X24 HT-stressed replicates vs. X0 Control replicates



D. MDS Plot for "Young"X6 and X24 HT-stressed replicates vs. X0 Control replicates

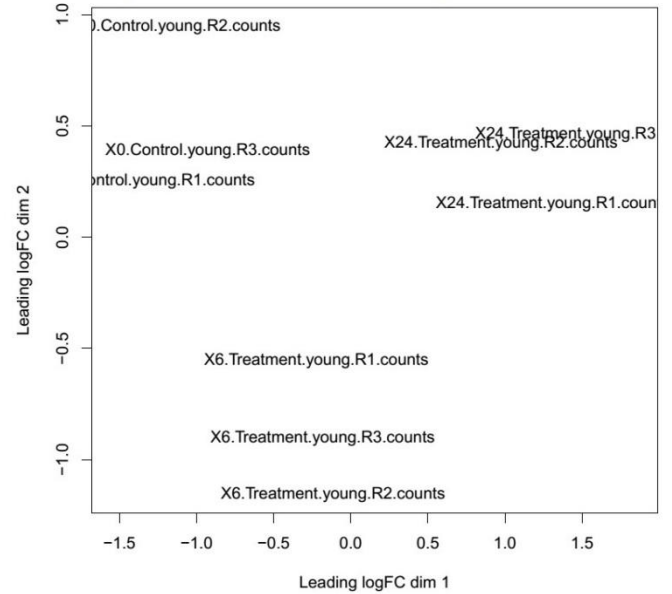
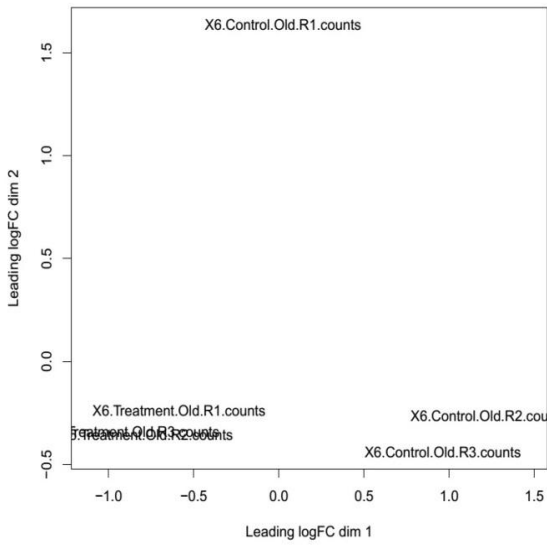


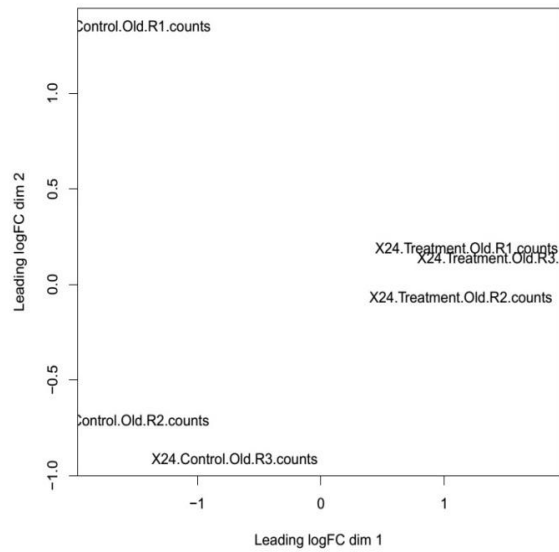
Figure 5.2 Multidimensional scaling (MDS) showing the relationship between replicates in two dimensions (Leading logFC dimension 1 and 2), generated by edgeR.

Figure 5.2 Multidimensional scaling (MDS) showing the relationship between replicates in two dimensions (Leading logFC dimension 1 and 2), generated by edgeR. A). MDS plot for all “Old” stage buds without HT-stress at different time points. Three replicates (R1, R2 and R3) for the samples X0.Control.Old, X6.Control.Old and X24.Control.Old are closely related in dimension 2 and separated in dimension 1. **B).** MDS plot for all “Young” stage buds without HT-stress at different time points. Three replicates (R1, R2 and R3) for the samples X0.Control.Young, X6.Control.Young and X24.Control.Young are closely related in dimension 1 and separated in dimension 2. **C).** MDS plot for “Old” stage buds with 6 and 24 hours HT-stress, respectively, vs. Control buds without HT-stress when HT-stress began. Three replicates (R1, R2 and R3) for the samples, X0.Control.Old, X6.Treatment.Old and X24. Treatment.Old, are closely related in both dimensions. **D).** MDS plot for “Young” stage buds with 6 and 24 hours HT-stress, respectively, vs. Control buds without HT-stress when HT-stress began. Three replicates (R1, R2 and R3) for the samples, X0.Control.Young, X6.Treatment.Young and X24. Treatment.Young, are closely related in both dimensions.

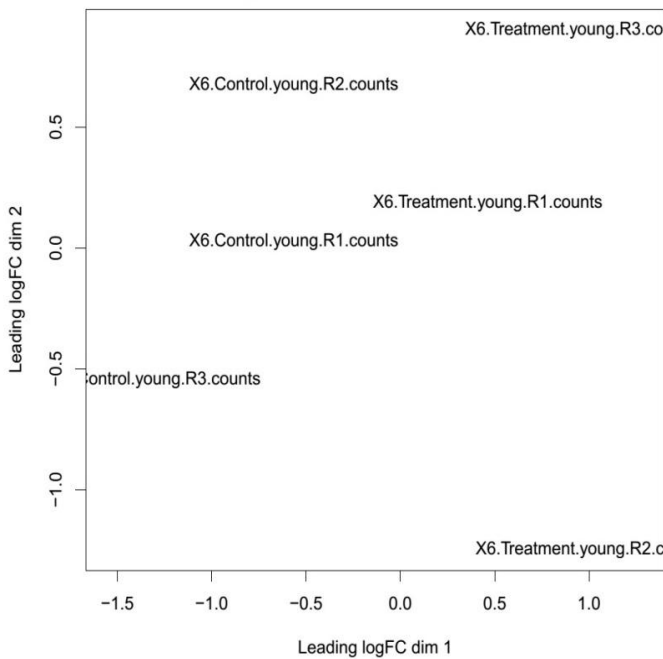
A. MDS Plot for "Old" replicates data between HT-stressed and Control groups at X6 time point



B. MDS Plot for "Old" replicates data between HT-stressed and Control groups at X24 time point



C. MDS Plot for "Young" replicates data between HT-stressed and Control groups at X6 time point



D. MDS Plot for "Young" replicates data between HT-stressed and Control groups at X24 time point

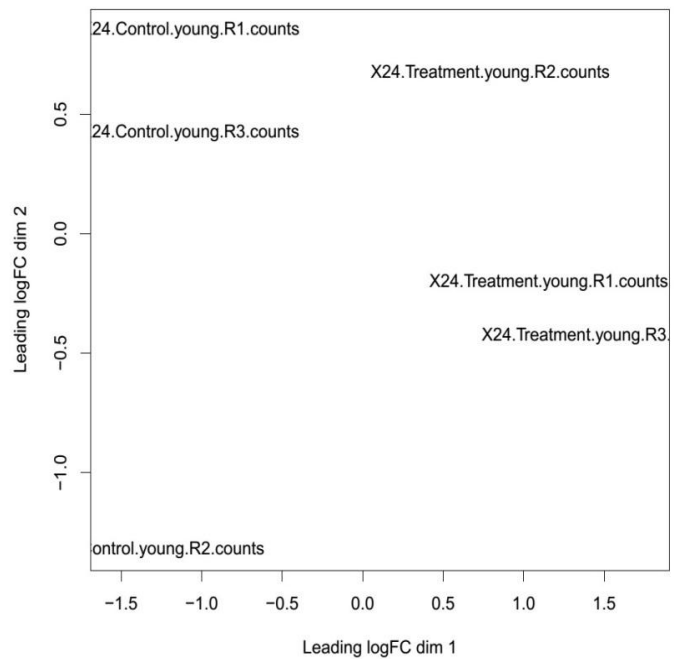


Figure 5.3 Multidimensional scaling (MDS) showing the relationship between replicates in two dimensions (Leading logFC dimension 1 and 2), generated by edgeR.

Figure 5.3 Multidimensional scaling (MDS) showing the relationship between replicates in two dimensions (Leading logFC dimension 1 and 2), generated by edgeR. A). MDS plot for “Old” stage buds with and without HT-stress at X6 time point. Three replicates (R1, R2 and R3) for the samples X6.Control.Old are more closely related in dimension 1 and more separated in dimension 2, whereas the X6.Treatment.Old replicates were closely related in both dimensions. **B).** MDS plot for “Old” stage buds with and without HT-stress at X24 time points. Three replicates (R1, R2 and R3) for the samples X24.Control.Young are closely related in dimension 1 and separated in dimension 2, whereas X24.Treatment.Old replicates were closely related in both dimensions. **C).** MDS plot for “Young” stage buds with and without HT-stress at X6 time point. Three replicates (R1, R2 and R3) for the samples X6.Control.Young and X6.Treatment.Old are closely related in dimension 1 and separated in dimension 2. **D).** MDS plot for “Young” stage buds with and without HT-stress at X24 time point. Three replicates (R1, R2 and R3) for the samples X24.Control.Young and X24.Treatment.Young are closely related in dimension 1 and separated in dimension 2.

5.3.4 Interpreting the differential expression analysis results

Differential expression analysis means identifying genes with RNA levels that are different across experimental treatments. Here, RNA levels were assessed

as the number of reads that overlap the entire gene region. The original read counts should be normalised after mapping to reduce the difference among each read counts database. To evaluate the efficiency of normalisation, an MA-plot was generated by the edgeR software. The variance estimates are used to determine if the HT-stress causes a significant change in gene expression through comparing the pairs of “Old” and “Young” samples between HT-stressed samples and non-stressed at each separate time point (Fig. 5.4).

The “MA-Plot” provides a useful overview for an experiment with a two-group comparison (Yang et al., 2002). This plot represents each gene with a dot. The x axis is the average expression measured in CPM (counts per million) (A-values), the y axis is the log₂ fold change between treatments (M-values). For a particular gene, a log₂ fold change of -1 for condition HT-stressed vs non-stressed means that the HT-stress induces a change in observed expression level of $2^{-1} = 0.5$ compared to the non-stressed condition. Analogously, a log₂ fold change of 1 means that the treatment induces a change in observed expression level of $2^1 = 2$ compared to the non-stressed condition. The horizontal dashed lines represent the genes which are altered 2-fold up-regulated or down-regulated than those are non-stressed. Red points indicate genes found to be significantly up-regulated with the HT-stress through an adjusted *P*-value ($P < 0.05$), and blue points indicate those are significantly down-regulated (Fig. 5.4).

The “Volcano Plot” is an effective and easy-to-interpret graph that summarizes both fold-change and a measure of statistical significance from a statistical test (P -value) (Li, 2012), which is used to deduce the distribution of differentially expressed genes. It is a scatter-plot of the negative \log_{10} -transformed P -values from the gene-specific test (on the y-axis) against the \log_2 fold change (on the x-axis) (Fig. 5.5). These results in data-points with low P -values appearing towards the top of the plot. The \log_2 of the fold-change is used so that changes in both directions (up and down) appear equidistant from the centre. Plotting points in this way results in two regions of interest in the plot: those points that are found towards the top of the plot that are far to either the left- or the right-hand side. These represent values that display large magnitude fold changes (hence being left- or right- of centre) as well as high statistical significance (hence being towards the top). In the “Volcano Plot”, the vertical dashed blue lines shows 2-fold changes. The red dots indicate the genes that display high statistical significance (P -value <0.05) and were up-regulated 2-fold after HT-stress than those were not stressed, while the blue dots present those genes that were down-regulated.

According to the two separate analysis methods, the numbers of genes that were statistically significantly differentially expressed in different staged buds with different HT-stress period are listed in Table 5.2. When a P -value <0.05 is used for statistical significance, there are 764 genes up-regulated and 531 down-regulated 2-fold in “Old” bud samples with 6 hours HT-stress, while 672

genes are up-regulated and 518 down-regulated 2-fold significantly in “Young” groups. After 24 hours HT-stressed samples showed 1588 genes up-regulated and 1478 down-regulated 2-fold level in “Old” groups, and 1509 up-regulated and 998 down-regulated 2-fold in “Young” groups. These results indicate that more genes are induced by 24 hours of HT-stress rather than only 6 hours treatment, and the genes in “Old” staged samples display more variation in expression than those in “Young” samples with sample HT-stress period.

Table 5.2 Number of genes that present significant difference on expression level with HT-stress. T6, samples were collected after 6 hours HT-stress; T24, samples were collected after 24 hours HT-stress; Old, “Old” group samples; Young, “Young” group samples (details see section 5.2.1). All of the genes are up-/down- 2-fold change on expression level in the HT-stressed samples than those without HT-stress.

Sample groups	<i>P</i> -value<0.05 Fold change>2	
T6-Old	Up-regulated	764
	Down-regulated	531
T6-Young	Up-regulated	672
	Down-regulated	518
T24-Old	Up-regulated	1588
	Down-regulated	1478
T24-Young	Up-regulated	1509
	Down-regulated	998

Figure 5.4 MA-plot generated in edgeR for evaluating the efficiency of normalisation. Red colour points indicate the genes where the adjusted P -value is less than 0.05 and up-regulated, and blue are down-regulated. A “smear” of points at low A value (x-axis) is presented to the left of the minimum A for counts that were low. The horizontal lines show 2-fold changes.

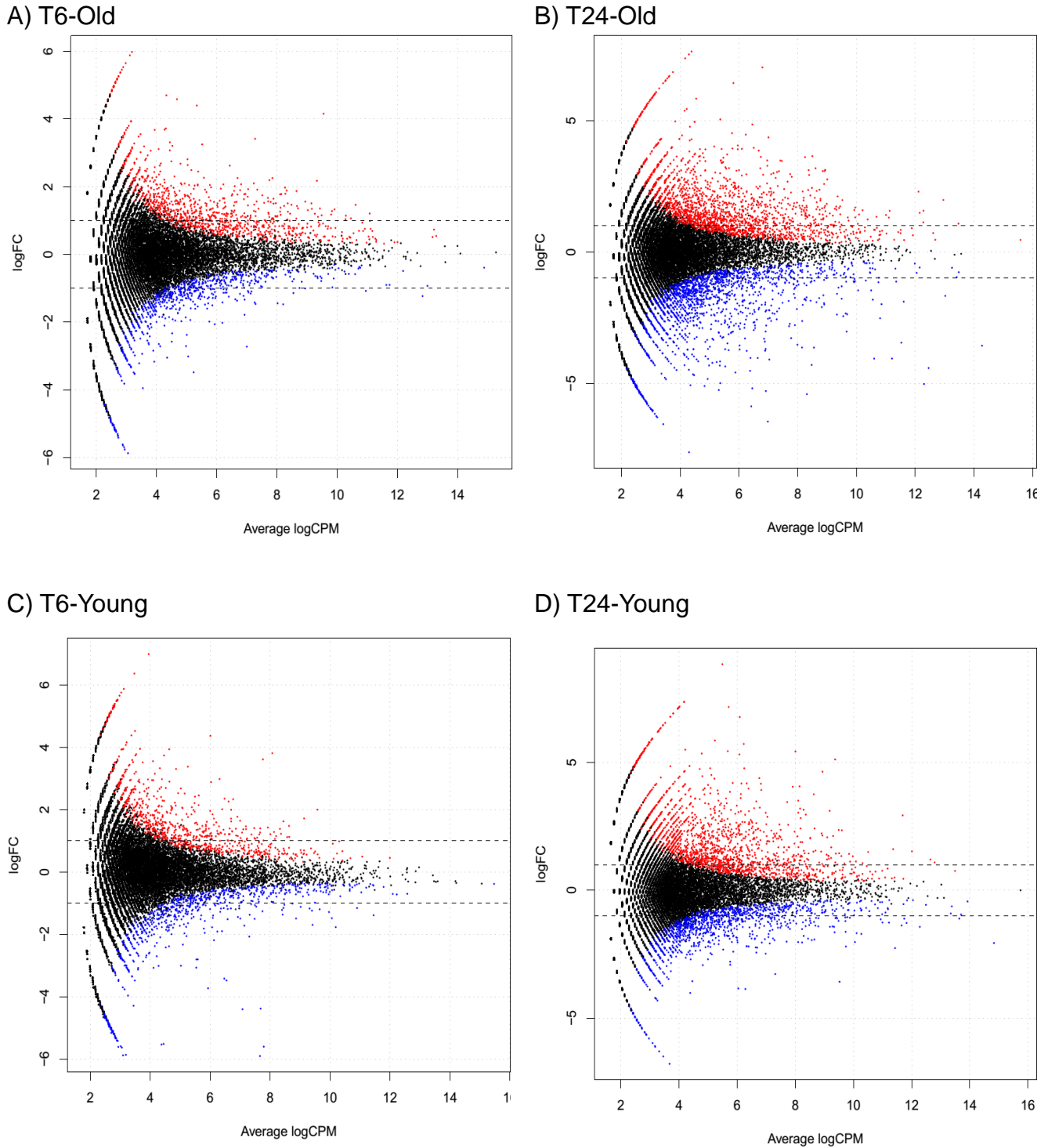
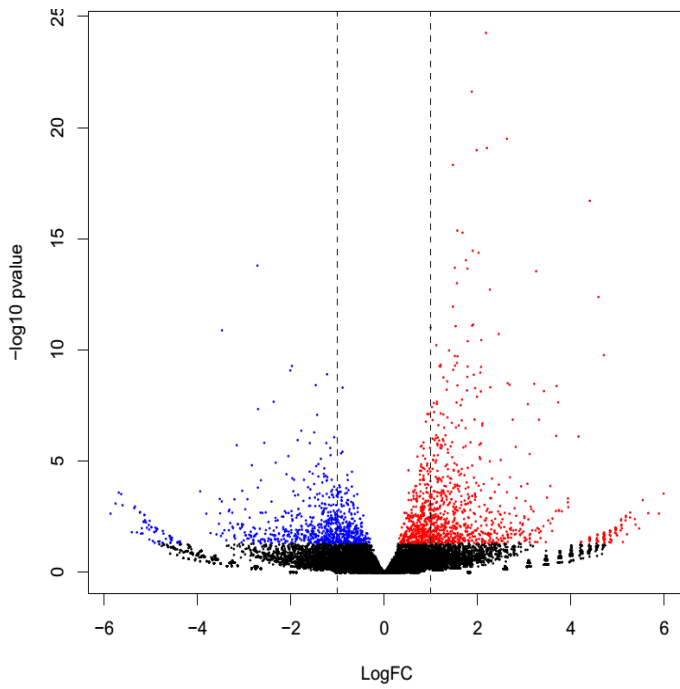
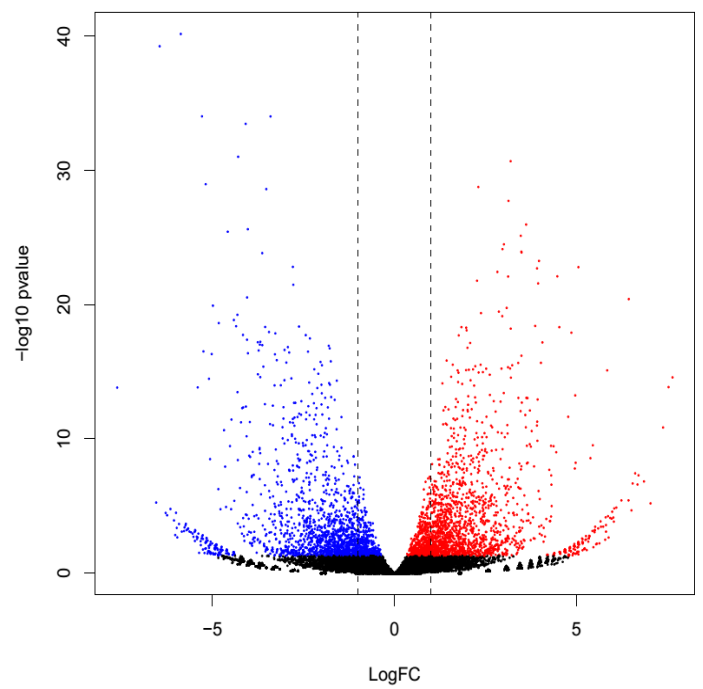


Figure 5.5 Volcano plot of gene expression and significance. The red points indicate genes that display both high statistical significance (P -value <0.05 , y-axis) as well as 2-fold up-regulated change on expression level (x-axis), and the blue for those are down-regulated. The vertical dashed lines show 2-fold changes.

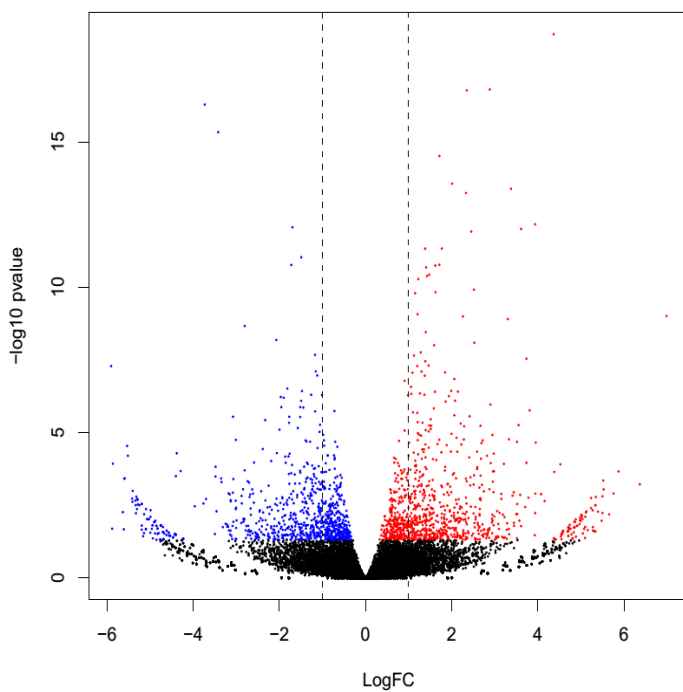
A) T6-Old



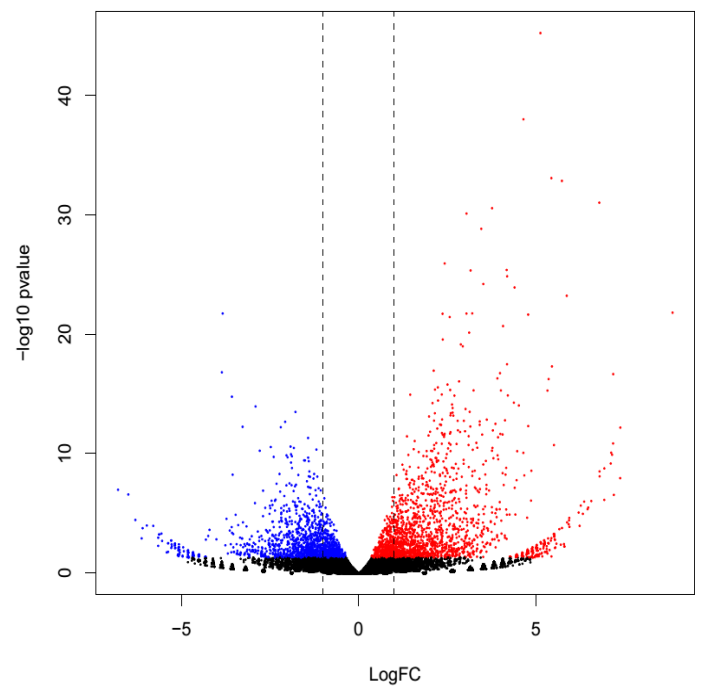
B) T24-Old



C) T6-Young



D) T24-Young



5.3.5 Gene ontology enrichment analysis and annotation of the significantly regulated genes

Gene Ontology (GO) classification of the significantly regulated genes was performed to identify the functional processes associated with the Arabidopsis inflorescence HT response. The predominant 45 sub-classifications of GO functions across all of the significantly regulated genes, which are statistically significant by *P*-value, as determined over the two HT-stress time points and two different staged sample groups are shown in Fig. 5.6, 5.7, 5.8, 5.9, 5.10, 5.11, 5.12 and 5.13. Based on these functional classifications, the genes which were most enriched were those in “other cellular process” and “other metabolic processes”, which are classified into Biological Processes. The most enriched categories of the genes are “nucleus”, “other membrane”, “other intracellular components”, and “other cytoplasmic components” in Cellular Component classification, and are enriched in “other binding” and “unknown molecular functions” in Molecular Function. The lowest enrichment category of the genes is “electron transport or energy pathways” in Biological Process and “receptor binding or activity” in Molecular. In the Cellular Component classification the lowest enrichment level is “ribosome”. However, the percentage of gene enrichment for “response to stress” does not present a significant difference with other categories, which suggests that some HT sensitive genes might not be reported to be related to HT.

A summary of the most down- and up- regulated genes in “Old” and “Young” group samples with 6 hours and 24 hours HT-stress is presented in Table 5.3, 5.4, 5.5 and 5.6 with significant value of P -value <0.05 . For example, with the significant value P -value <0.05 , the gene AT2G32950 (*COP1*), whose function is to repress photomorphogenesis and induce skotomorphogenesis in the dark (Hofmann, 2015), was most down-regulated (58.46 fold) in “Old” samples after 6 hours HT-stress and the most up-regulated one is AT4G00050 (*UNE10*) (63.2 fold), which is a sequence-specific DNA binding transcription factor (Leivar et al., 2008). However, in the same staged samples, the most down-regulated gene is AT1G47270 (*TLP6*) (196.87 fold), which is a transcription factor and encodes phosphoric diester hydrolase (Lai et al., 2012), and the most up-regulated one is AT3G59200 (198.47 fold), which encode F-box/RNI-like superfamily protein (Kuroda et al., 2012), with 24 hours HT-stress. In the “Young” group samples, the most down-regulated gene is AT3G27810 (*MYB21*) (59.74 fold), which encodes a member of the R2R3-MYB transcription factor gene family and Involves in jasmonate response during stamen development (Li et al., 2013, Peng, 2009), and the most up-regulated one is AT5G25451 (126.7 fold), which is a pseudo-gene of AT5G25450 and not reported the function, with 6 hours HT-stress. In 24 hours HT-stressed “Young” sample, the most down-regulated gene is AT1G33730 (*CYP76C5*)(110.66 fold), which is not identified the clear function, and the most up-regulated one is AT1G29410 (*PAI3*)(461.33 fold), whose function is to

encode phosphoribosylanthranilate isomerase which catalyzes the third step in tryptophan biosynthesis (He & Li, 2001). In addition, the the fold change of expression level in “Young” samples with 6 hours HT-stress is less than those with 24 hours stress. These results suggest that 24 hours HT-stress not only leads to a greater number of genes with altered expression levels but also the extent of fold change is much higher.

Figure 5.6 Gene Ontology (GO) enrichment analysis of up-regulated genes in “Old” sample with 6 hours HT-stress. The genes are up-regulated 2-fold in 6 hours HT-stressed samples compared to those not stressed in “Old” group samples, expression level is significantly different (P -value <0.05). Y-axis displays the percentage of significant genes corresponding to each functional type. X-axis displays the GO annotation corresponding to the three categories: Biological Process, Cellular Compartment, and Molecular Function.

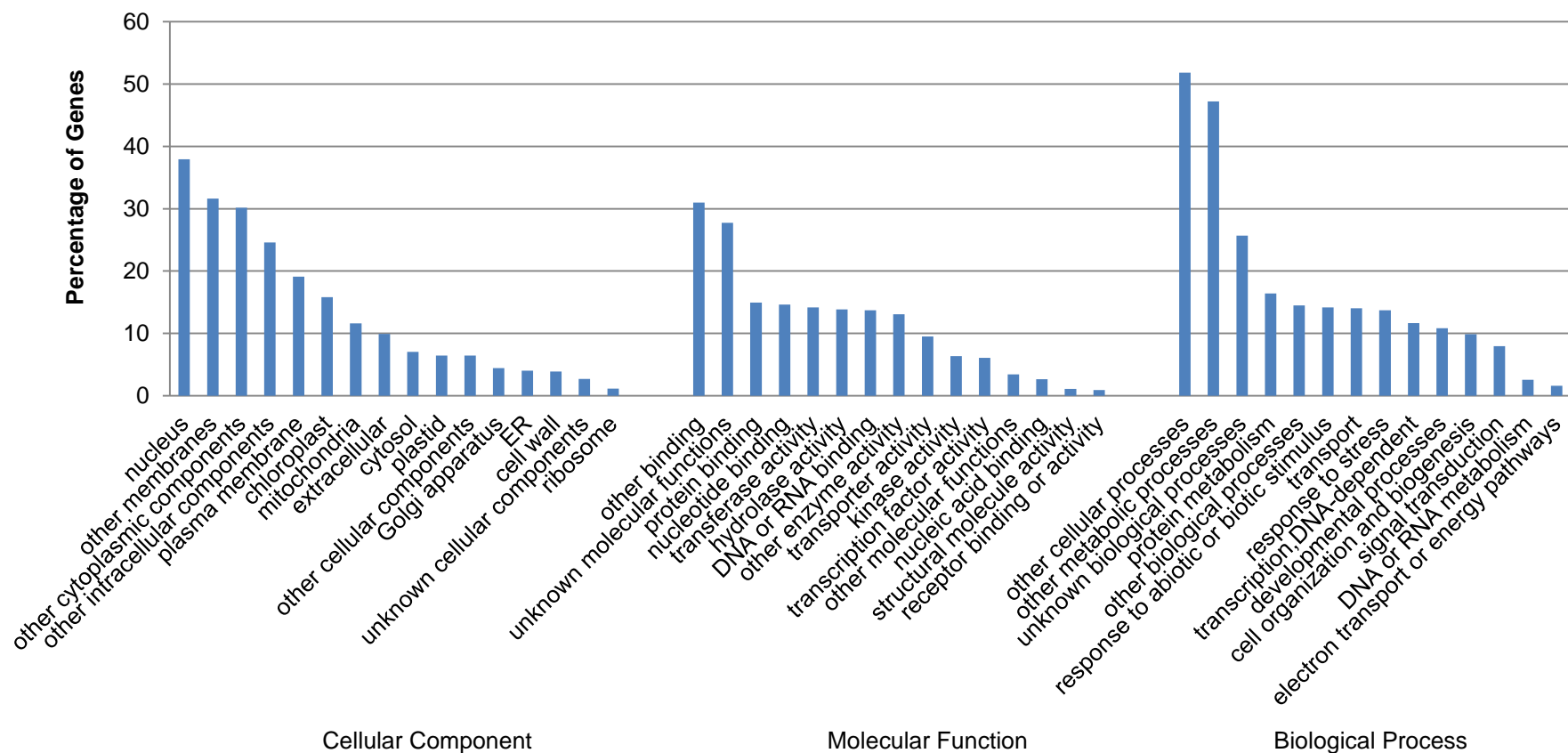


Figure 5.7 Gene Ontology (GO) enrichment analysis of down-regulated genes in “Old” sample with 6 hours HT-stress. The genes are down-regulated 2-fold in 6 hours HT-stressed samples compared to those not stressed in “Old” group samples, expression level is significantly different (P -value<0.05). Y-axis displays the percentage of significant genes corresponding to each functional type. X-axis displays the GO annotation corresponding to the three categories: Biological Process, Cellular Compartment, and Molecular Function.

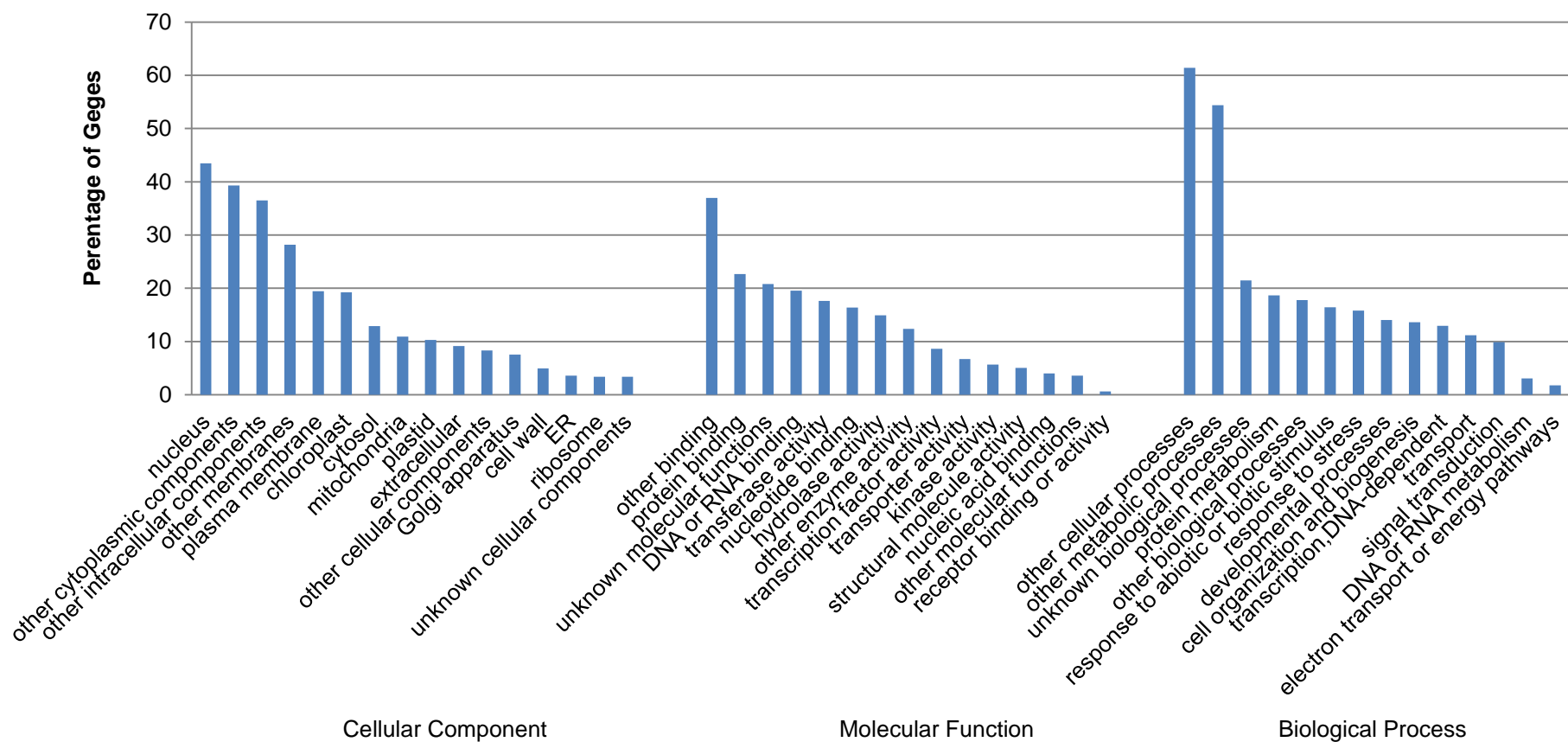


Figure 5.8 Gene Ontology (GO) enrichment analysis of up-regulated genes in “Young” sample with 6 hours HT-stress. The genes are up-regulated 2-fold in 6 hours HT-stressed samples compared to those not stressed in “Young” group samples, expression level is significantly different (P -value <0.05). Y-axis displays the percentage of significant genes corresponding to each functional type. X-axis displays the GO annotation corresponding to the three categories: Biological Process, Cellular Compartment, and Molecular Function.

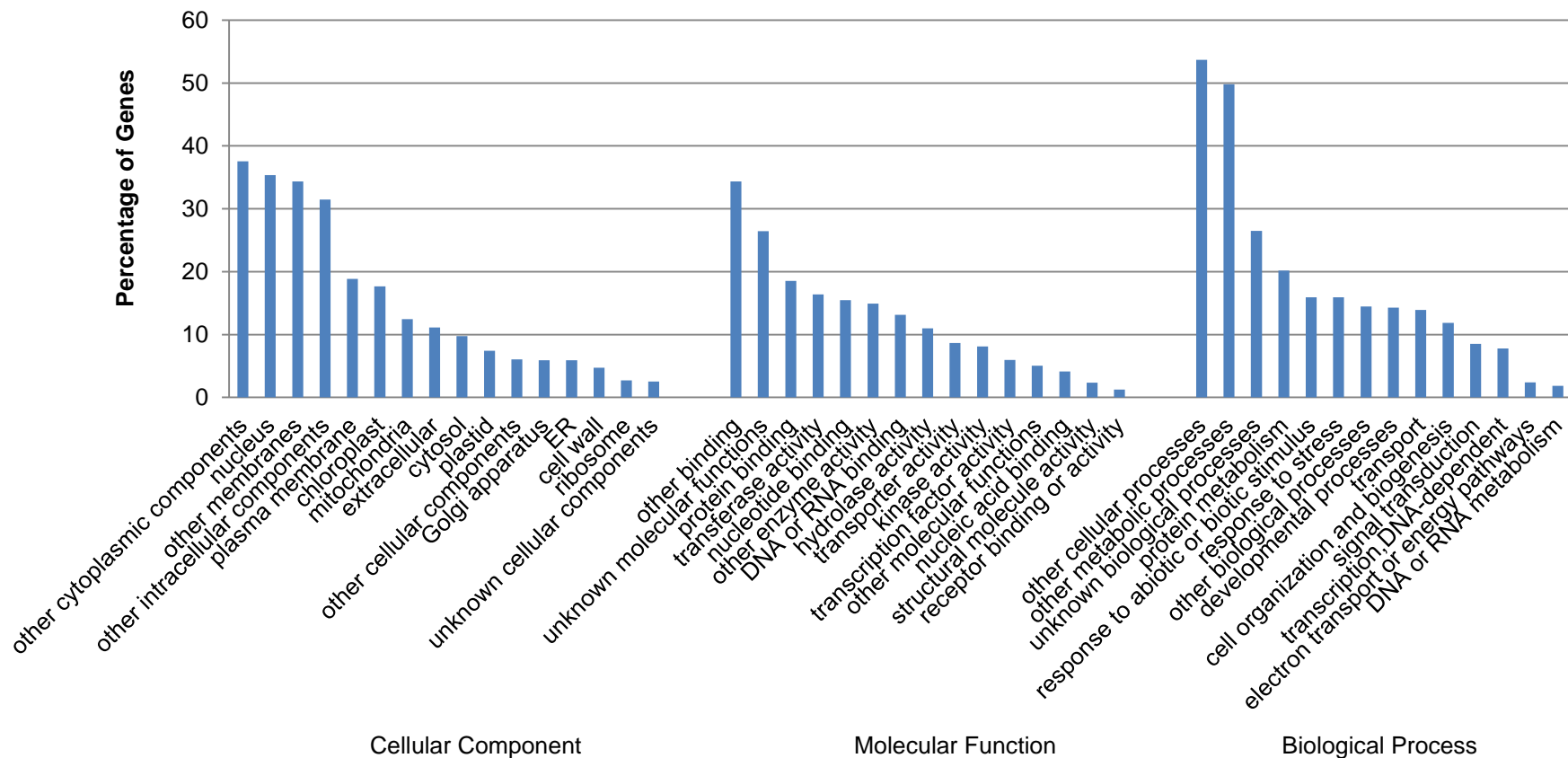


Figure 5.9 Gene Ontology (GO) enrichment analysis of down-regulated genes in “Young” sample with 6 hours HT-stress. The genes are down-regulated 2-fold in 6 hours HT-stressed samples compared to those not stressed in “Young” group samples, expression level is significantly different (P -value <0.05). Y-axis displays the percentage of significant genes corresponding to each functional type. X-axis displays the GO annotation corresponding to the three categories: Biological Process, Cellular Component, and Molecular Function.

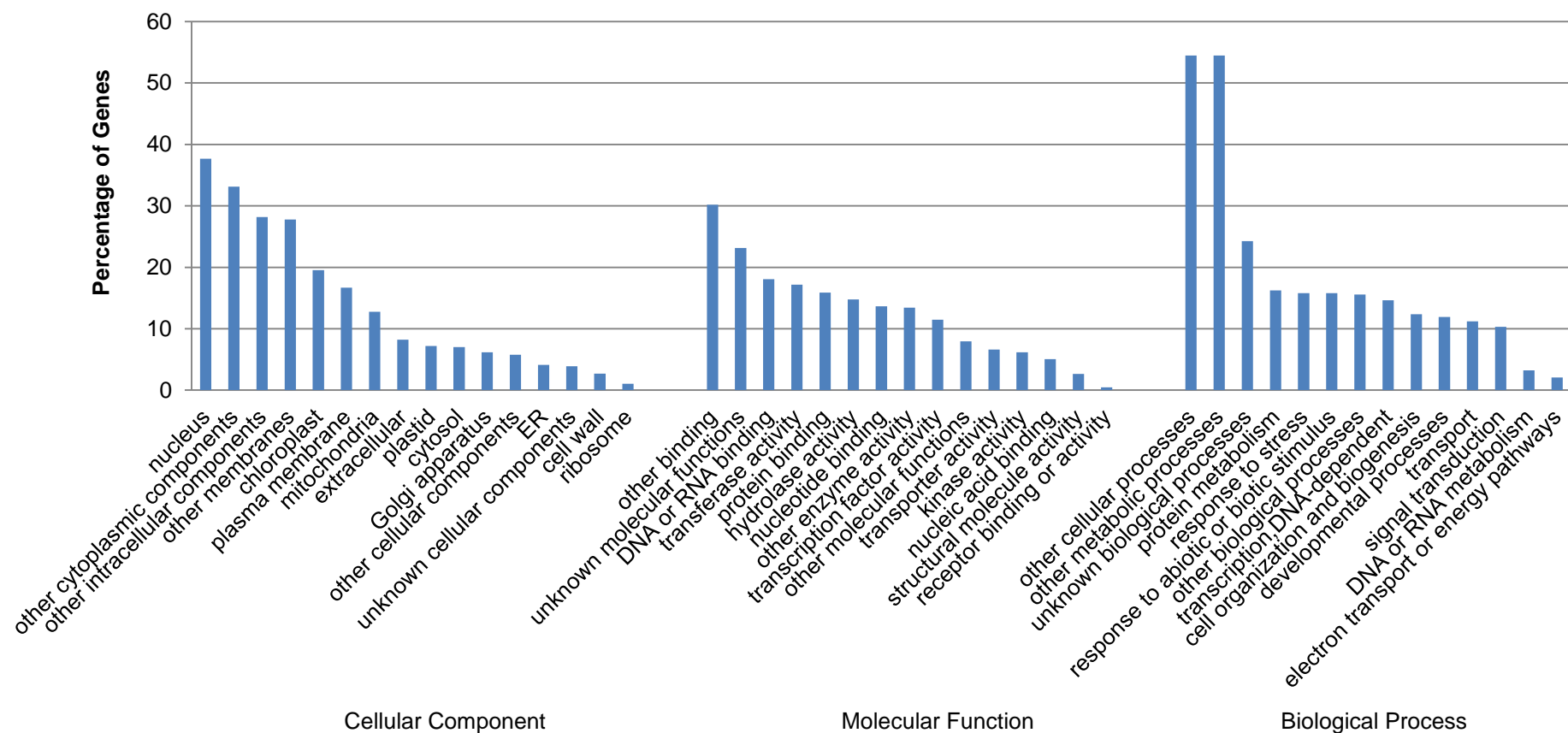


Figure 5.10 Gene Ontology (GO) enrichment analysis of up-regulated genes in “Old” sample with 24 hours HT-stress. The genes are up-regulated 2-fold in 24 hours HT-stressed samples compared to those not stressed in “Old” group samples, expression level is significantly different (P -value <0.05). Y-axis displays the percentage of significant genes corresponding to each functional type. X-axis displays the GO annotation corresponding to the three categories: Biological Process, Cellular Compartment, and Molecular Function.

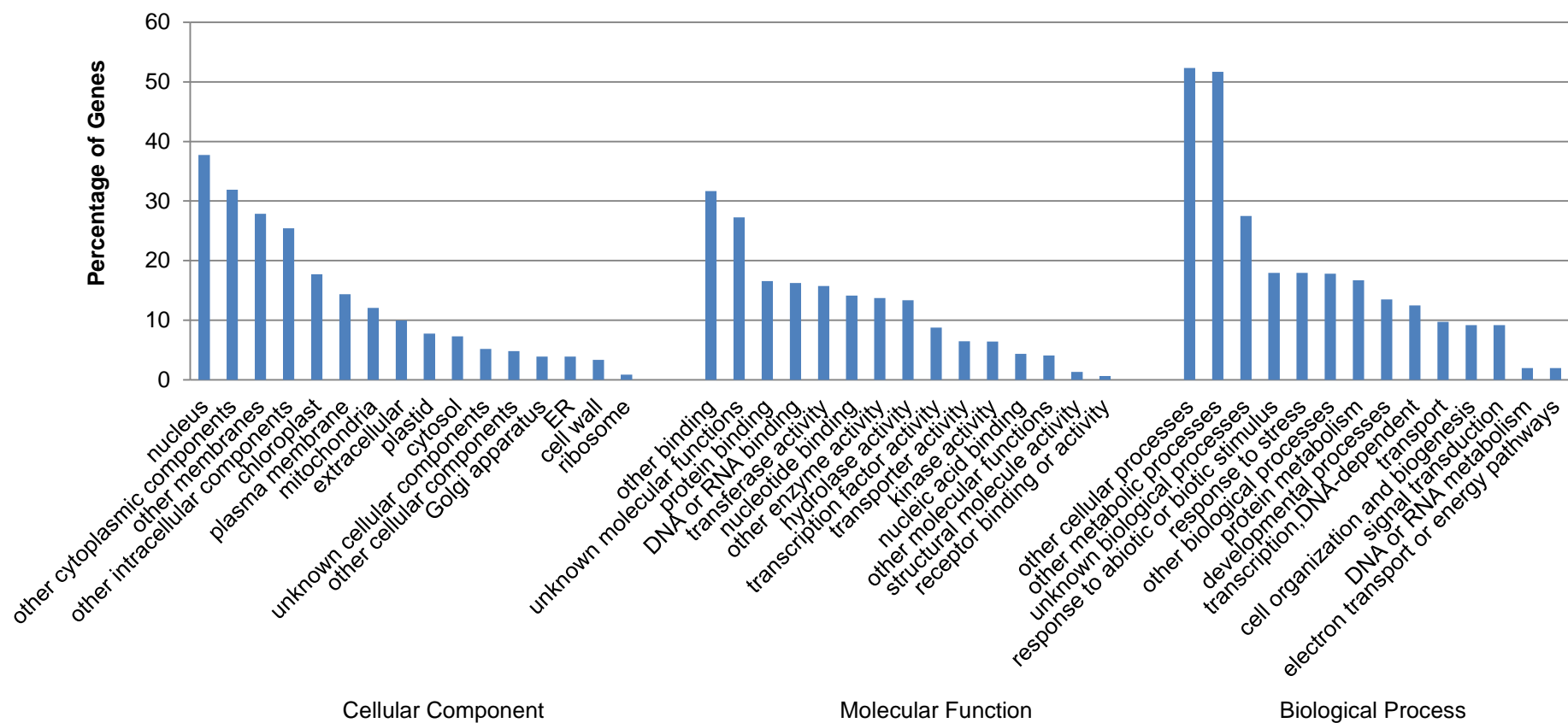


Figure 5.11 Gene Ontology (GO) enrichment analysis of down-regulated genes in “Old” sample with 24 hours HT-stress. The genes are down-regulated 2-fold in 24 hours HT-stressed samples compared to those not stressed in “Old” group samples, expression level is significantly different (P -value <0.05). Y-axis displays the percentage of significant genes corresponding to each functional type. X-axis displays the GO annotation corresponding to the three categories: Biological Process, Cellular Compartment, and Molecular Function.

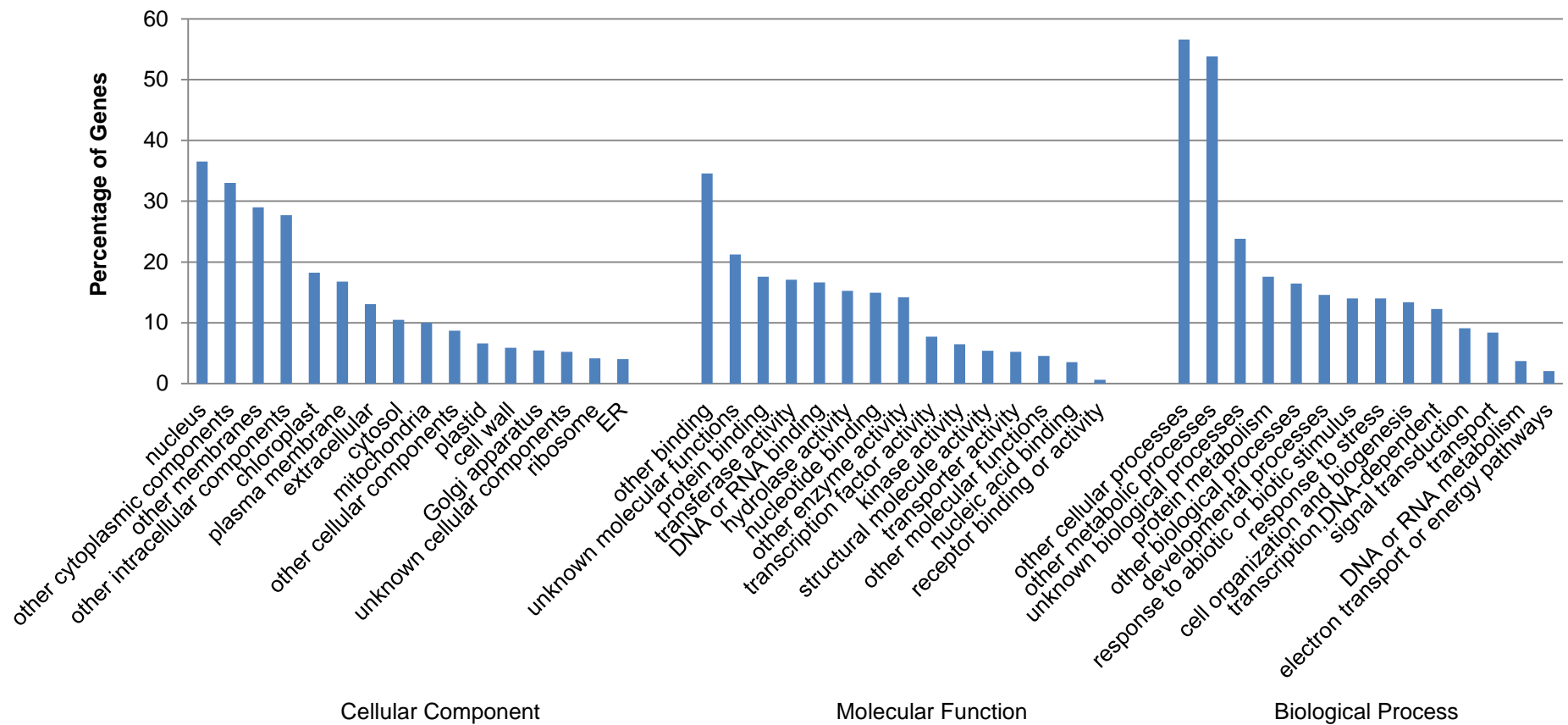


Figure 5.12 Gene Ontology (GO) enrichment analysis of up-regulated genes in “Young” sample with 24 hours HT-stress. The genes are up-regulated 2-fold in 24 hours HT-stressed samples compared to those not stressed in “Young” group samples, expression level is significantly different (P -value <0.05). Y-axis displays the percentage of significant genes corresponding to each functional type. X-axis displays the GO annotation corresponding to the three categories: Biological Process, Cellular Component, and Molecular Function.

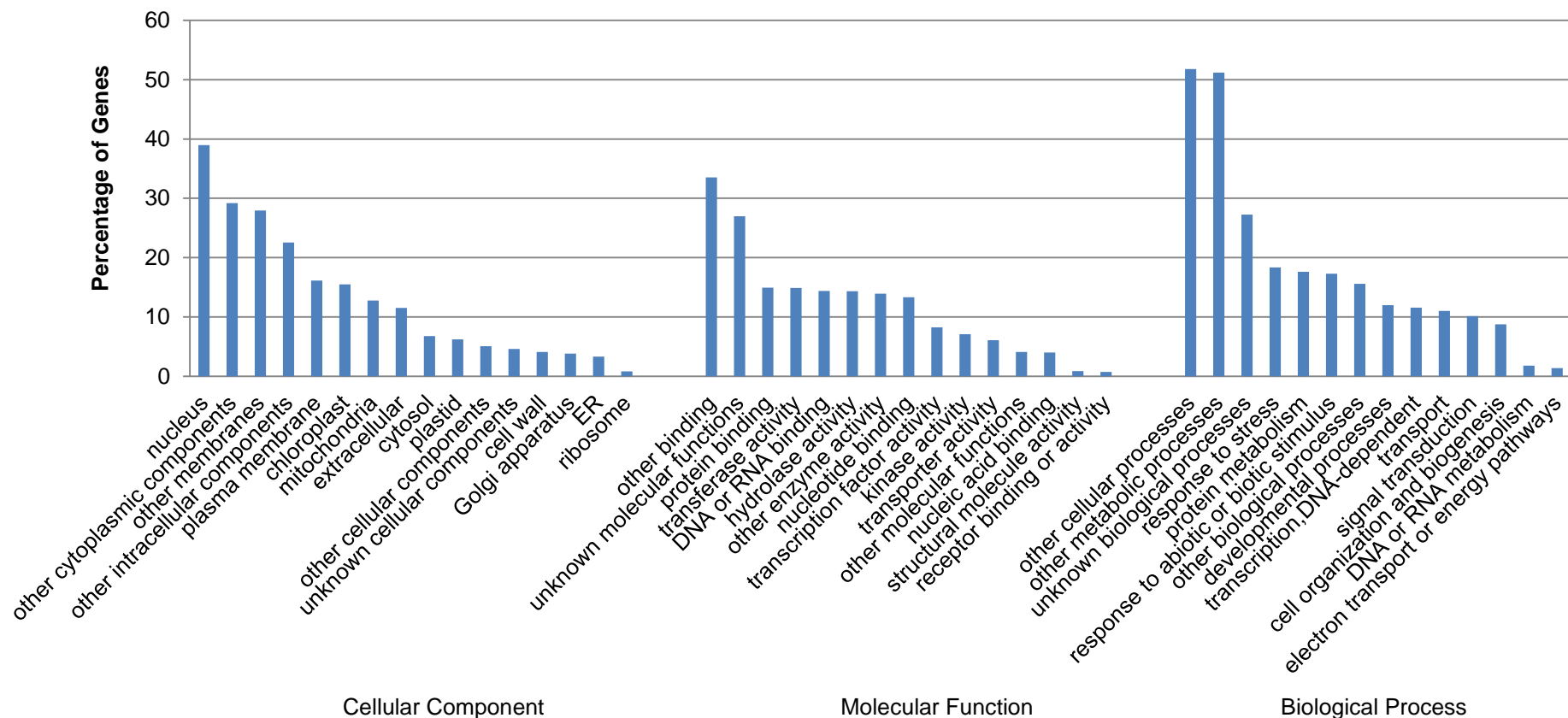


Figure 5.13 Gene Ontology (GO) enrichment analysis of down-regulated genes in “Young” sample with 24 hours HT-stress. The genes are down-regulated 2-fold in 24 hours HT-stressed samples compared to those not stressed in “Young” group samples, expression level is significantly different (P -value <0.05). Y-axis displays the percentage of significant genes corresponding to each functional type. X-axis displays the GO annotation corresponding to the three categories: Biological Process, Cellular Compartment, and Molecular Function.

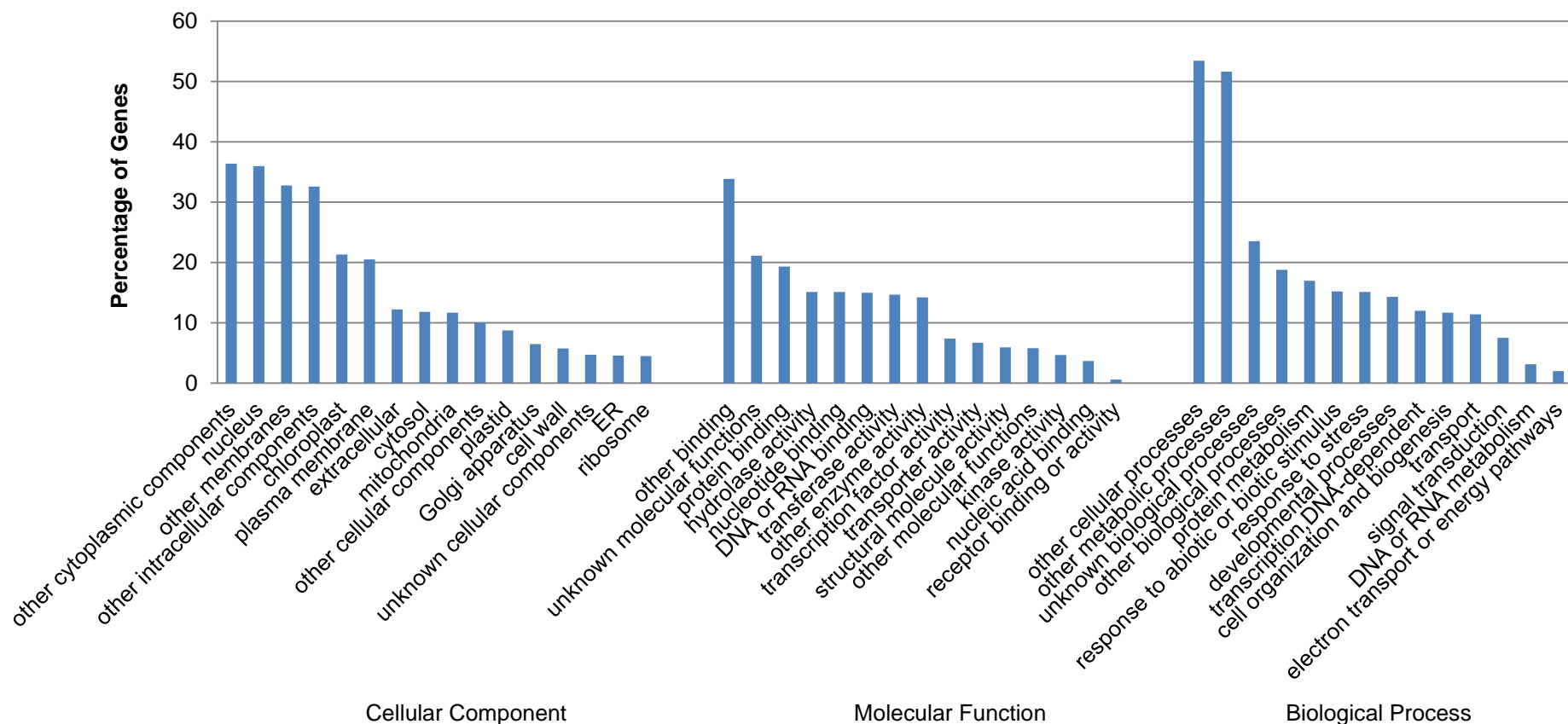


Table 5.3 Summary of the top 10 down- and up- regulated genes in “Old” group samples with 6 hours HT-stress (P -value<0.05). Down-regulated genes are labelled with blue colour and up-regulated ones are labelled with red colour.

AGI code	Symbol	Description	Fold change	Transcription factor
AT2G32950	<i>COP1</i>	Transducin/WD40 repeat-like superfamily protein	-58.46	
AT5G06920	<i>FLA21</i>	FASCICLIN-like arabinogalactan protein 21 precursor	-54.20	
AT5G40660	<i>AT5G40660</i>	ATP12 protein-like protein	-51.71	
AT3G17340	<i>AT3G17340</i>	ARM repeat superfamily protein	-49.82	
AT1G77520	<i>AT1G77520</i>	O-methyltransferase family protein	-48.92	
AT2G13440	<i>AT2G13440</i>	glucose-inhibited division family A protein	-42.57	
AT5G16970	<i>AER</i>	alkenal reductase	-41.08	
AT5G39220	<i>AT5G39220</i>	alpha/beta-Hydrolases superfamily protein	-40.69	
AT1G24070	<i>CSLA10</i>	cellulose synthase-like A10	-39.49	
AT2G18210	<i>AT2G18210</i>	hypothetical protein	-37.81	
AT5G50050	<i>AT5G50050</i>	Plant invertase/pectin methylesterase inhibitor superfamily protein	36.70	
AT5G40600	<i>AT5G40600</i>	bromodomain testis-specific protein	38.38	
AT4G12750	<i>AT4G12750</i>	Homeodomain-like transcriptional regulator	38.48	
AT2G36660	<i>PAB7</i>	poly(A) binding protein 7	41.24	
AT1G65430	<i>ARI8</i>	IBR domain-containing protein	41.67	
AT5G09210	<i>AT5G09210</i>	GC-rich sequence DNA-binding factor-like protein	43.97	
AT3G60310	<i>AT3G60310</i>	acyl-CoA synthetase family protein	46.32	
AT2G17380	<i>AP19</i>	associated protein 19	50.29	
AT1G07850	<i>AT1G07850</i>	transferring glycosyl group transferase (DUF604)	59.01	
AT4G00050	<i>UNE10</i>	basic helix-loop-helix (bHLH) DNA-binding superfamily protein	63.20	Yes

Table 5.4 Summary of the top 10 down- and up- regulated genes in “Young” group samples with 6 hours HT-stress (P -value<0.05). Down-regulated genes are labelled with blue colour and up-regulated ones are labelled with red colour.

AGI code	Symbol	Description	Fold change	Transcription factor
AT3G27810	<i>MYB21</i>	LURP-one-like protein (DUF567)	-59.74	Yes
AT3G10986	<i>AT3G10986</i>	indole-3-butyric acid response 5	-58.88	
AT2G40390	<i>AT2G40390</i>	basic helix-loop-helix (bHLH) DNA-binding superfamily protein	-58.25	
AT3G13210	<i>AT3G13210</i>	Chaperone DnaJ-domain superfamily protein	-49.59	
AT4G33870	<i>AT4G33870</i>	pseudogene of Protein kinase superfamily protein	-48.78	
AT5G40350	<i>MYB24</i>	myb domain protein 24	-48.54	Yes
AT1G79220	<i>AT1G79220</i>	3-hydroxyacyl-CoA dehydrogenase family protein	-48.19	Yes
AT2G30240	<i>ATCHX13</i>	myb domain protein 21	-46.32	
AT3G17670	<i>AT3G17670</i>	Pmr5/Cas1p GDSL/SGNH-like acyl-esterase family protein	-45.67	
AT4G28790	<i>AT4G28790</i>	photosystem II reaction center protein D	-42.78	Yes
AT3G20970	<i>NFU4</i>	Mitochondrial transcription termination factor family protein	44.54	
AT3G15290	<i>AT3G15290</i>	NFU domain protein 4	45.20	
ATCG00270	<i>PSBD</i>	Cation/hydrogen exchanger family protein	45.17	
AT5G40180	<i>AT5G40180</i>	crooked neck protein, putative / cell cycle protein	45.82	
AT2G04550	<i>IBR5</i>	peptide transporter 1	46.07	
AT3G54140	<i>PTR1</i>	Peroxidase superfamily protein	50.32	
AT4G37480	<i>AT4G37480</i>	neuronal PAS domain protein	53.96	
AT1G68610	<i>PCR11</i>	Unknown gene	58.48	
AT4G03038	<i>AT4G03038</i>	tetratricopeptide repeat (TPR)-containing protein	82.34	
AT5G25451	<i>AT5G25451</i>	PLANT CADMIUM RESISTANCE 11	126.70	

Table 5.5 Summary of the top 10 down- and up- regulated genes in “Old” group samples with 24 hours HT-stress (*P*-value<0.05). Down-regulated genes are labelled with blue colour and up-regulated ones are labelled with red colour.

AGI code	Symbol	Description	Fold change	Transcription factor
AT1G47270	<i>TLP6</i>	tubby like protein 6	-196.87	Yes
AT5G48210	<i>AT5G48210</i>	prolamin-like protein (DUF1278)	-93.78	
AT3G43210	<i>TES</i>	ATP binding microtubule motor family protein	-87.76	
AT2G38360	<i>PRA1.B4</i>	prenylated RAB acceptor 1.B4	-78.27	
AT4G36610	<i>AT4G36610</i>	alpha/beta-Hydrolases superfamily protein	-76.09	
AT3G03760	<i>LBD20</i>	LOB domain-containing protein 20	-71.42	Yes
AT3G16780	<i>AT3G16780</i>	Ribosomal protein L19e family protein	-66.78	
AT5G02540	<i>AT5G02540</i>	NAD(P)-binding Rossmann-fold superfamily protein	-65.27	
AT5G16240	<i>AT5G16240</i>	Plant stearyl-acyl-carrier-protein desaturase family protein	-64.30	
AT1G18600	<i>RBL12</i>	RHOMBOID-like protein 12	-63.34	
ATCG00270	<i>PSBD</i>	photosystem II reaction center protein D	90.84	
AT1G80430	<i>AT1G80430</i>	tRNA-Ser	92.88	
AT3G04184	<i>AT3G04184</i>	hypothetical protein	97.44	
AT1G70680	<i>AT1G70680</i>	Caleosin-related family protein	101.90	
AT5G40180	<i>AT5G40180</i>	Pmr5/Cas1p GDSL/SGNH-like acyl-esterase family protein	103.94	
ATCG00050	<i>RPS16</i>	ribosomal protein S16	115.28	
AT5G40350	<i>MYB24</i>	myb domain protein 24	130.70	Yes
ATCG00500	<i>ACCD</i>	acetyl-CoA carboxylase carboxyl transferase subunit beta	165.84	
AT4G04170	<i>AT4G04170</i>	transposable_element_gene	184.00	
AT3G59200	<i>AT3G59200</i>	F-box/RNI-like superfamily protein	198.47	

Table 5.6 Summary of the top 10 down- and up- regulated genes in “Young” group samples with 24 hours HT-stress (*P*-value<0.05). Down-regulated genes are labelled with blue colour and up-regulated ones are labelled with red colour.

AGI code	Symbol	Description	Fold change	Transcription factor
AT1G33730	<i>CYP76C5</i>	cytochrome P450, family 76, subfamily C, polypeptide 5	-110.66	
AT2G38320	<i>TBL34</i>	TRICHOME BIREFRINGENCE-LIKE 34	-90.56	
AT1G15570	<i>CYCA2;3</i>	CYCLIN A2;3	-78.86	
AT2G27690	<i>CYP94C1</i>	cytochrome P450, family 94, subfamily C, polypeptide 1	-69.73	
AT2G44250	<i>AT2G44250</i>	tRNA-splicing ligase, putative (DUF239)	-68.48	
AT5G50230	<i>AT5G50230</i>	Transducin/WD40 repeat-like superfamily protein	-63.10	
AT2G47370	<i>AT2G47370</i>	Calcium-dependent phosphotriesterase superfamily protein	-55.58	
AT1G09200	<i>AT1G09200</i>	Histone superfamily protein	-50.49	
AT4G31130	<i>AT4G31130</i>	keratin-associated protein (DUF1218)	-50.46	
AT2G40250	<i>AT2G40250</i>	SGNH hydrolase-type esterase superfamily protein	-49.59	
AT3G60690	<i>AT3G60690</i>	SAUR-like auxin-responsive protein family	121.48	
AT3G48275	<i>AT3G48275</i>	tRNA-Thr	137.80	
AT1G05340	<i>AT1G05340</i>	cysteine-rich TM module stress tolerance protein	138.94	
AT5G13330	<i>Rap2.6L</i>	related to AP2 6l	141.48	Yes
AT4G35690	<i>AT4G35690</i>	hypothetical protein (DUF241)	144.39	
AT4G03038	<i>AT4G03038</i>	Unknown gene	144.59	
AT3G10450	<i>SCPL7</i>	serine carboxypeptidase-like 7	146.38	
AT4G03039	<i>MIR826A</i>	Encodes a microRNA of unknown function	165.78	
AT5G49690	<i>AT5G49690</i>	UDP-Glycosyltransferase superfamily protein	166.24	
AT1G29410	<i>PAI3</i>	phosphoribosylanthranilate isomerase 3	461.33	

Venn diagrams were performed to reveal the overlap of the genes those are significantly different (Fig. 5.14). To compare the different HT-stress period samples in “Old” and “Young” stages with P -value <0.05 , 17 genes were significantly down-regulated in both the “Old” and “Young” samples with 6 and 24 hours HT-stress, and 93 genes were up-regulated. Moreover, 26 genes were significantly and excessively down-regulated in both “Old” and “Young” samples with 6 hours HT-stress and 259 genes excessively with 24 hours HT-stress. 37 genes were significantly down-regulated only in “Young” samples in both 6 and 24 hours HT-stress and 74 genes in “Old” samples. For the genes that were significantly up-regulated, 29 genes were only up-regulated in both “Old” and “Young” samples with 6 hours HT-stress and 470 genes were with 24 hours HT-stress. There were 61 genes significantly up-regulated only in “Young” sample in both 6 and 24 hours HT-stress, and 72 genes only in “Old” samples. These specific gene that were down- and up-regulated in all samples were used to generate a heat map visualization of the cluster pattern through a Hierarchical Clustering (HCL) algorithm with a statistically significant different P -Value <0.05 (Fig. 5.15). These genes that are expressed in both the “Old” and “Young” stage samples display a stable down- or up- regulation with 6 and 24 hours HT-stress, which suggests that the HT-stress induces sustained change in gene expression.

Figure 5.14 Venn diagram analysis of the significantly regulated genes at different stages with different HT-stress period. The clusters are related to each staged samples with different HT-stress period.

A) Genes are significantly down-regulated (P -value <0.05) B) Genes are significantly up-regulated (P -value <0.05)

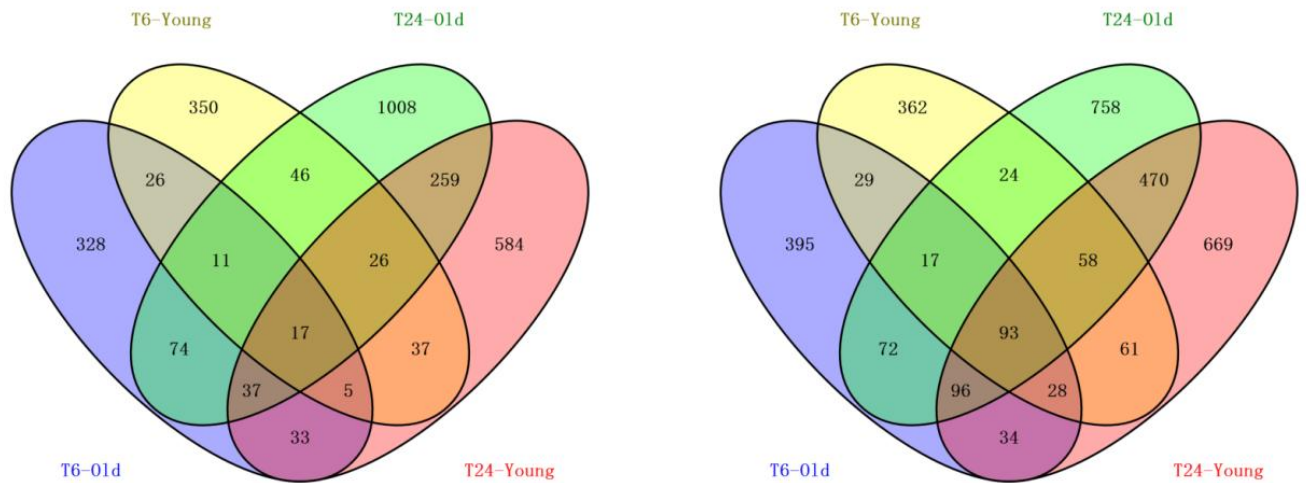
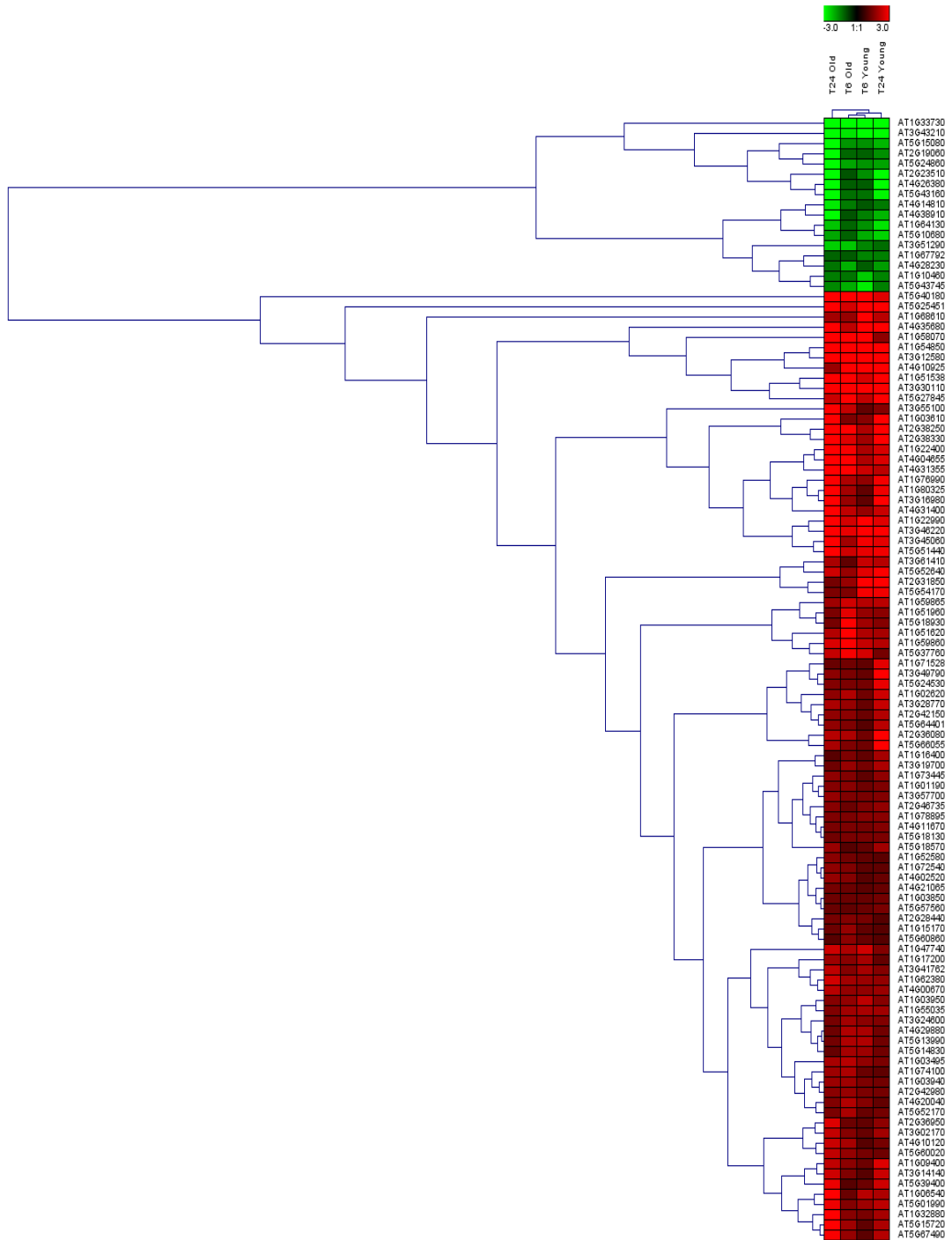


Figure 5.15 Heatmap of differential expression between all pairwise comparisons using ANOVA analysis. Heatmap clustering of expression fold change of the significantly regulated genes (P -value <0.05) conducted using Hierarchical Clustering (HCL) algorithm in “Old” and “Young” staged samples at the two HT-stress time points. The colour scale represents the values of log2FC (Expression level fold change).



5.3.6 Expression validation by quantitative RT-PCR

Ten genes were selected to verify the expression level results of RNA-seq by quantitative RT-PCR. Six of them have been used in Chapter 4 for expression analysis with HT-stress, and four others were selected as the method mentioned in section 4.1. The 24 hours HT-stress time point was used to compare the expression between quantitative RT-PCR and RNA-seq results. All of the 10 genes showed similar expression patterns in this analysis as seen from the differential analysis results from RNA-seq (Fig. 5.16, Fig. 5.17). The fold change of these genes in RNA-seq and quantitative RT-PCR are listed in Table 5.7.

Table 5.7 Comparison of gene expression fold change in RNA-seq and quantitative RT-PCR.

AGI code	Sample stages	Fold change in RNA-seq	Fold change in quantitative RT-PCR
AT1G09210	Old	-2.71	-1.81
	Young	-0.76	-0.98
AT2G02810	Old	-0.84	-1.00
	Young	-1.67	-1.38
AT2G21510	Old	-0.55	-0.41
	Young	-1.64	-0.57
AT2G45070	Old	-1.42	-0.76
	Young	-2.20	-1.65
AT5G28540	Old	-0.45	-0.81
	Young	-0.07	-0.65
AT3G12050	Old	1.00	0.30
	Young	1.51	0.70
AT3G24500	Old	1.56	1.21
	Young	1.16	1.05
AT4G12400	Old	1.71	1.87
	Young	1.80	1.86
AT4G26080	Old	1.39	2.28
	Young	1.02	1.62
AT5G52640	Old	2.43	4.23
	Young	2.96	3.50

Figure 5.16 Quantitative RT-PCR verification of the differentially down-regulated expressed genes. Error bars indicate standard error. Log₂FC: fold change value after log₂ transformation of expression levels. Primers used for quantitative RT-PCR: AT1G09210 (CRT1bF-qPCR and CRT1bR-qPCR), AT2G02810 (UTR1F-qPCR and UTR1R-qPCR), AT2G21510 (F3K23F-qPCR and F3K23R-qPCR), AT2G45070 (SEC61F-qPCR and SEC61R-qPCR), AT5G28540 (BIP1F-qPCR and BIP1R-qPCR), and ACTIN7 as reference gene (ACT7_2F and ACT7_443R) (primer sequences see section Appendix II).

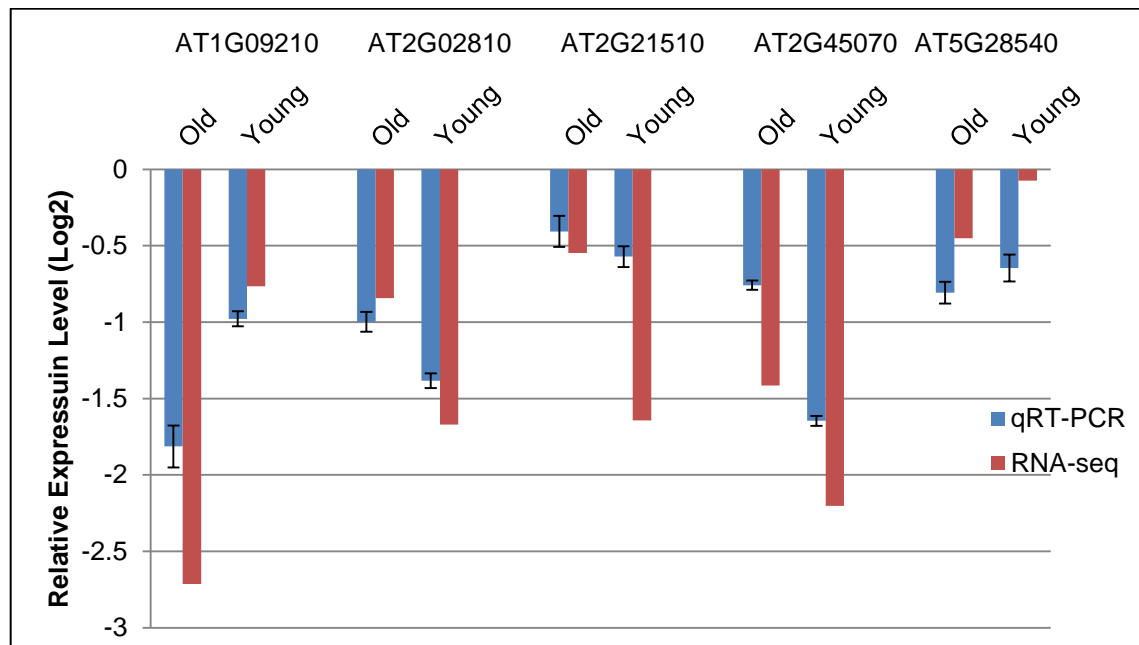
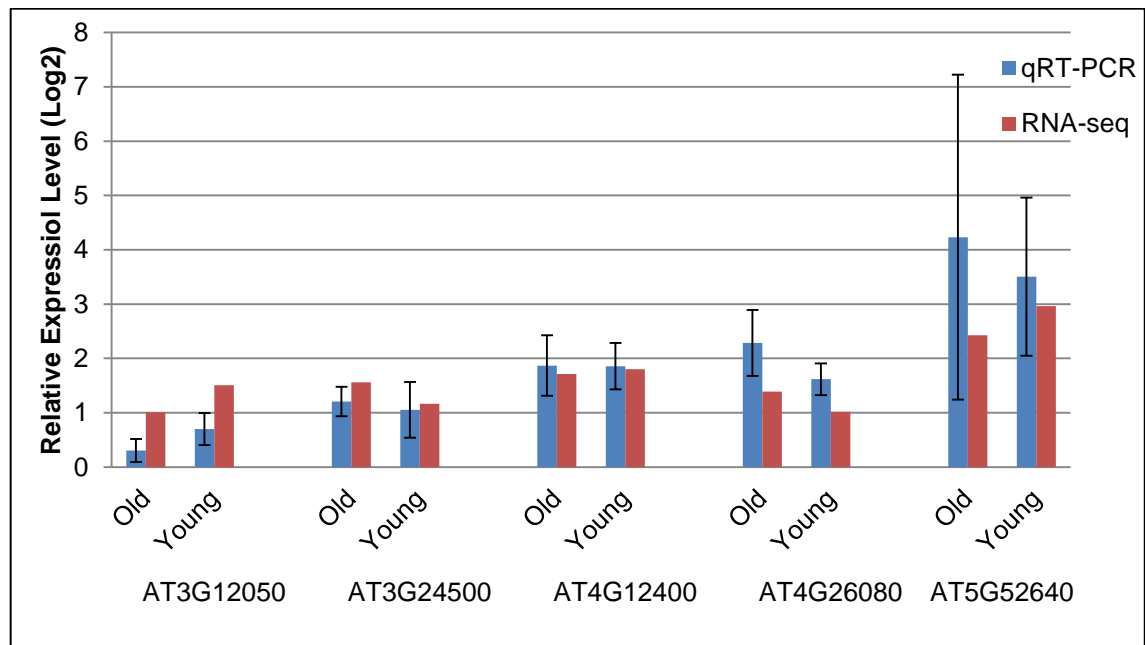


Figure 5.17 Quantitative RT-PCR verification of the differentially up-regulated expressed genes. Error bars indicate standard error. Log2FC: fold change value after log2 transformation of expression levels. Primers used for quantitative RT-PCR: AT3G12050 (MEC18F-qPCR and MEC18R-qPCR), AT3G24500 (MBF1cF-qPCR and MBF1cR-qPCR), AT4G12400 (HOP3F-qPCR and HOP3R-qPCR), AT4G26080 (ABI1F-qPCR and ABI1R-qPCR), AT5G52640 (HS83F-qPCR and HS83R-qPCR), and ACTIN7 as reference gene (ACT7_2F and ACT7_443R) (primer sequences see section Appendix II).



5.4 DISCUSSION

The aim of the RNA-seq analysis was to identify, on a genome-wide scale, genes differentially regulated by HT-stress. For this purpose, the bud samples from *Arabidopsis* Ler wild type plants were developmentally staged and the corresponding RNA was extracted for sequencing-based transcriptomic research. The data generated by the sequencing-based experiment were analysed with different software, expression data were produced using edgeR and the variation of gene expression were statistically analysed using ANOVA model to generate the fold-change using *P*-value values for identifying differentially expressed genes.

5.4.1 Data quality assessment

Arabidopsis Ler buds were treated within HT-stress. These buds were separated into two groups according to pollen developmental stages and collected at different time points during HT-stress. Total RNA was extracted from these bud samples by a QIAGEN protocol and the quality was identified using a Agilent 2100 Bioanalyzer before they were submitted for RNA-seq. Data was obtained from the RNA-seq experiments as base-pairs reads and the first step of RNA-seq analysis was to assess the data quality. The purpose of this experiment was to detect the differentially expressed genes under the HT-stress treatment. MDS plots were generated to provide a visual representation of the pattern of distances between the different biological replicates. The MDS plots revealed that the sample clusters that were HT-stressed for 24 hours displayed a larger distance from other clusters, which indicates longer HT treatment induces genes that are differentially expressed

more significantly (Fig. 5.1). Furthermore, control sample clusters that were not HT-stressed showed closer distance with other, while the HT-stressed samples were assembled together from all replicates which were treated with same period HT-stress but kept away with the replicates that were suffered different HT-stress treatment (Fig. 5.2). For each comparison between HT-stressed and non-stressed samples, which were in sample stage and collected at same time points, replicates from HT-stressed samples presented sufficient distance from that non-stressed to recognise the difference between samples (Fig. 5.3). This MDS plots indicated that the RNA-seq experiment design was efficient and that the data achieved from RNA-seq was sufficient quality for further analysis.

With the ANOVA model, the data from RNA-seq were formalised to generate the fold-change of gene expression in different stage samples which were collected at different HT-stressing time points. The purpose of RNA-seq was to find the genes showing differential expression, so *P*-values were used to identify if the difference was significant or not. The *P*-value is a measure of how likely you are to get this compound data if no real difference existed. Therefore, a small *P*-value (<0.05) indicates that there is a small chance of getting this data if no real difference existed and therefore you decide that the difference in group abundance data is significant. In this way, the number of differentially expressed genes is established (Table 5.2).

After mapped counts normalisation, MA-plots were generated to evaluate the results after normalisation (Fig. 5.4). In the MA-plot, the x axis is the average expression over the mean of normalized counts (A-values), which could represent the gene expression level, and the y axis is the log₂ fold change (FC)

between treatments (M-values). Most genes are not differentially and should distribute nearby the line of $\log_2FC=0$ and not alter with expression level. In this experiment, the gene distribution accumulated between $-1 < \log_2FC < 1$ with the average midline as $\log_2FC=0$, the significantly differentially expressed genes are coloured with red (for up-regulated) and blue (for down-regulated). These results indicated the normalisation of mapped read counts was of sufficiently high quality for further analysis.

The “volcano” plot is used to deduce the distribution of differentially expressed genes. In these plots, the x axis indicates the \log_2 of fold change of gene expression level in different samples, and y axis is the \log_{10} of *P*-value which present the significant difference of gene expression level. In this experiment, red dots display the genes that are significantly up-regulated and blue are those of down-regulated. The results represent the genes are distributed equally on both sides of the vertical line of $\log_2FC=0$, which indicated the distribution of gene is in a good quality (Fig. 5.5).

In summary, these results represent a sufficient evaluation for RNA-seq data. Firstly all of the replicates from different bud samples which were collected in different pollen developmental stages and treated with different periods of HT-stress displayed enough distance with each other according to MDS plots (Fig. 5.1, Fig. 5.2, Fig. 5.3), which indicates that each sample group was different from the others. Secondly, MA-plot results suggest the normalisation of gene expression was accurate since the gene distribution corresponded to a normal distribution (Fig. 5.4). And finally, Volcano plots indicate there was sufficient quantity of significantly differentially expressed genes which also

showed more than 2-fold change of expression for analysing (Fig. 5.5). Therefore, data of RNA-seq was of sufficiently high quality for further analysis.

5.4.2 Gene Ontology (GO) enrichment analysis

According to previous results, the gene lists that were significantly differentially expressed were generated for different sample stages with different HT-stress periods. GO enrichment analysis was performed to investigate the significantly differentially expressed gene enrichment in biological functional categories (Fig. 5.6, 5.7, 5.8, 5.9, 5.10, 5.11, 5.12 and 5.13). The highest enriched categories were cellular processes and metabolic processes, which indicate the most HT sensitive biological function should be related to cellular and metabolic processes. Interestingly, the functional category of “response to stress” presented a quite normal level with most other categories, which indicates the HT response or regulation genes might not represent too much of the differentially expressed genes with HT-stress.

According to GO enrichment analysis, the possible functions of the significantly differentially expressed genes were deduced. For example, AT1G29410 was the most up-regulated (461.33 fold) change in “Young” staged samples with 24 hours HT-stress. This gene is enriched “extracellular” category in Cellular Component cluster and also enriched in “unknown molecular functions” in Molecular Function cluster. Previous research reported that AT1G29410 belongs to the PAI family that encode the enzyme that catalysis the third step of the tryptophan biosynthetic pathway, phosphoribosylanthranilate isomerase (PAI) (Melquist et al., 1999). The most down-regulated gene was AT1G47270, which is a transcription factor and down-regulated 196.87 fold, in 24 hours

HT-stressed “Old” samples. This gene was enriched in several functional categories, such as “other cellular components” and “nucleus” in Cellular Component, “hydrolase activity”, “other binding” and “transcription factor activity” in Molecular Function, and “developmental processes”, “other cellular processes”, “other biological processes”, “other metabolic processes” and “transcription DNA-dependent” in Biological Process. This gene is a member of the Tubby and Tubby-like proteins (TLPs) family and specifically interacts with *Arabidopsis* Skp1-like (ASK) protein 11, it also possibly works in multiple physiological and developmental processes in *Arabidopsis* (Bao et al., 2014).

Moreover, the Venn diagrams reveal the overlap of the significantly differentially expressed gene lists in both “Old” and “Young” staged samples with 6 hours or 24 hours HT-stress (Fig. 5.14) The Heatmap cluster (Fig. 5.15), which is generated by Hierarchical Clustering (HCL) algorithm, of the expression pattern of these genes indicates that the expression level and variation of these genes is stable in different staged samples and stressed with different HT period.

5.4.3 RNA-seq data validation

To validate the accuracy of RNA-seq data, ten genes were selected to compare the expression level fold change between RNA-seq results and quantitative RT-PCR. In these ten genes, six of them have been used in Chapter 4 for expression analysis in *Arabidopsis* Ler wild type inflorescence, and four others are chosen according to the method that is mentioned in section 4.1. All of these genes are related to HT response in previous annotations and are also tapetum related (Pearce et al., 2015). Both of “Old”

and “Young” staged samples were used in quantitative RT-PCR and the samples were HT-stressed for 1 day to compare the RNA-seq samples that were collected after 24 hours HT-stress. The expression level results show that all of these genes display a similar fold change trend in different stage samples (Fig. 5.16, Fig. 5.17). However, the fold change of gene expression level in RNA-seq data and quantitative RT-PCR is not exactly same, which might be due to the samples being collected at a different time of the day and also the variation in developmental stage of plants.

In summary, this RNA-seq dataset is efficient and accurate for further research on gene function.

CHAPTER 6

PROGRAMMED CELL DEATH RELATED GENE EXPRESSION AND REGULATION

CHAPTER 6. PROGRAMMED CELL DEATH RELATED GENE EXPRESSION AND REGULATION

6.1 INTRODUCTION

Programmed cell death (PCD) is an actively controlled, genetically encoded self-destruct mechanism of the cell (Williams & Dickman, 2008). Although many kinds of PCD have been described and molecularly dissected in animals, less is known about the regulation of PCD processes in plants. However, plant PCD is a crucial component that response to abiotic and biotic stress and a core theme during plant development. Many communication events function to trigger, execute, and thus prevent PCD during plant reproductive development, which include intracellular communication, signalling within cells and tissues, and kinds of complex communication between genetically distinct individuals that are necessary for successful plant reproduction (Olvera-Carrillo et al., 2012).

As mentioned in section 1.5, PCD can be part of a developmental programme (dPCD) or be triggered by environmental conditions (ePCD) (Van Durme & Nowack, 2016). During regular plant development, dPCD initiates as the final step of cell-type specific differentiation programmes (Van Haute gem et al., 2015). Furthermore, although dPCD processes occur independently from stresses of environmental changes, the timing of differentiation-induced or

senescence-related dPCD can be influenced by stresses (Thomas, 2013).

According to Van Durme and Nowack (2016), there is a three-phase chronological progression of the molecular mechanisms involved in regulation of dPCD processes in plant cells.

The first phase is the differentiation programme that various cell types have to undergo in order to achieve the competency of PCD. The tapetum layer undergoes dPCD at the end of the differentiation programme during pollen mitosis stages. A number of genes that are involved with tapetum PCD have been identified. In *Arabidopsis*, the transcription of the mitochondria-localised aspartic protease UNDEAD, which acts as a negative regulator of tapetum dPCD, is directly controlled by a transcription factor (TF) MYB80. Furthermore, the mutants of loss of function of either *MYB80* or *UNDEAD* display premature tapetal PCD and then results in male sterility (Phan et al., 2011). On the contrary, bHLH TF ETERNAL TAPETUM1 in rice was found to promote tapetum PCD through activating the transcription of the cell death-inducing aspartic proteases AP25 and AP37 directly (Niu et al., 2013).

Plant cells then receive the internal or external signals that trigger a rapid PCD execution at the correct time and place during Phase II. Reactive oxygen species (ROS) are highly reactive molecules, which can damage cellular components directly (Zhang et al., 2016). ROS was also reported to associate with dPCD, and possibly functioned as a part of the signalling network that

triggers dPCD execution (Van Durme & Nowack, 2016). During anther development, existence of ROS regulates the right timing of tapetal dPCD. In *Arabidopsis* a tissue-specific NADPH oxidase (RBOHE) is the major contributor of H₂O₂ levels that promotes tapetal cell death, both of deficiency and over-expression of RBOHE abolish the regular ROS accumulation and results in male sterility (Xie et al., 2014). Finally, the cellular corpse is either partially or completely removed by cell clearance processes after breakdown of cellular compartmentalisation in Phase III.

Many male sterile genes have been reported to function in tapetum PCD as mentioned in section 1.5.1. Tapetum undergoes abnormal and early PCD in male sterility mutants and several male sterile genes regulate tapetum PCD during pollen development. To investigate the regulation network between male sterile genes and PCD genes, four PCD related genes were used. *APS REDUCTASE 1* (*APR1*, At4G04610), *BIFUNCTIONAL NUCLEASE 1* (*BFN1*, At1G11190), *CYSTEINE ENDOPEPTIDASE 1* (*CEP1*, At5G50260), and *SENESCENCE-ASSOCIATED GENE 12* (*SAG12*, At5G45890) have been reported to function during ovule PCD processing (Dr. Moritz Nowack, VIB UGent, unpub.) (Kumpf & Nowack, 2015, Zhang et al., 2014). It was expected that the expression of these may be altered in the male sterile mutants.

APR1 encodes a disulfide isomerase-like (PDIL) protein, a member of a multi-gene family of the thioredoxin (TRX) superfamily. This protein belongs to

the adenosine 5'-phosphosulfate reductase-like (APRL) group and reduces sulfate for Cys biosynthesis (Bick et al., 1998, Setya et al., 1996). There are three APR isoforms in the APR family. Previous research reported the key function of *APR1*, one of three APR family members, is to regulate sulphate assimilation in *Arabidopsis* plants (Takahashi et al., 2011). Several of these reports described *APR1* expression and function in root development, but they also mentioned there was not any obvious developmental effect or growth penalty in *Arabidopsis* plants which were lacking functional *APR1* and the plants were perfectly viable (Kopriva et al., 2009). The APR enzyme is a reductase that catalyzes the reduction of activated sulfate to sulfite in plants, and this enzyme is also a kind of glutathione (GSH) reductase that functions to the redox cofactor glutaredoxin similarly. The *APR1* cDNA encoding APS reductase from *Arabidopsis thaliana* is able to complement the cysteine auxotrophy of an *E. coli cysH* [3'-phosphoadenosine-5'-phosphosulfate (PAPS) reductase] mutant, only of the *E. coli* strain produce glutathione (Bick et al., 1998) . APR activity is reported to be regulated through nitrogen at a transcriptional level, and that the three APR isoforms are regulated differently in plants (Koprivova et al., 2000). APR is subject to coordinated metabolic control by carbon metabolism, and the signals from carbon and nitrogen metabolism act synergistically. Positive signalling from sugars can override negative signalling from nitrate assimilation (Hesse et al., 2003). Furthermore, a previous study also revealed APR activity and mRNA level of all three AP

isoforms increased 3-fold in roots after 5h treatment with 150mM NaCl (Koprivova et al., 2008). The regulation of APR was not affected in mutants, which is deficient in abscisic acid (ABA) synthesis, and the plants treated with ABA did not change the mRNA levels of APR isoforms but not in the mutants deficient in jasmonate, salicylate, or ethylene signalling, these results showed that APR was regulated by salt stress in an ABA-independent manner. However, APR enzyme activity was not affected by salt in these plants (Koprivova et al., 2008). *APR1* is a key enzyme in sulfur metabolism and is up-regulated by cytokinin during this process (Ohkama et al., 2002).

BFN1 encodes a bi-functional nuclease that involves in nucleic acid degradation and facilitates nucleotide and phosphate recovery in plant senescence (Perez-Amador et al., 2000). It has mismatch-specific endonuclease activity with wide recognition of single base mismatches, and the ability to cleave types of mismatches (heteroduplexes with loops) (Farage-Barhom et al., 2008, Triques et al., 2007). Level of *BFN1* mRNA was extremely low even undetectable in roots, stems, and leaves, but relatively high in flowers and during stem and leaf senescence (Perez-Amador et al., 2000). *BFN1* nuclease activity was also induced during stem and leaf senescence (Pérez-Amador et al., 2000). Farage-Barhom et al. (2008) also reported the high correlation between GUS expression with *BFN1* promoter-regulation and all examined developmental processes associated with PCD. However, there was no expression was detected in any other part of

plant, which suggested that *BFN1* was involved in developmental PCD-related and senescence processes in *Arabidopsis*. They latterly verified *BFN1*'s function was a nucleic acid-degrading enzyme in senescence and PCD by its localization pattern (Farage-Barhom et al., 2011). The results published by Fendrych et al. (2014) indicates that the lateral root cap (LRC) in *Arabidopsis* roots gives unambiguous evidence for *BFN1* function as a key enzyme for the cell-clearance process during cell death in planta.

CEP1 belongs to the Cysteine proteinases superfamily, and is involved in the final stage of developmental programmed cell death. *AtCEP1* is present in roots, stems, flowers and buds, and green siliques of wild-type *Arabidopsis*. During generative tissue developmental processes, activity of *CEP1* promoter was firstly found in flowers when the gynoecium elongates and extends beyond the top of the stamen, but disappeared when the siliques turned yellow, when the outer integument became slimy and the inner integument developed into the seed coat (Helm et al., 2008). *CEP1* also involves in tapetal PCD and pollen development in *Arabidopsis thaliana*. *CEP1* is a crucial executor during tapetal PCD, and precise expression of *CEP1* is necessary for degeneration of tapetal cells and functional pollen formation promptly (Zhang et al., 2014).

SAG12 is an *Arabidopsis* gene encoding a cysteine protease, that is expressed only in senescent tissues (Huynh le et al., 2005). *SAG12* is specifically activated through developmentally controlled senescence

pathways but not by stress- or hormone-controlled ones. Previous studies indicate that *SAG12* is a senescence marker gene in leaf senescence processes and regulated by several other genes (Dellero et al., 2016, Smykowski et al., 2015, Song et al., 2016). Furthermore, senescence in transgenic plants expressing *SAG12:ipt* is suppressed (Huynh le et al., 2005, Noh & Amasino, 1999, Zhang et al., 2000).

6.2 MATERIALS AND METHODS

6.2.1 Plant materials and growth

All of the seeds used in the research, including the GFP reporter constructs (*APR1:GFP*, *BFN1:GFP*, *CEP1:GFP*, and *SAG12:GFP*, seeds obtained from Dr. Moritz Nowack), male sterile mutants (*ams*, *ms1*, *myb26*, *dyl1* and *tdf1*), and the F1 and F2 generations were sown on Levington M3 and placed in the glasshouse. The F2 generations were sown in 4x3 block trays, with each block for 6-8 seeds. All of the growth conditions are according to section 2.1.

6.2.2 Introgression of PCD genes into male sterile mutants

The four GFP reporter constructs were introgressed into the male sterile mutants. As the mutants were male sterile, there was no need to remove stamens before crossing. F1 generation seeds were harvested from fertile siliques of the male sterile mutant plants and then sown in soil. F2 generation seeds were then harvested for screening.

6.2.3 BASTA screening

BASTA (glufosinate-ammonium) was sprayed onto the leaves of the 15-day old F2 generation plants to screen the homozygous male sterile mutants. The concentration of BASTA was 150mg/l. The spraying was carried out every second day 5 times. Dead plants were removed immediately. Fertile plants were discarded to make sure the samples analysed were homozygous male sterile. Bud samples were dissected to achieve individual anthers, and the buds on the main shoots were marked from the youngest to the oldest one numerical order from 1. Pollen developmental stages were confirmed by DAPI staining. However, as there was no pollen produced in *ams* and *ms1* mutants, pollen developmental stages were confirmed by comparing the anther size and development between mutants and WT samples.

6.2.4 Samples dissection and microscopy

One week after the BASTA screening, the F2 generation plants were confirmed by analysis of GFP expression in anthers. Six plants were selected in each line, the buds of a whole inflorescence were dissected using Zeiss stereomicroscopy Stemi SV6. The samples were stained with 3 µg/ml DAPI solution for stage identification and GFP expression analysis (see section 2.3 for DAPI staining protocol and section 2.13 for confocal microscopy and fluorescence microscopy set up). Also a WT with each GFP construct was analysed.

6.2.5 Bud samples collection

The bud samples on the main shoot of each homozygous male sterile line were collected. The buds from each inflorescence were divided into three staged groups as mentioned previously (see section 4.2.2), mature group, old group, and young group. The samples were collected into 1.5 ml tubes and frozen in liquid nitrogen, and then stored in a -80°C freezer before RNA extraction.

6.2.6 RNA extraction and cDNA synthesis

Total RNA of was extracted using a QIAGEN kit, and then the quality of RNA samples was tested by Nanodrop. cDNA was synthesised from the RNA template, and the quality was then checked by RT-PCR using a housekeeping gene (Actin 7) (see section 2.8 and 2.11).

6.2.7 Quantitative RT-PCR

Quantitative RT-PCR was conducted as in section 2.13. Primers for PCD genes are listed in Appendix II. The standard program for running the plate on the LightCycler was: 95°C 10 min; 45x (95°C 30 sec, 54 °C, 30 sec, 72°C for 1 min); 72°C 6 min. Cp values were calculated by the software of a LightCycler® 480. The expression level was analysed using MicroSoft Excel and statistical analysis was performed by GraphPad Prism 6.

6.3 RESULTS

6.3.1 PCD related genes expression analysis

Four PCD related gene (*APR1*, *BFN1*, *CEP1*, and *SAG12*) GFP reporter constructs plants were introgressed into different male sterile mutants (*ams*, *ms1*, and *myb26*). The sterile mutant plants were recovered after self-crossing of F1 populations and searching for expression in the segregating F2 populations. The results showed that the GFP expression in F1 generation samples was similar with that in the wild type plants.

6.3.1.1 *APR1* expression in WT and male sterile mutants

To investigate the expression and regulation of *APR1*, we used the *APR1*:GFP promoter reporter construct here to show the expression stages during *Arabidopsis* anther and pollen development. The result showed expression of *APR1* genes in *Arabidopsis* anthers at different stages (Fig. 6.1). *APR1*:GFP signal was seen in the nuclei of the anther wall cell rather than pollen, however, it was not clear to indicate the exact layers in which it was expressed. There was no *APR1*:GFP signal could be observed at the microsporocytes stage. GFP signal appeared from tetrad stage and was sustained until pollen developed to the mature pollen stage just before anther dehiscence. However, no GFP signal was seen in the older four anthers during the mature pollen stage (Fig. 6.1). The difference between these two staged anthers is that

breakage of epidermis and endothecium has occurred in the older anther, but epidermis and endothecium are still complete. This result indicates that breakage of epidermis and endothecium cell leads to the loss of APR1:GFP. The septum cell degeneration and stomium differentiation begins in the later stage of pollen mitosis II, and would be completed by the mature pollen stage before anther dehiscence. Mature pollen was seen in both the four older and two younger anthers in buds No.1 and 2, but a slight difference in developmental stage was seen between these two. However, there was no obvious change of GFP expression level according to confocal microscopy results since it was not possible to clearly recognise the difference in GFP brightness from these pictures (Fig. 6.1).

Figure 6.1 APR1:GFP expression in anther tissues in WT background

Scale bar: 75µm (No. 1-11), 150µm (No. 12-16)

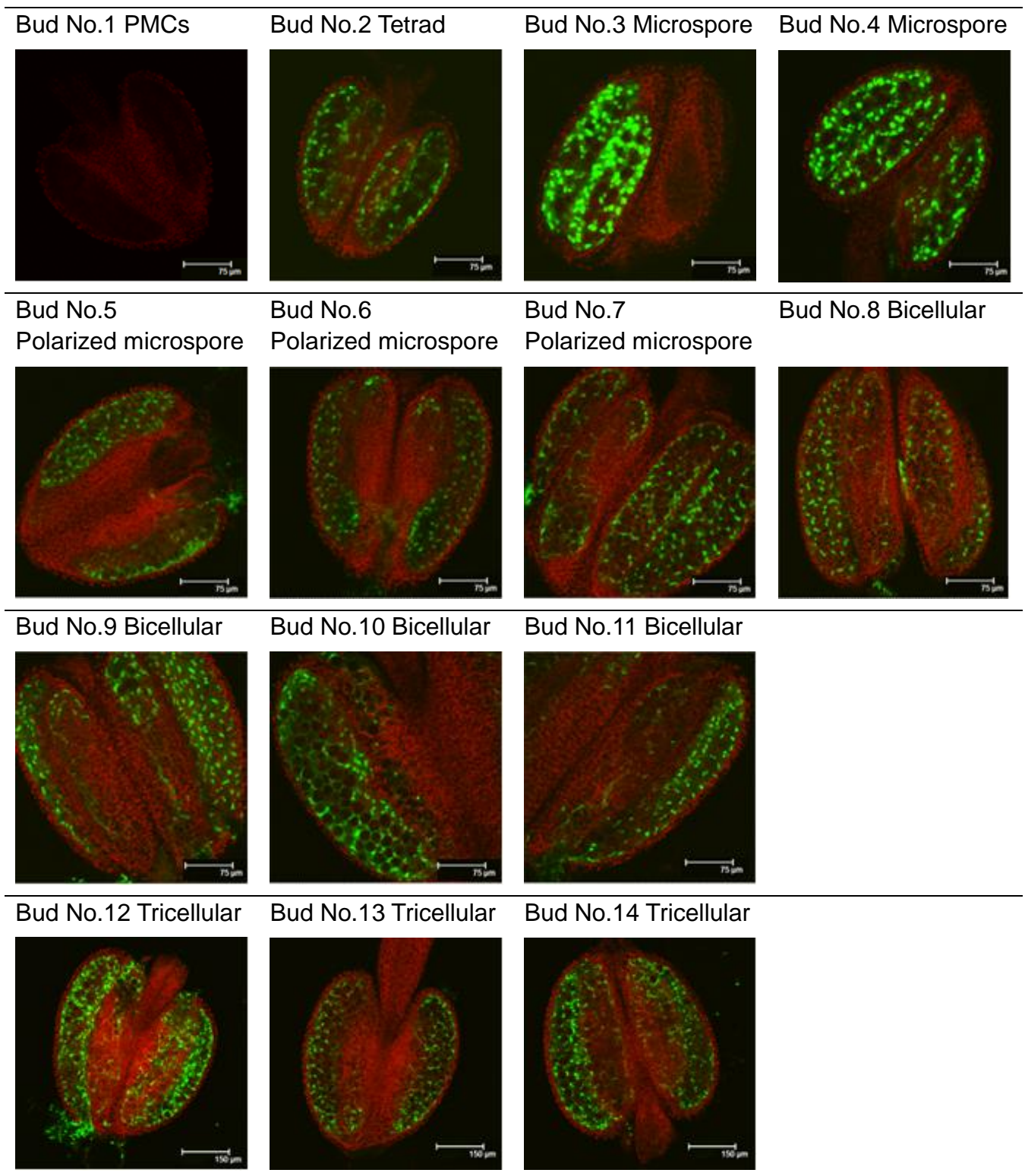
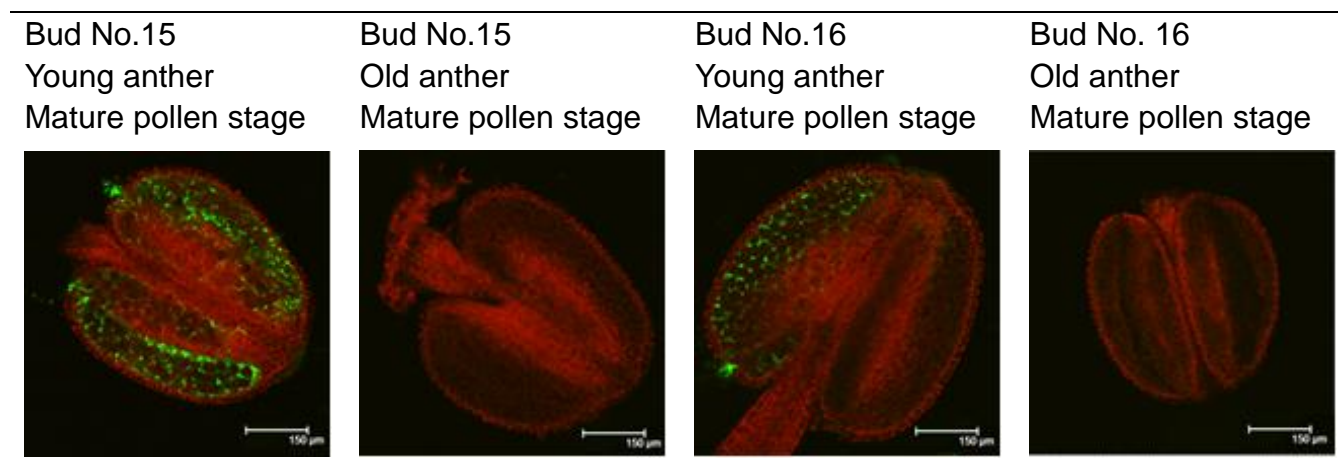


Figure 6.1 APR1:GFP expression in anther tissue in WT background

(Continued)



In the homozygous male sterile mutants, the expression of *APR1* showed a different expression (Fig. 6.2). In the *ams* homozygous mutant, the expression level of *APR1* was down-regulated which resulted in weaker GFP signal in anther tissues. No GFP signal could be found in the tetrad stage in the *ams* mutant, with GFP signal delayed to the microspore stage. Furthermore, this GFP signal could be observed in both the old and young anthers in the oldest bud samples of the inflorescences, rather than the lack of expression observed in old anthers in WT. However, the strength of APR1:GFP signal was significantly decreased in these anthers (Fig. 6.2).

APR1 expression showed a quite similar pattern in *ms1* homozygous mutants compared to *ams* mutant (Fig. 6.3). GFP signal in *ms1* mutant anthers was weaker than that in WT samples, but stronger than that in *ams* mutant. The expression stage was also delayed to the microspore stage as seen in *ams*.

Clear GFP signal was observed across all parts of the anther tissue of the oldest bud samples in the inflorescence in both the four older and two younger anthers (Fig. 6.3).

In the *myb26* homozygous mutant, GFP signal also appeared from microspore stage, which was delayed compare to WT plants. *APR1* expression level was down-regulated in the microspore stage but then increased to almost normal levels in polarized microspore stage. The GFP signal was reduced in the bicellular stage until nearly no clear expression was visible in the oldest bud samples (mature pollen stage and tricellular stage), there was very weak GFP signal could be found at the top of the anthers during these pollen developmental stages (Fig. 6.4).

According to these results, *APR1:GFP* signal exists in nuclei of anther wall cells, but it was not possible to clearly localise expression to specific cell layers. However, *APR1:GFP* signal was observed after tapetum degeneration but vanished with the breakage of the epidermis and the endothecium. Moreover, expression of *APR1* was delayed from tetrad stage in WT to microspore stage in *ams*, *ms1* and *myb26* homozygous mutants. And detailed summary of expression stages of *APR1:GFP* are listed in Table 6.1.

Figure 6.2 APR1:GFP expression in anther tissue in *ams* mutant

Scale bar: 75µm

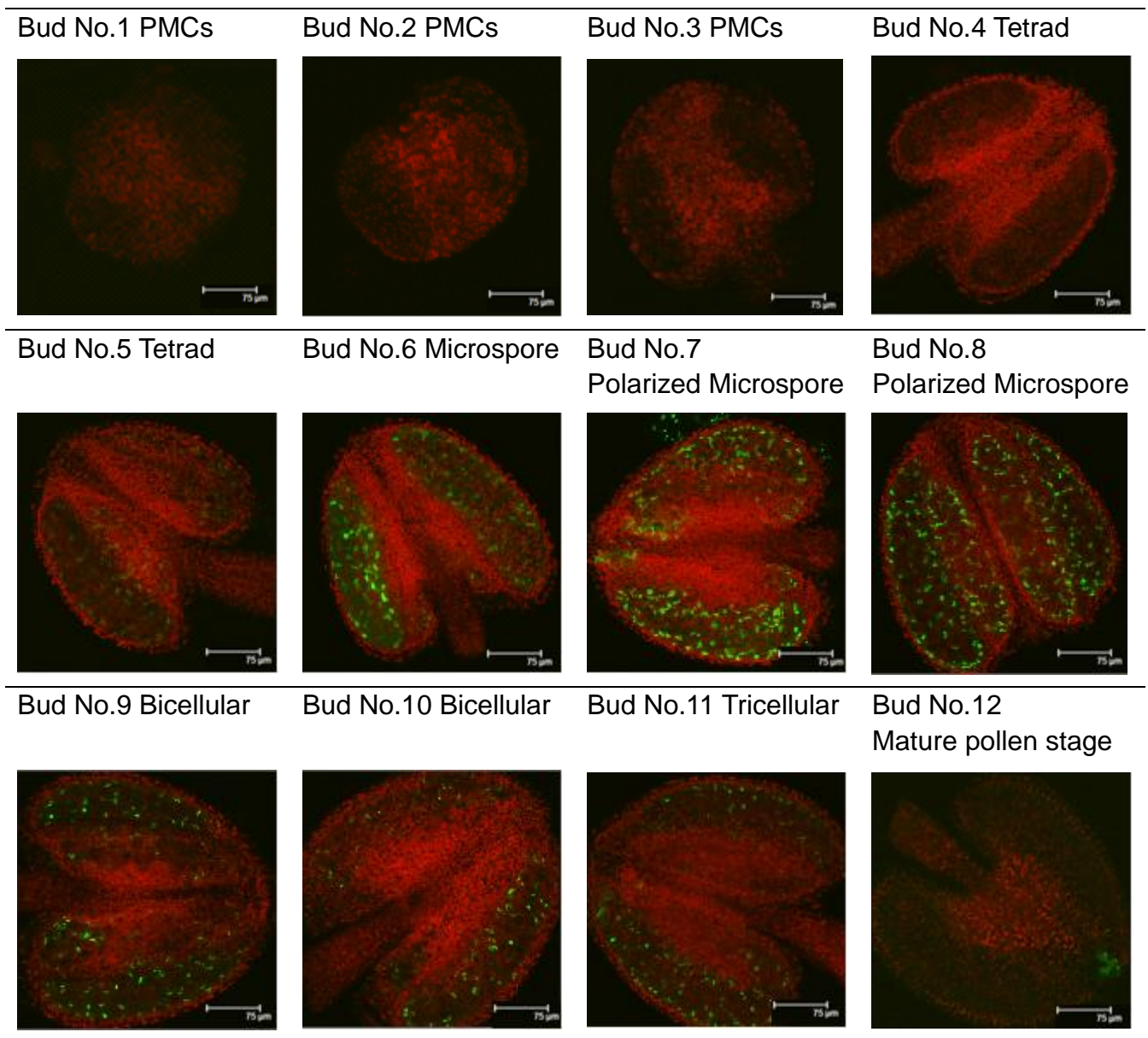


Figure 6.3 APR1:GFP expression in anther tissue in *ms1* mutant

Scale bar: 75µm

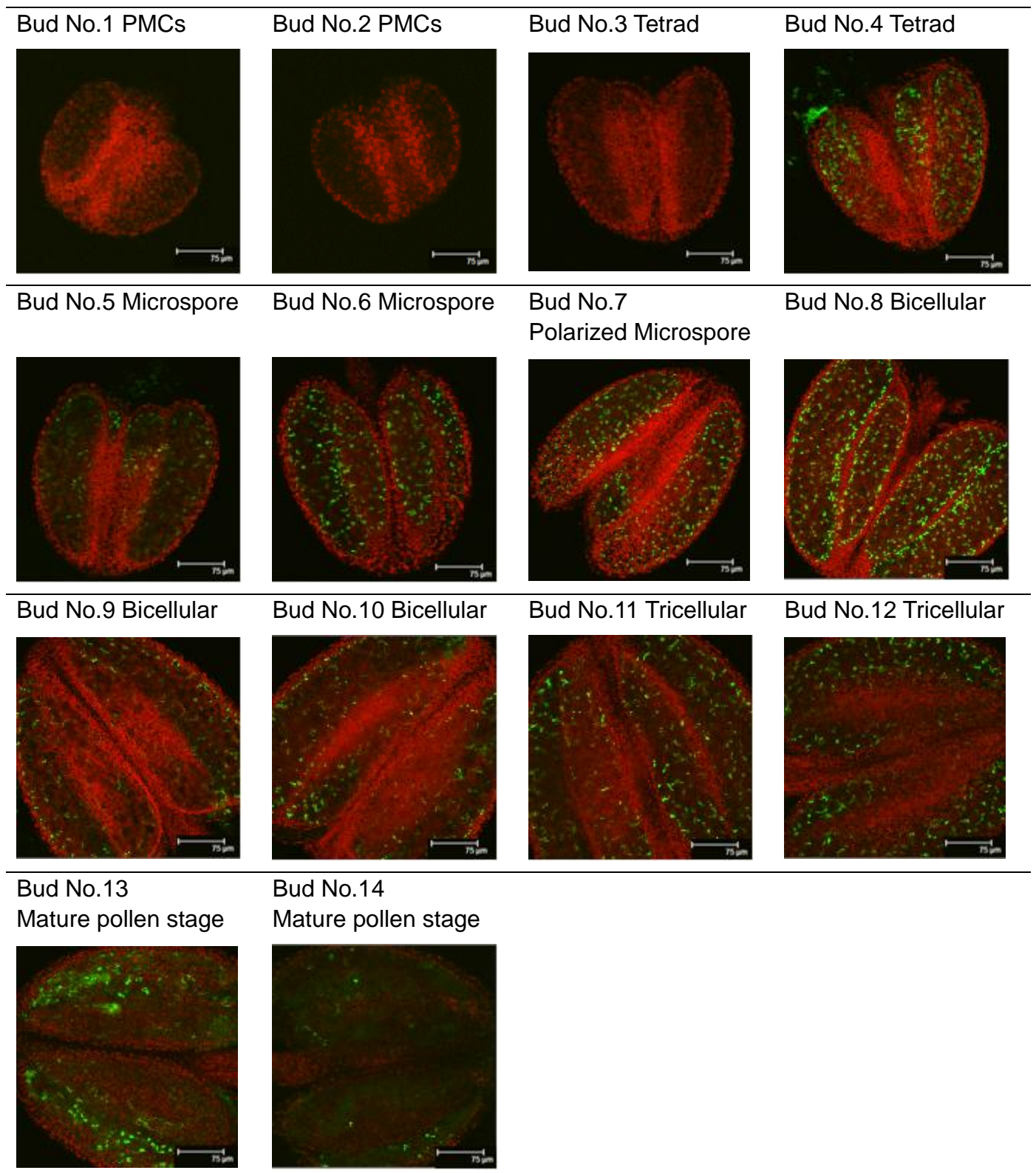
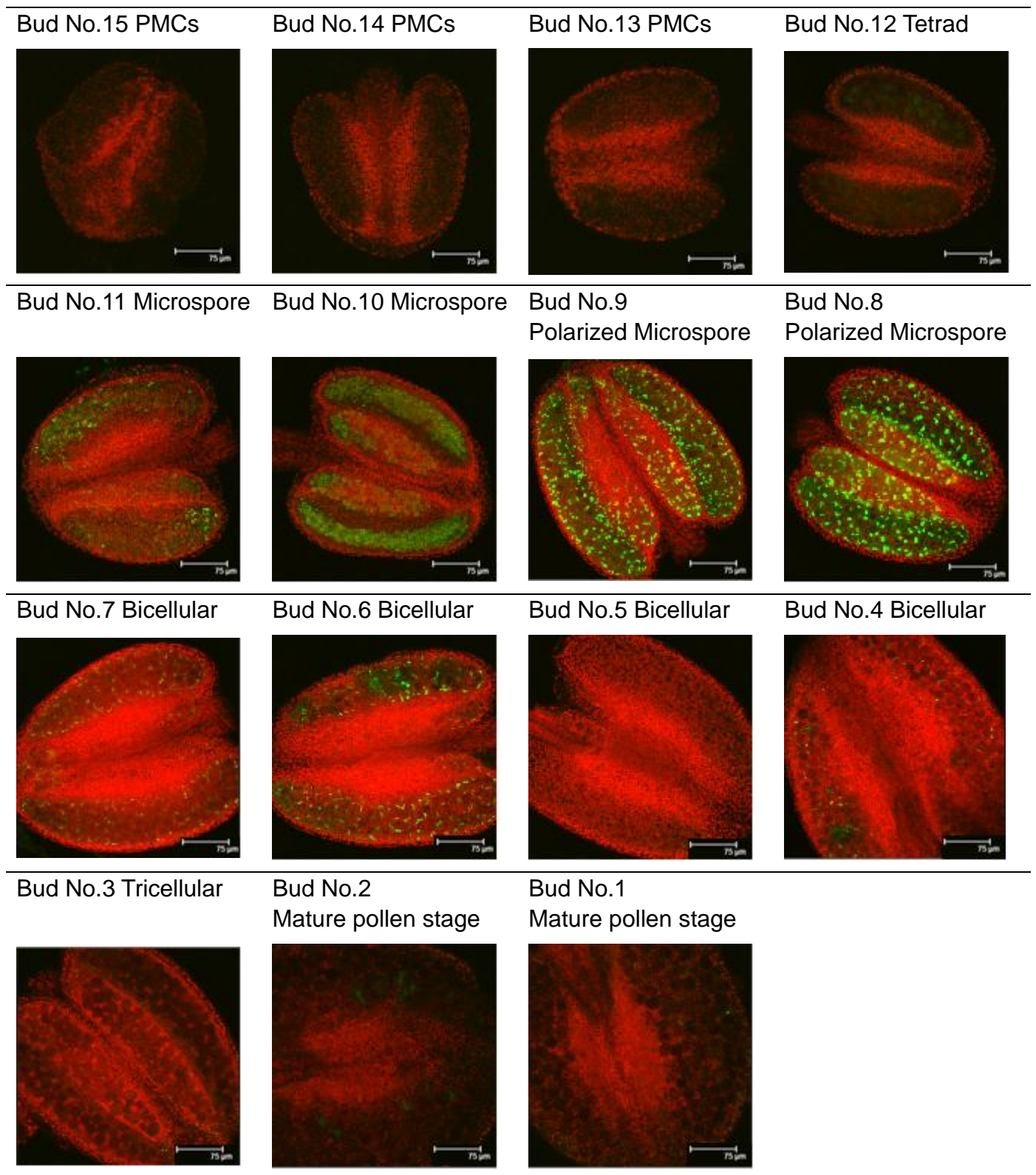


Figure 6.4 APR1:GFP expression in anther tissue in *myb26* mutant

Scale bar: 75µm

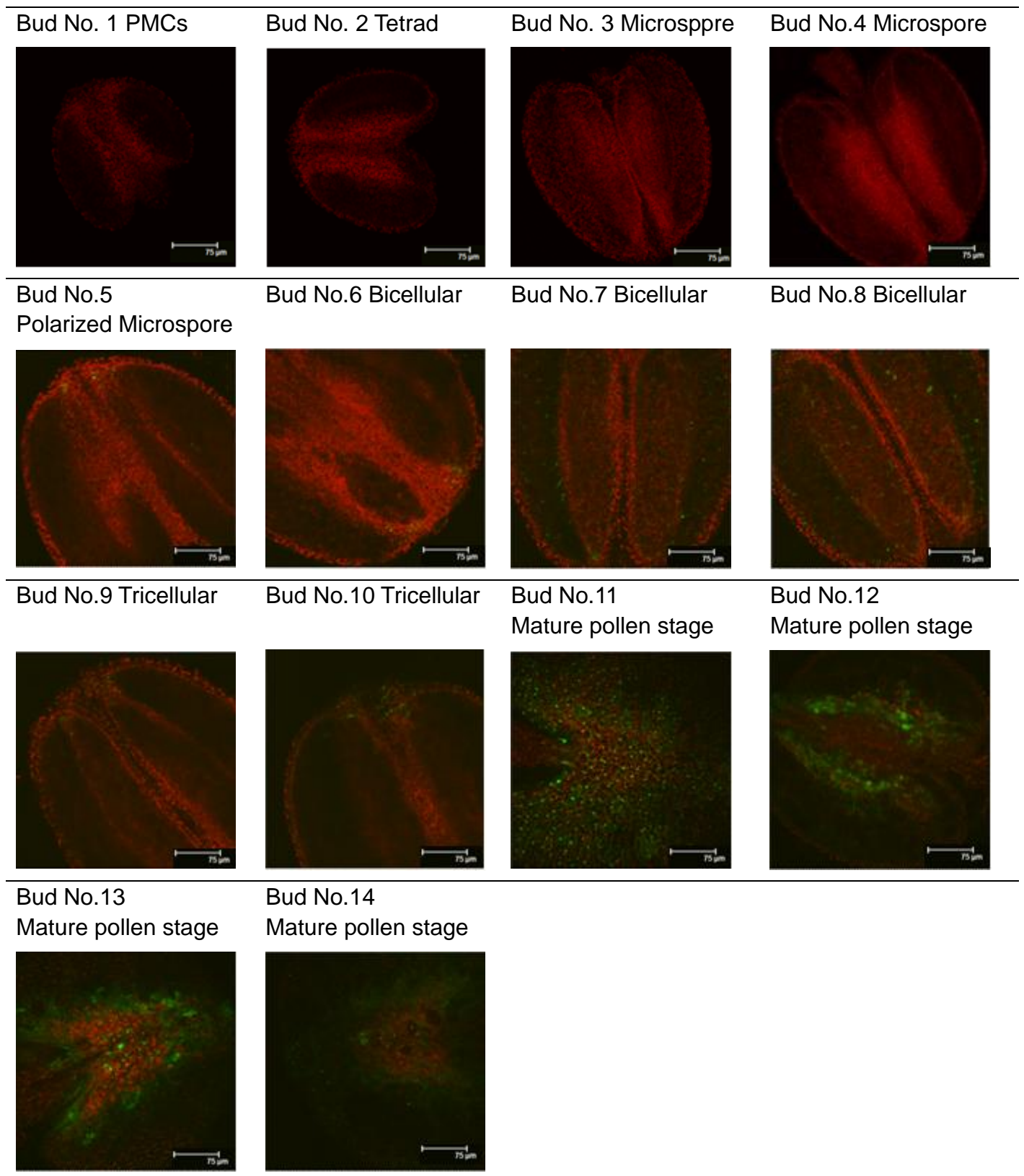


6.3.1.2 *BFN1* expression in WT and male sterile mutants

Previous research reported that *BFN1* protein was observed in filamentous structures that reorganised around the nuclei in senescing cells, and localised with fragmented nuclei in membrane-wrapped vesicles in late senescence, and then released into the entire cell during cell death (Farage-Barhom et al., 2011, Fendrych et al., 2014). During anther developmental processes, *BFN1*:GFP was observed at the polarized microspore stage during the differentiation of generative nuclei and vegetative nuclei (Fig. 6.5). However, this GFP was very weak in this stage and also the following bicellular and tricellular stages. The strongest *BFN1*:GFP was displayed in the anther, localised to the nuclei in anther wall cells but was dispersed into the entire cell in the mature pollen stage but before anther dehiscence. Furthermore, there was very weak *BFN1*:GFP signal seen only at the top of anther tissue in polarized microspore and tricellular pollen stages, but relatively stronger in the whole anther in bicellular stage at which time tapetum degeneration was occurring. Both the bicellular stage and mature pollen stage are the periods when major events of anther structure and morphology variation occur, with PCD processes occurring during these stages (Fig. 6.5).

Figure 6.5 BFN1:GFP expression in anther tissue in WT mutant

Scale bar: 75µm



BFN1:GFP was observed when free microspores were released in the *ams* homozygous mutant, which was in advance of that seen in WT samples. This signal then increased from the polarized microspore stage and was sustained during the whole pollen mitosis processes (PMI and PMII), but decreased at tricellular stage. GFP signal strength increased when mature pollen appeared and decreased later before anther dehiscence in the *ams* mutant (Fig. 6.6). The GFP fluorescence strength in the *ams* mutant was stronger enhanced level than that in WT samples.

The expression status was similar in the *ms1* homozygous mutant. GFP signal appeared in microspore stage, which was also in advance compared to that in the WT background, then increased in polarized microspore and bicellular stages, but decreased in tricellular stage. Increased BFN1:GFP signal was observed in early mature pollen stage (Fig. 6.7). The GFP signal showed some stronger fluorescence level than that in WT anthers.

There was no difference in the BFN1:GFP signal between WT and the *myb26* homozygous mutant background. BFN1:GFP was firstly observed in microspore stage at an extremely low level, which could be seen only as several green dots in the anther tissues through confocal microscopy, and also in the polarized microspore stage. This GFP fluorescence was enhanced in the bicellular stage, which was similar to that seen in WT plants. The difference observed was weaker GFP signal in the mature pollen stage in *myb26* mutant

than that in WT, although it was similar in that it showed dispensed GFP signal in very late pollen developmental stage before anther dehiscence (Fig. 6.8).

Figure 6.6 BFN1:GFP expression in anther tissue in *ams* mutant

Scale bar: 75µm

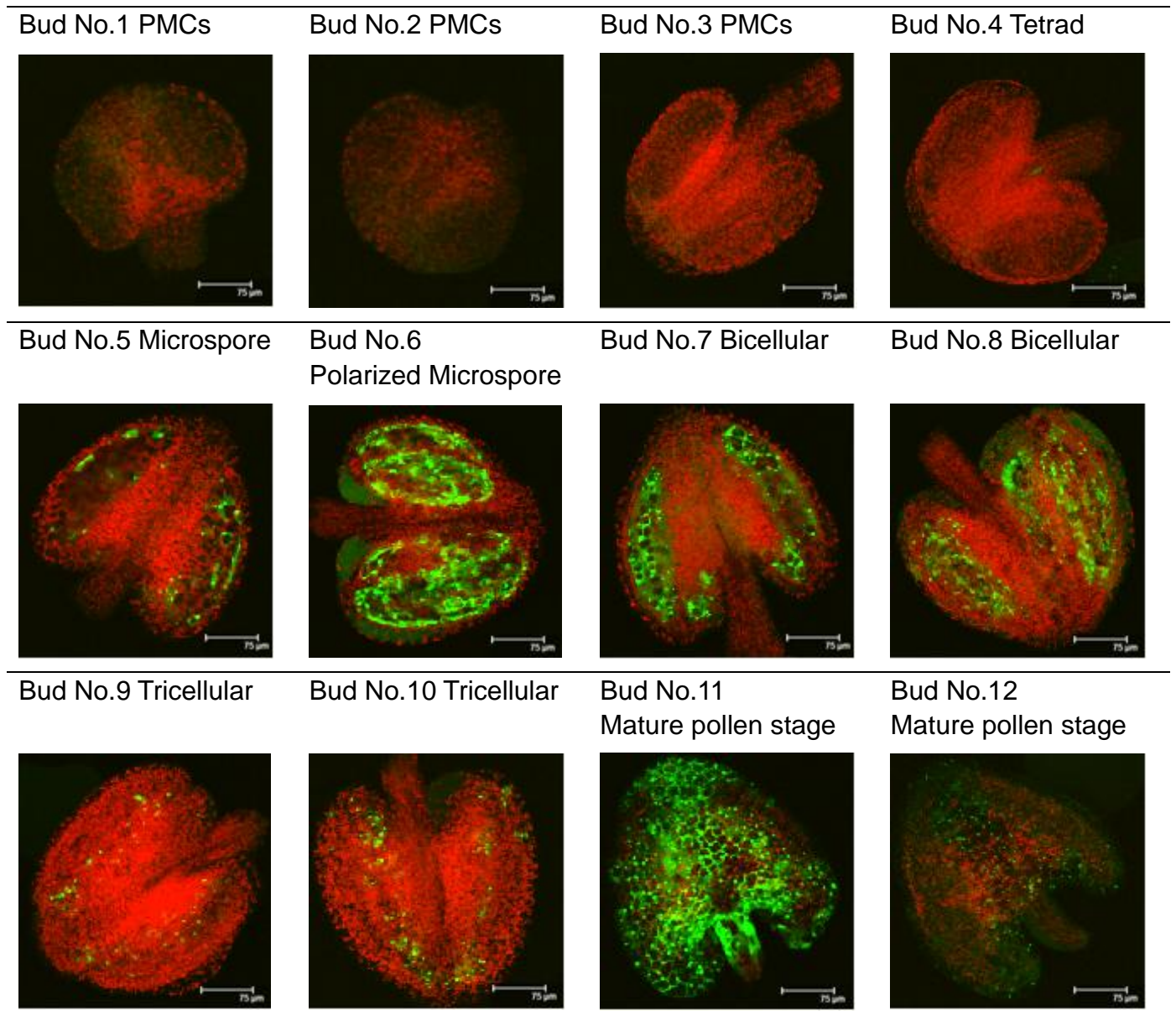


Figure 6.7 BFN1:GFP expression in anther tissue in *ms1* mutant

Scale bar: 75µm

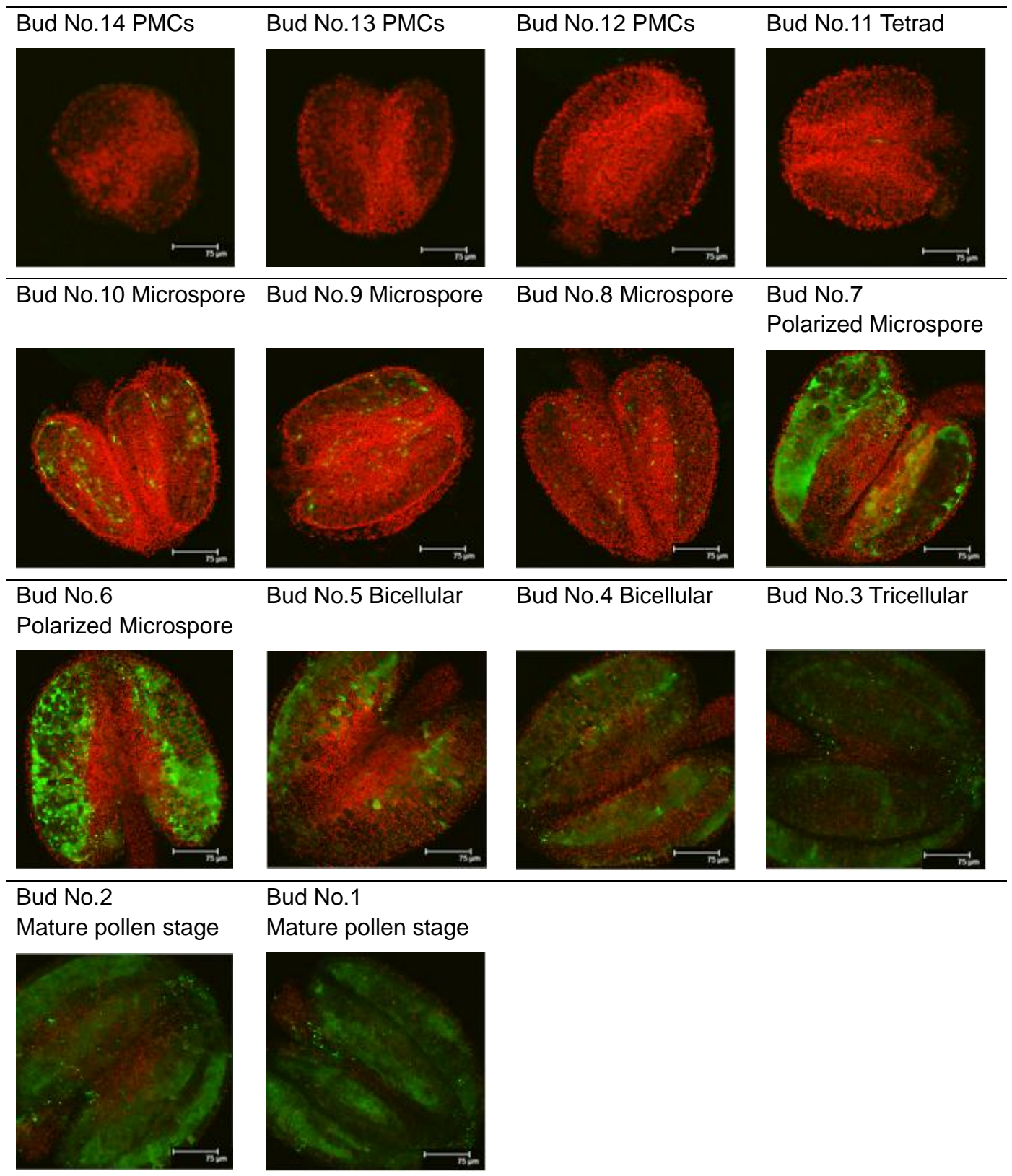
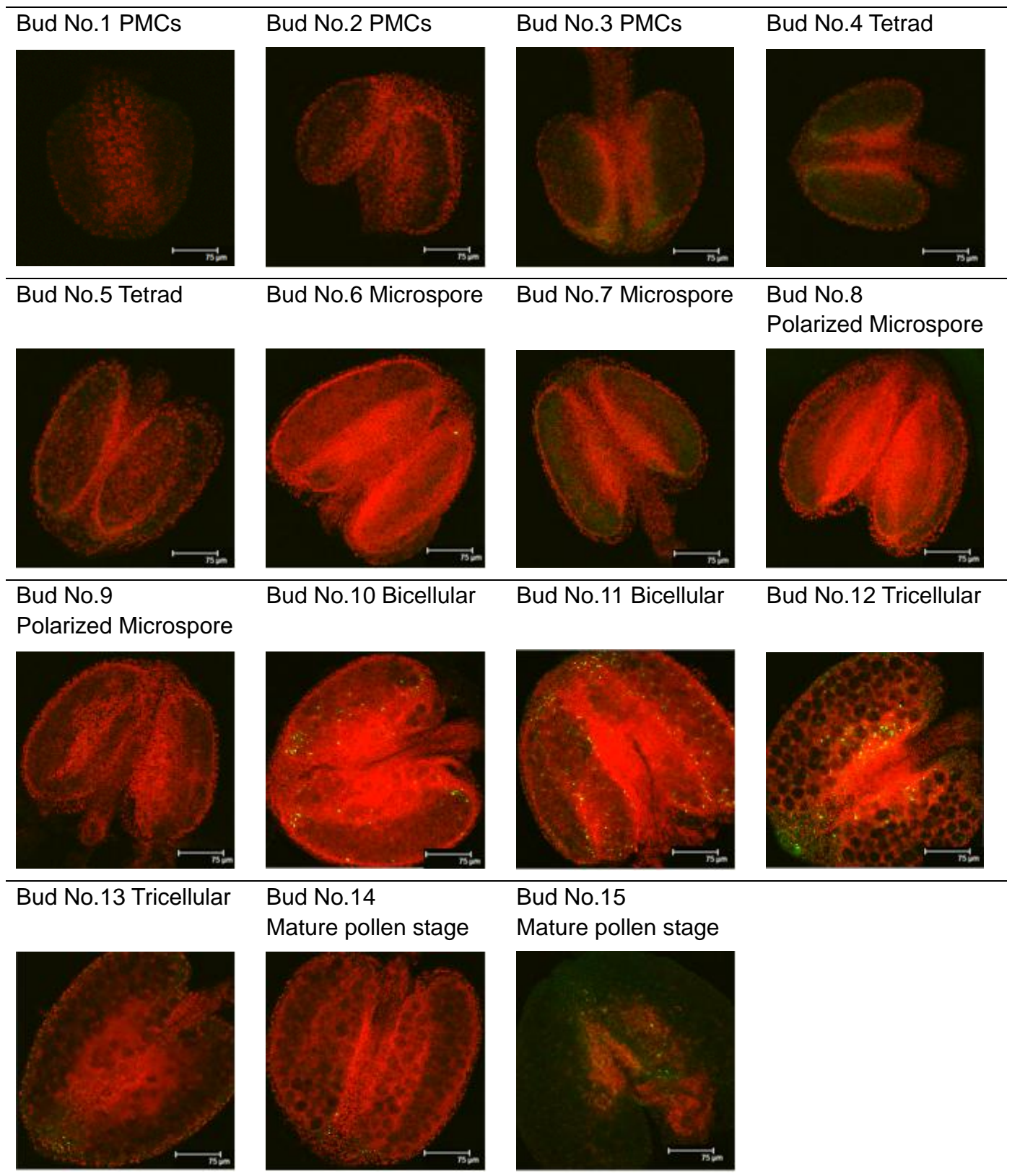


Figure 6.8 BFN1:GFP expression in anther tissue in *myb26* mutant

Scale bar: 75µm



6.3.1.3 *CEP1* expression in WT and male sterile mutants

It had been reported that KDEL-tailed cysteine endopeptidases are a group of papain-type peptidases found in senescing tissue undergoing programmed cell death (Helm et al., 2008). *CEP1* is a gene in this group its activity was confirmed by GUS during seedling, flowering, and root development, especially in tissues that collapse during final stages of PCD, and in the course of lateral root formation (Helm et al., 2008). Recent research also revealed *CEP1* as a key executor in tapetal PCD in the pollen developmental processes (Zhang et al., 2014). There was no CEP1:GFP signal observed before free microspores were released, which was also equated to tapetum degeneration initiation. This GFP fluorescence could be observed in polarized microspore stage firstly at a low level, and then GFP signal strength increased during pollen developmental stages to mature pollen until anther dehiscence. There was quite strong GFP fluorescence existed in late pollen stage, tricellular and mature pollen stages (Fig. 6.9).

In *ams* homozygous mutant anther samples, CEP1:GFP appeared in microspore stage, earlier than that in WT anther tissue, which was the period that tapetum degeneration was starting in *ams* mutant anther tissue. However, there was little difference in GFP fluorescence level between the *ams* mutant and WT samples. The GFP signal increased in polarized microspore and bicellular stages but did not show significant changes in tricellular and mature

pollen stage according to the confocal microscopy results (Fig. 6.10).

CEP1:GFP signal showed a similar pattern of expression period in *ms1* homozygous mutant. We could observe GFP fluorescence in another samples from microspore stage in *ms1* mutant, and this fluorescence lasted until the mature pollen stage. During the developmental stages, the GFP signal was not the same as that in WT and the *ams* mutant. In general, the GFP fluorescence was weaker in *ms1* mutant than in WT and the *ams* mutant, especially in tricellular and mature pollen stages. Furthermore, GFP fluorescence strength in the *ms1* mutant was stronger in bicellular than in tricellular, but it showed a reverse status in WT and *ams* mutants that the GFP fluorescence was stronger in tricellular than in bicellular (Fig. 6.11).

Strength of CEP1:GFP was clearly decreased in the *myb26* homozygous mutant, which resulted in extremely weak fluorescence level in the anther tissue, although the GFP signal appearance period was not advanced or delayed. The CEP1:GFP fluorescence could be observed in polarized microspore stage, which was same with that in WT samples. The signal was weak in the following stages but was enhanced during pollen development, and the strongest fluorescence was in mature pollen stage (Fig. 6.12).

Figure 6.9 CEP1:GFP expression in anther tissue in WT mutant.

Scale bar: 75µm (No. 1-8), 150µm (No. 9-14)

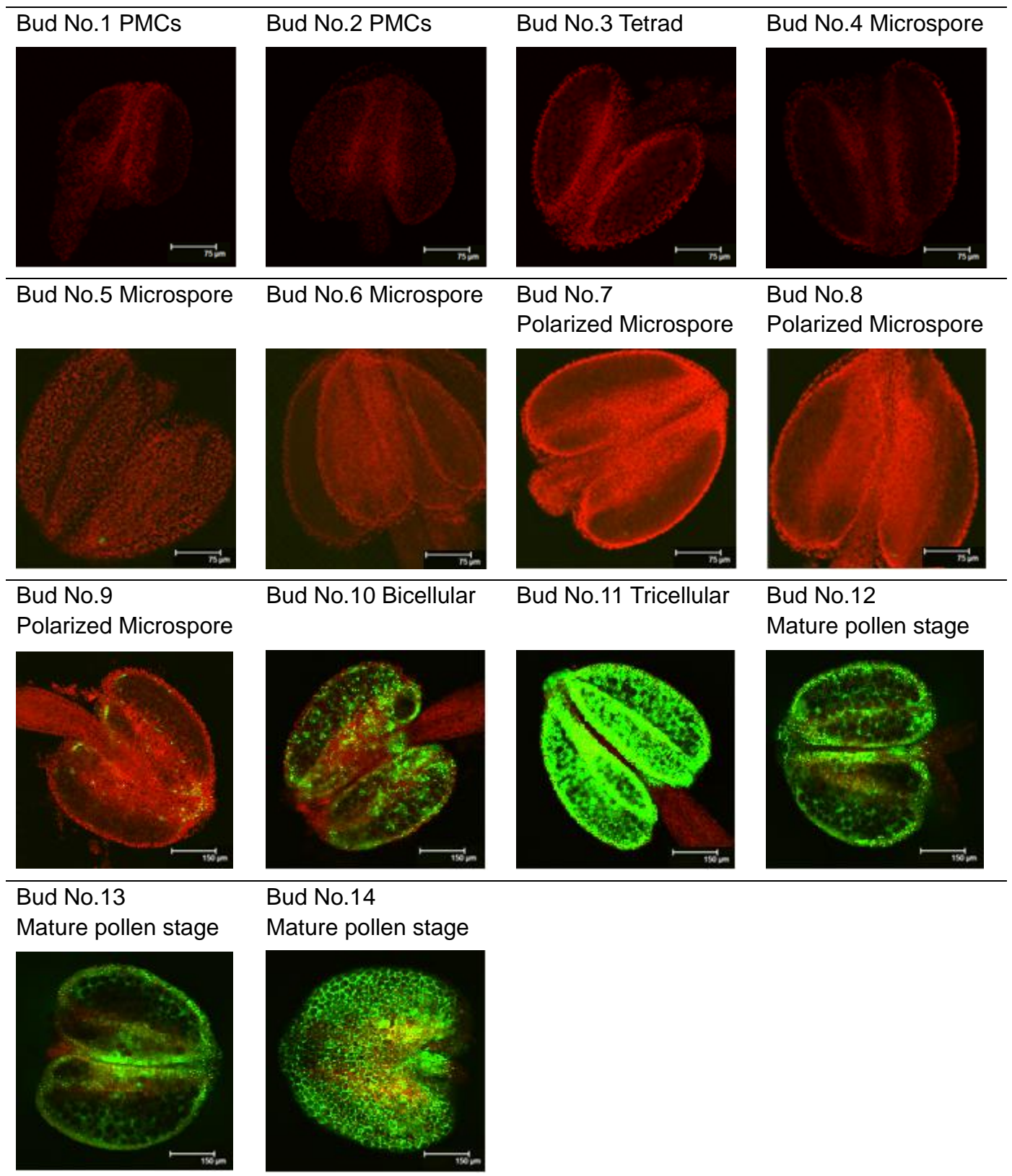


Figure 6.10 CEP1:GFP expression in anther tissue in *ams* mutant.

Scale bar: 75µm (No. 1-8), 150µm (No. 9-14)

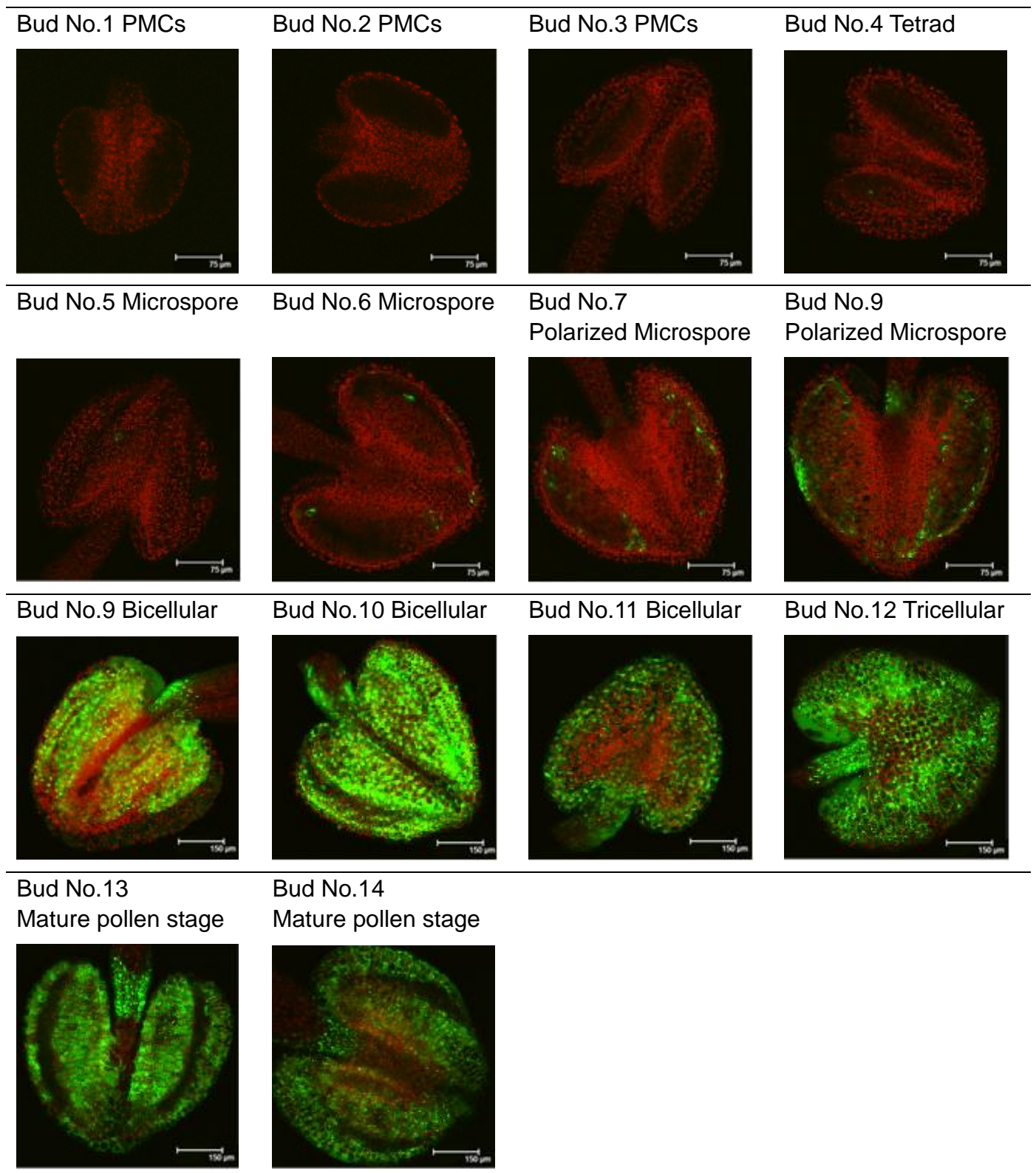


Figure 6.11 CEP1:GFP expression in anther tissue in *ms1* mutant.

Scale bar: 75 μ m (No. 1-8), 150 μ m (No. 9-12)

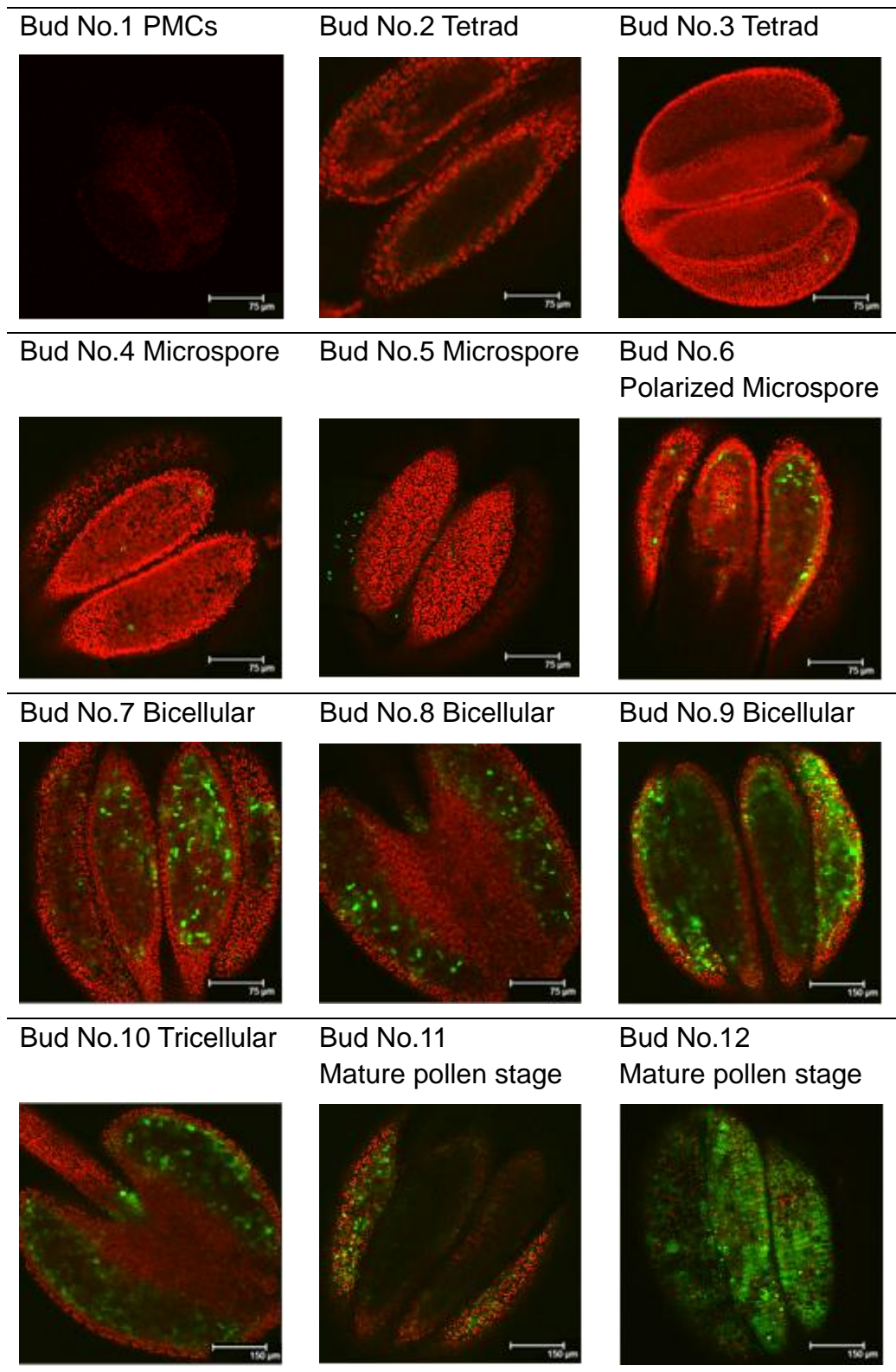
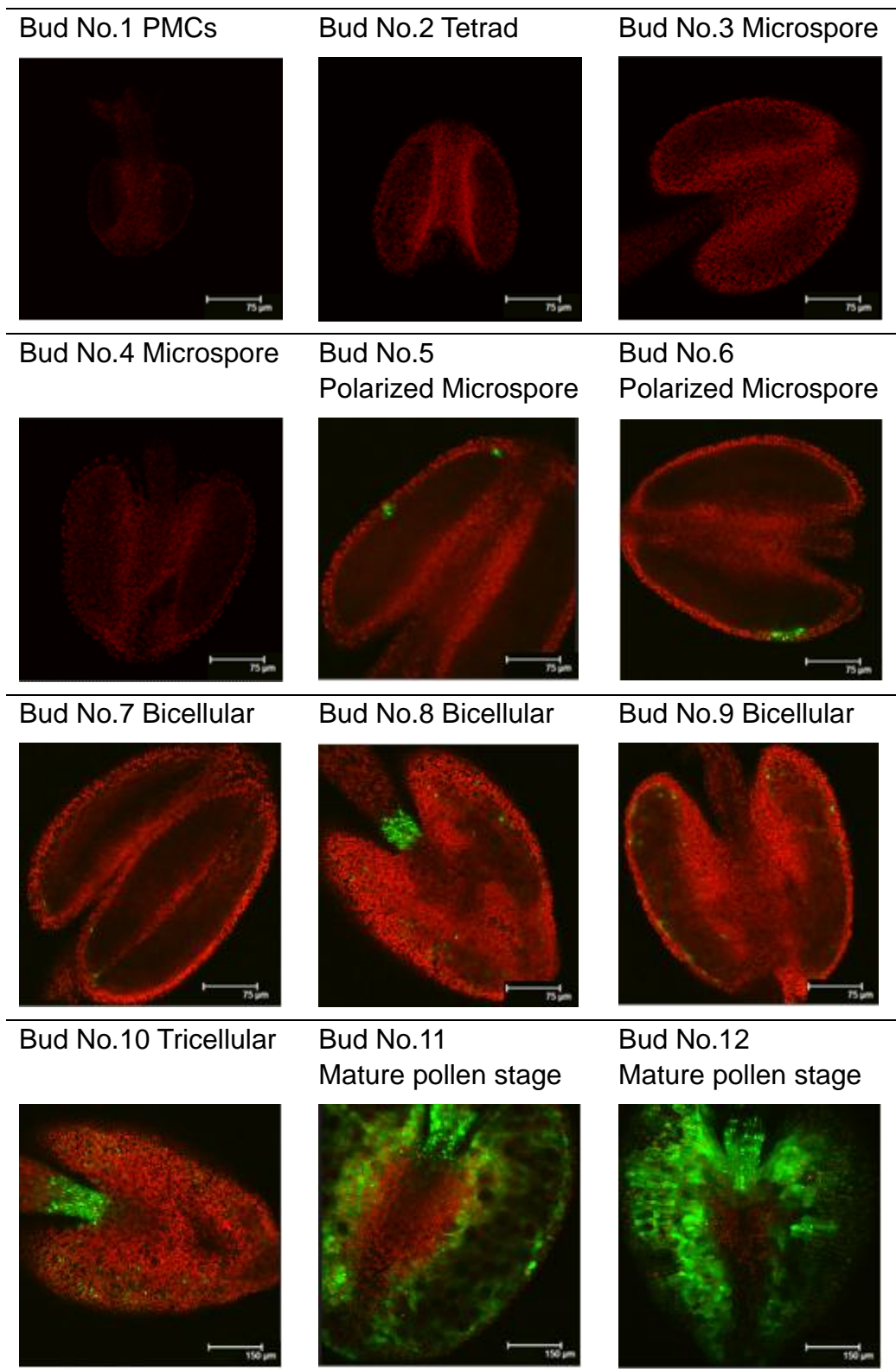


Figure 6.12 CEP1:GFP expression in anther tissue in *myb26* mutant.

Scale bar: 75µm (No. 1-9), 150µm (No. 10-12)



6.3.1.4 *SAG12* expression in WT and male sterile mutants

As a gene encoding a cysteine protease, *SAG12* is expressed only in senescent tissues, especially in senescent leaves and flower tissues (Noh & Amasino, 1999). Previous research has revealed that *SAG12* expression was specifically activated by developmentally controlled senescence pathways but not by stress- or hormone- controlled pathway (Lohman et al., 1994, Zhang et al., 2000, Otegui et al., 2005, Price et al., 2008). In WT samples, *SAG12*:GFP signal appeared only in the very late pollen stage, the oldest two buds in the inflorescence. GFP fluorescence could be observed in the old plants that were senescent rather than in the young plants that were still producing siliques, which was entirely different with the other three PCD genes discussed previously. Therefore, *SAG12*:GFP was observed only in the mature pollen stage in senescent plants. No GFP fluorescence appeared in any other pollen developmental stage or in the anther tissue in younger plants (Fig. 6.13).

No F₂ generation seedlings survived after BASTA screening of the *SAG12*♂ X *ams*♀ samples. However, the results of confocal microscopy indicated that this GFP signal could only be seen in mature pollen stage in *ms1* and *myb26* homozygous mutants from *SAG12*♂ X *ms1*♀ and *SAG12*♂ X *myb26*♀ F₂ generation plants. Furthermore, the GFP signal was extremely weak in these anther samples, even much weaker than that in WT plants. Nevertheless, no GFP signal was seen in any other pollen developmental stage, which is as

seen in WT plants (Fig. 6.14 and Fig. 6.15). According to these results, SAG12:GFP should be same in the anther of *ams* homozygous mutant with that in *ms1* and *myb26* mutants. As *SAG12* was a specific gene related to senescence processes it only was expressed in senescent tissues of plants. Therefore, *SAG12* was a senescence-specific gene, but did not appear to be involved in tapetum PCD in anther tissue during pollen development in *Arabidopsis*.

Figure 6.13 SAG12:GFP expression in anther tissue in WT mutant.

Scale bar: 75µm (No. 1), 150µm (No. 2-4)

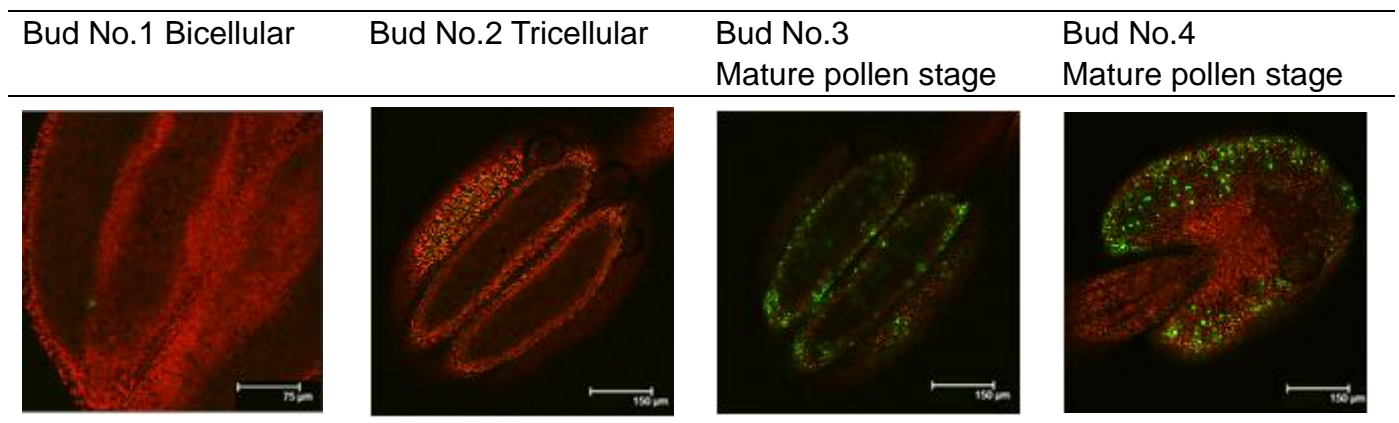


Figure 6.14 SAG12:GFP expression in anther tissue in *ms1* mutant.

Scale bar: 75µm

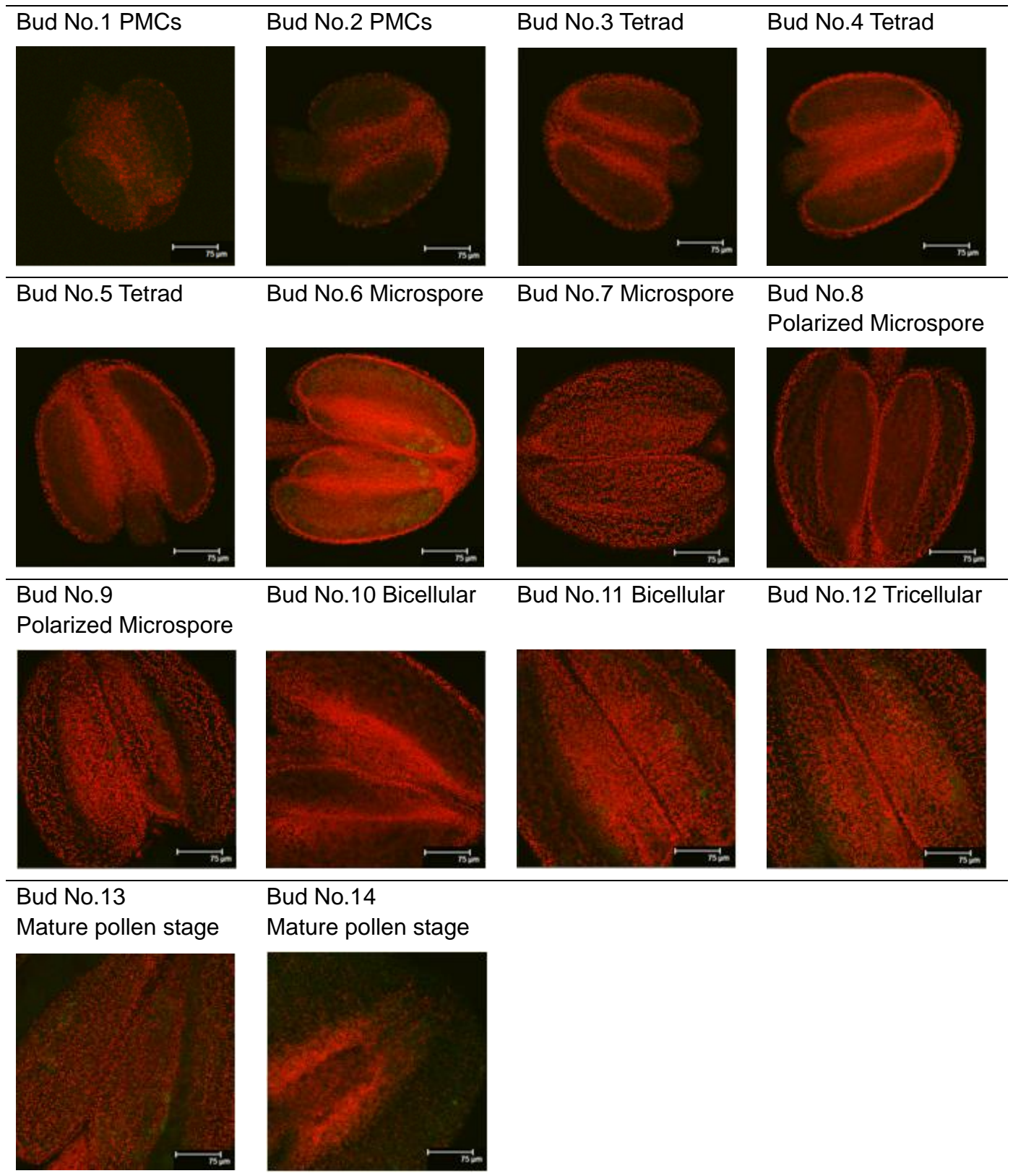
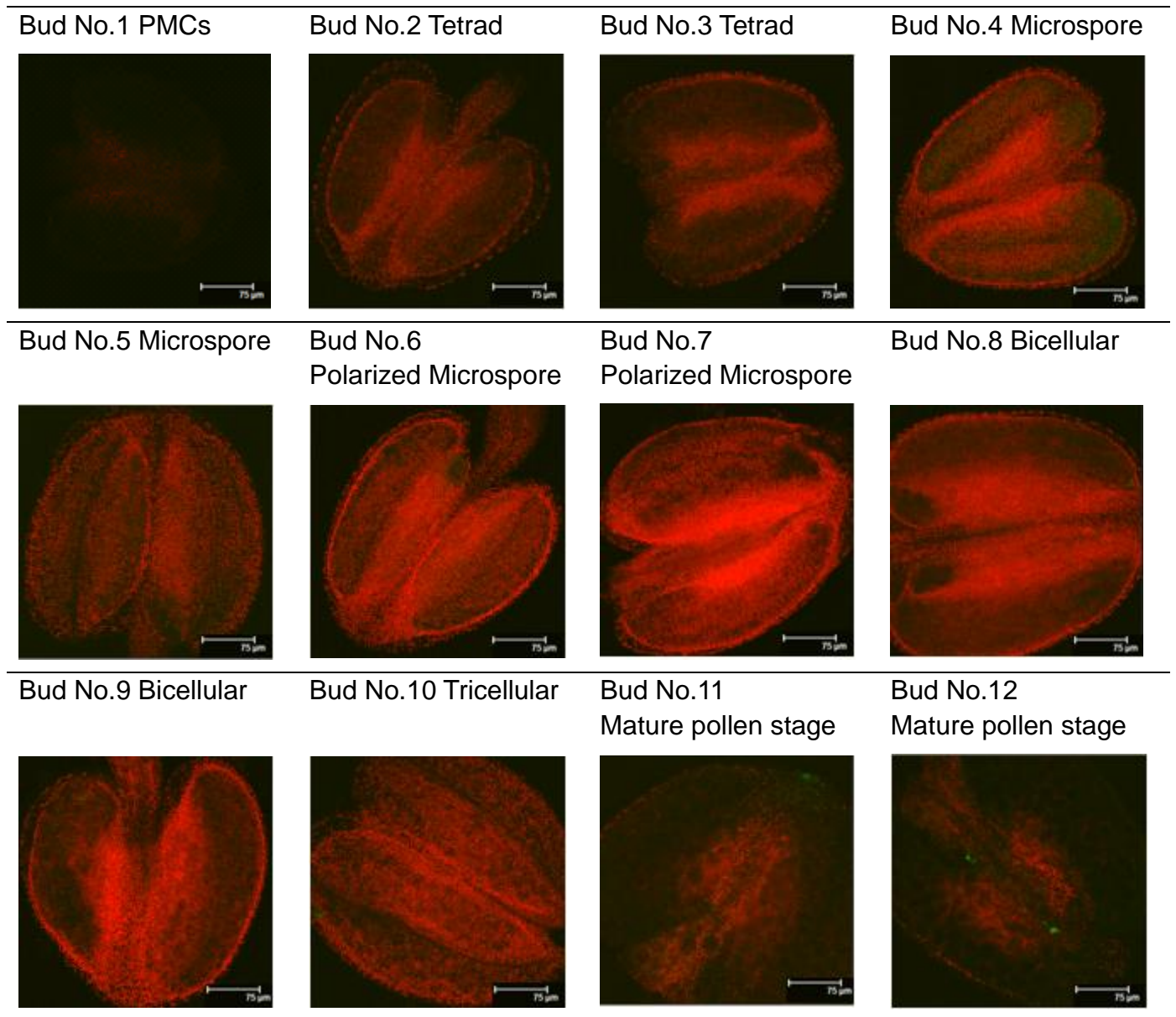


Figure 6.15 SAG12:GFP expression in anther tissue in *myb26* mutant.

Scale bar: 75µm



In conclusion, the expression pattern of these four PCD genes is summarised in Table 6.1. *APR1* expression existed before tapetum degeneration initiation with a high level but was delayed and also down-regulated in all of the three male sterile mutants according to observed GFP fluorescence, also *SAG12* could only function in the senescent parts of very old plants. These two genes did not exhibit a specific relationship on tapetum PCD regulation. Moreover, pollen would produce normal tetrads but pollen degeneration happened in the following processes in *ams* and *ms1* mutant, which mean tapetum abnormal and degeneration was advanced. Therefore, these results suggest that *BFN1* and *CEP1* gene had a greater relationship with the tapetum PCD process both of which were expressed from tapetum degeneration initiated in *ams* and *ms1* mutants. However, there was no evidence to reveal how the genes would be influenced in *myb26* mutant. According to the results of a weak relationship between *APR1/SAG12* and tapetum PCD, and also less regulation evidence in male sterile mutant (*ams*, *ms1* and *myb26*) mentioned above, we decided to focus on *BFN1* and *CEP1* in the following experiments.

Table 6.1 Expression pattern of PCD genes in *Arabidopsis* anther.

√, GFP signal was observed in this stage; X, GFP signal was not observed in this stage; blue and yellow background to highlight the expression stages in WT and mutants, respectively.

Genes	Background	PMCs	Tetrad	Microspore	Polarized Microspore	Bicellular	Tricellular	Mature pollen
<i>APR1</i>	WT	X	√	√	√	√	√	√
	<i>ams</i>	X	X	√	√	√	√	√
	<i>ms1</i>	X	X	√	√	√	√	√
	<i>myb26</i>	X	X	√	√	√	√	√
<i>BFN1</i>	WT	X	X	X	√	√	√	√
	<i>ams</i>	X	X	√	√	√	√	√
	<i>ms1</i>	X	X	√	√	√	√	√
	<i>myb26</i>	X	X	X	√	√	√	√
<i>CEP1</i>	WT	X	X	X	√	√	√	√
	<i>ams</i>	X	X	√	√	√	√	√
	<i>ms1</i>	X	X	√	√	√	√	√
	<i>myb26</i>	X	X	X	√	√	√	√
<i>SAG12</i>	WT	X	X	X	X	X	X	√
	<i>ms1</i>	X	X	X	X	X	X	√
	<i>myb26</i>	X	X	X	X	X	X	√

6.3.2 Quantitative RT-PCR analysis of PCD genes in WT plant

To investigate the expression level of *BFN1* and *CEP1* in different pollen developmental stages, *Arabidopsis* Ler bud samples were collected from three groups according to the developmental stages (See section 6.2.5). Quantitative RT-PCR was performed on staged Ler buds to measure *BFN1* and *CEP1* expression during anther development (Fig 6.16). The Ler buds in the “Old group” (Polarized microspore, PMI, bicellular and PMII stages) showed strongest *BFN1* expression, while buds in the “Mature group”

(tricellular stage and mature pollen stage) showed slightly reduced, but still at a high level compared to that in the “Young group” (Microspore, tetrad, PMCs and all of other younger buds). *CEP1* expression showed the highest level in the buds of “Mature group”, and then an extremely low level in other two groups. *CEP1* expression level was relatively higher in the “Old group” than that in “Young group”.

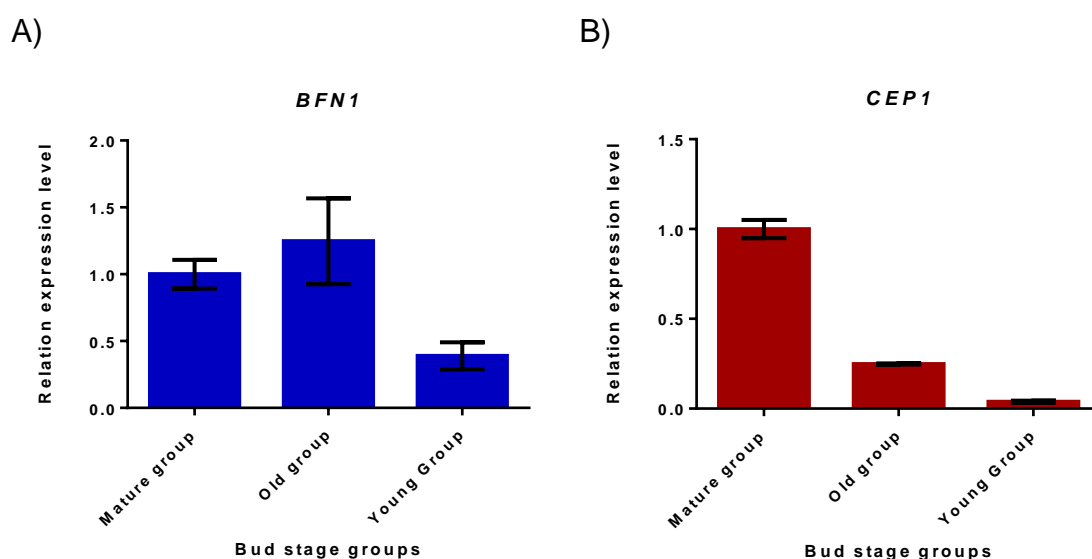


Figure 6.16 Quantitative RT-PCR of A) *BFN1* and B) *CEP1* expression in staged buds samples. Primers used for ACTIN7 amplification as reference gene were ACT7_2F and ACT7_443R; primers used for *BFN1* amplification were BFN1F and BFN1R; primers used for *CEP1* amplification were CEP1F and CEP1R (sequence of primers see Appendix II). *BFN1* and *CEP1* expression levels were normalised against internal control ACTIN7. Error bar: standard error.

6.3.3 Quantitative RT-PCR analysis of PCD genes in male sterile mutants

To evaluate *BFN1* and *CEP1* expression associated with male sterile mutants, quantitative RT-PCR was carried out on staged buds from *ams*, *ms1*, *dvt1* and *tdf1* homozygous mutant plants.

The buds in tricellular stage and mature pollen stage in the *ams* mutant showed an up-regulation of *BFN1* expression compared to WT buds, but showed a down-regulated expression level in both the younger bud. *BFN1* was down-regulated to a similar level in all of the *ms1* buds stages. *BFN1* was also down-regulated in *tdf1* mutant buds, while the old buds in tricellular stage and mature pollen stage showed a lower expression than younger buds. The most notable difference of *BFN1* expression was in *dvt1* mutant buds, where all of the buds showed a significantly up-regulated expression level. The buds in the “Mature group” and “Young group” showed a more than 35-fold up-regulation and the buds in “Old group” showed a more than 10-fold up-regulation (Fig. 6.17).

The expression level of *CEP1* gene was up-regulated in all of the staged buds samples in all of the male sterile mutants. The *ams* mutant buds of the “Young group” showed strongest *CEP1* expression in this male sterile, which was more than 70-fold up-regulation compared with that in same stages WT buds. *CEP1* expression in the buds of the “Old group” was also up-regulated more compared to 35-fold than WT ones. The “Mature group” buds showed the

weakest expression in the *ams* mutant but expression was still up-regulated more than 5-fold that of WT. In the *ms1* mutant samples, strongest *CEP1* expression level appeared in “Old group” buds, while the expression level was similar in other two groups. The expression level in all of the three groups was no more than 11-fold up-regulated compared to WT. *CEP1* expression showed the same change in the three developmental pollen stages in the *dyt1* and *tdf1* mutants. Weakest *CEP1* expression level was in the “Mature group”, then stronger in the “Old group”, and the strongest level was in the “Young group”. Moreover, the expression level was more than 300-fold up-regulation in “Mature” and “Old” group buds, and more than 3000-fold up-regulated in the “Young group” (Fig. 6.18). Detailed relative expression level changes are listed in Table 6.2.

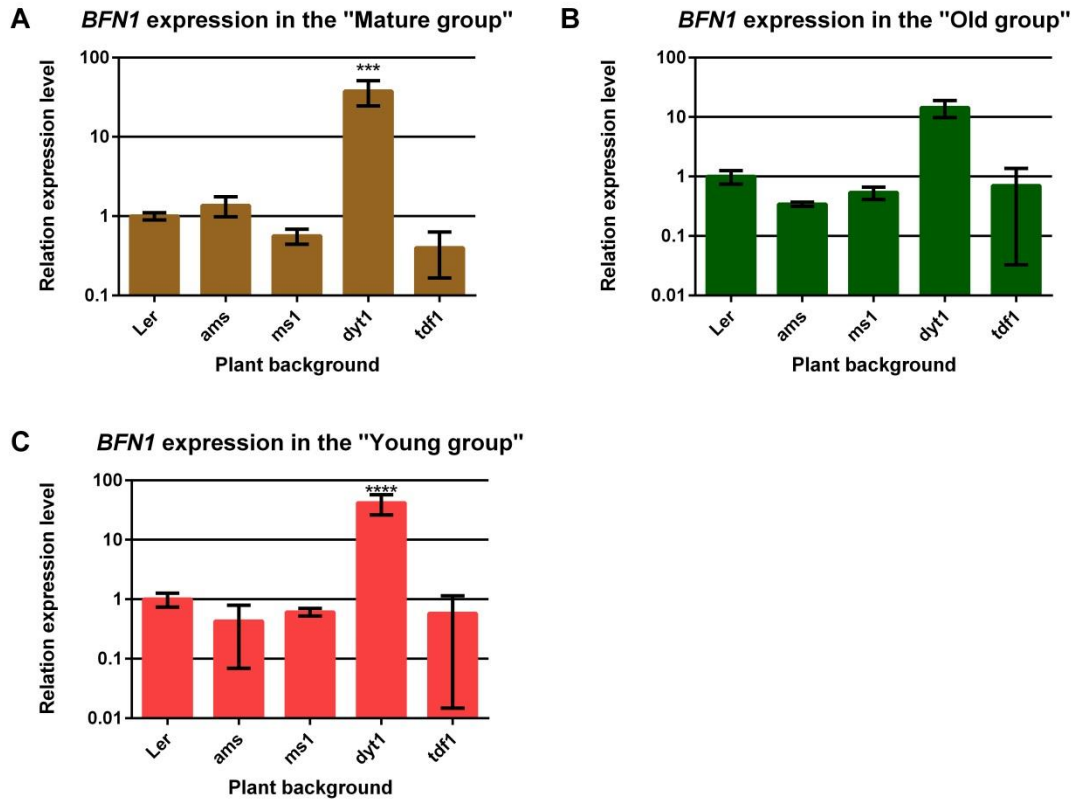


Figure 6.17 Quantitative RT-PCR of *BFN1* expression in male sterile mutant bud samples at different stages. A). *BFN1* expression in the "Mature group", B). *BFN1* expression in the "Old group", C). *BFN1* expression in the "Young group". Primers used for ACTIN7 amplification as reference gene were ACT7_2F and ACT7_443R; primers used for *BFN1* amplification were BFN1F and BFN1R (sequence of primers see Appendix II). *BFN1* expression levels were normalised against internal control ACTIN7. Error bar: standard error. ***, **** Relatively expression level in the mutant was significantly different from the wild type Ler by ANOVA. p value < 0.001, 0.0001, respectively.

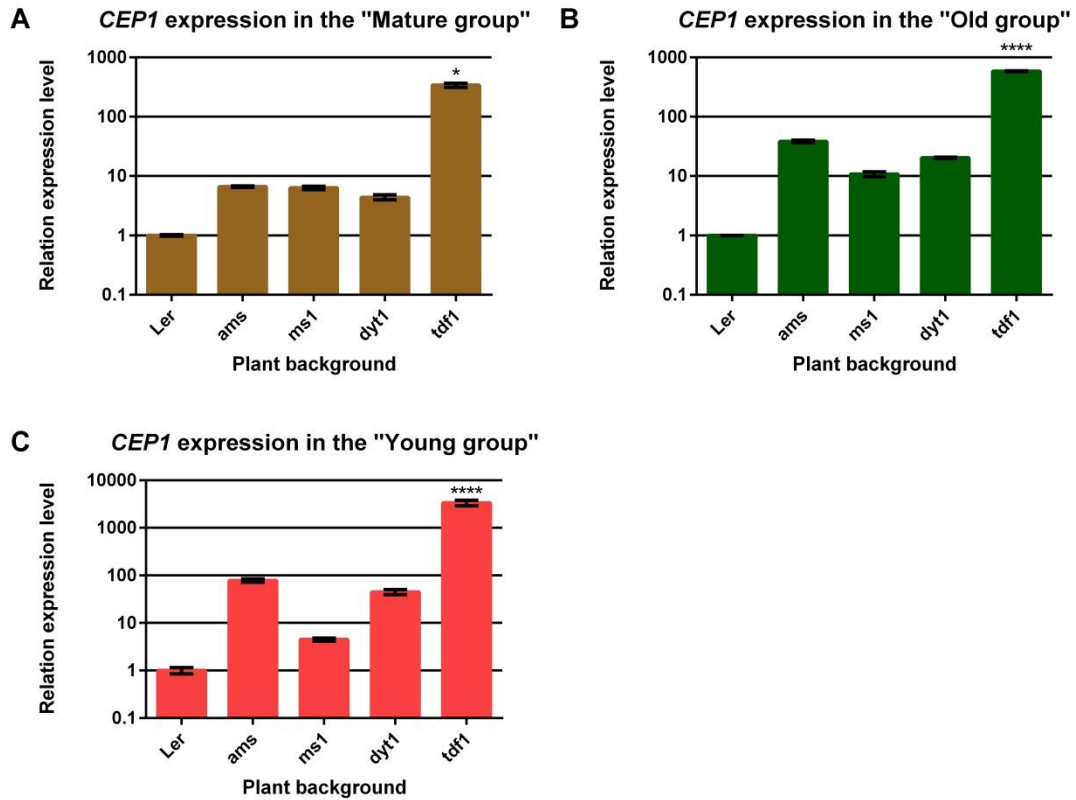


Figure 6.18 Quantitative RT-PCR of *CEP1* expression in staged male sterile mutant bud samples at different stages. A). *CEP1* expression in the “Mature group”, B). *CEP1* expression in the “Old group”, C). *CEP1* expression in the “Young group”. Primers used for ACTIN7 amplification as reference gene were ACT7_2F and ACT7_443R; primers used for *CEP1* amplification were CEP1F and CEP1R (sequence of primers see Appendix II). *CEP1* expression levels were normalised against internal control ACTIN7. Error bar: standard error. *, **** Relatively expression level in the mutant was significantly different from the wild type Ler by ANOVA. p value < 0.1, 0.0001, respectively.

Table 6.2 Detailed relative expression level of *BFN1* and *CEP1* in different staged buds.

Gene	Plant background	Relative expression level in different buds staged group		
		Mature	Old	Young
<i>BFN1</i>	WT	1.00	1.00	1.00
	<i>ams</i>	1.36	0.34	0.43
	<i>ms1</i>	0.56	0.54	0.61
	<i>dyt1</i>	37.80	14.40	41.70
	<i>tdf1</i>	0.40	0.70	0.58
<i>CEP1</i>	WT	1.00	1.00	1.00
	<i>ams</i>	6.64	38.49	78.19
	<i>ms1</i>	6.34	10.80	4.47
	<i>dyt1</i>	4.39	20.27	44.92
	<i>tdf1</i>	339.55	586.87	3359.38

6.3.4 HT-stress effected PCD genes expression during pollen development

HT-stress was performed to identify *BFN1* and *CEP1* expression changes in *Arabidopsis* anther tissue under high temperature stress. *Arabidopsis* Col-0 plants which were 30-days old with *BFN1*:GFP and *CEP1*:GFP constructs were treated at 32° C for two days. Whole inflorescences on the main shoot were collected and dissected and then the anther samples were used to identify GFP fluorescence through confocal microscopy. Buds were labelled as mentioned before (Section 6.3.1). Buds were collected at two time points, D1 and D2, which equate to 1 day after HT-stress began and 2 days after HT-stress began, respectively.

BFN1:GFP fluorescence could be observed from polarized microspore stage to mature pollen stage with variation of expression level in different pollen developmental stages in WT *Arabidopsis* plants (section 6.3.1.2). The confocal microscopy results showed there was not a distinct variation in expression of BFN1:GFP signal after 1 day HT-stress, where the GFP fluorescence was observed firstly in polarized microspore stage as well. However, the GFP signal was stronger in polarized microspore stage but weaker in bicellular stage compared with that in non-stressed anthers, which was the opposite status to the non-stressed anther tissue (Fig. 6.19). In the samples that were treated with HT for 2 days, GFP signal strength was significantly decreased. Clear GFP fluorescence was observed in polarized microspore stage and extremely weak signal showed in the following pollen developmental stages (bicellular, tricellular, and mature pollen stages) (Fig. 6.19).

CEP1:GFP signal showed a decrease in *Arabidopsis* anther tissue after both of 1 day and 2 days HT-stress. GFP fluorescence was notably reduced in every pollen developmental stage according to results by confocal microscopy. The HT-stressed buds in mature pollen stage showed the strongest GFP fluorescence strength, and then weaker in tricellular stage, this variation of expression pattern is same with that non-stressed. The GFP signal strength did not change from tetrad stage to early bicellular stage, which maintained at a low level, but increased in late bicellular stage after 1 day HT-stress. In the samples which were stressed with HT for 2 days, the strongest GFP

fluorescence was also observed in mature pollen stage, but it was stronger in bicellular stage than that was HT-stressed for 1 day. Furthermore, relatively stronger GFP fluorescence appeared in early polarized microspore stage and then decreased soon after. However, the most significant change of CEP1:GFP was that the GFP signal appearance was earlier after HT-stress in the microspore stage compared to non-stressed samples, which was observed firstly in polarized microspore stage in WT non-stressed samples (Fig. 6.20).

Figure 6.19 BFN1:GFP expression in Arabidopsis anther without HT-stress and HT-stressed for 1 day and 2 days. Anthers are presented according the positions in the inflorescence from young to old, pollen developmental stages are indicated. Scale bar: 75µm, and 150µm for last two of 1 day HT-stressed anthers.

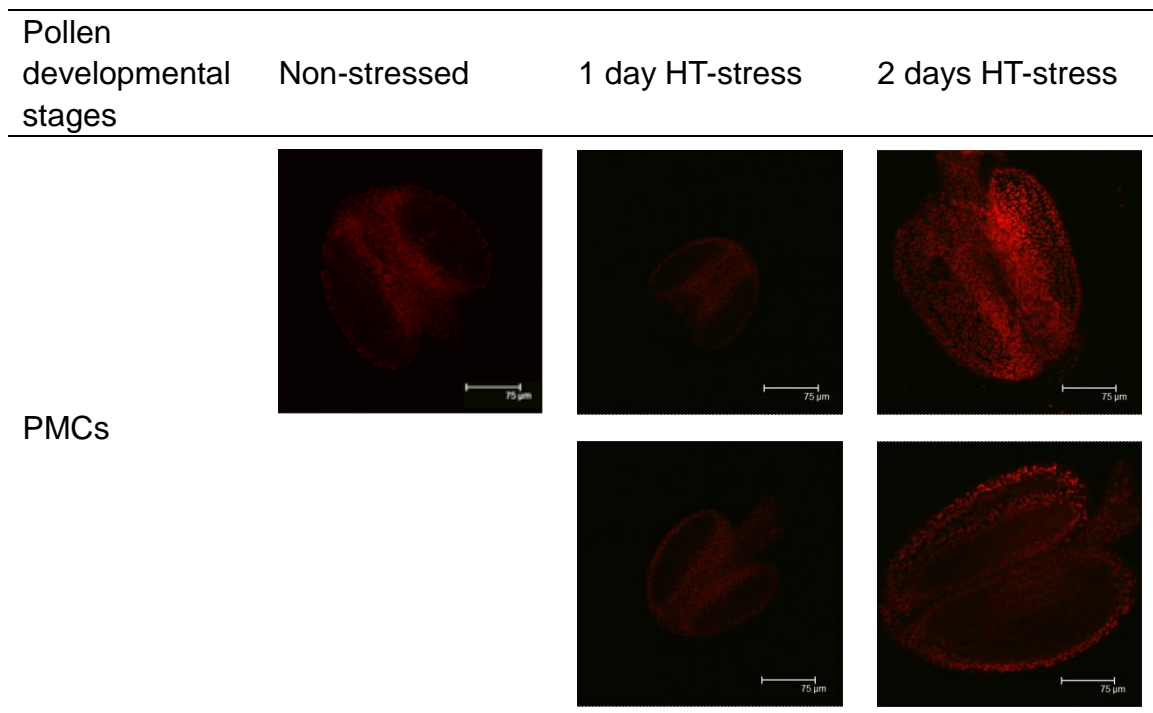


Figure 6.19 BFN1:GFP expression in Arabidopsis anther without HT-stress and HT-stressed for 1 day and 2 days. (continued)

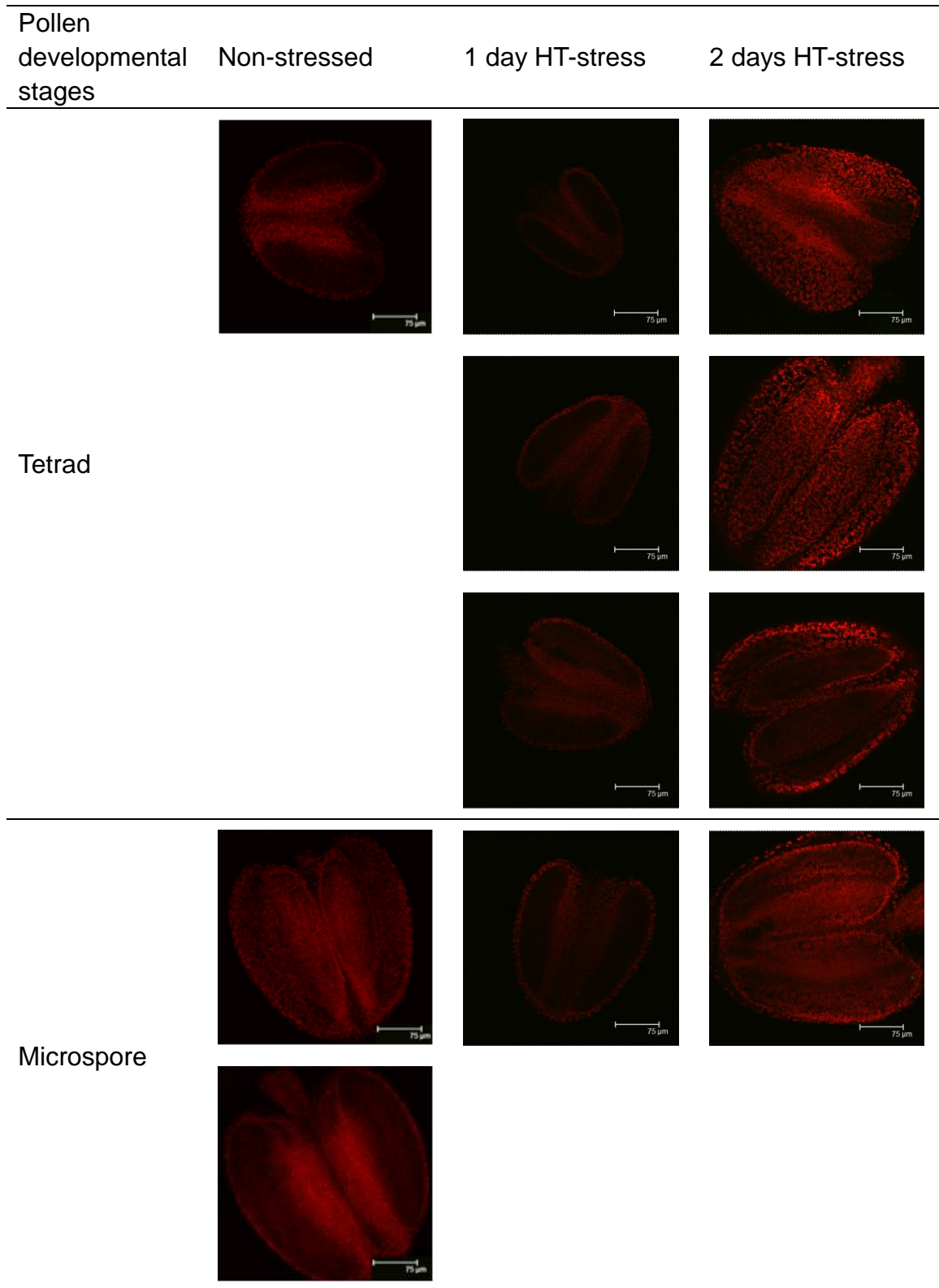


Figure 6.19 BFN1:GFP expression in Arabidopsis anther without HT-stress and HT-stressed for 1 day and 2 days. (continued)

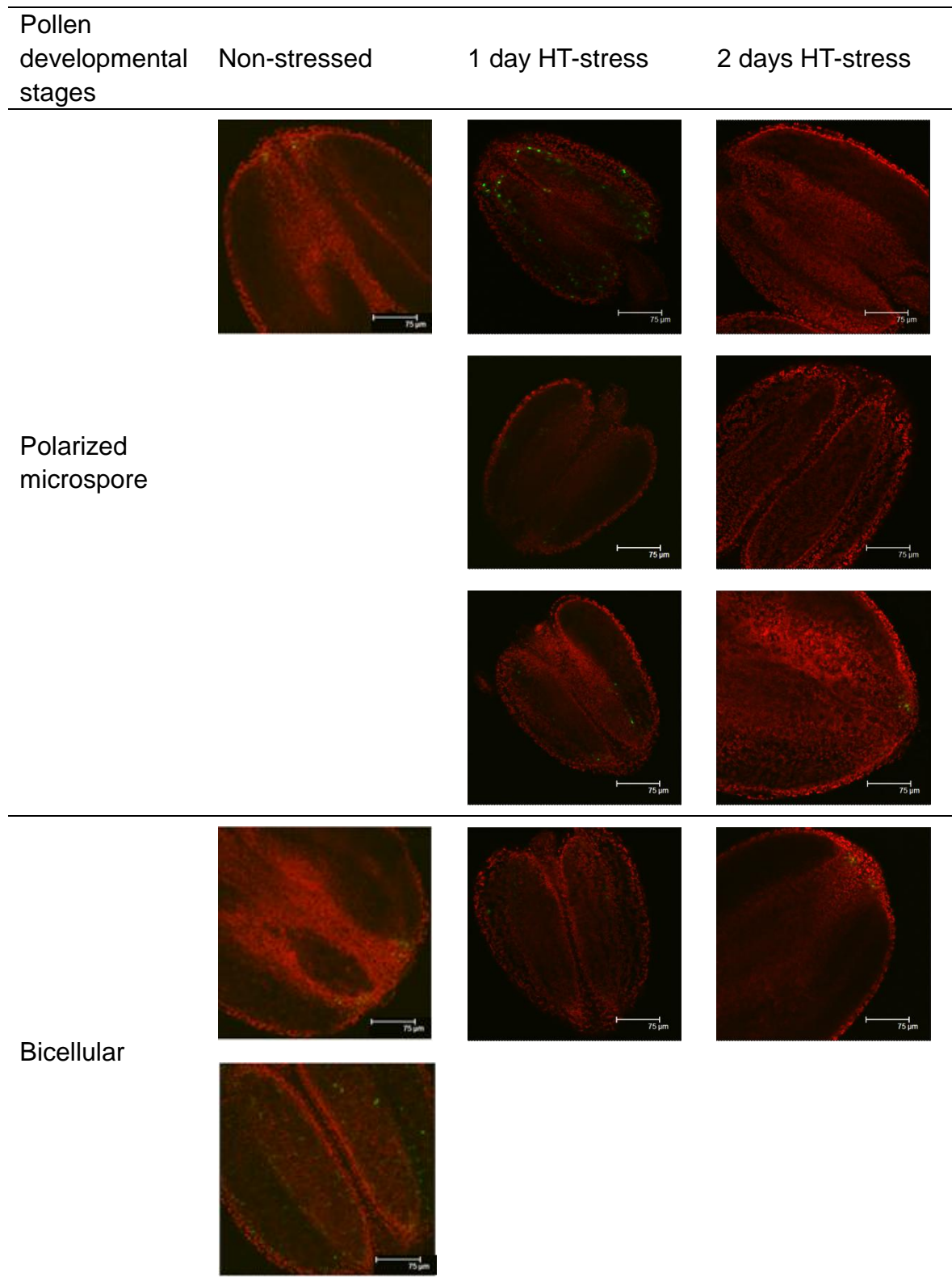


Figure 6.19 BFN1:GFP expression in Arabidopsis anther without HT-stress and HT-stressed for 1 day and 2 days. (continued)

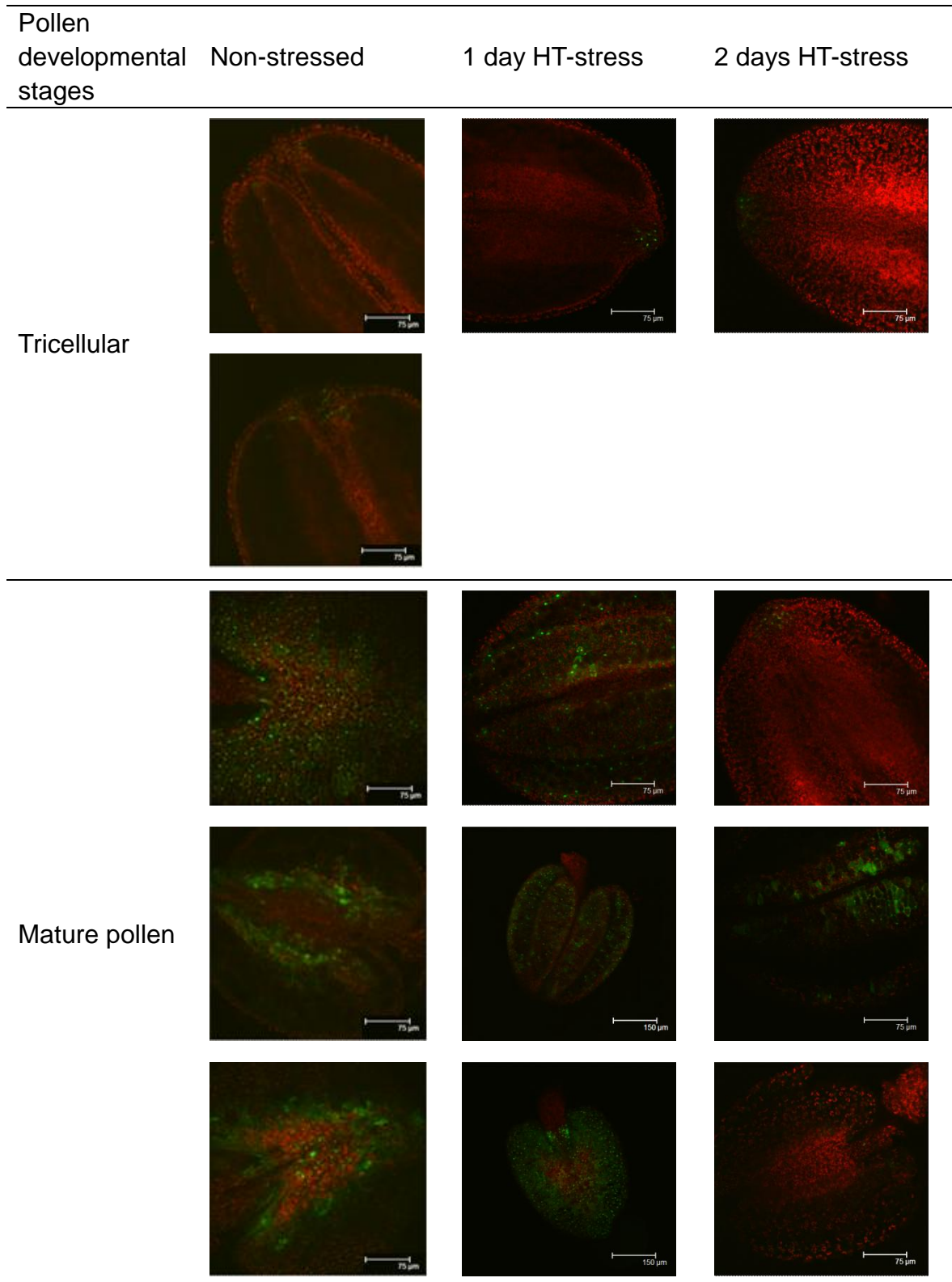


Figure 6.20 CEP1:GFP expression in Arabidopsis anther without HT-stress and HT-stressed for 1 day and 2 days. Anthers are presented according the positions in the inflorescence from young to old, pollen developmental stages are indicated. Scale bar: 75 μ m, and 150 μ m for the six oldest non-stressed anthers.

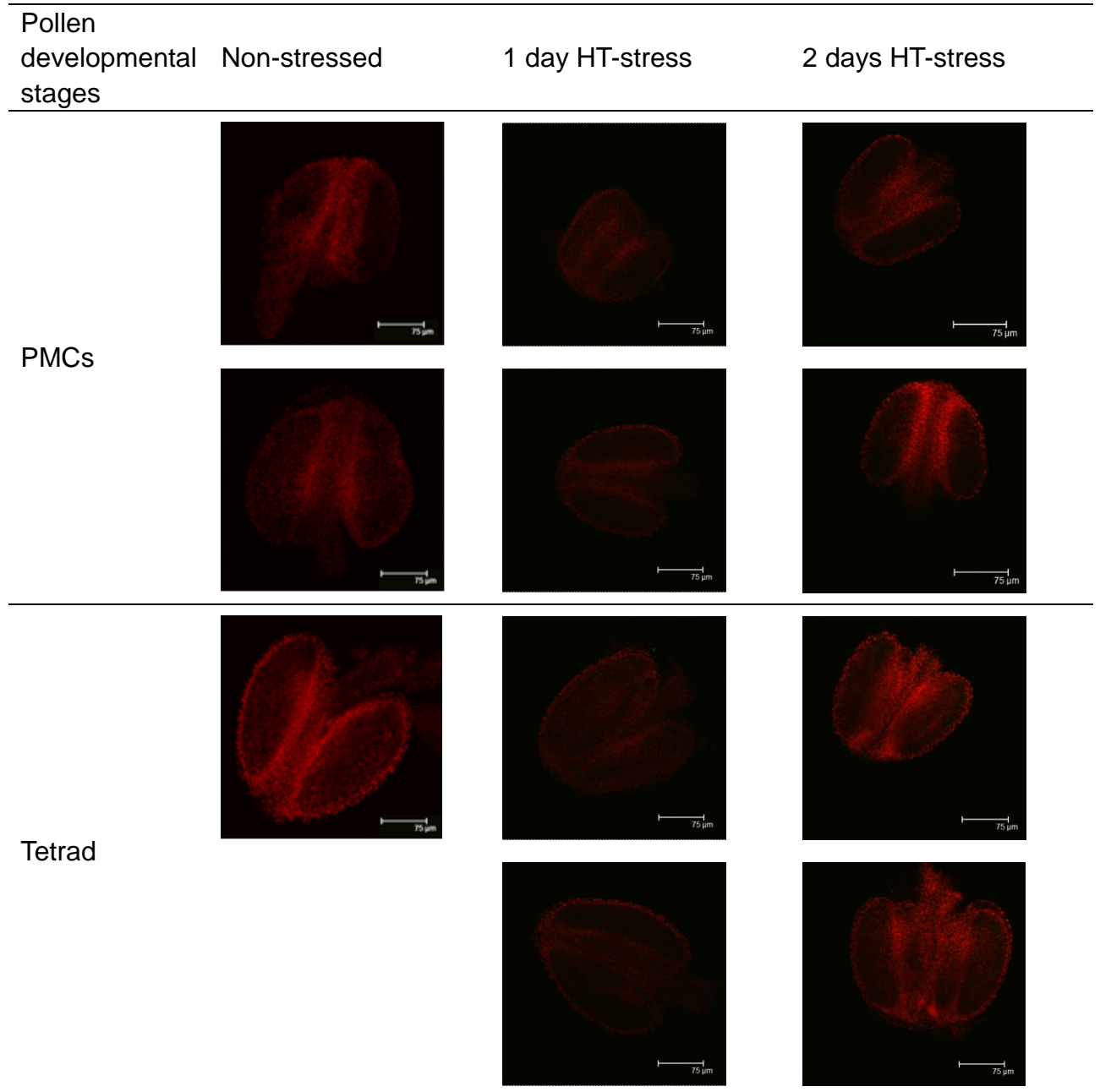


Figure 6.20 CEP1:GFP expression in Arabidopsis anther without HT-stress and HT-stressed for 1 day and 2 days. (continued)

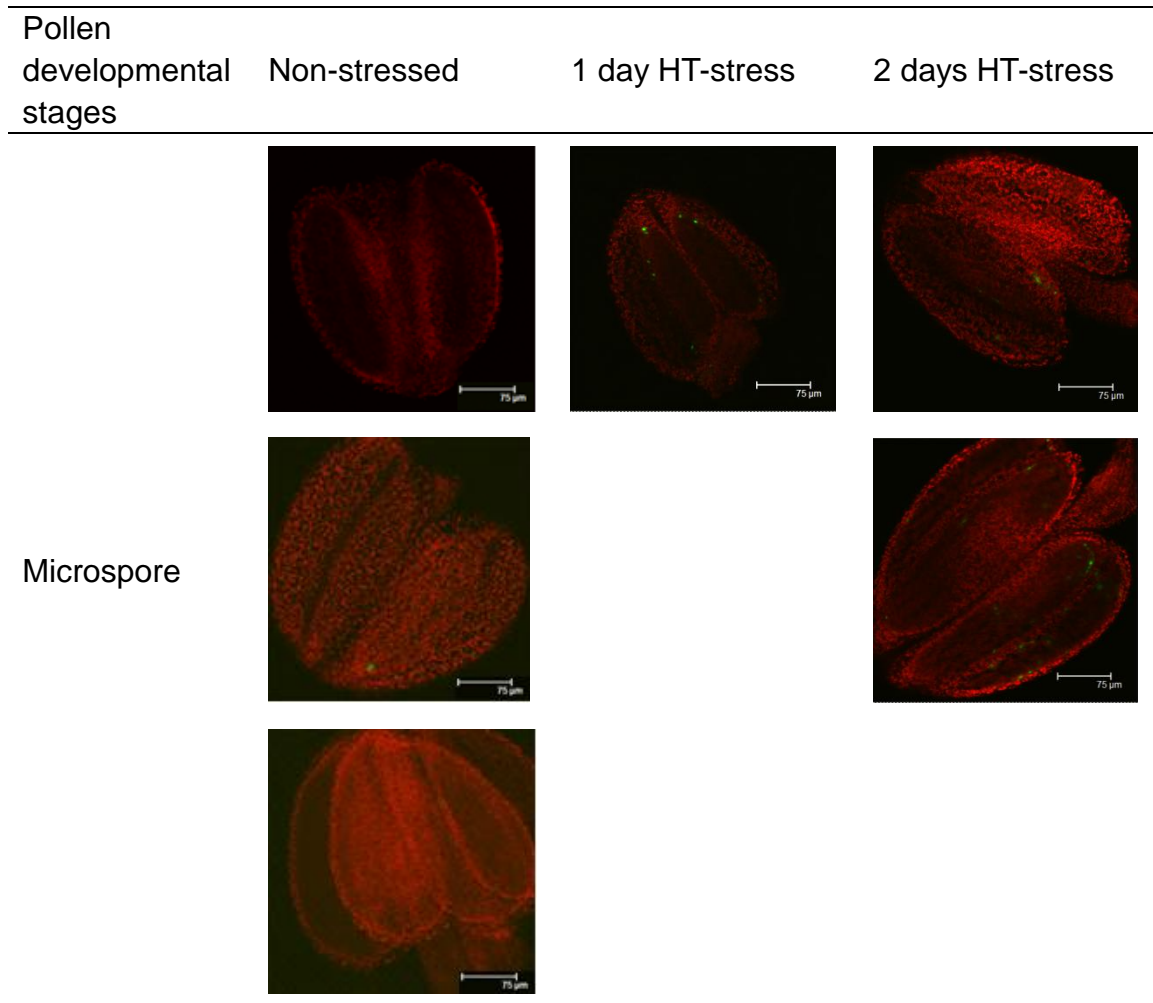


Figure 6.20 CEP1:GFP expression in Arabidopsis anther without HT-stress and HT-stressed for 1 day and 2 days. (continued)

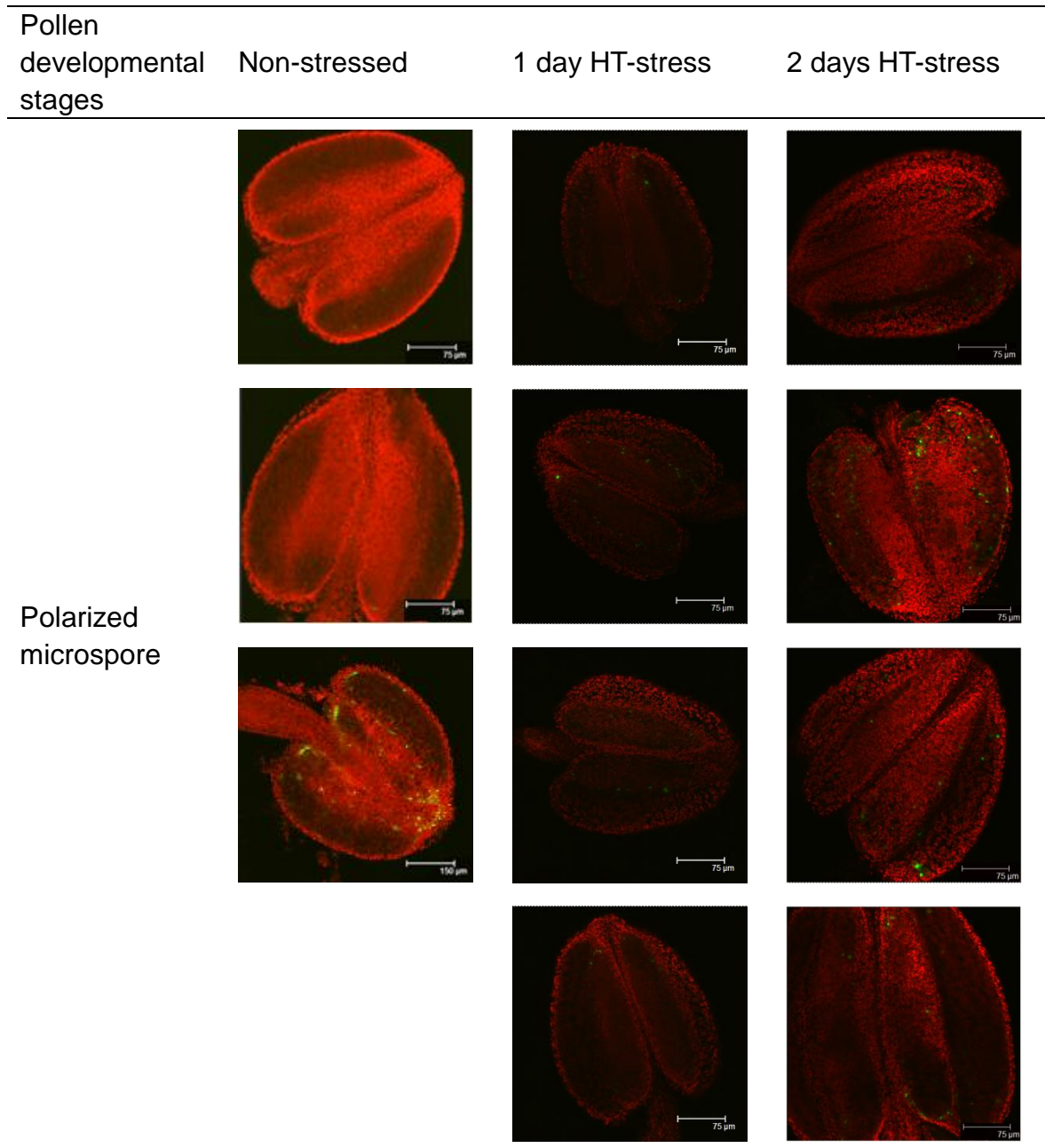


Figure 6.20 CEP1:GFP expression in Arabidopsis anther without HT-stress and HT-stressed for 1 day and 2 days. (continued)

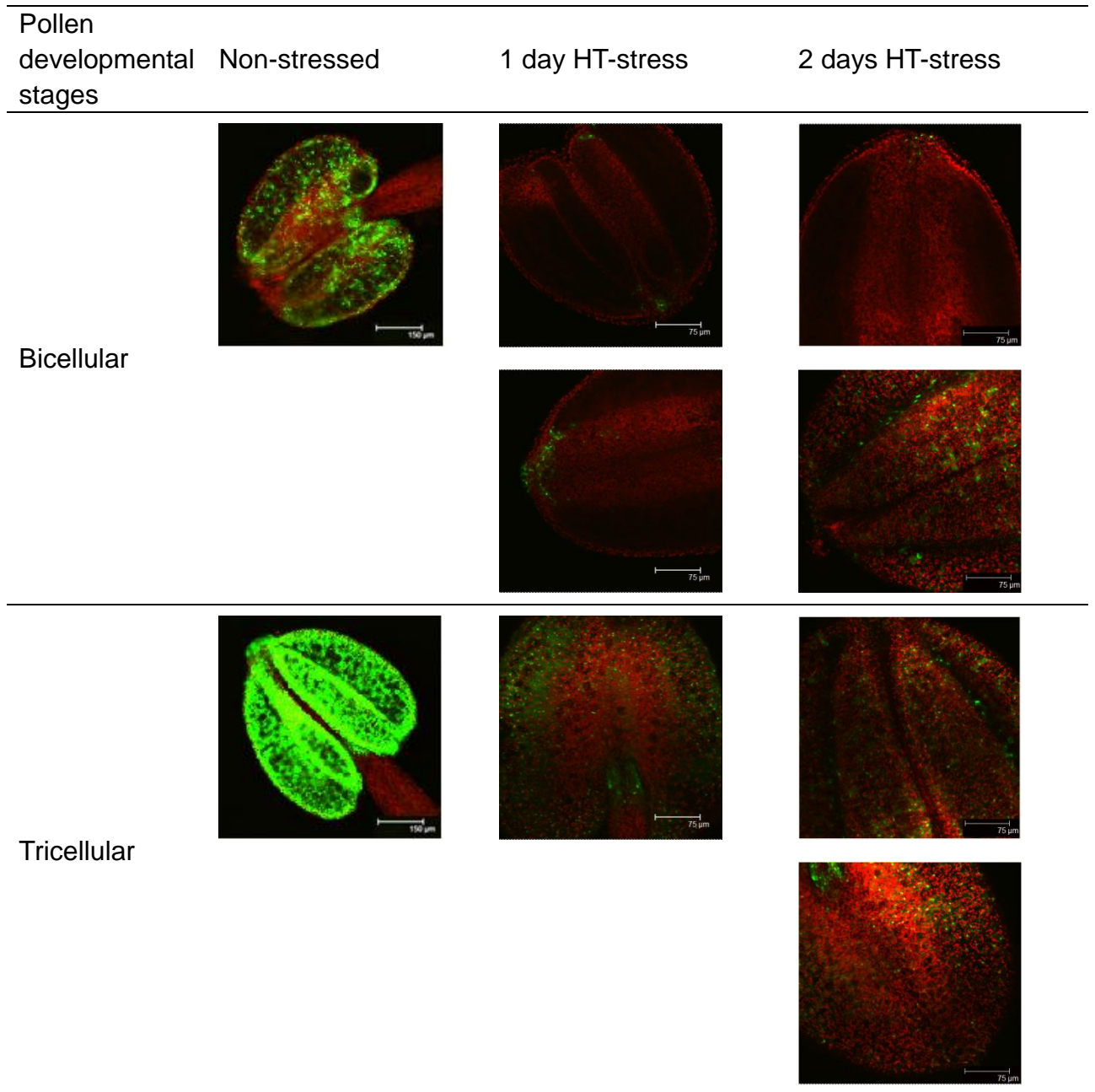
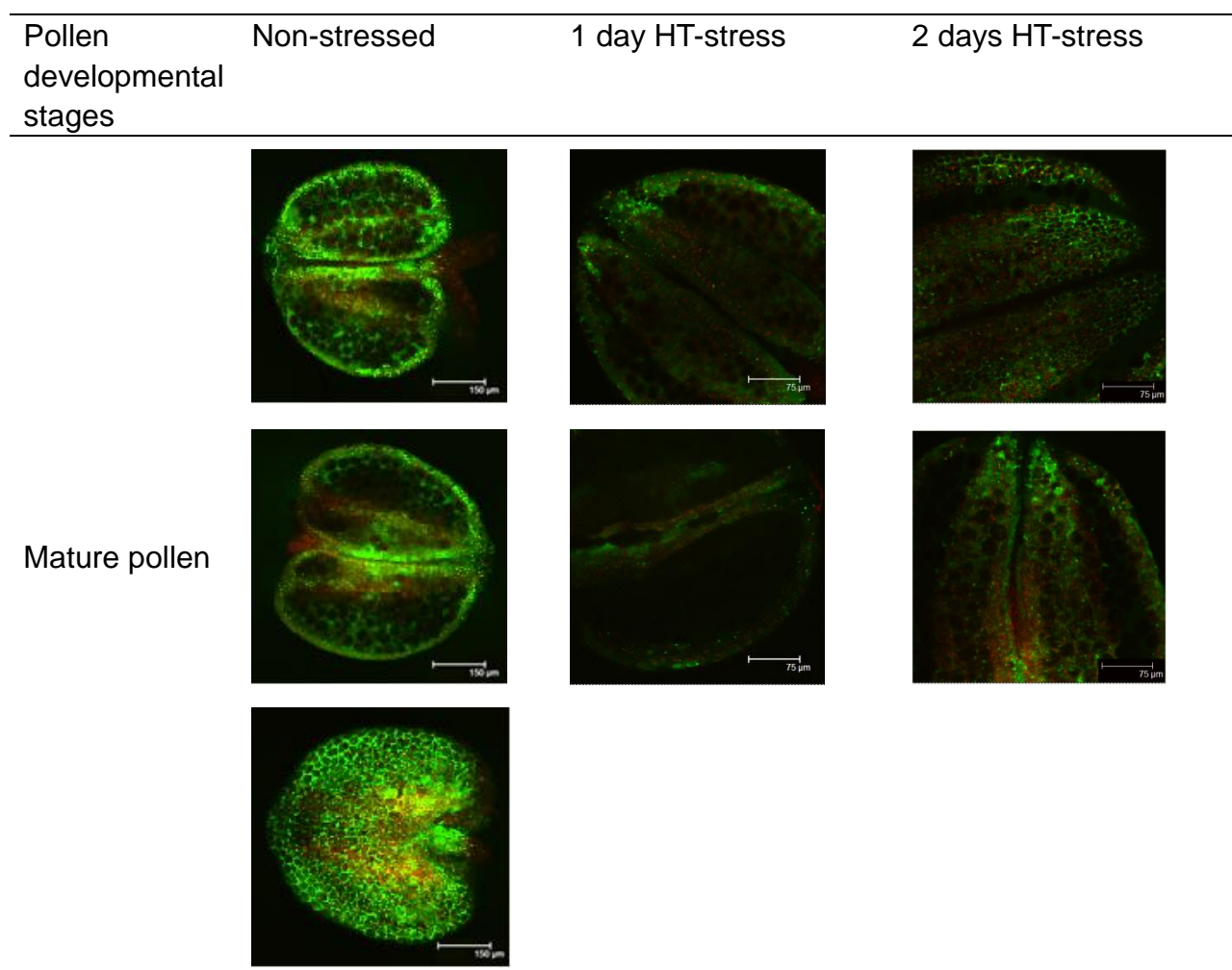


Figure 6.20 CEP1:GFP expression in Arabidopsis anther without HT-stress and HT-stressed for 1 day and 2 days. (continued)



6.3.5 RNA-seq results of *BFN1* and *CEP1*

To verify the confocal microscopy results, the RNA-seq results were analysed to perform the relative expression levels of *BFN1* and *CEP1* genes after HT-stress. The results showed the expression level of *BFN1* was down-regulated after 6 and 24 hours HT-stress in all of the samples (Fig. 6.21). The relative expression level was decreased more in the “Old group” than that in the “Young group”, which means *BFN1* gene was down-regulated more in

polarized microspore and pollen mitosis stages than in microspore, tetrad, PMCs and other younger stages. Furthermore, the longer HT-stress treatment depressed the expression level more than that with shorter HT-stress. These expression level results of *CEP1* were quite similar to *BFN1*, the difference was *CEP1* showed some up-regulation after 6 hours HT-stress, but then was decreased soon after.

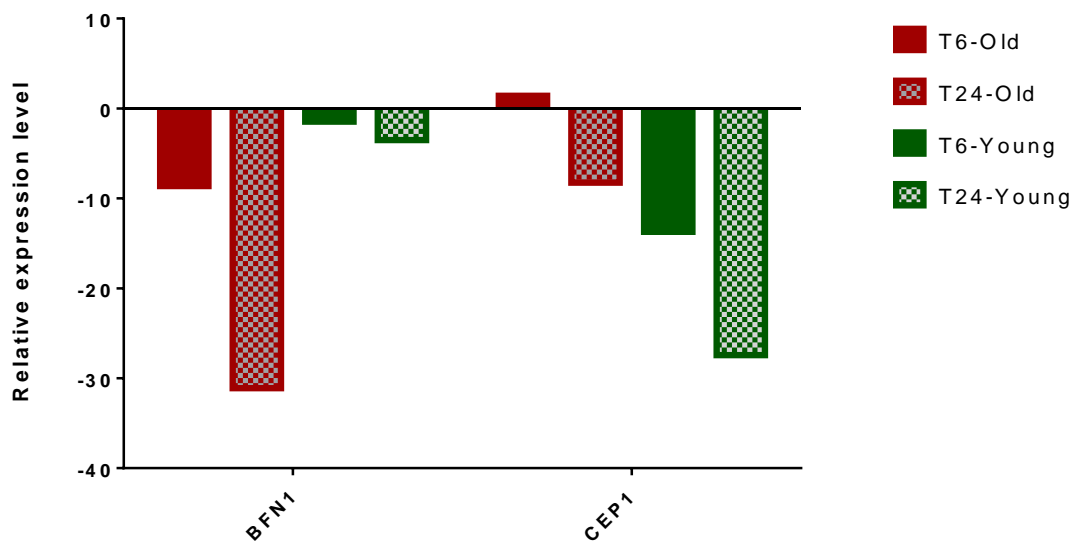


Figure 6.21 Relative expression levels of *BFN1* and *CEP1* in different pollen developmental stage after HT-stress. Bars indicate the expression fold change in HT-stressed samples compare with non-stressed which were collected at the same time points.

6.4 DISCUSSION

6.4.1 PCD genes expression with tapetum PCD

As previously discussed, the tapetum functions as a nutrition cell layer and for biosynthesis of pollen wall materials during pollen development, it is also thought to secrete an enzyme callase that is required for the breakdown of callase and the release of microspores from the tetrads (Pacini & Franchi, 1993). Tapetum PCD occurs in the later pollen developmental stages, immediately after microspore release from the tetrad and before mitosis II (Liu & Fan, 2013). The tapetum is rich in ER and the plasma membrane, lacking a cell wall, is often in contact with microspores. In the late tricellular pollen stage, the contents of tapetal cells are released into the locule and become closely associated with the pollen exine (Quilichini et al., 2014, Wilson & Zhang, 2009). The importance of the tapetal cells during anther development is emphasized through the fact that male sterility is often related with tapetal dysfunction, for example tapetal breakdown delayed in the *ms1* mutant shows a conversion from PCD degradation to necrotic-based breakdown (Vizcay-Barrena & Wilson, 2006). Also male-sterile plants have been constructed by using tapetum-specific promoters to express RNases in tapetal cells (Paul et al., 1992). Correct timing of tapetal PCD is important for pollen and anther development and plant fertility.

Previous research has indicated the function of APS reductase as the key

enzyme for plant sulphate assimilation, which undergoes extensive and complex regulation by multiple environment factors and signalling compounds (Kopriva & Koprivova, 2004, Koprivova et al., 2008). There are three genes in the family encoding APR in *Arabidopsis*, *APR1* was expressed in a different places compared to the other two genes in the family (Kopriva et al., 2009). The APR1:GFP signal was firstly observed in the tetrad stage which is after pollen meiosis. This GFP fluorescence decreased from polarized microspore stage which is the time at which the tapetum degeneration initiated. However, GFP signal disappeared in late pollen developmental stage that is just before anther dehiscence, which indicated that there was no *APR1* gene expression when septum and stomium breakage happened. It had been reported that tapetum degeneration was initiated from anther stage 10 (Sanders et al., 1999), which corresponds to the polarized microspore stage. In addition, confocal microscopy results reveal that APR1:GFP fluorescence exists in the nuclei of the anther wall cell, but it is hard to say the exact layer. Furthermore, the APR1:GFP signal exists even after tapetum degeneration but vanishes with breakage of the epidermis and endothecium. Therefore, *APR1* was not specifically expressed during tapetum degeneration.

As a senescence-associated nuclease I gene, *BFN1* encodes a bifunctional nuclease I enzyme, a protein with both RNase and DNase activities. Several previous researchers have reported the function and characterisation of *BFN1* of *Arabidopsis* during stem and leaf senescence, and high *BFN1* mRNA levels

were observed during leaf and stem senescence (Perez-Amador et al., 2000). BFN1 protein was observed localised in filamentous structures that reorganised around the nucleic in senescing cells in young *Arabidopsis* leaf. In the late senescence process, BFN1 was localised with fragmented nucleic in the membrane-wrapped vesicles (Farage-Barhom et al., 2011). This localisation pattern suggests *BFN1*'s function as a nuclei acid-degrading enzyme in senescence and PCD (Farage-Barhom et al., 2011). BFN1:GFP in WT anther samples was visible in polarized microspore stage at a low level, when tapetum PCD began. This GFP fluorescence increased during the bicellular stage and then reduced to similar low level as the polarized microspore stage in the tricellular stage. Strongest GFP signal was observed in the mature pollen prior to anther dehiscence (Fig. 6.5). However, the quantitative RT-PCR result indicated the expression level of *BFN1* was lowest before polarized microspore stage, which was before tapetum degeneration. Then the expression level increased during tapetum degeneration, including the polarized microspore stage and pollen mitosis I & II stages, but then was decreased in the tricellular stage and mature pollen stage (Fig. 6.16). This expression variation could be explained as although previous research reported that tapetum degeneration process during pollen development (Sanders et al., 1999). Tapetum PCD initiates from polarized microspore stage so that BFN1:GFP fluorescence appeared then. This fluorescence increased during pollen mitosis I and II as the tapetum PCD and degradation carried on

most serious, but the GFP signal decreased at tricellular stage for tapetum had been disappeared before tricellular pollen stage (Sanders et al., 1999). Furthermore, the strongest GFP fluorescence in mature pollen stage may be due to the accumulation fragmented DNA in the late senescence of stamen. Some other recent evidence also revealed that the tapetum cytoplasmic materials still existed in the later tricellular pollen stage in the locule after programmed cell death (Quilichini et al., 2014), which may also lead to BFN1:GFP fluorescence exists during tapetum degeneration and still could be observed in tricellular and mature pollen stage for the tapetum cytoplasmic constituents did not disappear. Another possibility of the difference between quantitative RT-PCR and GFP fluorescence might be the GFP stability and accumulated in anther, which then results in stronger GFP signal to be observed in the tricellular and mature stages. Further analysis of TUNEL and immunolocalisation at difference pollen developmental stages may be needed to identify the localisation of BFN1 protein and to verify the expression of *BFN1* gene, and mutants that are deficient in *BFN1* expression may be also needed to investigate the function of *BFN1* gene during tapetum PCD.

CEP1 is a gene encoding a KDEL-tailed cysteine endopeptidase, which belongs to a group of papain-type peptidases in senescing tissues undergoing PCD (Zhou et al., 2016). These peptidases are synthesized as pro-enzymes with a C-terminal KDEL endoplasmatic reticulum retention signal, and then is removed with the pro-sequence to activate enzyme activity (Helm et al., 2008).

CEP1 has been reported as a crucial executor during tapetal PCD and that “proper” *CEP1* expression is thought to be necessary for timely degeneration of tapetal cells and functional pollen formation (Zhang et al., 2014). However, unlike the results published before (Zhang et al., 2014), a different pattern of *CEP1*:GFP fluorescence during anther developmental processes was observed. The strongest GFP signal in WT anther samples appeared in late pollen developmental stages, tricellular stage and mature pollen stage, but was much lower in earlier stages (Fig. 6.9). These results were confirmed by the quantitative RT-PCR results, which showed the *CEP1* relative expression levels were 1, 0.25, and 0.04 in “Mature group”, “Old group”, and “Young group” bud samples, respectively. These results indicate the *CEP1* expression could still be detected in the late pollen developmental stages even when the tapetum had degenerated. A possible reason for this is because tapetum cytoplasmic materials still exist around pollen grains after degeneration (Quilichini et al., 2014). However, repeated verification is necessary to confirm the previous results.

Several researchers have previously mentioned that the cysteine protease gene *SENESCENCE ASSOCIATED GENE12* (*SAG12*) was involved in plant senescence and was up-regulated in different tissues with age, especially in leaves and petals (Otegui et al., 2005, Price et al., 2008, Song et al., 2016), and also it was reported that it could regulate plant flood tolerance (Huynh le et al., 2005, Zhang et al., 2000). We observed weak *SAG12*:GFP fluorescence

only in late pollen developmental stages in WT anther samples, at mature pollen stage just before pollen dehiscence, simultaneously in the senescing plants (Fig. 6.13). Furthermore, no GFP signal appeared in any other stages and also no such fluorescence existed in old bud samples if the plants were not senescent. According to these results, *SAG12* was specifically expressed during plant senescence but did not show any specific relationship with tapetum PCD.

6.4.2 PCD genes expression in the male sterile mutants

It is known that several genes which lead to male sterility are involved in tapetum PCD, such as *AMS*, *MS1*, and *DYT1*. Confocal microscopy of *APR1*, *BFN1*, *CEP1*, and *SAG12* with GFP expression in the *ams*, *ms1* and *myb26* homozygous mutants indicated how these four PCD related genes were regulated in male sterile mutants with altered tapetum PCD.

There was no *APR1*:GFP fluorescence in tetrad stage and other younger stages, GFP signal appeared in the microspore stage in *ams*, *ms1* and *myb26* mutants, which was delayed compared with WT. The GFP fluorescence strength in all the three male sterile mutants also showed a weaker level than WT (Fig. 6.2, 6.3, and 6.4). This was similar to *SAG12* for it also showed a decrease in GFP fluorescence strength in *ms1* and *myb26* mutants even though this *SAG12*:GFP could only be observed in later mature pollen stage (Fig. 6.14 and 6.15). *BFN1*:GFP and *CEP1*:GFP was observed firstly in the

microspore stage in *ams* and *ms1* mutants, which was in advance compared to that in WT samples, but did not show any variation in *myb26* mutant (Fig. 6.6, 6.7, 6.8, 6.10, 6.11, and 6.12). It has been reported that abnormal tapetum occurs in the tetrad stage in the *ams* mutant (Xu et al., 2010), and in late microspore stage in the *ms1* mutant (Wilson et al., 2001), which suggests that the expression of *BFN1* and *CEP1* may be anticipated along with earlier tapetum PCD in *ams* and *ms1* mutants. Moreover, there was no variation of the GFP signal appearance period in the *myb26* mutant of *BFN1* and *CEP1*, which would also support the possibility of a relationship between *BFN1*, *CEP1* and tapetum PCD because there was a limited relationship between *MYB26* and tapetum PCD since it is downstream of regulation by *ams* and *ms1* (Yang et al., 2007, Wilson et al., 2011).

Quantitative RT-PCR results indicated a similar trend in these different male sterile mutants (Fig 6.17 and 6.18). *BFN1* was down-regulated in the *ms1* mutant and also in “Old group” and “Young group” bud samples in *ams* mutant, but was up-regulated in “Mature group” buds in the *ams* mutant. The *CEP1* gene was up-regulated in all of the staged samples in *ams* and *ms1* mutant.

DYT1 is a gene that function during early stages of tapetum development, and *TDF1* which play a vital role in tapetum differentiation and function is a gene downstream of *DYT1* (Gu et al., 2014, Zhu et al., 2008). *BFN1* showed significantly up-regulation in the *dyt1* mutant buds, but was down-regulated in

tdf1 mutant. *CEP1* was significantly up-regulated in both the *dyt1* and *tdf1* mutants, and its expression level in *tdf1* mutant was higher compared to WT samples. As mentioned before, *AMS* and *MS1* operate downstream of *TDF1* (Fig. 1.8) in the transcriptional regulation (Wilson et al., 2011). These results indicated that *BFN1* might be down-stream of *DYT1* but up-stream of *AMS*, *MS1* and *TDF1*, while *CEP1* maybe down-stream of all of these four genes.

6.4.3 Impacts of HT-stress on *BFN1* and *CEP1* during pollen development

BFN1 and *CEP1* have been implicated in tapetum PCD processes; previous research has suggested HT-stress may result in premature degeneration of the tapetum (Sakata & Higashitani, 2008). *BFN1*:GFP and *CEP1*:GFP fluorescence strength in most of pollen developmental stages after HT-stress decreased as compared to non-stressed samples, which was also confirmed by the RNA-seq results (Fig. 6.21). *BFN1*:GFP decreased over time in all of the pollen developmental stages, and also the relative expression level by RNA-seq analysis showed similar trends. *CEP1*:GFP fluorescence strength showed decreased level after one day HT-stress, which was also seen in the RNA-seq (Fig. 6.21). However, *CEP1*:GFP signal appeared earlier in these HT-stressed samples than non-stressed, and the *CEP1* gene was more specific in tapetum PCD than *BFN1*. These results indicate that *CEP1* gene is sensitive to tapetum PCD and variation of tapetum PCD leads to a different expression of *CEP1*. In addition, the RNA-seq data indicates *CEP1* expression

level in polarized microspore stage and pollen mitosis stages showed an up-regulated level after 6 hours HT-stress than that was not HT-stressed, but then the expression level after 24 hours was down-regulated to below that of not HT-stressed. The confocal microscopy photos showed a stronger CEP1:GFP fluorescence level in bicellular stage after 2 days HT-stress than samples were HT-stressed for 1 day at the same stage. All of these results indicate that *CEP1* gene is sensitive to high temperature stress, as well as alteration of tapetum PCD caused by HT-stress.

In conclusion, *APR1* and *SAG12* are not specific only expressed during tapetum PCD processes, while expression of *BFN1* and *CEP1* showed a closer correlation with tapetum PCD. In addition, *BFN1* might be down-stream of *DYT1* but up-stream of *AMS*, *MS1* and *TDF1*, while *CEP1* is likely down-stream of all of these four genes. HT-stress depresses *BFN1* expression level during pollen development and this reduction was enhanced along with HT-stress. HT-stress leads to an earlier tapetum PCD and would result in earlier expression of *CEP1*, but the transient expression analysis by confocal microscopy revealed expression of *CEP1* is sensitive to HT-stress. The possible regulation network of *BFN1* and *CEP1* is shown in Fig 6.22.

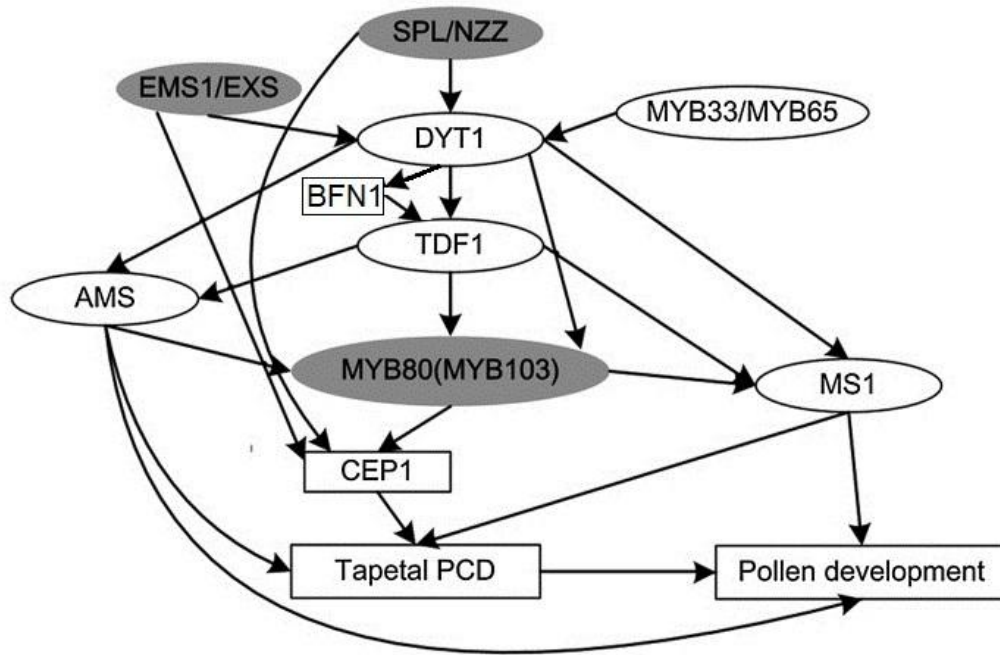


Figure 6.22 A model for *BFN1* and *CEP1* regulation during anther and pollen development. Solid arrows represent gene regulation and grey ovals represent direct gene regulation.

CHAPTER 7

GENERAL DISCUSSION

CHAPTER 7. GENERAL DISCUSSION

Global warming is predicted to effect on plant growth negatively due to the damaging effect of HT-stress on plant development, which is likely to result in a series problems for global food security (Stocker et al., 2013). HT-stress is a major environmental factor that influences plant growth, metabolism and productivity (Lobell & Field, 2007). The susceptibility of plant responses to HT vary with the developmental stage, but HT-stress affects all vegetative and reproductive stages to some extent (Sakata & Higashitani, 2008). In an extremely HT environment, plants suffer serious cellular damage and cell death within short period, which may result in a catastrophic collapse of cellular organization (Ahuja et al., 2010). Although all plant tissues are susceptible to HT-stress in almost all the developmental stages, the reproductive tissues are the most sensitive parts, and a slightly increasing of temperature during flowering time can cause critical damage during reproductive organ development and lead to the loss of entire crop yield (Lobell et al., 2011). HT can cause significant male reproductive organ damage resulting in male sterility, since the male gametophyte is particularly sensitive to high temperatures, whilst the pistil and the female gametophyte are considered to be more tolerant (Hedhly, 2011). In addition to pollen development, filament elongation is also impacted by HT-stress. The filaments in *Arabidopsis* flowers display a significant reduction in length after 2 days

HT-stress at 32° C (Fig. 3.8, Fig. 3.9), while no phenotype variation was observed in pistil development.

7.1 HIGH TEMPERATURE STRESS ON PLANT MORPHOLOGY DURING POLLEN DEVELOPMENT

The most direct impact of HT-stress for pollen development is variation of pollen viability and *in vitro* germination. During the HT-stress experiment, the percentage of viable pollen and germination displayed a significant reduction, which was reduced more than 4-fold compared to non-stressed pollen (Fig. 3.5, Fig. 3.6), and which was evident after 1 day HT-stress. According to the pollen developmental staging result (see section 3.3.1), the pollen samples, which were collected on the first day in the HT-stress experiment, were in tricellular and mature stages. This means the pollen which is in late developmental stages (tricellular and mature stages) was more seriously damaged after HT-stress, even though they suffered a shorter duration of HT-stress, than other earlier staged pollen. Moreover, pollen viability and germination show recovery over time. An important event during pollen development is the degeneration of tapetum, which ends before the tricellular stage (Sanders et al., 1999). This suggests that the presence of the tapetum may serve to protect pollen development from HT-stress.

HT-stressed *Arabidopsis* plants produced shorter siliques and less seeds than those not HT-stressed (Fig. 3.7, Fig.3.8). Endo et al. (2009) have reported that

HT-stress does not damage the ability of the pistil to receive pollen by the stigma, but impaired the ability of pollen to attach and/or germinate on the stigma. Hence, this reduction in silique length and seed number is likely to be due to the impact of HT-stress on pollen development and seeds. Injury of HT at different development stages implied that development of the oldest bud in the HT-stress experiment was suppressed the most, while the data of silique length and seed numbers showed some recovery from the oldest to youngest buds after 2 days HT-stress (Fig. 3.9, Fig. 3.10). Nevertheless, the seeds produced by the HT-stressed plants did not show a significant loss of vigour, and no significant difference in percentage of seed germination between HT-stressed and non-stressed samples (Fig. 3.13).

7.2 MOLECULAR ASPECT AND GENE FUNCTION ANALYSIS ON HT-STRESS DURING POLLEN DEVELOPMENT

The tapetum is a specialised layer of nutritive cells found within the sporangium of flowering plants, which is important for pollen nutrition and development, as well as a source of precursors for the pollen coat (Polowick & Sawhney, 1993). Tapetum development is essential for male fertility (Bita & Gerats, 2013). Major variations in gene expression under HT-stress are possibly related to tapetum degeneration and pollen sterility (Oshino et al., 2007, Endo et al., 2009).

A number of genes were therefore selected which were expressed in the

tapetum and showed expression variation as a result of HT stimulus (see section 4.1). All of the selected genes were inducible by HT-stress but most of them, except *ABI1* gene, showed some recovery when the plants were returned to normal temperature environment (Fig. 4.3).

The function of the endoplasmic reticulum (ER) in the endomembrane system is engaged with the folding and modification of proteins in to ensure their correct sorting, secretion and function (Ron & Walter, 2007). Disturbances in the ER or overload in secreted protein production results in the accumulation of unfolded proteins, which leading to the unfolded protein response (UPR) (Silva et al., 2015). *AtCRT1b* and *AtUTR1* are two UPR related genes. *AtCRT1b* belongs to the calreticulin (CRT) family, an ER-localized Ca²⁺-binding protein, which is up-regulated by UPR for ER-stress response (Kim et al., 2013). *AtUTR1* is a UDP-galactose/glucose transporter, which is also up-regulated by UPR (Reyes et al., 2006). There is no clear understanding as to how environmental stresses induce UPR in plants, but closer analysis of the effects of the different stress agents on UPR signalling in plants might provide greater insight into the mechanisms by which different environmental stresses activate UPR (Liu & Howell, 2010). HT-stress in plants induces ER stress and then leads to UPR, which results in up-regulation of stress-response genes (Howell, 2013), but the role of UPR in the general HT-stress response and thermo-tolerance is not well described in plants (Fragkostefanakis et al., 2016). However, the evidence of *AtCRT1b* and

AtUTR1 expression level in this experiment indicates these two genes are suppressed after HT-stress (Fig. 4.3a, Fig. 4.3b). This suggests UPR activation is not elevated by this treatment since previous research reported increased UPR led to up-regulation of *AtCRT1b* and *AtUTR1* (Reyes et al., 2006, Kim et al., 2013). Furthermore, the ectopic expression of sHsp21.5, a gene that regulates ER chaperone in maturing tomato microspores with HT-stress, was reported to cause the lower accumulation of UPR-related genes (Fragkostefanakis et al., 2016). Loss of function of *AtCRT1b* results in a reduction of HT resistance and reduced seed production after HT-stress, but there is no significant difference in the *atutr1* mutant. This might be due to that fact that loss of function of *AtUTR1* could be complemented by the *AtUTR3* gene (Reyes et al., 2010), but two other *CRT* family members, *AtCRT1* and *AtCRT3*, were reported not to contribute to recover the loss of function of *AtCRT1b* (Kim et al., 2013).

AtMBF1c is a transcriptional co-activator in *Arabidopsis*, which has been reported to function in enhancing the tolerance of transgenic plants to high temperature and osmotic stress, and bacterial infection , (Suzuki et al., 2005). Suzuki et al. (2005) reported the over-expression of *MBF1c* in *Arabidopsis* plants increased seed germination percentage and transgenic seedling survival rate with HT-stress. Multiprotein bridging factor 1 (MBF1) is a highly conserved transcriptional co-activator, MBF1c also involves in the regulation of diverse processes, while MBF1c is specifically elevated in *Arabidopsis* in

response to HT-stress in contrast with two other MBF1 family members, *MBF1a* and *MBF1b* (Rizhsky et al., 2004). *AtMBF1c* displayed rapidly HT-inducibility and was up-regulated within 1 day of HT-stress, which was reduced to normal levels in the following measurement time points (Fig. 4.3c). In addition, loss of function of *MBF1c* leads to a delay on the reduction of pollen viability but decreased HT tolerance to produce less seeds from HT-stressed plants (Fig. 4.18). Previous research reported that over-expressed *MBF1c* transgenic plants resulted in the constitutive expression of several signal transduction and defence transcripts, and also the enhanced accumulation of different stress-associated transcripts in response to HT-stress, which suggests that constitutive expression of *MBF1c* in transgenic plants changes the accumulation of specific transcripts in non-stressed control conditions and the stressed environment (Suzuki et al., 2005). Moreover, gain- and loss-of-function *MBF1c* plants provides strong evidence for a link between *MBF1c* and trehalose metabolism, suggests a role for *MBF1c* as a central regulator of thermo-tolerance in *Arabidopsis*, and demonstrates that *MBF1c* functions upstream to ethylene, PR-1, SA, and trehalose during HT-stress (Suzuki et al., 2008).

ABI1 is a key component of ABA signal transduction in *Arabidopsis* that regulates numerous ABA responses (Moes et al., 2008). Abscisic acid (ABA) is critical for plant growth in response to environment challenges (Lu et al., 2015). ABA is known to be required for several plant individual or combined abiotic

tolerances (Suzuki et al., 2016), and ABA could enhance plant stress tolerance by inducing genes encoding enzymes for the biosynthesis of compatible osmolytes and LEA-like proteins, which increase plant stress tolerance cooperatively (Bray, 2002). A reduced ABA sensitivity in *abi1* mutants (Arend et al., 2009), which leads to reduced HT tolerance in *Arabidopsis* plants. ABA content was previously shown not to be elevated in an HT environment (Baron et al., 2012), but ABA sensitivity of the plant is increased, this may be due to the expression level of *AtABI1* that displayed a significant up-regulation in all stages of WT bud samples during the entire HT-stress experiment (Fig. 4.3d). Therefore, plants that have lost *AtABI1* function may display a lower sensitivity to ABA and show reduction in pollen viability and reproductive development compared to wild type under HT-stress (Fig. 4.20).

Both *AtHOP3* and *AtHS83* were highly induced and significantly up-regulated by HT-stress but this dropped to a normal level when the plants were returned to a non-stressed environments. *AtHOP3* is a target gene of a putative heat-shock transcription factor *HsfA2*, which is a heat-inducible and essential for acquired thermo-tolerance in *Arabidopsis* (Charng et al., 2007, Nishizawa et al., 2006). *AtHS83* is member of the HSP90 family, which regulates heat-inducible genes by suppressing HSF activity, and HSP90 is transiently inactivated upon heat shock, leading to activation of heat shock factors (Yamada et al., 2007). The analysis of phenotype indicates that the loss of function of *AtHOP3* and *AtHS83* leads to a delay HT sensitivity but reduction of

HT tolerance, which produced less seeds on HT-stress *Arabidopsis* plants (Fig. 4.19, Fig. 4.21).

However, the link between these genes and tapetum development is unclear and ultrastructure investigations are needed to confirm this.

7.3 TRANSCRIPTOME ANALYSIS OF HT-STRESS DURING POLLEN DEVELOPMENT

Transcriptome analysis by next-generation sequencing (RNA-seq) allows a understanding of the transcriptome for identifying the functional components of the genome and revealing the molecular constituents of cells and tissues, and also for understanding development and disease (Hoeijmakers et al., 2013).

According to the previous expression analysis results, the genes which were analysed in chapter 4 presented more variation in expression level in bud samples which were collected after 1 day HT-stress than at other time points (Fig. 4.3). Hence, stages buds for RNA-seq were treated at 32° C for 1 day and collected at three time points as mentioned in section 5.2.1.

Datasets for each replicate were assessed for quality using in MDS plots (Fig. 5.1, Fig.5.2, Fig. 5.3). Each group cluster showed effective distance with others. The efficiency of normalisation was also evaluated and confirmed using edgeR, and displayed by MA-plot (Fig. 5.4), the distribution of significantly differentially expressed genes were presented with “volcano” plots

by comparing two values, the expression fold change and p-value of significance of differentially expression of gene (Fig. 5.5). In addition, P-value<0.05 was used to classify the significance of differentially expressed genes. Finally, DE gene lists were generated (Table 5.2). There are about 700 genes are transcription factors in these DE genes.

The GO enrichment analysis indicates that the DE genes were mostly enriched in “other cellular process” and “other metabolic processes” which are classified into Biological Processes in all of the classifications. In Cellular Component classification, the most enriched categories were “nucleus”, “other membrane”, “other intracellular components”, and “other cytoplasmic components”, while enriched in “other binding” and “unknown molecular functions” for Molecular Function. These results suggest that plant cellular and metabolic processes are more sensitive to HT-stress. However, the functional category of “response to stress” presents a quite normal level, which indicates the HT response or regulation genes might not represent too much differential expression level with HT-stress. This enrichment analysis indicates that HT-stress may lead to metabolic variation in cellular level, and then results in a series of morphological change during pollen development. These results may also help to find the target genes with specific function during pollen development undergo HT-stress.

Among these genes, AT1G29410 (*PAI3*) shows highest up-regulation to

461.33 fold in 24 hours HT-stressed “Young” staged buds by evaluating both of FDR and p-value. There is very limited research reported about the function of *PAI3*, which belongs to the PAI family that encode the enzyme that catalyses the third step of the tryptophan biosynthetic pathway, phosphoribosylanthranilate isomerase (PAI) (Melquist et al., 1999). *PAI3* is enriched in Biological Process according to GO analysis by TAIR [www.Arabidopsis.org].

AT4G00050 (*bHLH016*) is a member of basic/helix-loop-helix (bHLH) family (Toledo-Ortiz et al., 2003). It presents the highest expression level of 63.2 fold up-regulation among all of the genes in the 6 hours HT-stressed “Old” staged buds sample. This gene also shows several GO enrichment categories in Biological Process [www.Arabidopsis.org].

AT3G27810 (*MYB21*) expresses lowest down-regulation to 59.74 fold in the 6 hours HT-stressed “Young” staged buds sample. AT3G27810 is a transcription factor and is preferentially expressed in anther vascular tissue and in cells at the junction between the anther and stamen filament, and is involved in anther wall development (Li et al., 2013). AT3G27810 is also induced in flowers by drought, which might function in the recovery of those drought-tolerance (Su et al., 2013). AT3G27810 is jasmonate induced during petal and stamen filament elongation and anther dehiscence, but it also induces a negative feedback on jasmonate biosynthesis (Reeves et al., 2012).

AT2G32950 (*COP1*) is the most down-regulated gene to 58.46 fold in 6 hours HT-stressed “Old” bud samples. AT2G32950 is a central negative regulator of photomorphogenesis (Lin et al., 2016). AT2G32950 is a key regulator of flavonoid biosynthesis in seedlings but not of flavonoid deposition in seeds (Jaegle et al., 2016). AT2G32950 controls responses to abiotic stress, while salt stress and ethylene antagonistically regulate nucleocytoplasmic partitioning of AT2G32950, then to control *Arabidopsis* seed germination (Yu & Wang, 2016).

However, not all of these genes are reported to be specific functioned during pollen development. Furthermore, the RNA-seq database was validated by quantitative RT-PCR. Selected genes expressed showed a similar trend in both of RNA-seq data and quantitative RT-PCR experiment (Fig. 5.14, Fig. 5.15). These observations support the assertion that the RNA-seq database is efficient for further gene function analysis. Following analysis will be initiated with the genes which showed most up- and down- regulated expression to predict their possible function by GO enrichment analysis and regulation network, and also to be considered whether the candidate genes are functioned in tapetum PCD or not. Then phenotype analysis in loss of function of the genes under HT-stress will be preceded, such as pollen viability, plant reproductive growth and ultrastructure of anther tissue.

7.4 PROGRAMMED CELL DEATH WITH HT-STRESS DURING POLLEN DEVELOPMENT

Programmed cell death (PCD) is essential for proper plant growth and development, which is a highly and precisely controlled cell death process for elimination of unnecessary cells (Van Hautegeem et al., 2015). PCD is crucial for plant stress response systems within abiotic and biotic stress environments, and also for plant reproductive growth (Zhou et al., 2016). Failure of tapetum PCD during *Arabidopsis* pollen development would lead to sterility (Zhang et al., 2014). High temperature stress is also known as a factor to induce PCD in several plant species (Petrov et al., 2015).

The expression analyse imply that *AtBFN1* and *AtCEP1* genes present an earlier expression stage in two male sterile mutants, *ams* and *ms1*, than that in wild type plants (Fig. 6.5, 6.6, 6.7, 6.8, 6.9, 6.10, 6.11 and 6.12). Quantitative RT-PCR indicates *AtBFN1* was repressed in *ams* and *ms1* mutants except in late pollen developmental staged buds of the *ams* mutant, and *AtCEP1* expressed up-regulation in the entire inflorescence in both of the mutants (Fig.6.17, Fig. 6.18). Further expression analysis in other male sterile mutants suggests that *AtBFN1* was down-regulation in the *tdf1* mutant but up-regulated in *dyt1* mutant, while *ATCEP1* is up-regulated in both of them. *AtBFN1* may be repressed by loss function of *ams*, *ms1* and *tdf1*, but induced in the *dyt1* mutants. *AtCEP1* is induced in all of these four male sterile mutants, and in

tdf1 AtCEP1 expression was elevated significantly higher than in the other three. Therefore, *AtBFN1* might be down-stream of *DYT1* but up-stream of *AMS*, *MS1* and *TDF1*, while *AtCEP1* should be down-stream of all of these four genes.

HT-stress suppresses *BFN1* and *CEP1* expression during pollen development according to the GFP signal. *BFN1:GFP* and *CEP1:GFP* fluorescence strength in most pollen developmental stages after HT-stress decreased compared to non-stressed samples (Fig. 6.19 and 6.22) but *CEP1:GFP* signal appeared earlier in these HT-stressed samples than non-stressed. This expression variation was validated by RNA-seq data (Fig. 6.21), which indicate *BFN1* and *CEP1* are HT repressed genes.

CEP1 is a gene for a KDEL-tailed cysteine endopeptidase and has been shown to be involved in tapetum PCD (Zhang et al., 2014, Zhou et al., 2016). *BFN1* is a well-known leaf senescence reporter, which has also been shown to function in chromatin breakdown during root cap PCD in *Arabidopsis* (Farage-Barhom et al., 2008, Farage-Barhom et al., 2011, Kumpf & Nowack, 2015). The GFP expression under confocal microscopy implies *BFN1* expression was advanced in *ams* and *ms1* mutants, and the tapetum presents an earlier degeneration in *ams* and *ms1* mutants. However, it is not clear whether *BFN1* is involved in tapetum PCD. To investigate the function of *BFN1* in tapetum PCD, morphological analysis on loss of function *BFN1* mutants is

needed, possibly as well as proteomics and transcriptomics.

7.5 SUGGESTING RELATIONSHIP BETWEEN HT-STRESS AND POLLEN DEVELOPMENT

Developing microspores and pollen are most sensitive and to be easily affected by high temperatures (Iwahori, 1965). The earliest HT induced developmental defects occur in pollen meiosis (Boyko et al., 2005, Francis et al., 2007), which may affect chromosome behaviour and meiotic cell division, and then lead to a unbalanced chromosome separation between spores and the formation of diploid dyads (Omidi et al., 2014, Pecrix et al., 2011, Rezaei et al., 2010). HT is also known to affect in vegetative tissues and during pollen tube growth through cytoskeleton and microtubule dynamics (Smertenko et al., 1997, Parrotta et al., 2016, Muller et al., 2007). Pollen viability was seriously damaged during HT-stress, as well as seed production (Fig. 3.5, Fig. 3.8). Microsporogenesis is also defected, which suggests that a reduction in pollen number and viability may lead to defects in the supportive tapetal cells indirectly (Parish et al., 2012, De Storme & Geelen, 2014). Several aberrations have been observed during tapetum development and degeneration, such as hypertrophy and premature, delayed degeneration, and morphology of tapetal endoplasmic reticulum (Abiko et al., 2005, Endo et al., 2009, Oshino et al., 2007, Harsant et al., 2013). In addition, the amount of starch and sugars in maturing pollen grains is also affected by long-term and mildly elevated

temperature (Aloni et al., 2001, Pressman et al., 2002, Firon et al., 2006). It is still not clear that how HT affects the above developmental processes. Several cellular effects of HT have been identified in vegetative cells, such as accumulation of reactive oxygen species (ROS), increased membrane fluidity, misfolding of proteins, and changes in the specificity and kinetics of enzyme reactions (Alfonso et al., 2001, Atkin & Tjoelker, 2003, Sangwan et al., 2002).

A sophisticated HT stress response (HSR) exists in plants to contend the HT affections and to maintain cellular homeostasis. The heat shock transcription factors (HSFs) is central of the HSR through binding the heat shock element (HSE), a specific palindromic DNA sequence, and induce the expression of HT responsive genes (Kotak et al., 2007, Scharf et al., 2012). Most of HSFs are induced in response to HT, which suggests that HSFs have a major but similar role to response to HT in pollen (Müller & Rieu, 2016). Heat shock proteins (HSPs) function to prevent irreversible high temperature damage under HT-stress, such as preventing the formation of aggregates, resolubilising aggregated proteins and returning them to the native conformation (Hartl et al., 2011, Kotak et al., 2007), and also to maintain the integrity of cell membrane (Tsvetkova et al., 2002). Accumulation of ROS is another HSR. HT seriously induces the ROS scavenging enzymes and antioxidants, which is contributed to plant HT-tolerance (Chao et al., 2009, Mittal et al., 2012). Plant hormones have also been reported to link to HT stress signalling and pollen HT tolerance. For example, pollen HT-tolerance is

improved by ethylene that is produced through chemical induction before HT-stress, while application of an ethylene inhibitor reduces this HT-tolerance (Firon et al., 2012). Exogenous application of auxin could improve pollen HT-tolerance to HT-stress in *Arabidopsis* and barley plants (Higashitani, 2013, Sakata et al., 2010). The effect of HT-stress on pollen characteristics is associated with variations of carbohydrate metabolism and content in the developing anthers (Chung et al., 2014, Pressman et al., 2006, Kaur et al., 2015). But it is still not clear that changes in starch and sugar levels in developing pollen are the result of active adjustments of the primary metabolism as part of the pollen HT response or an adverse consequence of high temperature. It is possible that pollen and tapetum need an unusually strong demand for energy, which is indicated by the high number of mitochondria in these cells. The tapetum and pollen may be affected more serious than other cells by depleting in energy reserves (Müller & Rieu, 2016).

For the future, obtaining knowledge on function of DE genes from RNA-seq, by applying morphology and ultrastructure analysis in WT and loss of function mutants, and also regulation and enrichment research, may be necessary to further understand HT response and tolerance during pollen development.

REFERENCES

REFERENCES

Abiko M, Akibayashi K, Sakata T, Kimura M, Kihara M, Itoh K, Asamizu E, Sato S, Takahashi H, Higashitani A, 2005. High-temperature induction of male sterility during barley (*Hordeum vulgare* L.) anther development is mediated by transcriptional inhibition. *Sexual Plant Reproduction* **18**, 91-100.

Ahuja I, De Vos RC, Bones AM, Hall RD, 2010. Plant molecular stress responses face climate change. *Trends Plant Sci* **15**, 664-74.

Ainsworth EA, Beier C, Calfapietra C, Ceulemans R, Durand-Tardif M, Farquhar GD, Godbold DL, Hendrey GR, Hickler T, Kaduk J, Karnosky DF, Kimball BA, Korner C, Koornneef M, Lafarge T, Leakey AD, Lewin KF, Long SP, Manderscheid R, Mcneil DL, Mies TA, Miglietta F, Morgan JA, Nagy J, Norby RJ, Norton RM, Percy KE, Rogers A, Soussana JF, Stitt M, Weigel HJ, White JW, 2008. Next generation of elevated [CO₂] experiments with crops: a critical investment for feeding the future world. *Plant Cell Environ* **31**, 1317-24.

Albrecht C, Russinova E, Hecht V, Baaijens E, De Vries S, 2005. The *Arabidopsis thaliana* SOMATIC EMBRYOGENESIS RECEPTOR-LIKE KINASES1 and 2 control male sporogenesis. *The Plant Cell* **17**, 3337-49.

Alfonso M, Yruela I, Almarcegui S, Torrado E, Perez MA, Picorel R, 2001. Unusual tolerance to high temperatures in a new herbicide-resistant D1 mutant from *Glycine max* (L.) Merr. cell cultures deficient in fatty acid desaturation. *Planta* **212**, 573-82.

Alia HH, Sakamoto A, Murata N, 1998. Enhancement of the tolerance of *Arabidopsis* to high temperatures by genetic engineering of the synthesis of glycinebetaine. *Plant J* **16**, 155-61.

Aloni B, Peet M, Pharr M, Karni L, 2001. The effect of high temperature and high atmospheric CO₂ on carbohydrate changes in bell pepper (*Capsicum annuum*) pollen in relation to its germination. *Physiol Plant* **112**, 505-12.

Alonso-Peral MM, Li J, Li Y, Allen RS, Schnippenkoetter W, Ohms S, White RG, Millar AA, 2010. The microRNA159-regulated GAMYB-like genes inhibit growth and promote programmed cell death in *Arabidopsis*. *Plant Physiol* **154**, 757-71.

Anders S, Huber W, 2010. Differential expression analysis for sequence count data. *Genome biology* **11**, 1.

Anders S, Pyl PT, Huber W, 2014. HTSeq—a Python framework to work with high-throughput sequencing data. *Bioinformatics* **31**, 166-169.

Arabidopsis Genome Initiative, 2000. Analysis of the genome sequence of the flowering plant *Arabidopsis thaliana*. *Nature* **408**, 796.

Arend M, Schnitzler JP, Ehling B, Hansch R, Lange T, Rennenberg H, Himmelbach A, Grill E, Fromm J, 2009. Expression of the *Arabidopsis* mutant *ABI1* gene alters abscisic acid sensitivity, stomatal development, and growth morphology in gray poplars. *Plant Physiol* **151**, 2110-9.

Ariizumi T, Toriyama K, 2007. Pollen exine pattern formation is dependent on three major developmental processes in *Arabidopsis thaliana*. *Int J Plant Dev Biol* **1**, 106-15.

Ariizumi T, Toriyama K, 2011. Genetic regulation of sporopollenin synthesis and pollen exine development. *Annual review of plant biology* **62**, 437-60.

Atkin OK, Tjoelker MG, 2003. Thermal acclimation and the dynamic response of plant respiration to temperature. *Trends Plant Sci* **8**, 343-51.

Auer PL, Doerge R, 2010. Statistical design and analysis of RNA sequencing data. *Genetics* **185**, 405-16.

Avila-Ospina L, Moison M, Yoshimoto K, Masclaux-Daubresse C, 2014. Autophagy, plant senescence, and nutrient recycling. *Journal of Experimental Botany*, DOI: 10.1093/jxb/eru03.

Bao Y, Song WM, Jin YL, Jiang CM, Yang Y, Li B, Huang WJ, Liu H, Zhang HX, 2014. Characterization of *Arabidopsis* Tubby-like proteins and redundant function of AtTLP3 and AtTLP9 in plant response to ABA and osmotic stress. *Plant Mol Biol* **86**, 471-83.

Barnabas B, Jager K, Feher A, 2008. The effect of drought and heat stress on reproductive processes in cereals. *Plant Cell Environ* **31**, 11-38.

Baron KN, Schroeder DF, Stasolla C, 2012. Transcriptional response of abscisic acid (ABA) metabolism and transport to cold and heat stress applied at the reproductive stage of development in *Arabidopsis thaliana*. *Plant Sci* **188-189**, 48-59.

Battisti DS, Naylor RL, 2009. Historical warnings of future food insecurity with unprecedented seasonal heat. *Science* **323**, 240-4.

Bechtold U, Albihlal WS, Lawson T, Fryer MJ, Sparrow PA, Richard F, Persad R, Bowden L, Hickman R, Martin C, Beynon JL, Buchanan-Wollaston V, Baker NR, Morison JI, Schoffl F, Ott S, Mullineaux PM, 2013. *Arabidopsis* *HEAT SHOCK TRANSCRIPTION FACTOR1b* overexpression enhances water productivity, resistance to drought, and infection. *J Exp Bot* **64**, 3467-81.

Berendzen K, Searle I, Ravenscroft D, Koncz C, Batschauer A, Coupland G, Somssich IE, Iker B, 2005. A rapid and versatile combined DNA/RNA

extraction protocol and its application to the analysis of a novel DNA marker set polymorphic between *Arabidopsis thaliana* ecotypes Col-0 and Landsberg erecta. *Plant Methods* **1**, 1.

Bick J-A, slund F, Chen Y, Leustek T, 1998. Glutaredoxin function for the carboxyl-terminal domain of the plant-type 5'-adenylylsulfate reductase. *Proceedings of the National Academy of Sciences* **95**, 8404-9.

Bitá C, Gerats T, 2013. Plant tolerance to high temperature in a changing environment: scientific fundamentals and production of heat stress-tolerant crops. *Front Plant Sci* **4**, 273.

Bloom JS, Khan Z, Kruglyak L, Singh M, Caudy AA, 2009. Measuring differential gene expression by short read sequencing: quantitative comparison to 2-channel gene expression microarrays. *BMC Genomics* **10**, 1.

Bowman JL, Smyth DR, Meyerowitz EM, 1991. Genetic interactions among floral homeotic genes of *Arabidopsis*. *Development* **112**, 1-20.

Boyko A, Filkowski J, Kovalchuk I, 2005. Homologous recombination in plants is temperature and day-length dependent. *Mutat Res* **572**, 73-83.

Bray EA, 2002. Abscisic acid regulation of gene expression during water-deficit stress in the era of the *Arabidopsis* genome. *Plant Cell Environ* **25**, 153-61.

Bray Ea B-SJ, Weretilnyk E, 2000. Responses to abiotic stresses. In: W Gruissem BB, R Jones, ed. *Biochemistry and Molecular Biology of Plants*. Rockville, MD: American Society of Plant Physiologists, 1158-249.

Canales C, Bhatt AM, Scott R, Dickinson H, 2002. EXS, a putative LRR receptor kinase, regulates male germline cell number and tapetal identity and promotes seed development in *Arabidopsis*. *Current Biology* **12**, 1718-27.

Carter C, Pan S, Zouhar J, Avila EL, Girke T, Raikhel NV, 2004. The vegetative vacuole proteome of *Arabidopsis thaliana* reveals predicted and unexpected proteins. *The Plant Cell Online* **16**, 3285-303.

Cha JY, Ahn G, Kim JY, Kang SB, Kim MR, Su'udi M, Kim WY, Son D, 2013. Structural and functional differences of cytosolic 90-kDa heat-shock proteins (Hsp90s) in *Arabidopsis thaliana*. *Plant Physiol Biochem* **70**, 368-73.

Chak RK, Thomas TL, Quatrano RS, Rock CD, 2000. The genes *ABI1* and *ABI2* are involved in abscisic acid-and drought-inducible expression of the *Daucus carota* L. Dc3 promoter in guard cells of transgenic *Arabidopsis thaliana* (L.) Heynh. *Planta* **210**, 875-83.

Changsong Z, Diqui Y, 2010. Analysis of the cold-responsive transcriptome in the mature pollen of *Arabidopsis*. *Journal of Plant Biology* **53**, 400-16.

Chao Y-Y, Hsu Y, Kao C, 2009. Involvement of glutathione in heat shock–and hydrogen peroxide–induced cadmium tolerance of rice (*Oryza sativa* L.) seedlings. *Plant and Soil* **318**, 37-45.

Charng YY, Liu HC, Liu NY, Chi WT, Wang CN, Chang SH, Wang TT, 2007. A heat-inducible transcription factor, HsfA2, is required for extension of acquired thermotolerance in *Arabidopsis*. *Plant Physiol* **143**, 251-62.

Chaudhury AM, 1993. Nuclear genes controlling male fertility. *The Plant Cell* **5**, 1277.

Chen HY, Hsieh EJ, Cheng MC, Chen CY, Hwang SY, Lin TP, 2016. *ORA47 (octadecanoid-responsive AP2/ERF-domain transcription factor 47)* regulates jasmonic acid and abscisic acid biosynthesis and signaling through binding to a novel *cis*-element. *New Phytol* **211**, 599-613.

Christensen A, Svensson K, Thelin L, Zhang W, Tintor N, Prins D, Funke N, Michalak M, Schulze-Lefert P, Saijo Y, 2010. Higher plant calreticulins have acquired specialized functions in *Arabidopsis*. *PLoS One* **5**, e11342.

Christensen JH, Christensen OB, 2007. A summary of the PRUDENCE model projections of changes in European climate by the end of this century. *Climatic Change* **81**, 7-30.

Chung P, Hsiao H-H, Chen H-J, Chang C-W, Wang S-J, 2014. Influence of temperature on the expression of the rice sucrose transporter 4 gene, *OsSUT4*, in germinating embryos and maturing pollen. *Acta Physiologiae Plantarum* **36**, 217-29.

Cloonan N, Forrest AR, Kollé G, Gardiner BB, Faulkner GJ, Brown MK, Taylor DF, Steptoe AL, Wani S, Bethel G, 2008. Stem cell transcriptome profiling via massive-scale mRNA sequencing. *Nature Methods* **5**, 613-9.

Colcombet J, Boisson-Dernier A, Ros-Palau R, Vera CE, Schroeder JI, 2005. *Arabidopsis* SOMATIC EMBRYOGENESIS RECEPTOR KINASES1 and 2 are essential for tapetum development and microspore maturation. *Plant Cell* **17**, 3350-61.

Conner TW, Lafayette PR, Nagao RT, Key JL, 1990. Sequence and expression of a HSP83 from *Arabidopsis thaliana*. *Plant Physiology* **94**, 1689-95.

De Storme N, Geelen D, 2014. The impact of environmental stress on male reproductive development in plants: biological processes and molecular mechanisms. *Plant Cell Environ* **37**, 1-18.

Dellero Y, Jossier M, Glab N, Oury C, Tcherkez G, Hodges M, 2016. Decreased glycolate oxidase activity leads to altered carbon allocation and leaf senescence after a transfer from high CO₂ to ambient air in *Arabidopsis thaliana*. *J Exp Bot* **67**, 3149-63.

Dept AOOTUNF, 2002. *The state of world fisheries and aquaculture, 2002*. Food & Agriculture Org.

Dinneny JR, Weigel D, Yanofsky MF, 2006. NUBBIN and JAGGED define stamen and carpel shape in *Arabidopsis*. *Development* **133**, 1645-55.

Dumas C, Berger F, Faure J-E, 1998. Gametes, Fertilization and Early Embryogenesis in Flowering. *Advances in Botanical Research* **28**, 231.

Eady C, Lindsey K, Twell D, 1995. The significance of microspore division and division symmetry for vegetative cell-specific transcription and generative cell differentiation. *The Plant Cell* **7**, 65-74.

Edlund AF, Swanson R, Preuss D, 2004. Pollen and stigma structure and function: the role of diversity in pollination. *The Plant Cell Online* **16**, S84-S97.

Endo M, Tsuchiya T, Hamada K, Kawamura S, Yano K, Ohshima M, Higashitani A, Watanabe M, Kawagishi-Kobayashi M, 2009. High temperatures cause male sterility in rice plants with transcriptional alterations during pollen development. *Plant and Cell Physiology* **50**, 1911-22.

Faghihi MA, Wahlestedt C, 2009. Regulatory roles of natural antisense transcripts. *Nature Reviews Molecular Cell Biology* **10**, 637-43.

Fan LM, Wang YF, Wang H, Wu WH, 2001. *In vitro Arabidopsis* pollen germination and characterization of the inward potassium currents in *Arabidopsis* pollen grain protoplasts. *Journal of Experimental Botany* **52**, 1603-14.

Fang Z, Cui X, 2011. Design and validation issues in RNA-seq experiments. *Briefings in Bioinformatics*, bbr004.

Farage-Barhom S, Burd S, Sonogo L, Mett A, Belausov E, Gidoni D, Lers A, 2011. Localization of the *Arabidopsis* senescence-and cell death-associated BFN1 nuclease: from the ER to fragmented nuclei. *Molecular Plant* **4**, 1062-73.

Farage-Barhom S, Burd S, Sonogo L, Perl-Treves R, Lers A, 2008. Expression analysis of the *BFN1* nuclease gene promoter during senescence, abscission, and programmed cell death-related processes. *Journal of Experimental Botany* **59**, 3247-58.

Fellerer C, Schweiger R, Schongrubler K, Soll J, Schwenkert S, 2011. Cytosolic HSP90 cochaperones HOP and FKBP interact with freshly synthesized chloroplast preproteins of *Arabidopsis*. *Mol Plant* **4**, 1133-45.

Fendrych M, Van Hautegeem T, Van Durme M, Olvera-Carrillo Y, Huysmans M, Karimi M, Lippens S, Guérin CJ, Krebs M, Schumacher K, 2014. Programmed cell death controlled by ANAC033/SOMBRERO determines root cap organ size in *Arabidopsis*. *Current Biology* **24**, 931-40.

Feng B, Lu D, Ma X, Peng Y, Sun Y, Ning G, Ma H, 2012. Regulation of the *Arabidopsis* anther transcriptome by DYT1 for pollen development. *Plant J* **72**, 612-24.

Feng X, Dickinson HG, 2007. Packaging the male germline in plants. *Trends in Genetics* **23**, 503-10.

Feng X, Dickinson HG, 2010. Cell-cell interactions during patterning of the *Arabidopsis* anther. *Biochem Soc Trans* **38**, 571-6.

Firon N, Pressman E, Meir S, Khoury R, Altahan L, 2012. Ethylene is involved in maintaining tomato (*Solanum lycopersicum*) pollen quality under heat-stress conditions. *AoB Plants* **2012**, pls024.

Firon N, Shaked R, Peet M, Pharr D, Zamski E, Rosenfeld K, Althan L, Pressman E, 2006. Pollen grains of heat tolerant tomato cultivars retain higher carbohydrate concentration under heat stress conditions. *Scientia Horticulturae* **109**, 212-7.

Fragkostefanakis S, Mesihovic A, Hu Y, Schleiff E, 2016. Unfolded protein response in pollen development and heat stress tolerance. *Plant Reproduction*, 1-11.

Francis KE, Lam SY, Harrison BD, Bey AL, Berchowitz LE, Copenhaver GP, 2007. Pollen tetrad-based visual assay for meiotic recombination in *Arabidopsis*. *Proc Natl Acad Sci U S A* **104**, 3913-8.

Frankel R, 1973. *The use of male sterility in hybrid seed production*. New York: Wiley.

Friedlander M, Atsmon D, Galun E, 1977. Sexual differentiation in cucumber: The effects of abscisic acid and other growth regulators on various sex genotypes. *Plant and Cell Physiology* **18**, 261-9.

Fryer MJ, Ball L, Oxborough K, Karpinski S, Mullineaux PM, Baker NR, 2003. Control of Ascorbate Peroxidase 2 expression by hydrogen peroxide

and leaf water status during excess light stress reveals a functional organisation of *Arabidopsis* leaves. *The Plant Journal* **33**, 691-705.

Ge W, Song Y, Zhang C, Zhang Y, Burlingame AL, Guo Y, 2011. Proteomic analyses of apoplastic proteins from germinating *Arabidopsis thaliana* pollen. *Biochimica et Biophysica Acta (BBA)-Proteins and Proteomics* **1814**, 1964-73.

Goldberg RB, Beals TP, Sanders PM, 1993. Anther development: basic principles and practical applications. *The Plant Cell* **5**, 1217.

Gomez JF, Talle B, Wilson ZA, 2015. Anther and pollen development: A conserved developmental pathway. *Journal of integrative plant biology* **57**, 876-91.

Gu JN, Zhu J, Yu Y, Teng XD, Lou Y, Xu XF, Liu JL, Yang ZN, 2014. DYT1 directly regulates the expression of *TDF1* for tapetum development and pollen wall formation in *Arabidopsis*. *Plant J* **80**, 1005-13.

Gurley WB, 2000. HSP101: a key component for the acquisition of thermotolerance in plants. *Plant Cell* **12**, 457-60.

Harsant J, Pavlovic L, Chiu G, Sultmanis S, Sage TL, 2013. High temperature stress and its effect on pollen development and morphological components of harvest index in the C3 model grass *Brachypodium distachyon*. *J Exp Bot* **64**, 2971-83.

Hartl FU, Bracher A, Hayer-Hartl M, 2011. Molecular chaperones in protein folding and proteostasis. *Nature* **475**, 324-32.

Hasanuzzaman M, Nahar K, Alam MM, Roychowdhury R, Fujita M, 2013. Physiological, biochemical, and molecular mechanisms of heat stress tolerance in plants. *International Journal of Molecular Sciences* **14**, 9643-84.

Hatfield JL, Prueger JH, 2015. Temperature extremes: effect on plant growth and development. *Weather and Climate Extremes* **10**, 4-10.

He D, Wang Q, Wang K, Yang P, 2015. Genome-Wide Dissection of the MicroRNA Expression Profile in Rice Embryo during Early Stages of Seed Germination. *PLoS One* **10**, e0145424.

He Y, Li J, 2001. Differential expression of triplicate phosphoribosylanthranilate isomerase isogenes in the tryptophan biosynthetic pathway of *Arabidopsis thaliana* (L.) Heynh. *Planta* **212**, 641-7.

Hedhly A, 2011. Sensitivity of flowering plant gametophytes to temperature fluctuations. *Environmental and Experimental Botany* **74**, 9-16.

Hedhly A, Hormaza JI, Herrero M, 2009. Global warming and sexual plant reproduction. *Trends Plant Sci* **14**, 30-6.

Helm M, Schmid M, Hierl G, Terneus K, Tan L, Lottspeich F, Kieliszewski MJ, Gietl C, 2008. KDEL-tailed cysteine endopeptidases involved in programmed cell death, intercalation of new cells, and dismantling of extensin scaffolds. *American Journal of Botany* **95**, 1049-62.

Hernández-Pinzón I, Ross JH, Barnes KA, Damant AP, Murphy DJ, 1999. Composition and role of tapetal lipid bodies in the biogenesis of the pollen coat of *Brassica napus*. *Planta* **208**, 588-98.

Hesse H, Trachsel N, Suter M, Kopriva S, Von Ballmoos P, Rennenberg H, Brunold C, 2003. Effect of glucose on assimilatory sulphate reduction in *Arabidopsis thaliana* roots. *Journal of Experimental Botany* **54**, 1701-9.

Heyndrickx KS, Vandepoele K, 2012. Systematic identification of functional plant modules through the integration of complementary data sources. *Plant Physiology* **159**, 884-901.

Higashitani A, 2013. High temperature injury and auxin biosynthesis in microsporogenesis. *Front Plant Sci* **4**, 47.

Hinton JC, Hautefort I, Eriksson S, Thompson A, Rhen M, 2004. Benefits and pitfalls of using microarrays to monitor bacterial gene expression during infection. *Current Opinion in Microbiology* **7**, 277-82.

Hoeijmakers WA, Bartfai R, Stunnenberg HG, 2013. Transcriptome analysis using RNA-Seq. *Methods Mol Biol* **923**, 221-39.

Hofmann NR, 2015. A mechanism for inhibition of COP1 in photomorphogenesis: direct interactions of phytochromes with SPA proteins. *Plant Cell* **27**, 8.

Hord CL, Chen C, Deyoung BJ, Clark SE, Ma H, 2006. The BAM1/BAM2 receptor-like kinases are important regulators of *Arabidopsis* early anther development. *Plant Cell* **18**, 1667-80.

Howell SH, 2013. Endoplasmic reticulum stress responses in plants. *Annu Rev Plant Biol* **64**, 477-99.

Huynh Le N, Vantoai T, Streeter J, Banowitz G, 2005. Regulation of flooding tolerance of SAG12:ipt *Arabidopsis* plants by cytokinin. *J Exp Bot* **56**, 1397-407.

Ito T, Ng KH, Lim TS, Yu H, Meyerowitz EM, 2007. The homeotic protein AGAMOUS controls late stamen development by regulating a jasmonate biosynthetic gene in *Arabidopsis*. *Plant Cell* **19**, 3516-29.

Ito T, Wellmer F, Yu H, Das P, Ito N, Alves-Ferreira M, Riechmann JL, Meyerowitz EM, 2004. The homeotic protein AGAMOUS controls microsporogenesis by regulation of SPOROCTELESS. *Nature* **430**, 356-60.

Iwahori S, 1965. High temperature injuries in tomato. IV. *Journal of the Japanese Society for Horticultural Science* **34**, 33-41.

Jaegle B, Uroic MK, Holtkotte X, Lucas C, Termath AO, Schmalz HG, Bucher M, Hoecker U, Hulskamp M, Schrader A, 2016. A fast and simple LC-MS-based characterization of the flavonoid biosynthesis pathway for few seed(ling)s. *BMC Plant Biol* **16**, 190.

Jaggard KW, Qi A, Ober ES, 2010. Possible changes to arable crop yields by 2050. *Philos Trans R Soc Lond B Biol Sci* **365**, 2835-51.

Jia G, Liu X, Owen HA, Zhao D, 2008. Signaling of cell fate determination by the TPD1 small protein and EMS1 receptor kinase. *Proc Natl Acad Sci U S A* **105**, 2220-5.

Jiang Y, Yang B, Harris NS, Deyholos MK, 2007. Comparative proteomic analysis of NaCl stress-responsive proteins in *Arabidopsis* roots. *Journal of Experimental Botany* **58**, 3591-607.

Katiyar-Agarwal S, Agarwal M, Grover A, 2003. Heat-tolerant basmati rice engineered by over-expression of hsp101. *Plant Mol Biol* **51**, 677-86.

Katoh H, Fujita K, Takuhara Y, Ogawa A, Suzuki S, 2011. ER stress-induced protein, VIGG, disturbs plant cation homeostasis, which is correlated with growth retardation and robustness to ER stress. *Biochem Biophys Res Commun* **405**, 514-20.

Kaul ML, 1988. *Male sterility in higher plants*. Berlin. Heidelberg.: Springer-Verlag.

Kaur R, Bains T, Bindumadhava H, Nayyar H, 2015. Responses of mungbean (*Vigna radiata* L.) genotypes to heat stress: effects on reproductive biology, leaf function and yield traits. *Scientia Horticulturae* **197**, 527-41.

Kaya H, Shibahara KI, Taoka KI, Iwabuchi M, Stillman B, Araki T, 2001. FASCIATA genes for chromatin assembly factor-1 in *Arabidopsis* maintain the cellular organization of apical meristems. *Cell* **104**, 131-42.

Kim D, Langmead B, Salzberg SL, 2015. HISAT: a fast spliced aligner with low memory requirements. *Nature Methods* **12**, 357-60.

Kim JH, Nguyen NH, Nguyen NT, Hong SW, Lee H, 2013. Loss of all three calreticulins, *CRT1*, *CRT2* and *CRT3*, causes enhanced sensitivity to water stress in *Arabidopsis*. *Plant Cell Rep* **32**, 1843-53.

Kim SH, Lee JH, Seo KI, Ryu B, Sung Y, Chung T, Deng XW, Lee JH, 2014. Characterization of a Novel DWD protein that participates in heat stress response in *Arabidopsis*. *Mol Cells* **37**, 833-40.

Kimchi A, 2007. Programmed cell death: from novel gene discovery to studies on network connectivity and emerging biomedical implications. *Cytokine Growth Factor Rev* **18**, 435-40.

Kong L, Cheng J, Zhu Y, Ding Y, Meng J, Chen Z, Xie Q, Guo Y, Li J, Yang S, Gong Z, 2015. Degradation of the ABA co-receptor ABI1 by PUB12/13 U-box E3 ligases. *Nat Commun* **6**, 8630.

Kopriva S, Koprivova A, 2004. Plant adenosine 5'-phosphosulphate reductase: the past, the present, and the future. *Journal of Experimental Botany* **55**, 1775-83.

Kopriva S, Mugford SG, Matthewman C, Koprivova A, 2009. Plant sulfate assimilation genes: redundancy versus specialization. *Plant Cell Rep* **28**, 1769-80.

Koprivova A, North KA, Kopriva S, 2008. Complex signaling network in regulation of adenosine 5'-phosphosulfate reductase by salt stress in *Arabidopsis* roots. *Plant Physiology* **146**, 1408-20.

Koprivova A, Suter M, Den Camp RO, Brunold C, Kopriva S, 2000. Regulation of sulfate assimilation by nitrogen in *Arabidopsis*. *Plant Physiology* **122**, 737-46.

Kotak S, Larkindale J, Lee U, Von Koskull-Doring P, Vierling E, Scharf KD, 2007. Complexity of the heat stress response in plants. *Curr Opin Plant Biol* **10**, 310-6.

Kovtun Y, Chiu W-L, Tena G, Sheen J, 2000. Functional analysis of oxidative stress-activated mitogen-activated protein kinase cascade in plants. *Proceedings of the National Academy of Sciences* **97**, 2940-5.

Krishna P, Gloor G, 2001. The Hsp90 family of proteins in *Arabidopsis thaliana*. *Cell Stress Chaperones* **6**, 238-46.

Krzywinska E, Bucholc M, Kulik A, Ciesielski A, Lichoicka M, Debski J, Ludwikow A, Dadlez M, Rodriguez PL, Dobrowolska G, 2016. Phosphatase ABI1 and okadaic acid-sensitive phosphoprotein phosphatases inhibit salt stress-activated SnRK2.4 kinase. *BMC Plant Biol* **16**, 136.

Kumpf RP, Nowack MK, 2015. The root cap: a short story of life and death. *66*, 5651-62.

Kuroda H, Yanagawa Y, Takahashi N, Horii Y, Matsui M, 2012. A comprehensive analysis of interaction and localization of *Arabidopsis* SKP1-like (ASK) and F-box (FBX) proteins. *PLoS One* **7**, e50009.

Lai C-P, Chen P-H, Huang J-P, Tzeng Y-H, Chaw S-M, Shaw J-F, 2012. Functional diversification of the Tubby-like protein gene families (TULPs) during eukaryotic evolution. *Biocatalysis and Agricultural Biotechnology* **1**, 2-8.

Lalanne E, Twell D, 2002. Genetic control of male germ unit organization in *Arabidopsis*. *Plant Physiology* **129**, 865-75.

Lam E, 2004. Controlled cell death, plant survival and development. *Nature Reviews Molecular Cell Biology* **5**, 305-15.

Larkindale J, Hall JD, Knight MR, Vierling E, 2005. Heat stress phenotypes of *Arabidopsis* mutants implicate multiple signaling pathways in the acquisition of thermotolerance. *Plant Physiol* **138**, 882-97.

Larkindale J, Huang B, 2004. Thermotolerance and antioxidant systems in *Agrostis stolonifera*: involvement of salicylic acid, abscisic acid, calcium, hydrogen peroxide, and ethylene. *J Plant Physiol* **161**, 405-13.

Lee JH, Hübel A, Schöffl F, 1995. Derepression of the activity of genetically engineered heat shock factor causes constitutive synthesis of heat shock proteins and increased thermotolerance in transgenic *Arabidopsis*. *The Plant Journal* **8**, 603-12.

Leivar P, Monte E, Al-Sady B, Carle C, Storer A, Alonso JM, Ecker JR, Quail PH, 2008. The *Arabidopsis* phytochrome-interacting factor PIF7, together with PIF3 and PIF4, regulates responses to prolonged red light by modulating phyB levels. *Plant Cell* **20**, 337-52.

Lenartowski R, Suwińska A, Prusińska J, Gumowski K, Lenartowska M, 2014. Molecular cloning and transcriptional activity of a new *Petunia* calreticulin gene involved in pistil transmitting tract maturation, progamic phase, and double fertilization. *Planta* **239**, 437-54.

Leung J, Bouvier-Durand M, Morris PC, Guerrier D, Cheddor F, Giraudat J, 1994. *Arabidopsis* ABA response gene ABI1: features of a calcium-modulated protein phosphatase. *Science* **264**, 1448-52.

Li C, Shen H, Wang T, Wang X, 2015. ABA Regulates Subcellular Redistribution of OsABI-LIKE2, a Negative Regulator in ABA Signaling, to Control Root Architecture and Drought Resistance in *Oryza sativa*. *Plant Cell Physiol* **56**, 2396-408.

Li H, Handsaker B, Wysoker A, Fennell T, Ruan J, Homer N, Marth G, Abecasis G, Durbin R, 2009. The sequence alignment/map format and SAMtools. *Bioinformatics* **25**, 2078-9.

Li W, 2012. Volcano plots in analyzing differential expressions with mRNA microarrays. *J Bioinform Comput Biol* **10**, 1231003.

Li W, Ma H, 2002. Gametophyte development. *Curr Biol* **12**, R718-21.

Li Y, Jiang J, Du ML, Li L, Wang XL, Li XB, 2013. A cotton gene encoding MYB-like transcription factor is specifically expressed in pollen and is involved in regulation of late anther/pollen development. *Plant Cell Physiol* **54**, 893-906.

Lin XL, Niu D, Hu ZL, Kim DH, Jin YH, Cai B, Liu P, Miura K, Yun DJ, Kim WY, Lin R, Jin JB, 2016. An *Arabidopsis* SUMO E3 Ligase, SIZ1, Negatively Regulates Photomorphogenesis by Promoting COP1 Activity. **12**, e1006016.

Lister R, O'malley RC, Tonti-Filippini J, Gregory BD, Berry CC, Millar AH, Ecker JR, 2008. Highly integrated single-base resolution maps of the epigenome in *Arabidopsis*. *Cell* **133**, 523-36.

Liu J-X, Howell SH, 2010. Endoplasmic reticulum protein quality control and its relationship to environmental stress responses in plants. *The Plant Cell* **22**, 2930-42.

Liu L, Fan X-D, 2013. Tapetum: regulation and role in sporopollenin biosynthesis in *Arabidopsis*. *Plant Mol Biol* **83**, 165-75.

Liu Y, Zhou J, White KP, 2014. RNA-seq differential expression studies: more sequence or more replication? *Bioinformatics* **30**, 301-4.

Lobell DB, Field CB, 2007. Global scale climate–crop yield relationships and the impacts of recent warming. *Environmental research letters* **2**, 014002.

Lobell DB, Gourdji SM, 2012. The influence of climate change on global crop productivity. *Plant physiology* **160**, 1686-97.

Lobell DB, Schlenker W, Costa-Roberts J, 2011. Climate trends and global crop production since 1980. *Science* **333**, 616-20.

Lohman KN, Gan S, John MC, Amasino RM, 1994. Molecular analysis of natural leaf senescence in *Arabidopsis thaliana*. *Physiologia Plantarum* **92**, 322-8.

Lu Y, Sasaki Y, Li X, Mori IC, Matsuura T, Hirayama T, Sato T, Yamaguchi J, 2015. ABI1 regulates carbon/nitrogen-nutrient signal transduction independent of ABA biosynthesis and canonical ABA signalling pathways in *Arabidopsis*. *J Exp Bot* **66**, 2763-71.

Ma H, 2005. Molecular genetic analyses of microsporogenesis and microgametogenesis in flowering plants. *Annu. Rev. Plant Biol.* **56**, 393-434.

Maestri E, Klueva N, Perrotta C, Gulli M, Nguyen HT, Marmioli N, 2002. Molecular genetics of heat tolerance and heat shock proteins in cereals. *Plant Mol Biol* **48**, 667-81.

Mang HG, Qian W, Zhu Y, Qian J, Kang HG, Klessig DF, Hua J, 2012. Abscisic acid deficiency antagonizes high-temperature inhibition of disease resistance through enhancing nuclear accumulation of resistance proteins SNC1 and RPS4 in *Arabidopsis*. *Plant Cell* **24**, 1271-84.

Marioni JC, Mason CE, Mane SM, Stephens M, Gilad Y, 2008. RNA-seq: an assessment of technical reproducibility and comparison with gene expression arrays. *Genome Research* **18**, 1509-17.

Mccarthy DJ, Chen Y, Smyth GK, 2012. Differential expression analysis of multifactor RNA-Seq experiments with respect to biological variation. *Nucleic Acids Res* **40**, 4288-97.

Mccormick S, 1993. Male gametophyte development. *The Plant Cell* **5**, 1265.

Mccormick S, 2004. Control of male gametophyte development. *The Plant Cell* **16**, S142-S53.

Meiri D, Breiman A, 2009. *Arabidopsis* ROF1 (FKBP62) modulates thermotolerance by interacting with HSP90.1 and affecting the accumulation of HsfA2-regulated sHSPs. *Plant J* **59**, 387-99.

Melquist S, Luff B, Bender J, 1999. *Arabidopsis* PAI gene arrangements, cytosine methylation and expression. *Genetics* **153**, 401-13.

Mepham R, Lane G, 1969. Formation and development of the tapetal periplasmodium in *Tradescantia bracteata*. *Protoplasma* **68**, 175-92.

Mi H, Poudel S, Muruganujan A, Casagrande JT, Thomas PD, 2016. PANTHER version 10: expanded protein families and functions, and analysis tools. *Nucleic Acids Res* **44**, D336-42.

Michalak M, Corbett EF, Mesaeli N, Nakamura K, Opas M, 1999. Calreticulin: one protein, one gene, many functions. *Biochem J* **344 Pt 2**, 281-92.

Mitsuda N, Iwase A, Yamamoto H, Yoshida M, Seki M, Shinozaki K, Ohme-Takagi M, 2007. NAC transcription factors, NST1 and NST3, are key regulators of the formation of secondary walls in woody tissues of *Arabidopsis*. *The Plant Cell* **19**, 270-80.

Mittal D, Madhyastha DA, Grover A, 2012. Genome-wide transcriptional profiles during temperature and oxidative stress reveal coordinated expression patterns and overlapping regulons in rice. *PLoS One* **7**, e40899.

Mittler R, Vanderauwera S, Suzuki N, Miller G, Tognetti VB, Vandepoele K, Gollery M, Shulaev V, Van Breusegem F, 2011. ROS signaling: the new wave? *Trends Plant Sci* **16**, 300-9.

Moes D, Himmelbach A, Korte A, Haberer G, Grill E, 2008. Nuclear localization of the mutant protein phosphatase *abi1* is required for insensitivity towards ABA responses in *Arabidopsis*. *Plant J* **54**, 806-19.

Montero-Barrientos M, Hermosa R, Cardoza RE, Gutierrez S, Nicolas C, Monte E, 2010. Transgenic expression of the *Trichoderma harzianum* hsp70 gene increases *Arabidopsis* resistance to heat and other abiotic stresses. *Journal of Plant Physiology* **167**, 659-65.

Morin RD, Bainbridge M, Fejes A, Hirst M, Krzywinski M, Pugh TJ, McDonald H, Varhol R, Jones SJ, Marra MA, 2008. Profiling the HeLa S3 transcriptome using randomly primed cDNA and massively parallel short-read sequencing. *Biotechniques* **45**, 81.

Mortazavi A, Williams BA, Mccue K, Schaeffer L, Wold B, 2008. Mapping and quantifying mammalian transcriptomes by RNA-Seq. *Nature methods* **5**, 621-8.

Muller J, Menzel D, Samaj J, 2007. Cell-type-specific disruption and recovery of the cytoskeleton in *Arabidopsis thaliana* epidermal root cells upon heat shock stress. *Protoplasma* **230**, 231-42.

Murakami T, Matsuba S, Funatsuki H, Kawaguchi K, Saruyama H, Tanida M, Sato Y, 2004. Over-expression of a small heat shock protein, sHSP17. 7, confers both heat tolerance and UV-B resistance to rice plants. *Molecular Breeding* **13**, 165-75.

Müller F, Rieu I, 2016. Acclimation to high temperature during pollen development. *Plant Reproduction*, 1-12.

Nagalakshmi U, Wang Z, Waern K, Shou C, Raha D, Gerstein M, Snyder M, 2008. The transcriptional landscape of the yeast genome defined by RNA sequencing. *Science* **320**, 1344-9.

Nawkar GM, Maibam P, Park JH, Sahi VP, Lee SY, Kang CH, 2013. UV-induced cell death in plants. *International Journal of Molecular Sciences* **14**, 1608-28.

Nikolovski N, Rubtsov D, Segura MP, Miles GP, Stevens TJ, Dunkley TP, Munro S, Lilley KS, Dupree P, 2012. Putative glycosyltransferases and other plant Golgi apparatus proteins are revealed by LOPIT proteomics. *Plant Physiology* **160**, 1037-51.

Nishizawa A, Yabuta Y, Yoshida E, Maruta T, Yoshimura K, Shigeoka S, 2006. *Arabidopsis* heat shock transcription factor A2 as a key regulator in response to several types of environmental stress. *The Plant Journal* **48**, 535-47.

Niu N, Liang W, Yang X, Jin W, Wilson ZA, Hu J, Zhang D, 2013. EAT1 promotes tapetal cell death by regulating aspartic proteases during male reproductive development in rice. *Nat Commun* **4**, 1445.

Noh YS, Amasino RM, 1999. Identification of a promoter region responsible for the senescence-specific expression of SAG12. *Plant Mol Biol* **41**, 181-94.

Norambuena L, Marchant L, Berninsone P, Hirschberg CB, Silva H, Orellana A, 2002. Transport of UDP-galactose in Plants (IDENTIFICATION AND FUNCTIONAL CHARACTERIZATION OF AtUTr1, AN *ARABIDOPSIS THALIANA* UDP-GALACTOSE/UDP-GLUCOSE TRANSPORTER). *Journal of Biological Chemistry* **277**, 32923-9.

Nover L, Bharti K, Doring P, Mishra SK, Ganguli A, Scharf KD, 2001. *Arabidopsis* and the heat stress transcription factor world: how many heat stress transcription factors do we need? *Cell Stress Chaperones* **6**, 177-89.

Ohkama N, Takei K, Sakakibara H, Hayashi H, Yoneyama T, Fujiwara T, 2002. Regulation of sulfur-responsive gene expression by exogenously applied cytokinins in *Arabidopsis thaliana*. *Plant and Cell Physiology* **43**, 1493-501.

Olvera-Carrillo Y, Salanenko Y, Nowack MK, 2012. Control of programmed cell death during plant reproductive development. In. *Biocommunication of Plants*. Springer, 171-96.

Olvera-Carrillo Y, Van Bel M, Van Hautegeem T, Fendrych M, Huysmans M, 2015. A Conserved Core of Programmed Cell Death Indicator Genes Discriminates Developmentally and Environmentally Induced Programmed Cell Death in Plants. *Plant Physiol* **169**, 2684-99.

Omidi M, Siahpoosh MR, Mamghani R, Modarresi M, 2014. The influence of terminal heat stress on meiosis abnormalities in pollen mother cells of wheat. *Cytologia* **79**, 49-58.

Ono K, Hibino T, Kohinata T, Suzuki S, Tanaka Y, Nakamura T, Takabe T, 2001. Overexpression of DnaK from a halotolerant cyanobacterium *Aphanothece halophytica* enhances the high-temperature tolerance of tobacco during germination and early growth. *Plant Science* **160**, 455-61.

Oshino T, Abiko M, Saito R, Ichiishi E, Endo M, Kawagishi-Kobayashi M, Higashitani A, 2007. Premature progression of anther early developmental programs accompanied by comprehensive alterations in transcription during high-temperature injury in barley plants. *Mol Genet Genomics* **278**, 31-42.

Oshino T, Miura S, Kikuchi S, Hamada K, Yano K, Watanabe M, Higashitani A, 2011. Auxin depletion in barley plants under high - temperature conditions represses DNA proliferation in organelles and nuclei via transcriptional alterations. *Plant, Cell & Environment* **34**, 284-90.

Otegui MS, Noh YS, Martínez DE, Vila Petroff MG, Andrew Staehelin L, Amasino RM, Guamet JJ, 2005. Senescence - associated vacuoles with intense proteolytic activity develop in leaves of *Arabidopsis* and soybean. *The Plant Journal* **41**, 831-44.

Pérez-Amador MA, Abler ML, De Rocher EJ, Thompson DM, Van Hoof A, Lebrasseur ND, Lers A, Green PJ, 2000. Identification of BFN1, a bifunctional nuclease induced during leaf and stem senescence in *Arabidopsis*. *Plant Physiology* **122**, 169-80.

Pachauri RK, Allen MR, Barros V, Broome J, Cramer W, Christ R, Church J, Clarke L, Dahe Q, Dasgupta P, 2014. *Climate change 2014: synthesis Report. Contribution of working groups I, II and III to the fifth assessment report of the intergovernmental panel on climate change*. IPCC.

Pacini E, 1996. Types and meaning of pollen carbohydrate reserves. *Sexual plant reproduction* **9**, 362-6.

Pacini E, Franchi G, 1993. Role of the tapetum in pollen and spore dispersal. In. *The Tapetum*. Springer, 1-11.

Panchuk, li, Volkov RA, Schoffl F, 2002. Heat stress- and heat shock transcription factor-dependent expression and activity of ascorbate peroxidase in *Arabidopsis*. *Plant Physiol* **129**, 838-53.

Parcy F, Giraudat J, 1997. Interactions between the ABI1 and the ectopically expressed ABI3 genes in controlling abscisic acid responses in *Arabidopsis* vegetative tissues. *The Plant Journal* **11**, 693-702.

Parish RW, Phan HA, Iacuone S, Li SF, 2012. Tapetal development and abiotic stress: a centre of vulnerability. *Functional Plant Biology* **39**, 553-9.

Park SM, Hong CB, 2002. Class I small heat-shock protein gives thermotolerance in tobacco. *Journal of Plant Physiology* **159**, 25-30.

Parrotta L, Faleri C, Cresti M, Cai G, 2016. Heat stress affects the cytoskeleton and the delivery of sucrose synthase in tobacco pollen tubes. *Planta* **243**, 43-63.

Paul W, Hodge R, Smartt S, Draper J, Scott R, 1992. The isolation and characterisation of the tapetum-specific *Arabidopsis thaliana* A9 gene. *Plant Mol Biol* **19**, 611-22.

Pearce S, Ferguson A, King J, Wilson ZA, 2015. FlowerNet: a gene expression correlation network for anther and pollen development. *Plant Physiology* **167**, 1717-30.

Pecrix Y, Rallo G, Folzer H, Cigna M, Gudin S, Le Bris M, 2011. Polyploidization mechanisms: temperature environment can induce diploid gamete formation in *Rosa* sp. *J Exp Bot* **62**, 3587-97.

Peng J, 2009. Gibberellin and jasmonate crosstalk during stamen development. *J Integr Plant Biol* **51**, 1064-70.

Perez-Amador MA, Abler ML, De Rocher EJ, Thompson DM, Van Hoof A, Lebrasseur ND, Lers A, Green PJ, 2000. Identification of BFN1, a

bifunctional nuclease induced during leaf and stem senescence in *Arabidopsis*. *Plant Physiol* **122**, 169-80.

Pertea M, Pertea GM, Antonescu CM, Chang T-C, Mendell JT, Salzberg SL, 2015. StringTie enables improved reconstruction of a transcriptome from RNA-seq reads. *Nature biotechnology* **33**, 290-5.

Petrov V, Hille J, Mueller-Roeber B, Gechev TS, 2015. ROS-mediated abiotic stress-induced programmed cell death in plants. *Front Plant Sci* **6**, 69.

Phan HA, Iacuone S, Li SF, Parish RW, 2011. The MYB80 transcription factor is required for pollen development and the regulation of tapetal programmed cell death in *Arabidopsis thaliana*. *Plant Cell* **23**, 2209-24.

Phan HA, Li SF, Parish RW, 2012. MYB80, a regulator of tapetal and pollen development, is functionally conserved in crops. *Plant Mol Biol* **78**, 171-83.

Piffanelli P, Ross JH, Murphy D, 1998. Biogenesis and function of the lipidic structures of pollen grains. *Sexual plant reproduction* **11**, 65-80.

Plackett AR, Thomas SG, Wilson ZA, Hedden P, 2011. Gibberellin control of stamen development: a fertile field. *Trends Plant Sci* **16**, 568-78.

Platt KA, Huang AH, Thomson WW, 1998. Ultrastructural study of lipid accumulation in tapetal cells of *Brassica napus* L. cv. Westar during microsporogenesis. *International Journal of Plant Sciences*, 724-37.

Polowick P, Sawhney V, 1993. Differentiation of the tapetum during microsporogenesis in tomato (*Lycopersicon esculentum* Mill.), with special reference to the tapetal cell wall. *Annals of Botany* **72**, 595-605.

Prasad BD, Goel S, Krishna P, 2010. In silico identification of carboxylate clamp type tetratricopeptide repeat proteins in *Arabidopsis* and rice as putative co-chaperones of Hsp90/Hsp70. *PLoS One* **5**, e12761.

Prasad NG, Dey S, Shakarad M, Joshi A, 2003. The evolution of population stability as a by-product of life-history evolution. *Proc Biol Sci* **270 Suppl 1**, S84-6.

Pressman E, Harel D, Zamski E, Shaked R, Althan L, Rosenfeld K, Firon N, 2006. The effect of high temperatures on the expression and activity of sucrose-cleaving enzymes during tomato (*Lycopersicon esculentum*) anther development. *The Journal of Horticultural Science and Biotechnology* **81**, 341-8.

Pressman E, Peet MM, Pharr DM, 2002. The effect of heat stress on tomato pollen characteristics is associated with changes in carbohydrate concentration in the developing anthers. *Ann Bot* **90**, 631-6.

Price AM, Orellana DFA, Salleh FM, Stevens R, Acock R, Buchanan-Wollaston V, Stead AD, Rogers HJ, 2008. A comparison of leaf and petal senescence in wallflower reveals common and distinct patterns of gene expression and physiology. *Plant physiology* **147**, 1898-912.

Qin D, Wang F, Geng X, Zhang L, Yao Y, Ni Z, Peng H, Sun Q, 2015. Overexpression of heat stress-responsive *TaMBF1c*, a wheat (*Triticum aestivum* L.) Multiprotein Bridging Factor, confers heat tolerance in both yeast and rice. *Plant Mol Biol* **87**, 31-45.

Queitsch C, Hong S-W, Vierling E, Lindquist S, 2000. Heat shock protein **101** plays a crucial role in thermotolerance in *Arabidopsis*. *The Plant Cell* **12**, 479-92.

Quilichini TD, Douglas CJ, Samuels AL, 2014. New views of tapetum ultrastructure and pollen exine development in *Arabidopsis thaliana*. *Annals of Botany*, mcu042.

Raghavendra AS, Gonugunta VK, Christmann A, Grill E, 2010. ABA perception and signalling. *Trends Plant Sci* **15**, 395-401.

Reeves PH, Ellis CM, Ploense SE, Wu MF, Yadav V, Tholl D, Chetelat A, Haupt I, Kennerley BJ, Hodgens C, Farmer EE, Nagpal P, Reed JW, 2012. A regulatory network for coordinated flower maturation. *PLoS Genet* **8**, e1002506.

Regan SM, Moffatt BA, 1990. Cytochemical analysis of pollen development in wild-type *Arabidopsis* and a male-sterile mutant. *The Plant Cell* **2**, 877-89.

Reyes F, León G, Donoso M, Brandizzi F, Weber AP, Orellana A, 2010. The nucleotide sugar transporters AtUTr1 and AtUTr3 are required for the incorporation of UDP - glucose into the endoplasmic reticulum, are essential for pollen development and are needed for embryo sac progress in *Arabidopsis thaliana*. *The Plant Journal* **61**, 423-35.

Reyes F, Marchant L, Norambuena L, Nilo R, Silva H, Orellana A, 2006. AtUTr1, a UDP-glucose/UDP-galactose transporter from *Arabidopsis thaliana*, is located in the endoplasmic reticulum and up-regulated by the unfolded protein response. *J Biol Chem* **281**, 9145-51.

Reyes F, Orellana A, 2008. Golgi transporters: opening the gate to cell wall polysaccharide biosynthesis. *Curr Opin Plant Biol* **11**, 244-51.

Rezaei M, Arzani A, Sayed-Tabatabaei BE, 2010. Meiotic behaviour of tetraploid wheats (*Triticum turgidum* L.) and their synthetic hexaploid wheat derivatives influenced by meiotic restitution and heat stress. *J Genet* **89**, 401-7.

Riebeek H, 2010. Global warming: Feature articles. http://earthobservatory.nasa.gov/Features/GlobalWarming/global_warming_2007.pdf

Rizhsky L, Liang H, Shuman J, Shulaev V, Davletova S, Mittler R, 2004. When defense pathways collide. The response of *Arabidopsis* to a combination of drought and heat stress. *Plant Physiol* **134**, 1683-96.

Roberts A, Trapnell C, Donaghey J, Rinn JL, Pachter L, 2011. Improving RNA-Seq expression estimates by correcting for fragment bias. *Genome biology* **12**, 1.

Robinson MD, McCarthy DJ, Smyth GK, 2010. edgeR: a Bioconductor package for differential expression analysis of digital gene expression data. *Bioinformatics* **26**, 139-40.

Robles P, Pelaz S, 2004. Flower and fruit development in *Arabidopsis thaliana*. *International Journal of Developmental Biology* **49**, 633-43.

Rodziewicz P, Swarcewicz B, Chmielewska K, Wojakowska A, Stobiecki M, 2014. Influence of abiotic stresses on plant proteome and metabolome changes. *Acta Physiologiae Plantarum* **36**, 1-19.

Ron D, Walter P, 2007. Signal integration in the endoplasmic reticulum unfolded protein response. *Nat Rev Mol Cell Biol* **8**, 519-29.

Ruan YL, Jin Y, Yang YJ, Li GJ, Boyer JS, 2010. Sugar input, metabolism, and signaling mediated by invertase: roles in development, yield potential, and response to drought and heat. *Mol Plant* **3**, 942-55.

Sage TL, Bagha S, Lundsgaard-Nielsen V, Branch HA, Sultmanis S, Sage RF, 2015. The effect of high temperature stress on male and female reproduction in plants. *Field Crops Research* **182**, 30-42.

Saidi Y, Finka A, Muriset M, Bromberg Z, Weiss YG, Maathuis FJ, Goloubinoff P, 2009. The heat shock response in moss plants is regulated by specific calcium-permeable channels in the plasma membrane. *Plant Cell* **21**, 2829-43.

Sakata T, Higashitani A, 2008. Male sterility accompanied with abnormal anther development in plants—genes and environmental stresses with special reference to high temperature injury. *Int. J. Plant Dev. Biol* **2**.

Sakata T, Oshino T, Miura S, Tomabechi M, Tsunaga Y, Higashitani N, Miyazawa Y, Takahashi H, Watanabe M, Higashitani A, 2010. Auxins reverse plant male sterility caused by high temperatures. *Proceedings of the National Academy of Sciences* **107**, 8569-74.

Sakata T, Takahashi H, Nishiyama I, Higashitani A, 2000. Effects of high temperature on the development of pollen mother cells and microspores in barley *Hordeum vulgare* L. *Journal of Plant Research* **113**, 395-402.

Samakovli D, Margaritopoulou T, Prassinos C, Milioni D, Hatzopoulos P, 2014. Brassinosteroid nuclear signaling recruits HSP90 activity. *New Phytol* **203**, 743-57.

Sanders PM, Bui AQ, Weterings K, Mcintire K, Hsu Y-C, Lee PY, Truong MT, Beals T, Goldberg R, 1999. Anther developmental defects in *Arabidopsis thaliana* male-sterile mutants. *Sexual Plant Reproduction* **11**, 297-322.

Sangwan V, Orvar BL, Beyerly J, Hirt H, Dhindsa RS, 2002. Opposite changes in membrane fluidity mimic cold and heat stress activation of distinct plant MAP kinase pathways. *Plant J* **31**, 629-38.

Sanmiya K, Suzuki K, Egawa Y, Shono M, 2004. Mitochondrial small heat - shock protein enhances thermotolerance in tobacco plants. *FEBS letters* **557**, 265-8.

Sawhney VK, Shukla A, 1994. Male sterility in flowering plants: are plant growth substances involved? *American Journal of Botany*, 1640-7.

Scharf KD, Berberich T, Ebersberger I, Nover L, 2012. The plant heat stress transcription factor (Hsf) family: structure, function and evolution. *Biochim Biophys Acta* **1819**, 104-19.

Schmidhuber J, Tubiello FN, 2007. Global food security under climate change. *Proceedings of the National Academy of Sciences* **104**, 19703-8.

Schwacke R, Grallath S, Breitzkreuz KE, Stransky E, Stransky H, Frommer WB, Rentsch D, 1999. LeProT1, a transporter for proline, glycine betaine, and γ -amino butyric acid in tomato pollen. *The Plant Cell* **11**, 377-91.

Scott RJ, Spielman M, Dickinson HG, 2004. Stamen structure and function. *The Plant Cell* **16**, S46-S60.

Setya A, Murillo M, Leustek T, 1996. Sulfate reduction in higher plants: molecular evidence for a novel 5'-adenylylsulfate reductase. *Proc Natl Acad Sci U S A* **93**, 13383-8.

Shi W, Muramoto Y, Ueda A, Takabe T, 2001. Cloning of peroxisomal ascorbate peroxidase gene from barley and enhanced thermotolerance by overexpressing in *Arabidopsis thaliana*. *Gene* **273**, 23-7.

Shu-Lan Y, Jiang L, San Puaah C, Xie L-F, 2005. Overexpression of *TAPETUM DETERMINANT1* Alters the Cell Fates in the *Arabidopsis* Carpel and Tapetum via Genetic Interaction with *EXCESS MICROSPOROCTES1/EXTRA SPOROGENOUS CELLS*. *Plant Physiology* **139**, 186.

Silva PA, Silva JC, Caetano HD, Machado JP, Mendes GC, Reis PA, Brustolini OJ, Dal-Bianco M, Fontes EP, 2015. Comprehensive analysis of the endoplasmic reticulum stress response in the soybean genome: conserved and plant-specific features. *BMC Genomics* **16**, 783.

Smertenko A, Dr ber P, Viklický V, Opatrný Z, 1997. Heat stress affects the organization of microtubules and cell division in *Nicotiana tabacum* cells. *Plant, Cell & Environment* **20**, 1534-42.

Smykowski A, Fischer SM, Zentgraf U, 2015. Phosphorylation Affects DNA-Binding of the Senescence-Regulating bZIP Transcription Factor GBF1. *Plants (Basel)* **4**, 691-709.

Smyth DR, Bowman JL, Meyerowitz EM, 1990. Early flower development in *Arabidopsis*. *The Plant Cell* **2**, 755-67.

Sohn S, Back K, 2007. Transgenic rice tolerant to high temperature with elevated contents of dienoic fatty acids. *Biologia Plantarum* **51**, 340-2.

Solís M-T, Chakrabarti N, Corredor E, Cortés-Eslava J, Rodríguez-Serrano M, Biggiogera M, Risueño MC, Testillano PS, 2014. Epigenetic changes accompany developmental programmed cell death in tapetum cells. *Plant and Cell Physiology* **55**, 16-29.

Soneson C, Delorenzi M, 2013. A comparison of methods for differential expression analysis of RNA-seq data. *BMC Bioinformatics* **14**, 1.

Song Y, Xiang F, Zhang G, Miao Y, Miao C, Song CP, 2016. Abscisic Acid as an Internal Integrator of Multiple Physiological Processes Modulates Leaf Senescence Onset in *Arabidopsis thaliana*. *Front Plant Sci* **7**, 181.

Sorensen AM, Kröber S, Unte US, Huijser P, Dekker K, Saedler H, 2003. The *Arabidopsis* *ABORTED MICROSPORES (AMS)* gene encodes a MYC class transcription factor. *The Plant Journal* **33**, 413-23.

Steiner-Lange S, Unte U, 2003. Eckstein, L., Yang, C., and Wilson, ZA (2003). Disruption of *Arabidopsis thaliana* *MYB26* results in male sterility due to non-dehiscent anthers. *Plant J* **34**, 519-28.

Stocker T, Qin D, Plattner G, Tignor M, Allen S, Boschung J, Nauels A, Xia Y, Bex B, Midgley B, 2013. IPCC, 2013: climate change 2013: the physical science basis. Contribution of working group I to the fifth assessment report of the intergovernmental panel on climate change.

Sturn A, Quackenbush J, Trajanoski Z, 2002. Genesis: cluster analysis of microarray data. *Bioinformatics* **18**, 207-8.

Su Z, Ma X, Guo H, Sukiran NL, Guo B, Assmann SM, Ma H, 2013. Flower development under drought stress: morphological and transcriptomic analyses reveal acute responses and long-term acclimation in *Arabidopsis*. *Plant Cell* **25**, 3785-807.

Suzuki N, Bajad S, Shuman J, Shulaev V, Mittler R, 2008. The transcriptional co-activator MBF1c is a key regulator of thermotolerance in *Arabidopsis thaliana*. *J Biol Chem* **283**, 9269-75.

Suzuki N, Bassil E, Hamilton JS, Inupakutika MA, Zandalinas SI, Tripathy D, Luo Y, Dion E, Fukui G, Kumazaki A, Nakano R, Rivero RM, Verbeck GF, Azad RK, Blumwald E, Mittler R, 2016. ABA Is Required for Plant

Acclimation to a Combination of Salt and Heat Stress. *PLoS One* **11**, e0147625.

Suzuki N, Miller G, Sejima H, Harper J, Mittler R, 2013. Enhanced seed production under prolonged heat stress conditions in *Arabidopsis thaliana* plants deficient in cytosolic ascorbate peroxidase 2. *Journal of Experimental Botany* **64**, 253-63.

Suzuki N, Rizhsky L, Liang H, Shuman J, Shulaev V, Mittler R, 2005. Enhanced tolerance to environmental stress in transgenic plants expressing the transcriptional coactivator multiprotein bridging factor 1c. *Plant Physiol* **139**, 1313-22.

Suzuki N, Sejima H, Tam R, Schlauch K, Mittler R, 2011. Identification of the MBF1 heat-response regulon of *Arabidopsis thaliana*. *Plant J* **66**, 844-51.

Sweetlove L, Heazlewood J, Herald V, Holtzapffel R, Day D, Leaver C, Millar A, 2002. The impact of oxidative stress on *Arabidopsis* mitochondria. *The Plant Journal* **32**, 891-904.

Tajdel M, Mitula F, Ludwikow A, 2016. Regulation of *Arabidopsis* MAPKKK18 by ABI1 and SnRK2, components of the ABA signaling pathway. *Plant Signal Behav* **11**, e1139277.

Takahashi H, Kopriva S, Giordano M, Saito K, Hell R, 2011. Sulfur assimilation in photosynthetic organisms: molecular functions and regulations of transporters and assimilatory enzymes. *Annu Rev Plant Biol* **62**, 157-84.

Talanova V, Akimova T, Titov A, 2003. Effect of whole plant and local heating on the ABA content in cucumber seedling leaves and roots and on their heat tolerance. *Russian Journal of Plant Physiology* **50**, 90-4.

Tanaka I, 1997. Differentiation of generative and vegetative cells in angiosperm pollen. *Sexual Plant Reproduction* **10**, 1-7.

Tang R-S, Zheng J-C, Jin Z-Q, Zhang D-D, Huang Y-H, Chen L-G, 2008. Possible correlation between high temperature-induced floret sterility and endogenous levels of IAA, GAs and ABA in rice (*Oryza sativa* L.). *Plant Growth Regulation* **54**, 37-43.

Tauber E, Zordan M, Sandrelli F, Pegoraro M, Osterwalder N, Breda C, Daga A, Selmin A, Monger K, Benna C, Rosato E, Kyriacou CP, Costa R, 2007. Natural selection favors a newly derived timeless allele in *Drosophila melanogaster*. *Science* **316**, 1895-8.

Thomas H, 2013. Senescence, ageing and death of the whole plant. *New Phytologist* **197**, 696-711.

Thorstensen T, Grini PE, Mercy IS, Alm V, Erdal S, Aasland R, Aalen RB, 2008. The *Arabidopsis* SET-domain protein ASHR3 is involved in stamen development and interacts with the bHLH transcription factor ABORTED MICROSPORES (AMS). *Plant Mol Biol* **66**, 47-59.

Toh S, Imamura A, Watanabe A, Nakabayashi K, Okamoto M, Jikumaru Y, Hanada A, Aso Y, Ishiyama K, Tamura N, Iuchi S, Kobayashi M, Yamaguchi S, Kamiya Y, Nambara E, Kawakami N, 2008. High temperature-induced abscisic acid biosynthesis and its role in the inhibition of gibberellin action in *Arabidopsis* seeds. *Plant Physiol* **146**, 1368-85.

Toledo-Ortiz G, Huq E, Quail PH, 2003. The *Arabidopsis* basic/helix-loop-helix transcription factor family. *Plant Cell* **15**, 1749-70.

Triques K, Sturbois B, Gallais S, Dalmais M, Chauvin S, Clepet C, Aubourg S, Rameau C, Caboche M, Bendahmane A, 2007.

Characterization of *Arabidopsis thaliana* mismatch specific endonucleases: application to mutation discovery by TILLING in pea. *Plant J* **51**, 1116-25.

Tsuda K, Yamazaki K, 2004. Structure and expression analysis of three subtypes of *Arabidopsis MBF1* genes. *Biochim Biophys Acta* **1680**, 1-10.

Tsuji H, Aya K, Ueguchi-Tanaka M, Shimada Y, Nakazono M, Watanabe R, Nishizawa NK, Gomi K, Shimada A, Kitano H, Ashikari M, Matsuoka M, 2006. GAMYB controls different sets of genes and is differentially regulated by microRNA in aleurone cells and anthers. *Plant J* **47**, 427-44.

Tsvetkova NM, Horvath I, Torok Z, Wolkers WF, Balogi Z, Shigapova N, Crowe LM, Tablin F, Vierling E, Crowe JH, Vigh L, 2002. Small heat-shock proteins regulate membrane lipid polymorphism. *Proc Natl Acad Sci U S A* **99**, 13504-9.

Twell D, Howden R, 1998. Mechanisms of asymmetric division and cell fate determination in developing pollen. *Androgenesis and haploid plants. INRA-Springer-Verlag, Berlin Heidelberg*, 69-103.

Twell D, Oh S-A, Honys D, 2006. Pollen development, a genetic and transcriptomic view. In. *The Pollen Tube*. Springer, 15-45.

Van Durme M, Nowack MK, 2016. Mechanisms of developmentally controlled cell death in plants. *Curr Opin Plant Biol* **29**, 29-37.

Van Hautegeem T, Waters AJ, Goodrich J, Nowack MK, 2015. Only in dying, life: programmed cell death during plant development. *Trends Plant Sci* **20**, 102-13.

Vera JC, Wheat CW, Fescemyer HW, Frilander MJ, Crawford DL, Hanski I, Marden JH, 2008. Rapid transcriptome characterization for a nonmodel organism using 454 pyrosequencing. *Molecular Ecology* **17**, 1636-47.

Vizcay-Barrena G, Wilson ZA, 2006. Altered tapetal PCD and pollen wall development in the *Arabidopsis ms1* mutant. *Journal of Experimental Botany* **57**, 2709-17.

Voesenek LA, Bailey - Serres J, 2015. Flood adaptive traits and processes: an overview. *New Phytologist* **206**, 57-73.

Vollenweider P, Gunthardt-Goerg MS, 2006. Diagnosis of abiotic and biotic stress factors using the visible symptoms in foliage. *Environ Pollut* **140**, 562-71.

Wang R, Zhang Y, Kieffer M, Yu H, Kepinski S, Estelle M, 2016. HSP90 regulates temperature-dependent seedling growth in *Arabidopsis* by stabilizing the auxin co-receptor F-box protein TIR1. *Nat Commun* **7**, 10269.

Wang Z, Gerstein M, Snyder M, 2009. RNA-Seq: a revolutionary tool for transcriptomics. *Nature Reviews Genetics* **10**, 57-63.

Wassmann R, Jagadish S, Sumfleth K, Pathak H, Howell G, Ismail A, Serraj R, Redona E, Singh R, Heuer S, 2009. Regional vulnerability of climate change impacts on Asian rice production and scope for adaptation. *Advances in Agronomy* **102**, 91-133.

Weis E, Berry JA, 1988. Plants and high temperature stress. *Symp Soc Exp Biol* **42**, 329-46.

Wilhelm BT, Marguerat S, Watt S, Schubert F, Wood V, Goodhead I, Penkett CJ, Rogers J, Bähler J, 2008. Dynamic repertoire of a eukaryotic transcriptome surveyed at single-nucleotide resolution. *Nature* **453**, 1239-43.

Williams B, Dickman M, 2008. Plant programmed cell death: can't live with it; can't live without it. *Molecular Plant Pathology* **9**, 531-44.

Wilson ZA, Dawson J, Russell J, Mulligan BJ, 1991. Exploited plants. *Arabidopsis thaliana. Biologist* **38**, 163-9.

Wilson ZA, Morroll SM, Dawson J, Swarup R, Tighe PJ, 2001. The *Arabidopsis* MALE STERILITY1 (MS1) gene is a transcriptional regulator of male gametogenesis, with homology to the PHD - finger family of transcription factors. *The Plant Journal* **28**, 27-39.

Wilson ZA, Song J, Taylor B, Yang C, 2011. The final split: the regulation of anther dehiscence. *Journal of Experimental Botany* **62**, 1633-49.

Wilson ZA, Zhang D-B, 2009. From *Arabidopsis* to rice: pathways in pollen development. *Journal of Experimental Botany* **60**, 1479-92.

Wu L, Chen H, Curtis C, Fu ZQ, 2014. Go in for the kill: How plants deploy effector-triggered immunity to combat pathogens. *Virulence* **5**, 710-21.

Wyatt SE, Tsou PL, Robertson D, 2002. Expression of the high capacity calcium-binding domain of calreticulin increases bioavailable calcium stores in plants. *Transgenic Res* **11**, 1-10.

Xie HT, Wan ZY, Li S, Zhang Y, 2014. Spatiotemporal Production of Reactive Oxygen Species by NADPH Oxidase Is Critical for Tapetal Programmed Cell Death and Pollen Development in *Arabidopsis*. **26**, 2007-23.

Xu J, Ding Z, Vizcay-Barrena G, Shi J, Liang W, Yuan Z, Werck-Reichhart D, Schreiber L, Wilson ZA, Zhang D, 2014a. ABORTED MICROSPORES Acts as a Master Regulator of Pollen Wall Formation in *Arabidopsis*. *Plant Cell* **26**, 1544-56.

Xu J, Yang C, Yuan Z, Zhang D, Gondwe MY, Ding Z, Liang W, Zhang D, Wilson ZA, 2010. The ABORTED MICROSPORES regulatory network is required for postmeiotic male reproductive development in *Arabidopsis thaliana*. *The Plant Cell* **22**, 91-107.

Xu Y, Iacuone S, Li SF, Parish RW, 2014b. MYB80 homologues in *Arabidopsis*, cotton and Brassica: regulation and functional conservation in tapetal and pollen development. *BMC Plant Biol* **14**, 278.

Yamada K, Fukao Y, Hayashi M, Fukazawa M, Suzuki I, Nishimura M, 2007. Cytosolic HSP90 regulates the heat shock response that is responsible for heat acclimation in *Arabidopsis thaliana*. *Journal of Biological Chemistry* **282**, 37794-804.

Yang C, Xu Z, Song J, Conner K, Barrena GV, Wilson ZA, 2007. *Arabidopsis* MYB26/MALE STERILE35 regulates secondary thickening in the endothecium and is essential for anther dehiscence. *The Plant Cell* **19**, 534-48.

Yang SL, Xie LF, Mao HZ, Puaah CS, Yang WC, Jiang L, Sundaresan V, Ye D, 2003. *Tapetum determinant 1* is required for cell specialization in the *Arabidopsis* anther. *Plant Cell* **15**, 2792-804.

Yang X, Liang Z, Lu C, 2005. Genetic engineering of the biosynthesis of glycinebetaine enhances photosynthesis against high temperature stress in transgenic tobacco plants. *Plant Physiology* **138**, 2299-309.

Yang YH, Dudoit S, Luu P, Lin DM, Peng V, Ngai J, Speed TP, 2002. Normalization for cDNA microarray data: a robust composite method addressing single and multiple slide systematic variation. *Nucleic Acids Res* **30**, e15.

Yano T, Aydin M, Haraguchi T, 2007. Impact of climate change on irrigation demand and crop growth in a Mediterranean environment of Turkey. *Sensors* **7**, 2297-315.

Young LW, Wilen RW, Bonham-Smith PC, 2004. High temperature stress of *Brassica napus* during flowering reduces micro- and megagametophyte fertility, induces fruit abortion, and disrupts seed production. *J Exp Bot* **55**, 485-95.

Yu Y, Wang J, 2016. Salt Stress and Ethylene Antagonistically Regulate Nucleocytoplasmic Partitioning of COP1 to Control Seed Germination. **170**, 2340-50.

Zhang D, Liu D, Lv X, Wang Y, Xun Z, Liu Z, Li F, Lu H, 2014. The cysteine protease CEP1, a key executor involved in tapetal programmed cell death, regulates pollen development in *Arabidopsis*. *The Plant Cell* **26**, 2939-61.

Zhang J, Van Toai T, Huynh L, Preiszner J, 2000. Development of flooding-tolerant *Arabidopsis thaliana* by autoregulated cytokinin production. *Molecular Breeding* **6**, 135-44.

Zhang J, Wang X, Vikash V, Ye Q, Wu D, Liu Y, Dong W, 2016. ROS and ROS-Mediated Cellular Signaling. *Oxidative medicine and cellular longevity* **2016**.

Zhang W, Sun Y, Timofejeva L, Chen C, Grossniklaus U, Ma H, 2006. Regulation of *Arabidopsis* tapetum development and function by

DYSFUNCTIONAL TAPETUM1 (DYT1) encoding a putative bHLH transcription factor. *Development* **133**, 3085-95.

Zhang Z, Quick MK, Kanelakis KC, Gijzen M, Krishna P, 2003. Characterization of a plant homolog of hop, a cochaperone of hsp90. *Plant Physiol* **131**, 525-35.

Zhao DZ, Wang GF, Speal B, Ma H, 2002. The *excess microsporocytes 1* gene encodes a putative leucine-rich repeat receptor protein kinase that controls somatic and reproductive cell fates in the *Arabidopsis* anther. *Genes Dev* **16**, 2021-31.

Zhou L-Z, Höwing T, Müller B, Hammes UZ, Gietl C, Dresselhaus T, 2016. Expression analysis of KDEL-CysEPs programmed cell death markers during reproduction in *Arabidopsis*. *Plant Reproduction* **29**, 265-72.

Zhu J, Chen H, Li H, Gao JF, Jiang H, Wang C, Guan YF, Yang ZN, 2008. *Defective in Tapetal development and function 1* is essential for anther development and tapetal function for microspore maturation in *Arabidopsis*. *The Plant Journal* **55**, 266-77.

Zhu J, Lou Y, Xu X, Yang ZN, 2011. A genetic pathway for tapetum development and function in *Arabidopsis*. *J Integr Plant Biol* **53**, 892-900.

Zinn KE, Tunc-Ozdemir M, Harper JF, 2010. Temperature stress and plant sexual reproduction: uncovering the weakest links. *J Exp Bot* **61**, 1959-68.

APPENDICES

APPENDIX I Chemicals and Reagents

10 X TBE buffer

NaCl	0.89 M
Tris-HCl (pH 7.5)	10 mM
Na ₂ -EDTA	1 mM

Dilute to 0.5 X to use in electrophoresis

Murashige and Skoog Basal (MS) medium

MS powder	2.15 g
Sucrose (optional)	10 g
Agar	9 g
ddH ₂ O	add up to 1L
Total volume	1 L

Adjust pH to 5.2-5.7 and autoclave to sterilize; antibiotics added when sterilized medium cools to ~50°C

Sucrose buffer

Component	Concentration	for 10 ml
Tris-Cl (pH 7.5)	50 mM	0.5ml of 1M stock
NaCl	300 mM	0.75ml of 4M stock
Sucrose	300 mM	1.5ml of 2M stock
ddH ₂ O		7.25ml

APPENDIX I Chemicals and Reagents (continued)

BK buffer S15 MOPS (pH 7.5)

Ca(NO ₃) ₂ •4H ₂ O	30 mg/L (0.127 mM)
MgSO ₄ •7H ₂ O	20 mg/L (0.081 mM)
KNO ₃	10 mg/L (0.1 mM)
Sucrose	15%
MOPS	10 mM (pH 7.5)

Stored at -20 °C

APPENDIX II Primers

Primers information for RT-PCR and quantitative RT-PCR

Primers for housekeeping gene *ACTIN7* RT-PCR and quantitative RT-PCR (5' to 3')

For forward primer: ACT7_2F	TGGCCGATGGTGAGGATATT
For reverse primer: ACT7_443R	AACGGCCTGAATGGCAACAT

Primers for *CRT1b* (AT1G09210) RT-PCR and quantitative RT-PCR (5' to 3')

For forward primer: CRT1bF-qPCR	GCGAGGAAACCTCTGAGAAAGACG
For reverse primer: CRT1bR-qPCR	GGGGAGCAGTGAACGAATACACC

Primers for *UTR1* (AT2G02810) RT-PCR and quantitative RT-PCR (5' to 3')

For forward primer: UTR1F-qPCR	TCGCTGGAGGAGTATCCATCTTTGC
For reverse primer: UTR1R-qPCR	CGCTTCCGGGTGTAGCTTACAGAAC

Primers for *MBF1c* (AT3G24500) RT-PCR and quantitative RT-PCR (5' to 3')

For forward primer: MBF1cF-qPCR	GATGCCGAGCAGATACCCAG
For reverse primer: MBF1cR-qPCR	CCGCCGTAGATTTCCCCTTT

Primers for *HOP3* (AT4G12400) RT-PCR and quantitative RT-PCR (5' to 3')

For forward primer: HOP3F-qPCR	CTGAACCGGAGATGGAACCTATGGA
For reverse primer: HOP3R-qPCR	AGCATCTCGCCATTTTCACTAGAGC

Primers for *ABI1* (AT4G26080) RT-PCR and quantitative RT-PCR (5' to 3')

For forward primer: ABI1F-qPCR	CGGCAAACCTGCACTTCCATTATCC
For reverse primer: ABI1R-qPCR	TCCTCCGAGGCTTCAAATCAACC

APPENDIX II Primers (continued)

Primers information for RT-PCR and quantitative RT-PCR (continued)

Primers for <i>HS83</i> (AT5G52640) RT-PCR and quantitative RT-PCR (5' to 3')	
For forward primer: HS83F-qPCR	TTTGCGTTGAATCAAAGTTCGTTGC
For reverse primer: HS83R-qPCR	TGGTTCCCAAGTTGTTACACCAAATC
Primers for <i>F3K23</i> (AT2G21510) RT-PCR and quantitative RT-PCR (5' to 3')	
For forward primer: F3K23F-qPCR	TCGCTGGAGGAGTATCCATCTTTGC
For reverse primer: F3K23R-qPCR	CGCTTCCGGGTGTAGCTTACAGAAC
Primers for <i>SEC61</i> (AT2G45070) RT-PCR and quantitative RT-PCR (5' to 3')	
For forward primer: SEC61F-qPCR	CTACACCGATGACGCACCTGG
For reverse primer: SEC61R-qPCR	AGCGACGAAAGCAATGAAACC
Primers for <i>MEC18</i> (AT3G12050) RT-PCR and quantitative RT-PCR (5' to 3')	
For forward primer: MEC18F-qPCR	GAGGCCCGTGTAGGGATGAATTG
For reverse primer: MEC18R-qPCR	CGAAAACTGCACGGATCCTATGGAA
Primers for <i>BIP1</i> (AT5G28540) RT-PCR and quantitative RT-PCR (5' to 3')	
For forward primer: BIP1F-qPCR	CGGAGTGTTTGAGGTTCTCTCCACA
For reverse primer: BIP1R-qPCR	CTCACATTCCCTTCGGAGCTTACCA
Primers for <i>BFN1</i> (AT1G11190) RT-PCR and quantitative RT-PCR(5' to 3')	
For forward primer: BFN1F-qPCR	GCATCGGCTTTTAGATCATCCACGA
For reverse primer: BFN1R-qPCR	TGCTGGTCCGGCTTCTAAAAGATTC
Primers for <i>CEP1</i> (AT5G50260) RT-PCR and quantitative RT-PCR (5' to 3')	
For forward primer: CEP1F-qPCR	TTGCTAATCAGCCTGTTTCTG
For reverse primer: CEP1R-qPCR	ACTTTGTTCCGTCTATCGTTG

APPENDIX II Primers (continued)

Primers information for genotyping.

Primers for SALK_062083 genotyping (5' to 3')	
LP: SALK_062083LP	AGACGCCAATAAACCTTTTGG
RP: SALK_062083RP	TTTGGTCCTGATATCTGTGGC
Primers for SALK_099778 genotyping (5' to 3')	
LP: SALK_099778LP	TATGCACAGCCTTCTTTCTCC
RP: SALK_099778RP	TAGCGTCACCAGACCAATTTC
Primers for SALK_123541 genotyping (5' to 3')	
LP: SALK_123541LP	ACTTCAGAGAGAGGCATGTGCG
RP: SALK_123541RP	AGTATTGTATATGCGGTGCCG
Primers for GABI_493A10 genotyping (5' to 3')	
LP: GABI_493A10LP	TATCAATCCGACCAAGATTTCG
RP: GABI_493A10RP	TTCCCTGAATACATGTGCACC
Primers for SALK_083813 genotyping (5' to 3')	
LP: SALK_083813LP	ATCCAATGATAATAAGGCGGC
RP: SALK_083813RP	TAAAACCATTGAGCCAAATCG
Primers for GABI_434G08 genotyping (5' to 3')	
LP: GABI_434G08LP	TAAAACCATTGAGCCAAATCG
RP: GABI_434G08RP	TGTGTTACCCCCACAAAATG
Primers for SALK_072009 genotyping (5' to 3')	
LP: SALK_072009LP	TGAATATAGGAAGTCTGAAGCAAGTG
RP: SALK_072009RP	CGAAACAGCATCTTCCATCTC
Primers for GABI_334A12 genotyping (5' to 3')	
LP: GABI_334A12LP	TTATGTTTCTCTGCTAGTGGTGG
RP: GABI_334A12RP	CTCGGAGATTGAGTCAGTTGC

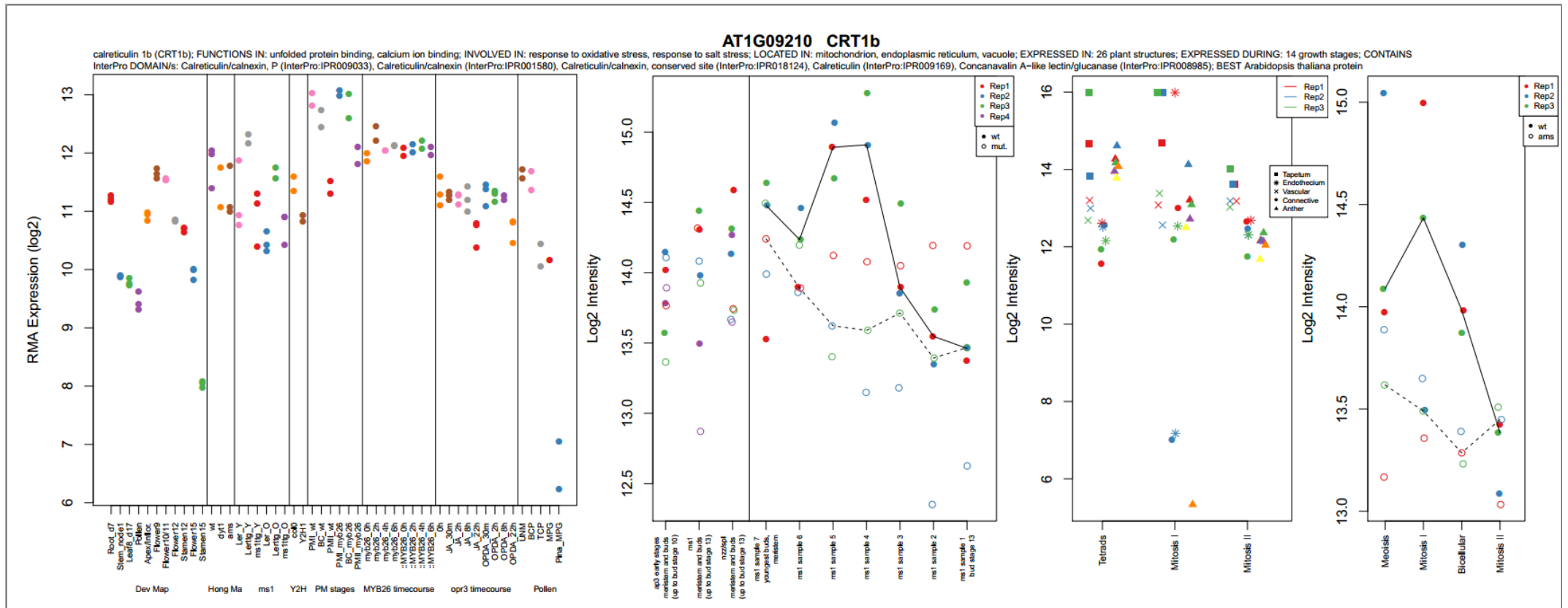
APPENDIX II Primers (continued)

Primers information for genotyping (continued).

Primers for SALK_000794 genotyping (5' to 3')	
LP: SALK_000794LP	AATGGAATTGAACCACTCAGG
RP: SALK_000794RP	GGAAGAAGCAAATCCAAAGG
Primers for SALK_023494 genotyping (5' to 3')	
LP: SALK_023494LP	TTGGTTGGTTACAAGTATTTGGAG
RP: SALK_023494RP	CCTCTGAATCTCCTTCATCGTC
Primers for SALK_004008 genotyping (5' to 3')	
LP: SALK_004008LP	GATTTACCCGCCTTCTCTTTG
RP: SALK_004008RP	TCAGGAAGAGAGCTGAAGCAG
Primers for SALK_075596 genotyping (5' to 3')	
LP: SALK_075596LP	TCAGACCCAACCTTCAACATCC
RP: SALK_075596RP	CACTTCTCAGTGGAGGGTCAG
Left border primer for SALK lines (5' to 3')	
LBb1.3	ATTTTGCCGATTTTCGGAAC
Left border primer for GABI lines (5' to 3')	
o8409	ATATTGACCATCATACTCATTGC

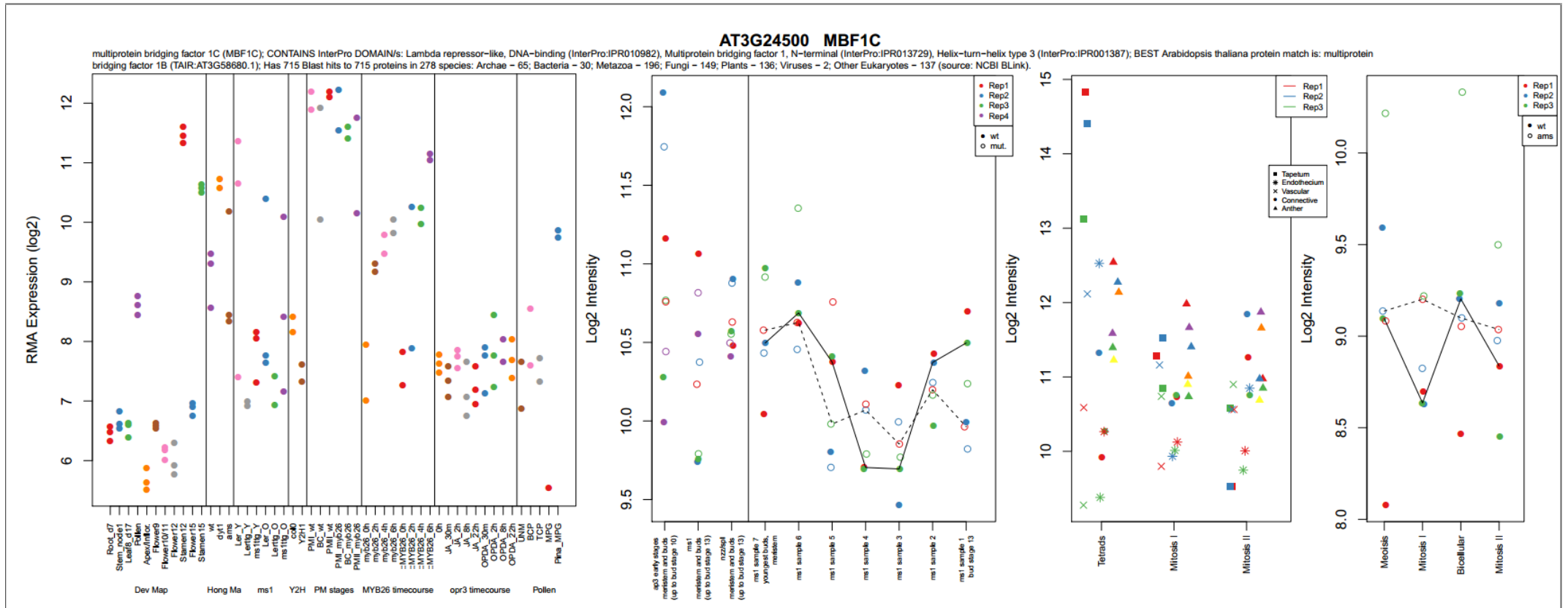
APPENDIX III Arabidopsis Anther/Floral Expression Plots

CRT1b (AT1G09210)



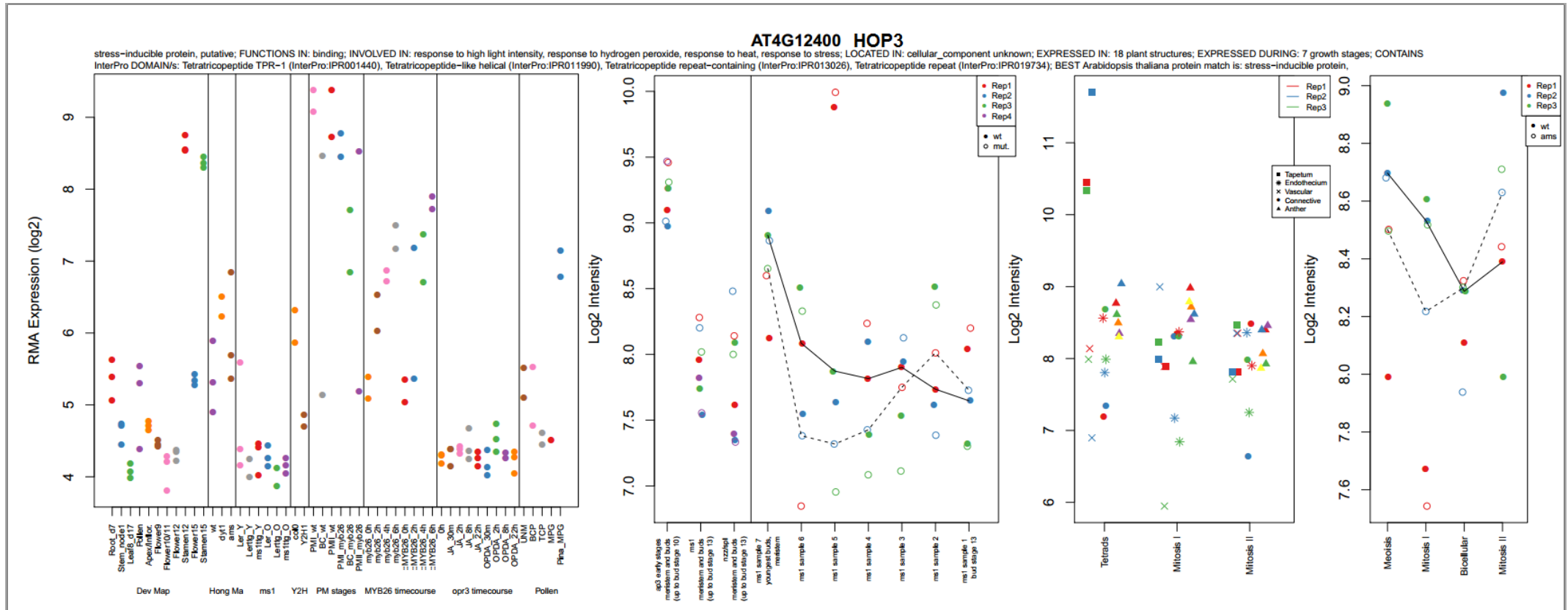
APPENDIX III Arabidopsis Anther/Floral Expression Plots (continued)

MBF1c (AT3G24500)



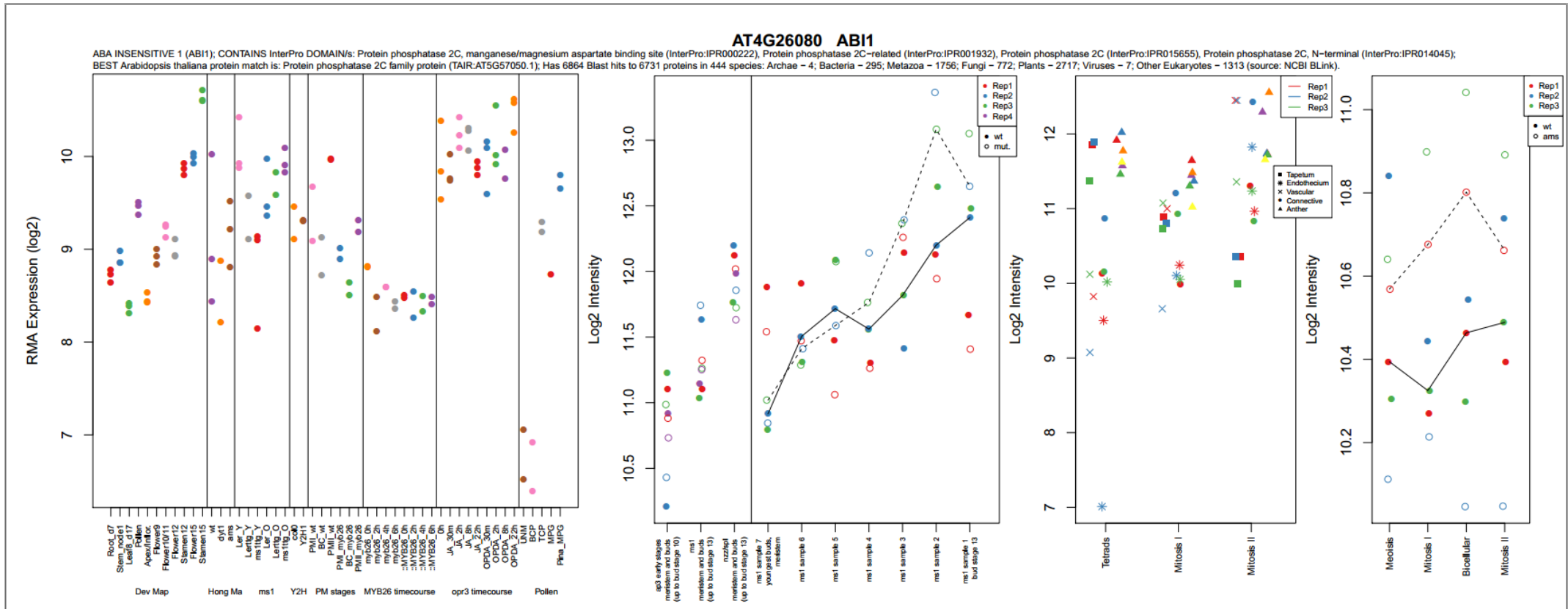
APPENDIX III Arabidopsis Anther/Floral Expression Plots (continued)

HOP3 (AT4G12400)



APPENDIX III Arabidopsis Anther/Floral Expression Plots (continued)

ABI1 (AT4G26080)



APPENDIX III Arabidopsis Anther/Floral Expression Plots (continued)

HS83 (AT5G52640)

